Investigations of Transport in Complex Atmospheric Flow Systems

I. Small Scale Studies of Diffusion through Porous Media, Impact of Fumehood Exhaust Reentry on Indoor Air Quality, and Pollutant Transport near an Isolated Island

II. Pollutant Transport in Mountain-Valley and Coastal Regions of California

Thesis by

Danny David Reible

In Partial Fulfillment of the Requirements

for the Degree of

Doctor of Philosophy

California Institute of Technology

Pasadena, California

1982

(Submitted October 20, 1981)

This thesis is dedicated to my parents, who started it

and to my wife, who completed it

Acknowledgements

This thesis would clearly not be possible without the guidance and assistance of my advisor, Dr. Fred Shair. I am grateful that I was able to conduct my research while maintaining a close personal and professional relationship with him. I am also thankful that my advisor was able to allow me to research topics that have a direct impact on the lives of everyone in California. It was deeply satisfying to be exposed, through my academic research, to the political machinery necessary to balance the often conflicting claims on the air resources of this state.

I also feel quite lucky to have been able to work closely with Dr.Ted Smith and Don Lehrman of Meteorology Research, Inc. Much of the thesis represents joint work between them, my advisor and myself.

Much of the research was supported by the California Air Resources Board and I gratefully acknowledge the assistance of Chuck Bennett, Chuck Unger and Jack Suder.

I also wish to thank Dr. Peter Drivas and Dr. Brian Lamb, whose work provided the foundation on which this thesis was built.

Because of the size and scope of the research projects that are described in this thesis, there are many people who particpated in these studies and contributed to their success. Ernie Sasaki, John King, Phil Sackinger, Anita Jakub and Willie Brown were especially helpful.

A special acknowledgement should be given to David Strand, who assisted my professional development in fields other than those described in this thesis.

Finally, I would like to thank my wife, Susie, who supported me throughout the common absences from home required by this research, and who is willing to move far from family and friends in the pursuit of my professional goals.

Abstract

This thesis details some applications of tracer techniques from laboratory scale studies of diffusion in porous media to the analysis of the transport and dispersion of pollutants in the mountain-valley and coastal environments that form the majority of the state of California.

Chapter 1 describes a technique for estimating gaseous diffusivities in porous media that is based on the general solution to Fick's second law for diffusion in a tube between two well-mixed volumes. In beds of essentially non-porous particles, the ratio of the measured effective diffusivity to the air diffusivity of a gas was found to be proportional to the bed porosity raised to the 1.43 power, a result in agreement with previous studies on similar materials. High moisture content (>15-20% moisture in sand) was found to significantly reduce the gas diffusivity with respect to that found in dry materials.

Chapter 2 indicates the importance of ventilation system imbalance upon the reentrainment of pollutants exhausted from a building. Tracer was released from a fumehood in a "clean" room at the Jet Propulsion Laboratory. Indoor concentrations as high as 235 PPB/gr-mole tracer released/hr were observed due to infiltration of the exhausted tracer. This concentration is about an order of magnitude higher than has been observed in buildings with more balanced venitilation systems. Predictions of single and multi-compartment stirred-tank models were compared to the dynamics of the tracer infiltration. A simple one-compartment model provided a better description of the infiltration dynamics

than a three-compartment model suggested by the design of the ventilation system.

Chapter 3 describes a series of atmospheric tracer studies of the transport and dispersion of pollutants over the ocean and near an isolated island cape. The experiments were designed to determine the impact of local sources on a background air quality sampling program. The horizontal dispersion of the tracer over the ocean surface could be approximated by the Gaussian plume model assuming a neutrally stable atmosphere, in general agreement with the expected atmospheric stability. Tracer releases from the surface of the isolated cape indicated that an essentially well-mixed separated zone existed above and downwind of the cape. The height of this zone extended to 35-40% above the height of the cape, about the same height as the wake downwind of an isolated building. Limited mixing between the separated zone and the freestream resulted in a sharp concentration gradient above this height.

Chapter 5 indicates the difficulties of describing the behavior of pollutants in complex terrain. A series of tracer experiments conducted in the northern and central California Coastal Mountains are described. The Gaussian plume model could be used to describe the dispersion of the tracer during strong, unidirectional winds. During an elevated tracer release, however, wind directional shear with altitude led to plume bifurcation, with the majority being transported through a stable nighttime drainage layer to ground level. The transport through the stable layer occurred at a vertical velocity of about 2 cm/s,

surprisingly rapid transport between stably stratified layers of the atmosphere.

Chapter 6 describes the uncertainties associated with mass balance and Gaussian parameter estimates from tracer data. The uncertainty in the calculated final result can be less than the errors (assumed random) associated with any individual experimental measurement, indicating that such calculations can be made with greater accuracy than would initially be expected.

Chapter 7 details the transport of pollutants in the San Joaquin Valley during stable wintertime conditions. The relatively limited net ventilation of the valley indicates that pollutants can remain within the valley for several days subsequent to their release. During one tracer experiment, about 50% of the released tracer was observed to be well-mixed within the southern valley about 72 hours after the beginning of the release. The most significant ventilation mechanism for the valley during the winter was the occasional passage of low pressure frontal systems. Long periods without frontal system passage can lead to significant pollutant buildup.

Chapter 8 describes the transport of pollutants in the San Joaquin Valley during summertime conditions. While much more effectively ventilated than during the winter, the increased solar insolation leads to significant ozone levels within the valley. A strong influx of air at the northern mouth of the valley is balanced during the day by a corresponding efflux at its southern end and by daytime upslope flow on the Sierra Nevada Mountains. At night, an eddy forms in the southern valley due to low level

stabilization and terrain blockage of the afternoon efflux over the southern boundary of the valley. This eddy grows as more air is entrained from the influx at the northern mouth of the valley. An accelerated layer of air aloft also develops during the night due to surface layer stabilization and decoupling. These dynamic flow structures are significant factors in the transport and dispersion of pollutants in the valley during the summer.

Chapter 9 details the impact of the San Joaquin Valley on the northern Mojave Desert. The transport of pollutants from the southern valley was linked through both tracer and aerosol data to the rapid nighttime reduction in visibility in the northern Mojave Desert. Unlike winter conditions, most of the pollutants in the southern valley were transported out of the valley within a day after their release.

Chapter 10 describes the impact on the Sierra Nevada Mountains of pollutant sources within the San Joaquin Valley. Tracer released within the valley was efficiently transported upslope, impacting National Park and Forest areas. The maximum concentrations observed upslope could be approximated with the Gaussian plume model, assuming very unstable atmospheric conditions. Nighttime stabilization arrested the upslope movement of the tracer and led to slope and valley impacts throughout the night. The limited nighttime ventilation of the slopes may result in the significant ozone concentrations typically observed at slope sites throughout the night.

Chapter 11 describes the transport characteristics of the Sacramento Valley, the northern half of the California Central

Valley. Tracer experiments indicated that San Francisco Bay area pollutants have only a small effect on the air quality in the Sacramento Valley. A midday flow divergence over Sacramento resulted in tracer impacts in both the northern part of the valley and the slopes northeast of the city. A counterclockwise eddy that forms in the southern valley during the morning was a potential mechanism for recirculating aged pollutants within the valley. During one tracer experiment, most of the released tracer was trapped within an elevated layer of air, a potentially important mechanism for multi-day impacts of pollutants.

Chapter 12 evaluates the transport of pollutants in the Santa Barbara Channel off the coast of southern California. Limited vertical mixing combined with diurnal wind reversals resulted in multi-day onshore impacts of the tracer released offshore. Efficient lateral mixing of the tracer during wind reversals led to a widespread coastal impact from a single point source. The existence of many point sources could result in a diluted background concentration (i.e. after wind reversals) that equals or exceeds the concentration directly downwind of a single source.

Chapter 13 develops a two layer model of the atmosphere that semi-quantitatively incorporates much of the basic transport structure observed in the above studies. The method of characteristics and the method of moments were used to examine the implications of the model. The model indicates that the air aloft must be considered in order to accurately predict the impact of a pollutant source, especially when considering the multi-day or long range impact of the source.

Table of Contents

Introduction

This thesis is separated into two parts. The first part (Chapters 1 through 3), details three experimental studies that were conducted to illustrate the potential of using an atmospheric tracer, sulfur hexafluoride, to solve specific transport problems that are not easily solved by any other means. This is especially true in Chapter 2, in which the impact of fumehood exhaust reentry on indoor air quality is examined, and in Chapter 3, in which the contamination of a background air quality sampling program by local pollutant sources is examined. Chapter 1 details an experimental technique that allows determination of gaseous diffusivities in porous media. In all three experiments, the use of a tracer that can be detected at concentrations as low as 1 part in a trillion (1 PPT) allows the transport characteristics to be easily quantified. Each chapter includes a separate introduction that gives the background and objectives of that work.

The second part of the thesis details the characteristics of pollutant transport and dispersion in the mountain-valley and coastal regions of California. While this section describes investigations that strictly pertain only to California, the transport mechanisms demonstrated are probably repeated elsewhere in the world. At the very least, the implications of these studies for other locales are worthy of further investigation.

Chapter 4 introduces this part of the thesis and outlines the basic problems, the objectives of these studies, and the method of

investigation. A short introduction is also included in each subsequent chapter to give the background and objectives of each study.

Chapter 5 describes a series of tracer experiments in the mountainous regions of central and northern California, illustrating many of the difficulties in describing the transport and dispersion of pollutants in complex terrain.

Chapter 6 analyzes the accuracy with which tracer data can be used to estimate mass balances (a comparison of released and observed amounts of tracer) and air quality model parameters (for the Gaussian plume model). Many of the results in the later chapters are based upon estimates of the total amount of mass remaining in a particular area after a tracer release, indicating the importance of an accurate mass balance estimate.

Chapters 7-10 analyze the transport and dispersion of pollutants in the southern half of the Central Valley of California, the San Joaquin Valley. Chapter 7 describes the fate of air pollutants in the San Joaquin Valley of California during winter conditions. Chapter 8 examines the San Joaquin Valley during summer conditions. The emphasis in these studies was on developing the overall ventilation balance for the valley during the respective season, and the implications of the overall ventilation in determining the structure of the flow field and the resulting pollutant transport and dispersion. Chapters 9 and 10 probe the impact of the San Joaquin Valley on two downwind receptor zones, the northern Mojave Desert and the western slopes of the Sierra Nevada Mountains.

Chapter 11 analyzes the summertime structure of the winds and the resulting pollutant transport in the northern half of the Central Valley, the Sacramento Valley.

Chapter 12 extends this analysis to the Santa Barbara Channel area of southern California. This chapter details the effect of diurnal wind reversals on the transport and dispersion of pollutants.

Chapter 13 incorporates many of the important characteristics of the transport of pollutants in the mountain-valley and coastal regions of California into a two layer model of the atmosphere. This model is used to indicate the implications of significant transport between the surface layer of the atmosphere and the air aloft.

Part I.

Small Scale Studies of Diffusion through Porous Media, Impact of Fumehood Exhaust Reentry on Indoor Air Quality, and Pollutant Transport near an Isolated Island

Chapter 1
A Technique for the Measurement of Gaseous Diffusion in Porous Media

by

D.D. Reible and F.H. Shair

(In Press, Journal of Soil Science)

ABSTRACT

An apparatus composed of two well-mixed vessels connected by a tube was used to measure the effective diffusivity of a gas (sulfur hexafluoride, SF_6) in porous beds of sand, steel wool and glass beads. The general solution to Fick's second law for the apparatus was employed in the analysis. The ratio of the measured effective diffusivity of SF_6 to the SF_6-air diffusivity was found to approximately equal the void fraction of the porous bed raised to the 1.43 power. This relationship agreed well with previously collected data and with the theoretical models of Millington (1959) and Marshall (1959). The effective diffusivity of wet porous materials was also measured and, at higher moisture contents, found to deviate strongly from that measured in dry materials. The effective diffusivity of SF_6 in sand with 20% moisture (volume basis) was found to be about one-fourth as large as the value expected from the dry bed experiments. No significant deviation was found for sand of 10% moisture content or lower.

INTRODUCTION

Many important industrial and agricultural processes require knowledge of the rate of gaseous diffusive transport through porous media. Applications of such knowledge include transport of oxygen and nutrients to plant root systems, the movement of gases in underground reservoirs, and transport of reactants to catalytic surfaces. Due to the complex nature of such transport, however, no model of such processes has universal applicability and experiment must generally be relied upon. The objective of this study is the demonstration of an experimental technique suitable for measuring gas diffusion rates in porous media. This technique serves to generalize some of the currently available methods. This technique is applied, in this work, to the estimation of gas diffusivities in both dry and wet porous beds composed of non-porous particles such as sand.

REVIEW OF PREVIOUS INVESTIGATIONS

A host of investigators have attempted to quantify the rate of gaseous diffusion through soils. The effective diffusivity of a gas through a porous media, D_e, is normally related to its diffusivity in air (if pore spaces within the media are air-filled) by a relation of the form,

$$D_e = \frac{\varepsilon}{\tau} D \qquad (1)$$

where D is the air diffusivity of the gas. The porosity of the medium, ε, is the fractional volume available for transport, and the tortuosity factor, τ, is a measure of the deviation of the flow path from uniform cylinders. The tortuosity factor is generally used as an adjustable parameter to fit experimentally determined diffusivities to Equation (1). The data of Penman (1940) suggested that the tortuosity was essentially constant and equal to about 1.5 for various materials and porosities between about 0.1 and 0.6. At higher porosities, Penman noted significant deviations from this approximation. Van Bavel's measurements (1951), indicated that the tortuosity was between 1.7 and 2 for beds of sand and glass spheres with porosities between 0.250 and 0.415. Millington (1959), taking a theoretical approach, found the tortuosity to be equal to the -1/3 power of the porosity. His approach considered spherical pores and the probability of two such pores on adjacent planes being connected. Marshall (1959) considered the interaction of cylindrical pores in adjacent planes to show that the tortuosity is equal to the -1/2 power of the porosity. Other investigators have attempted to quantify diffusive rates in catalysts, which like soils are porous. Wheeler (1955) assumed that diffusion occurs through parallel cylinders of uniform size. His analysis suggested that the tortuosity factor is equal to 2. Johnson and Stewart (1965) extended this model to uniform cylindrical capillaries that are not parallel and developed

an equation for the tortuosity factor which is not strictly dependent upon geometric factors. Wakao and Smith (1962) envisioned a bidisperse pore network of macro- and micropores and developed a model based on the possible interactions between the pores. For the limiting case of systems composed only of macropores, their results simplify to give the tortuosity as the inverse of the porosity.

Many of the measurements of diffusion rates are made via steady-state experiments in which gas streams of different compositions are passed over each end of a column of porous material. The composition of the streams is analyzed to determine the effective diffusivity. Buckingham (1904) was apparently the first to use an apparatus of this type. This technique has commonly been used to obtain binary diffusivities of H_2 and N_2 in porous media. A short description of this method may be found in Smith (1970). Penman (1940) and van Bavel (1951) also employed a steady-state method using a volatile liquid to provide a constant concentration of diffusing vapor at one end of the porous column. The primary disadvantage of such experiments is the lengthy amount of time typically required to achieve steady-state.

In order to shorten experimental time requirements and due to the the importance of transient diffusion in real systems, a number of unsteady-state techniques have been suggested. Pappendick and Runkles (1965) measured the transient diffusion of oxygen in a soil column that was initially flushed and then sealed on one end. Davis and Scott (1965) employed an approximate theory of gas chromatography developed by van Deemter, et al. (1956). The technique involves pulsing a porous column with the gas to be studied. The response of the system, as measured by the exit concentration profile, allows determination of the diffusivity. Barrer (1953) observed the transient flow of a test

gas through a porous plug. Barrer showed that the total volume of gas that diffuses through the plug asymptotically approaches a linear function of time if the concentrations at the plug faces remain essentially constant. Ball, et al. (1981) applied Fick's first law to measure the rate of diffusion of krypton-85 through a porous plug between two well-mixed volumes. Their analysis assumed that the concentration gradient through the porous plug was linear and that the total amount of tracer in the plug was constant. The solution of Fick's second law for diffusion betwen two well-mixed volumes, as presented in the current work, indicates that these assumptions are valid after a period of time which depends upon the geometry of the apparatus and the rate of diffusion. The reader is referred to Ball, et al. for a summary and critique of several other methods of measuring diffusion rates in porous media.

METHOD

Apparatus and Procedures

The apparatus employed for this investigation was composed of two Lucite cubes connected by a cylindrical tube. A diagram of the test facility is shown in Figure 1. A porous test material (either sand, glass beads, steel wool or mixtures of the three) was placed within the cylindrical tube. During an experiment, a known amount of sulfur hexafluoride (SF_6) was injected into one of the Lucite cubes. After allowing the cube to become well-mixed, the seals were removed allowing transport between the two cubes. The concentration of SF_6 in each cube was then followed as a function of time by regularly withdrawing 15 cm^3 syringe samples. The sample volume (and thus the cube pressure) was balanced by the injection of 15 cm^3 of "clean" air. The dilution error introduced by adding 15 cm^3 of laboratory air to the 3500 cm^3 cube volume during the collection of each sample was not significant. The gases within each cube were kept well-mixed by small fans rotated by hand 3 or 4 times every 5 minutes. The pump was used to mix the entire system at the completion of an experiment so that the steady-state concentration could be measured. In addition, the final mixing allowed an independent estimate of the mass originally injected and ensured that no SF_6 was lost.

All syringe samples were analyzed by electron capture gas chromatography. For this study, the SF_6-oxygen separating column was packed with 80-100 mesh 0.5 nm molecular sieve and was approximately 100 cm long. The detectors were calibrated by exponential dilution of a known concentration as described by Lamb (1978). The detectable range of SF_6 was approximately 5-10 parts per trillion (PPT) to 10 parts per billion (PPB). Higher SF_6 concentrations were

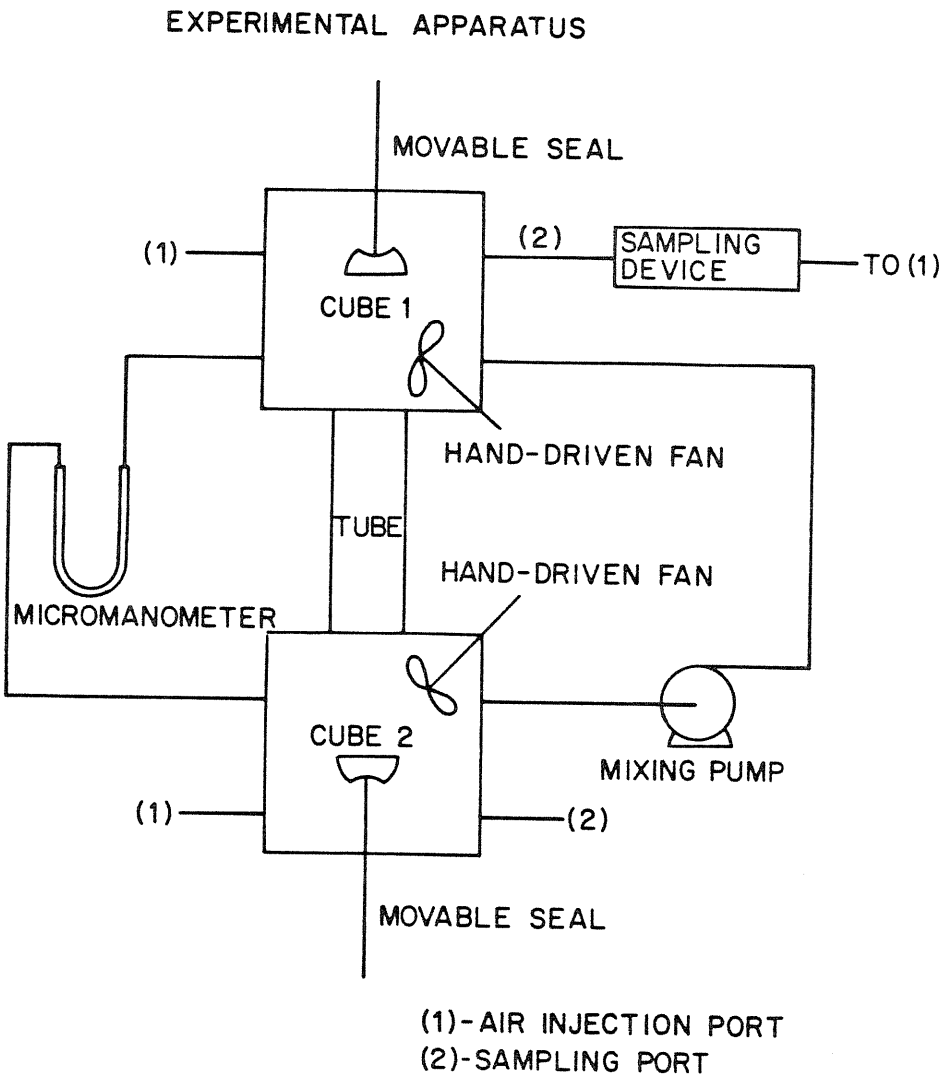

Figure 1 - Diagram of experimental apparatus.

analyzed by dilution of the sample. Further details of the analytical method are described in Lamb (1978). The use of SF_6 as a test gas is advantageous in that low concentrations, which correspond to short times, can be measured. While not generally necessary in a controlled laboratory environment, the ability to detect these low concentrations allows considerable flexibility in the arrangement of experiments. In addition, diffusivities through moist materials can be accurately measured due to the low solubility of SF_6 in water.

As mentioned previously, each Lucite cube had a volume of approximately 3500 cm^3. The inside diameter of the connecting tube was 2.54 cm and their lengths were 14.4 cm, 27.7 cm and 53.2 cm. The porous material within the connecting tube was either glass beads (1 cm and 0.2 mm dia), steel wool, sieved sand (-35,+60 mesh) or mixtures of these. In this manner, the porosity of the materials investigated was varied from 0.26 to 0.95. Steel wool with an 8.5% moisture content (vol H_2O/vol porous plug) and sand with 10, 15 and 20% moisture contents were also investigated. The porosity of the materials studied was estimated at the conclusion of an experiment by measuring the volume of water required to just fluidize the porous bed within the connecting tube. The moist samples were prepared by the addition of a known quantity of water to the porous material and then mixing thoroughly before placement in the apparatus.

It was possible to measure pressure differentials as low as about 0.25 N/m^2 across the porous column with the micromanometer. At the initiation of an experiment, the measured pressure differential was occasionally as high as 2.5 N/m^2. The convective transport induced by a pressure differential of this magnitude is small and not significant compared to the diffusive transport. As an example, Scheidegger (1957), suggested that sand permeabilities range from about 10^{-7} to 10^{-9}. Using the larger permeability and the maximum pressure gradient encountered during testing, the viscous flow flux was

smaller than the diffusive flux by a factor of about 300. An upper bound on convective effects was also established by experimentally determining the diffusivity of SF_6 in air. At 22°C and atmospheric pressure, the measured SF_6-air diffusivity was 0.109 cm^2/sec. This can be compared to the value of about 0.093 cm^2/sec suggested by the correlation of Fuller, Schettler and Giddings (see Reid, Prausnitz, and Sherwood, 1977). The damping action of the porous column further reduced the effect of convection during the experiments.

Estimation of Diffusivity

The measured concentration in the receiving cube as a function of time can be used to estimate the effective diffusivity of the SF_6 through the porous column. Fick's second law is applicable to diffusion through a tube with well-mixed end bulbs if the bulk transport of the diffusing gas is negligible. This is true if equimolar counter diffusion prevails or if the diffusing gas is present in low concentrations, as in this experiment. Thus the applicable equation for the concentration of component A, C_A, can be written as follows

$$\frac{\partial C_A}{\partial t} = D_e \frac{\partial^2 C_A}{\partial x^2} \qquad (2)$$

Where D_e is the effective diffusity through the porous medium. The boundary conditions are that the molar flux of component A out of each end bulb is equal to the time rate of change of C_A times the end bulb's volume, or

$$V_1 \frac{\partial C_A}{\partial t} = SD_e \frac{\partial C_A}{\partial x} \quad @\ x = 0$$

$$-V_2 \frac{\partial C_A}{\partial t} = SD_e \frac{\partial C_A}{\partial x} \quad @\ x = L \qquad (3)$$

End bulb 1 of volume V_1 is situated at x=0, and end bulb 2 of volume V_2 at x=L. S is the cross-sectional area of the connecting tube. The direction of transport of A is taken to be from x=0 to x=L. If we consider a given initial concentration, C_o, uniformly distributed over volume 1 and a length, l_o, down the tube, the concentration being zero elsewhere, then the necessary initial condition becomes

$$C_A(x,o) = \begin{cases} C_o \text{ for } 0 \leq x \leq l_o \\ 0 \text{ for } l_o < x \leq L \end{cases} \tag{4}$$

Shair and Cohen (1969) showed that the solution of Equation (2), for $x > l_o$, and subject to (3) and (4) is

$$C_A(x,t) = C_{A\infty} + 2C_o \sum_{n=1}^{\infty} \frac{\left(\cos \lambda_n(1-\frac{x}{L}) - \delta_2\lambda_n \sin\lambda_n(1-\frac{x}{L})\right)}{\lambda_n} \cdot \tag{5}$$

$$\frac{\left(\sin \lambda_n \frac{l_o}{L} + \delta_2\lambda_n \cos\lambda_n \frac{l_o}{L}\right) \exp\{-\lambda_n^2 D_e t/L^2\}}{(1+\delta_1+\delta_2 - \delta_1\delta_2\lambda_n^2)\cos\lambda_n - (\delta_1 + \delta_2 + 2\delta_1\delta_2)\lambda_n \sin\lambda_n}$$

where $\delta_1 = V_1/SL$, $\delta_2 = V_2/SL$, $C_{A\infty}$ is the concentration of A at equilibrium (infinite time) and the eigenvalues, λ_n, are the solutions to

$$\tan\lambda_n = -\frac{(\delta_1 + \delta_2)\lambda_n}{1 - \delta_1\delta_2\lambda_n^2} \tag{6}$$

It should be noted that this differs slightly from the solution presented by Shair and Cohen due to a typographical error in the earlier paper. The

existence of a general solution to Fick's second law for diffusion between two well-mixed volumes allows a great deal of flexibility in the design of experiments.

The apparatus employed during this study is similar to that used by Ball, et al. (1981), and for such a system, the general solution can be simplified by assuming:

(1) end bulbs of equal volume, $\delta_1 = \delta_2$

(2) the initial concentration is zero everywhere except in end bulb 1, $1_o = 0$

(3) the only concentration of interest after t = 0 is that in end bulb 2, at x = L

With these modifications, Equation (5) simplifies to

$$C_A(L,t) = C_{A\infty} + 2C_o \sum_{n=1}^{\infty} \frac{\delta \quad \exp \{-\lambda_n^2 D_e t/L^2\}}{\left((1 + 2\delta - \delta^2\lambda_n^2) \cos \lambda_n - (2\delta + 2\delta^2)\lambda_n \sin \lambda_n\right)} \tag{7}$$

The magnitude of each term in the infinite series is controlled, at large times, by the exponential factor. Since the second and subsequent eigenvalues are at least and order of magnitude larger than the first eigenvalue (see Table 1), the first term in the series dominates. Thus, at large time, it is possible to write

$$C_A(L,t) = C_{A\infty} - K' \exp \{-\lambda_1^2 D_e t/L^2\} \tag{8}$$

or

$$\ln \{1 - \frac{C_A(L,t)}{C_{A\infty}}\} = \ln K - \frac{\lambda_1^2}{L^2} D_e t \tag{9}$$

where K and K' are constants.

Table 1

Typical Values of λ_n, $\delta_1 = \delta_2$

δ	λ_1	λ_2	λ_3	λ_4	λ_5
13	0.3896	3.190	6.308	9.441	12.579
25	0.2817	3.167	6.296	9.433	12.573
49	0.2016	3.154	6.290	9.429	12.570

Equation (9) indicates that a plot of $\ln(1- \frac{C_A(L,t)}{C_{A\infty}})$ versus time should yield a curve that approaches a straight line whose slope is $\frac{\lambda_1^2}{L^2} D_e$. Since λ_1 and L are known geometric factors, the effective diffusivity through a porous medium can be estimated directly from the slope of such a plot. Evaluation of Equation (7), assuming a diffusivity of about 0.1 cm^2/sec, indicates that this linearization procedure should be valid after about 15 minutes for the smallest connecting tube employed during the experiment and about an hour for the longest. It should be noted that while the simplifications employed for our apparatus are convenient, effective diffusivities could be estimated under less restrictive assumptions by directly fitting the general solution, Equation (5), to experimental data.

Employing the assumptions outlined above, the data collected during a typical experiment was plotted as shown in Figure 2. The slope of the linear portion of the curve was accurately determined by a linear least squares fit and thus the effective diffusivity of SF_6 through the test medium estimated. By dividing the experimental diffusivity by the SF_6 diffusivity in air, the results can be compared to those of other researchers employing different gases. The SF_6 diffusivity in air was estimated using the empirical correlation of Fuller, Schettler and Giddings (see Reid, Prausnitz and Sherwood, 1977). For non-polar gas mixtures, such as SF_6 in air, this correlation can generally be expected to be accurate within about 5%. It was felt that the calculated SF_6-air diffusivity would be more accurate than the experimental determination due to the possibility of convective transport in the apparatus.

FIGURE 2 - LINEARIZED CONCENTRATIONS, TYPICAL EXPERIMENT

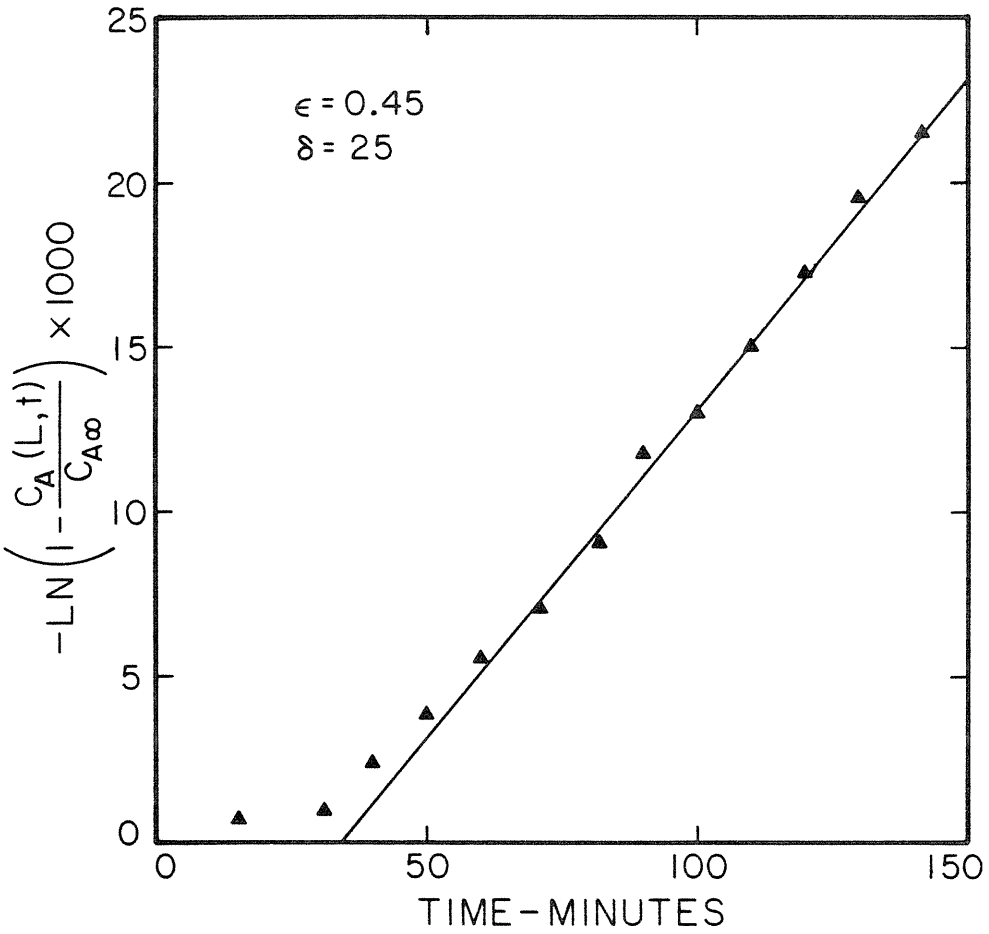

Figure 2 - Linearized analysis of a typical experiment.

RESULTS AND DISCUSSION

A summary of the experimentally determined effective diffusivities for dry test materials can be found in Table 2. The uncertainty in the measured effective diffusivities was about $\pm$ 5%. The experimentally determined diffusivity ratios (measured effective diffusivity divided by calculated air diffusivity) versus material porosity are also included in Table 2 and in Figure 3. Also included in Figure 3 are the theoretically based relationships suggested by Wakao and Smith ($D_e/D=\varepsilon^2$ in macropores), Millington ($D_e/D=\varepsilon^{4/3}$) and Marshall ($D_e/D=\varepsilon^{3/2}$). Over the range of materials studied, the experimental data agree well with the proposed relationships of both Millington and Marshall, the average deviations being 7.1% and 5.0%, respectively. Average deviation from the Wakao and Smith relationship is 41%, primarily due to large differences in the mid to lower porosity range. Also included in Figure 3 are representative data points from Penman (1940), van Bavel (1951), and Ball, et al. (1981). Except for the data of Ball and coworkers, agreement between previous investigations and the current work is good. An equation of the form $D_e/D=\varepsilon^n$ has been fitted to the experimental data by a least-mean-squares technique. The result, n=1.43, falls between the relationships proposed by Millington and Marshall. Table 2, mentioned previously, also shows the experimental deviation from this curve-fitted relationship. The average deviation is 3.5%.

It should be noted that these results are only applicable to beds of particles where the primary diffusion path is in the relatively large pore spaces between particles. Traditionally, the deviation in measured diffusion rates for different materials of similar porosities is modeled by adjusting the tortuosity factor. A different approach, however, can be useful in

Table 2

Experimental Diffusivities, Dry Materials

($22^{o}C$, atmospheric pressure)

Material	ε(%)	D_e(cm^2/sec)	D_e/D	Dev. from $\varepsilon^{1.43}$
Steel Wool	95	0.088	0.94	1.2%
compacted	88	0.098	0.81	-2.0%
Mixture of Steel Wool Glass Beads	70	0.052	0.56	-6.7%
Sieved Sand	50	0.032	0.34	-6.2%
compacted	45	0.031	0.33	4.0%
Glass Beads	26	0.014	0.15	0.9%

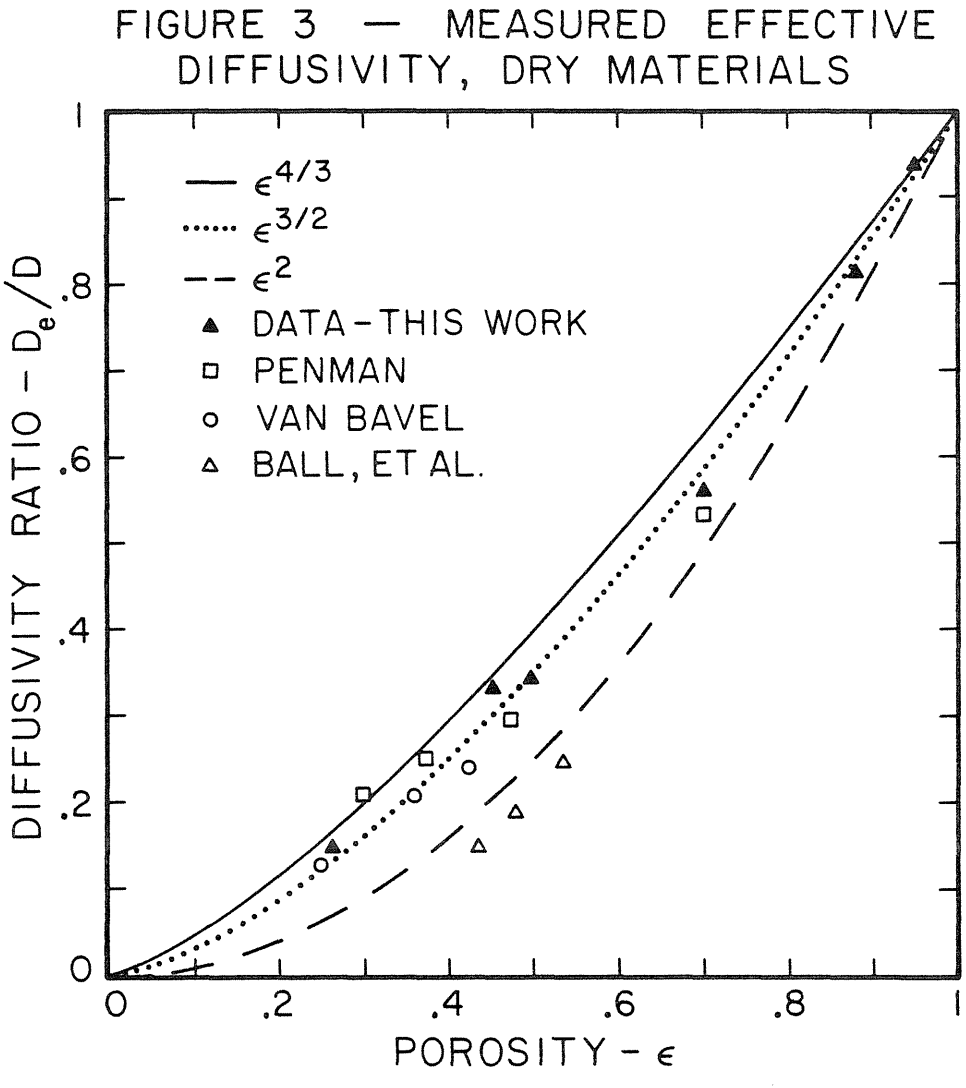

Figure 3 - Experimentally determined diffusivities as a function of bed porosity for dry materials.

understanding the effective diffusivity of gases in moist soils. Experimentally, wet material diffusivities showed large deviations from those measured in dry materials. The effect of moisture contents of 0, 10, 15 and 20% (vol. water/vol. porous bed) on the measured diffusivity ratio in sand is shown in Figure 4 and Table 3. Dry and 8.5% moisture steel wool diffusivities are also included. The reference curve in the figure is the best fit relationship found experimentally for dry materials, $D_e/D=\varepsilon^{1.43}$. The reduction of void volume due to moisture has been included as shown by the change in material porosity for each of the data points. If this reduction in void volume were the only effect of the addition of moisture, the data points would coincide with the reference curve. For small moisture contents (< = 10% in sand), this does occur. As the moisture content increases, however, dead end pores are apparently formed due to the presence of pockets of moisture and significant deviations from the reference curve result. This deviation is not the result of a change in the geometry of the individual pore spaces, i.e. tortuosity, but, instead, is the result of a reduction in the effective pore volume. The diffusive transport through the non-blocked pore space probably occurs at the same rate as in the dry material. An effective porosity, ε_e, can thus be defined as that value of the porosity that gives the experimentally determined diffusivity ratio when raised to the 1.43 power. As shown in Table 3, the decrease in effective porosity can be substantial between dry materials, where the effective porosity is assumed to equal the actual porosity, and wet materials.

FIGURE 4 — MEASURED EFFECTIVE DIFFUSIVITY, MOIST MATERIALS

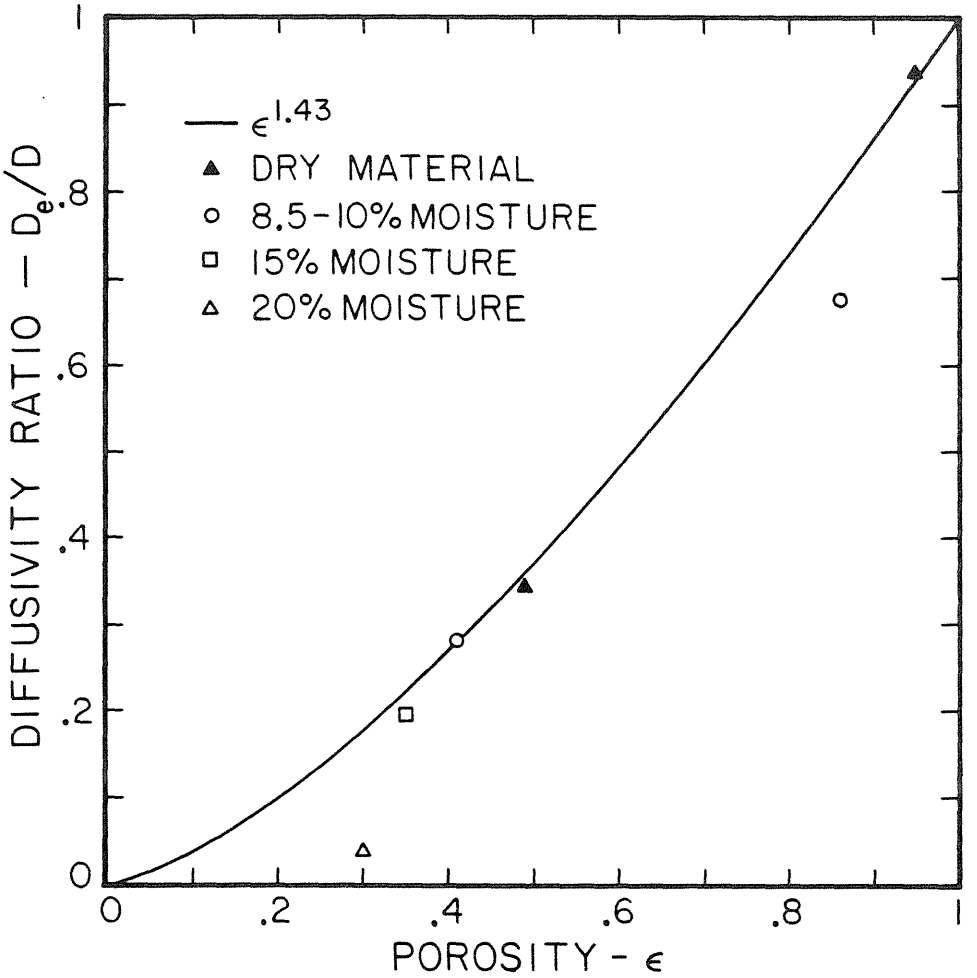

Figure 4 - Experimentally determined diffusivities as a function of bed porosity for moist materials.

Table 3

Experimental Diffusivities, Moist Materials

Material	% Water Content	ε(%)	ε_e(%)	D_e/D
Sieved Sand	0	50	48	0.34
	10	41	41	0.28
	15	35	32	0.20
	20	30	11	0.04
Steel Wool	0	95	96	0.94
	8.5	86	76	0.68

References

Ball, B. C., Harris W., and Burford, J. R., 1981. A laboratory method to measure gas diffusion and flow in soil and other porous materials. Journal of Soil Science, in press.

Barrer, M., 1953. A new approach to gas flow in capillary systems. Journal of Physical Chemistry, 57, 35-40.

van Bavel, C. H. M., 1952. Gaseous diffusion and porosity in porous media. Soil Science, 73, #2, 91-104.

Buckingham, E., 1904. Contributions to our knowledge of the aeration of soils. United States Department of Agricultural Bureau Soils Bulletin, 25.

Davis, B. R. and Scott, D. S., 1965. Measurement and effective diffusivities in porous particles. Symposium on Fundamentals of Heat and Mass Transfer, 58th annual meeting, American Institute of Chemical Engineers.

van Deemter, J. J., Zvider, F. J., and Klinkenberg, A., 1956. Longitudinal diffusion and resistance to mass transfer as causes of nonideality in chromatography. Chemical Engineering Science, 5, 271.

Johnson, M. F. L., and Stewart, W. E., 1965. Pore structure and gaseous diffusion in solid catalysts. Journal of Catalysis, 4, 248-252.

Lamb, B. K., 1978. Development and application of dual atmospheric tracer techniques for the characterization of pollutant transport and dispersion. Ph.D. Thesis, California Institute of Technology.

Marshall, T. J., 1959. The diffusion of gases through porous media. Journal of Soil Science, 10, #1, 79-82.

Millington, R. J., 1959. Gas diffusion in porous media. Science, 130, 100-102.

Pappendick, R. L. and Runkles, J. R., 1965. Transient state oxygen diffusion in soil. Soil Science, 100, #4, 251-261.

Penman, H. L., 1940. Gas and vapour movements in the soil. Journal of Agricultural Science, 30, 437-462.

Reid, R. C., Prausnitz, J. M., and Sherwood, T. K., 1977. "The Properties of Gases and Liquids". McGraw-Hill, 3rd ed.

Scheidegger A. E., 1957. "The Physics of Flow Through Porous Media". Macmillan Co.

Shair, F. H., and Cohen, D. S., 1969. Transient ordinary and forced diffusion in a tube connecting stirred-tank end bulbs of finite size. Chemical Engineering Science, 24, 39-48.

Smith, J. M., 1970. "Chemical Engineering Kinetics". McGraw-Hill.

Wakao, N. and Smith, J. M., 1962. Diffusion in catalyst pellets. Chemical Engineering Science, 17, 825-834.

Wheeler, A., 1955. "Catalysis". 2, P. H. Emmett, editor, Reinhold.

Chapter 2

The Reentrainment of Exhausted Pollutants into a Building due to Ventilation System Imbalance

by

D.D. Reible and F.H. Shair

(Submitted to Environmental Science and Technology)

Abstract

In order to illustrate the potential for significant indoor air quality problems in an imbalanced ventilation system, a sulfur hexafluoride tracer experiment was conducted in such a building. Even though the building was in overall balance, excess air exhaust capacity (over and above the air intake capacity) in a single room led to reentrainment of some of the exhausted tracer resulting in a steady-state indoor concentration of about 235 PPB/gr-mole SF_6 exhausted/hr. Overall, about 10-11% of the exhausted tracer was detected within the building at steady-state. Three stirred-tank models were developed to describe the dynamics of the air infiltration into the most heavily impacted rooms. A simple one compartment model provided a reasonable fit to the experimental data while a three compartment model based upon the design of the ventilation system was least satisfactory. The experiment indicated that a ventialtion system imbalance can lead to significant indoor impacts of exhausted pollutants and that some type of tracer experiment is necessary to determine the transport mechanism and magnitude of the impact.

Introduction

In recent years, the relationship between the air quality indoors to that outside has become increasingly important. Initially, this problem was investigated with respect to the stack height necessary to avoid reentrainment of exhaust gases from factories and laboratories back into the source facility. As the ventilation rate of homes and small buildings has decreased in order to conserve energy, however, the air quality in these structures has become increasingly suspect. Due to the difficulty in investigating these problems in full-scale systems, most researchers have resorted to small-scale wind tunnel studies that evaluate the building surface impacts of the pollutant source (e.g. Halitsky, (1), Vincent, (2). While such small-scale studies undoubtedly have some application to real systems, they suffer from a number of serious drawbacks. First and foremost is that it is generally impossible to determine the accuracy with which the full-scale flow is being modeled due to the inability to exactly reproduce atmospheric conditions in a wind tunnel. In addition, wind tunnel models are generally used to estimate the concentration profile exterior to the building due to a specific pollutant source. Such studies cannot hope to directly address the often more important question of the <u>indoor</u> pollutant impact. Thus, for example, the relationship between the ventilation rate of the building and the indoor air quality cannot generally be evaluated. Wind tunnel studies can be used to investigate the qualitative behavior of pollutants near buildings and to provide estimates of the surface impact from particular sources, but

studies on the full-scale system are generally necessary to evaluate and model the indoor impact of the pollutant source.

Drivas and Shair (3) probed the wake downwind of a building as well as as concentrations within the building with an atmospheric tracer. The studies of Drivas and Shair indicated that the building's near-wake tends to be relatively well-mixed, causing the indoor impact of the pollutant to also be relatively uniform. Their studies indicated that lumped parameter, stirred-tank models could be used to quantify the interraction of the outdoor air with that inside. Sabersky, et al. (4) and Shair and Heitner (5), showed that a stirred-tank model that included reaction terms could accurately describe indoor ozone concentrations resulting from high exterior concentrations. An review of the applications of well-mixed stirred tank models to indoor air quality was reported by the Committee on Indoor Pollutants (6). Generally such models assume that the section of a building served by a single ventilation system make up the well-mixed compartment.

As mentioned previously, the importance of assessing indoor air quality has increased recently as ventilation rates of buildings have decreased in an effort to conserve energy. In the case of laboratory buildings, which generally contain auxiliary ventilation systems such as fumehoods, the reduction of the overall ventilation rate can result in the development of a negative pressure in the building when compared to that outside. An imbalanced ventilation system can greatly increase the infiltration of exterior pollutants into parts of a building.

While the concentration uniformity noted in balanced ventilation systems suggests that relatively simple stirred-tank models are applicable, a ventilation imbalance can lead to significant concentration variations within a building. The purpose of the current work is to illustrate the significance of a ventilation system imbalance upon indoor air quality. In addition, various stirred-tank models were analyzed to test their validity to the dynamic behavior of the indoor concentrations in an imbalanced ventilation system. A number of studies conducted by the authors in previous years, primarily on laboratory buildings on college campuses, have indicated that an imbalanced ventilation system is quite common and thus a potentially significant problem.

Experimental Procedure

The building chosen for study was located on the campus of the Jet Propulsion Laboratory, Pasadena, California (Building #158). The building was approximately 49 m long, 24 m wide and 10 m high (2 stories). The building had intake and exhaust vents on the roof and on the exterior walls. Based upon the design air rates, the building was at a slight positive pressure, i.e.,the design intake rates exceeded the design forced exhaust rates. As shown in Figure 1, however, Room 115 in the southeast corner of the building was strongly imbalanced by a design exhaust rate of 1605 l/s more than the design intake rate. The fumehood in this room was exhausted to the outside via a flush vent on the east wall of the building. This fumehood was used to release an atmospheric tracer, sulfur hexafluoride, into the building environment.

Sulfur hexafluoride has proven useful in full scale atmospheric tracer studies (e.g. Drivas and Shair (3). It can be detected at concentrations as low as 1-10 parts-per-trillion (PPT) by electron capture gas chromatography. SF_6 concentrations between 10 and 10,000 PPT can generally be measured with an accuracy of better than +/- 20%. Higher concentrations can be measured by sample dilution. During the current study, the tracer was released from a small lecture bottle containment cylinder at a rate of 0.026 l SF_6/min, as measured via a calibrated rotameter. SF_6 was released between 1230 PDT and 1315 PDT, 7/11/80 under unstable atmospheric conditions and 2-3 mps southerly winds.

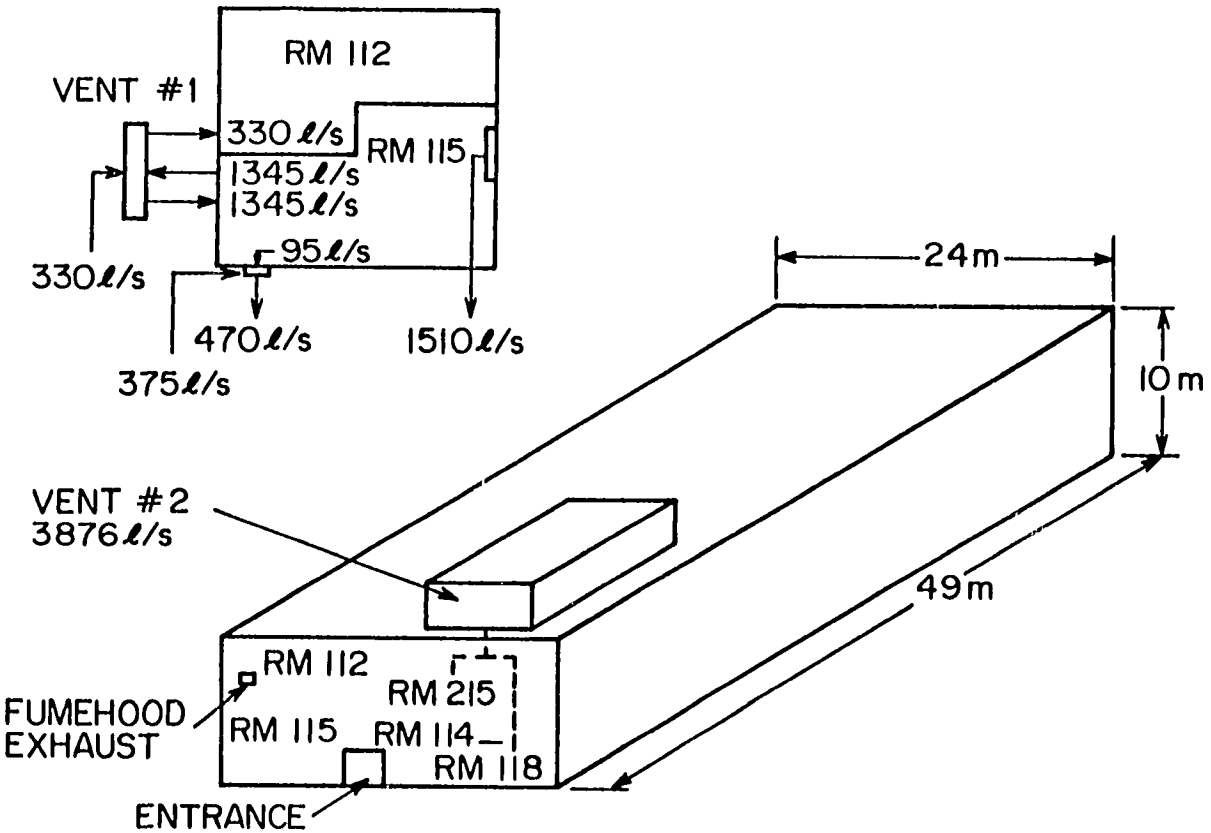

Figure 1 - General plan of test building indicating ventilation rates in rooms of interest.

Essentially instantaneous air samples (i.e. grab samples) were collected at one or two minute intervals at locations within and outside of the building. All air samples were collected in 30 cm^3 disposable plastic syringes. A more detailed description of the analytical and experimental procedure can be found in Drivas (7) or Lamb (8).

Presentation and Discussion of Results

As indicated in Figure 2, essentially none of the released tracer was observed at locations other than ventilation system #2 (Vent #2, Rm 215, Rm 114 and Rm 118), and in Rooms 115 and 112, which are on their own separate (and imbalanced) ventilation system. Rooms 115 and 112 were heavily impacted even though their normal air intake was through Vent #1, where very little SF_6 was observed. As indicated in the figure, the tracer was not spread uniformly throughout the inside of the test building. Instead, only those locations which had an air inlet located close to the exterior flush vent (i.e. the source) were affected significantly by the tracer. The inlet to ventilation system #2 was located on the roof on the easterly side of the building, the same side as the fumehood exhaust. The average ventilation inlet flowrate of 3880 l/s and concentration of 5530 PPT corresponded to about 5% of the SF_6 released. While SF_6 was introduced to ventilation system #2 via the normal air inlet, the ventilation system imbalance in Rooms 115 and 112 apparently led to the infiltration of the SF_6 contaminated air through an entrance on the east side of the building. This conclusion was verified by several samples collected outside of the building entrance that showed that the exterior tracer concentration at that location was virtually indistinguishable from the steady-state room concentration (about 15 PPB or 235 PPB/gr-mole released/hr). The 15 PPB concentrations and the 1605 l/s of required makeup air account for about 6% of the released tracer. It should be made clear that the contamination of Rooms 115 and 112 was not due to the

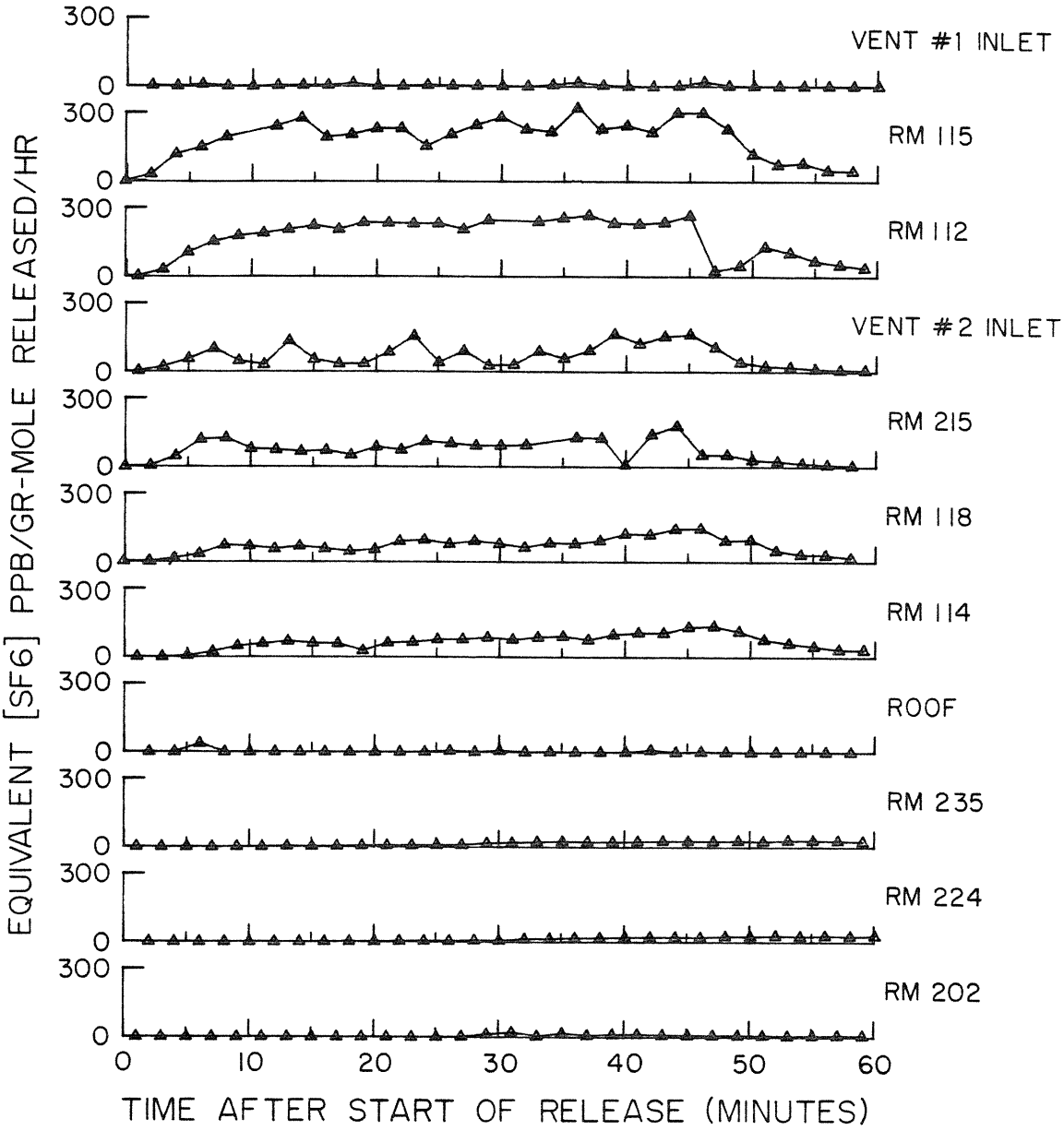

Figure 2 - Tracer concentrations observed at each sampling location during the test.

ineffectiveness of the fumehood, but instead due to the ineffectiveness of the exterior wind field in transporting the tracer away from the building. Unfortunately, fumehood design procedures and installation codes are generally based upon only the interior flow characteristics of the fumehood (e.g. face velocity). In more than one hundred fumehood experiments conducted by the authors, however, the local contamination problem at the fumehood was always insignificant compared to the return of contaminated air via reentrainment of the exhausted air. While this problem is aggravated by a ventilation imbalance, as in this test, it occurs even in more balanced ventilation systems. As mentioned previously, however, a balanced ventilation system results in a more uniform indoor impact (e.g. Drivas and Shair, 3). During this study, the concentration gradient with distance from the source was quite pronounced. As shown in Figure 3, the steady-state concentration observed in all rooms was well correlated with the time lag between the start of the release and the observation of tracer in that room, a result that is clearly at odds with the existence of a single well-mixed zone. The time lag was calculated from the release time and the time when concentrations exceeding 10% of the steady-state were observed in the room. The shaded characters in the figure, which show a somwhat larger lag time for the same concentrations than is indicated by the rest of the data, represent interior rooms, i.e. rooms which were contaminated by air drawn from other rooms and not the outside. The solid line represents a best-fit to all of the data (including interior rooms), for which the correlation

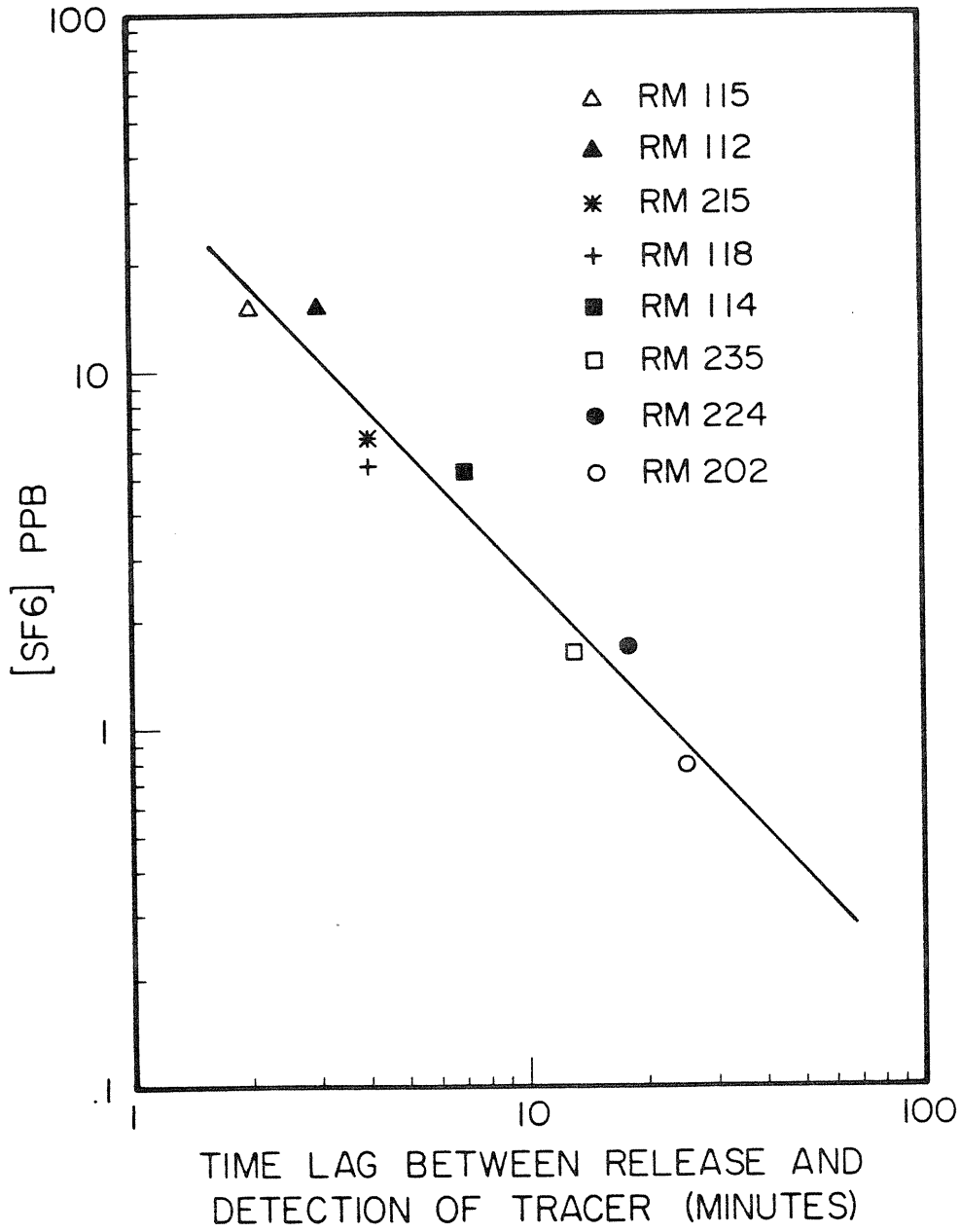

Figure 3 - Steady state concentrations in each room versus time lag between beginning of release and detection of 10% of the steady state concentration in that room.

coefficient was 0.929. Further tests are required before the significance, if any, of the good correlation between time lag and steady-state concentration is understood.

While neither the interior or exterior of the building was entirely well-mixed, this approximation was applicable to small zones within the building. A steady-state average of 89+/-11 PPB/gr-mole released/hr was observed in those rooms that received air through ventilation inlet #2 (Rooms 215, 118 and 114). A steady-state average of 235+/-1 PPB/gr-mole released/hr was observed in Rooms 115 and 112. Because of the existence of these well-mixed zones, stirred tank models were developed in an attempt to describe the dynamics of the concentration levels within the building. Because the highest concentration levels were observed in Rooms 115 and 112, the emphasis was to describe the dynamics of those rooms. Three models were considered: 1) a simple single compartment stirred-tank model that combined Rooms 115 and 112, 2) a two compartment model which assumed that Rooms 115 and 112 were interacting with a wake-like structure of unknown volume and adjustable ventilation rate, and 3) a three compartment model based upon the ventilation system design from building blueprints. The model equations are presented in Table 1 and schematics of the three models are shown in Figure's 4, 5 and 6, respectively. Below each schematic is the predicted concentration profiles as a function of time after the start of the release using the parameters included in each figure. Although an analytical solution to the model equations can be easily developed, the predicted concentration profiles were calculated using a

Table 1

Model Equations

(1) Single Compartment Model

$$V_1 \frac{dC_1}{dt} = q_{w1}C_w + q_{01}C_0 - q_{10}C_1 - q_{10}C_1$$

(2) Two Compartment Model

$$V_1 \frac{dC_1}{dt} = q_{w1}C_w + q_{01}C_0 - q_fC_f - q_{10}C_1$$

$$V_w \frac{dC_w}{dt} = q_{0w}C_0 + fq_fC_f - q_{w1}C_w - q_{w0}C_w$$

(3) Three Compartment Model

$$V_1 \frac{dC_1}{dt} = q_{01}C_0 + q_{31}C_3 - q_{10}C_1 - q_{13}C_1$$

$$V_2 \frac{dC_2}{dt} = q_{32}C_3 - q_{20}C_2$$

$$V_3 \frac{dC_3}{dt} = q_{03}C_0 + q_{13}C_1 - q_{31}C_3 - q_{32}C_3$$

where

V_i - volume of compartment i

t - time

q_{ij} - volumetric flowrate between zone i and zone j

C_i - concentration in zone or component i

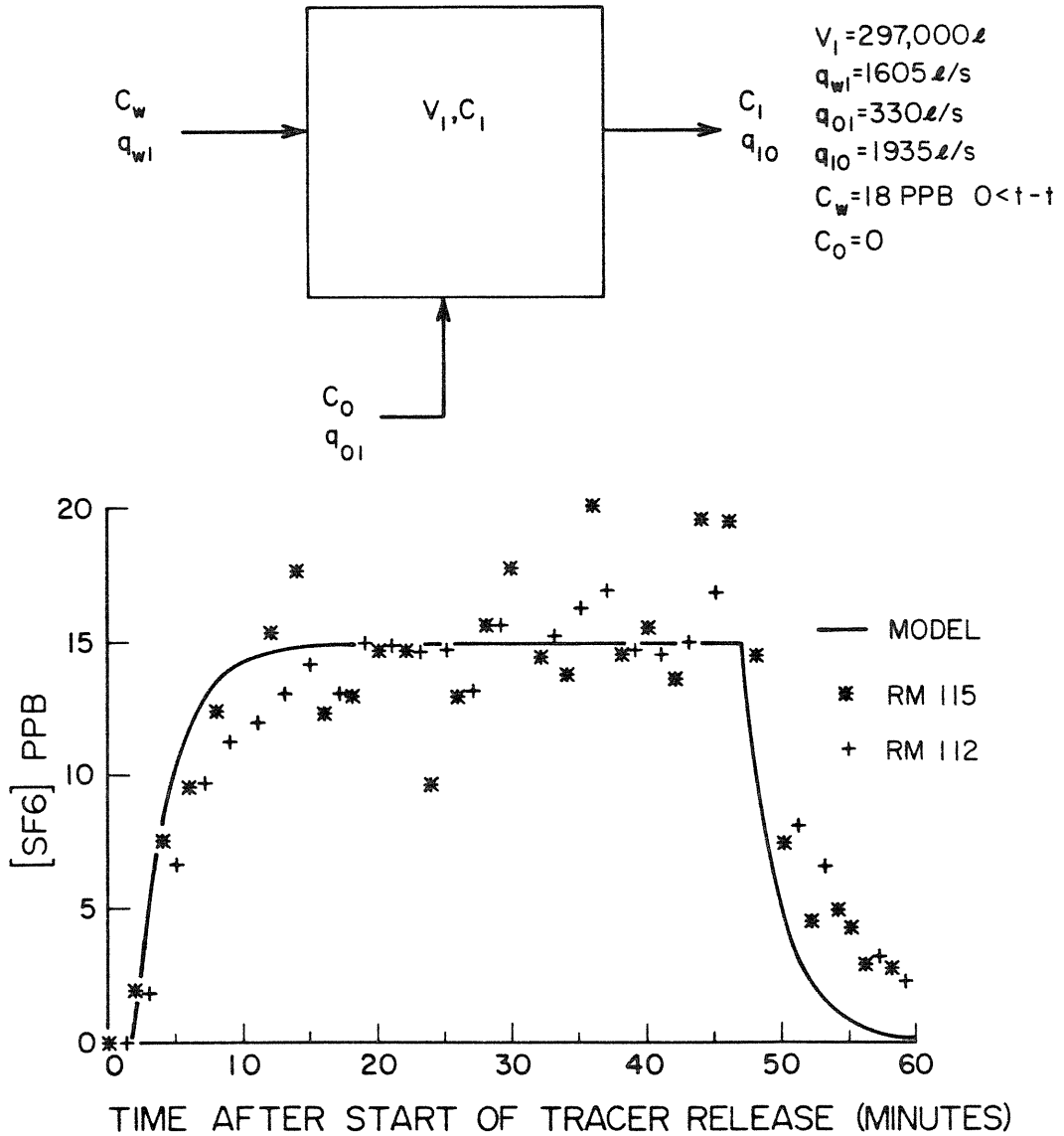

Figure 4 - Single compartment model and predicted concentration profiles. Compartment composed of Rooms 115 and 112.

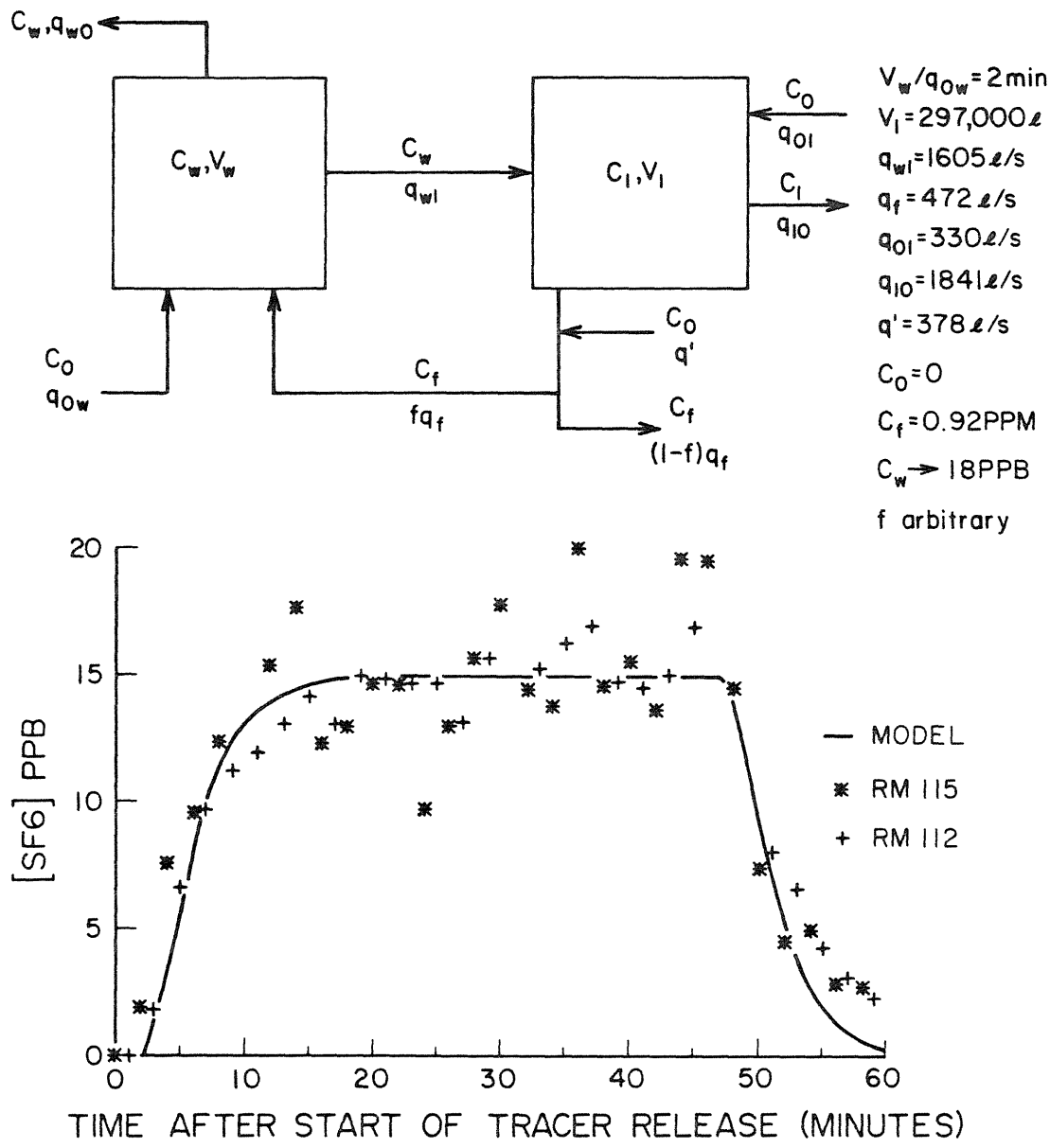

Figure 5 - Two compartment model and predicted concentration profiles. Rooms 115 and 112 form a compartment while the second compartment represents a wake-like zone exterior to the building.

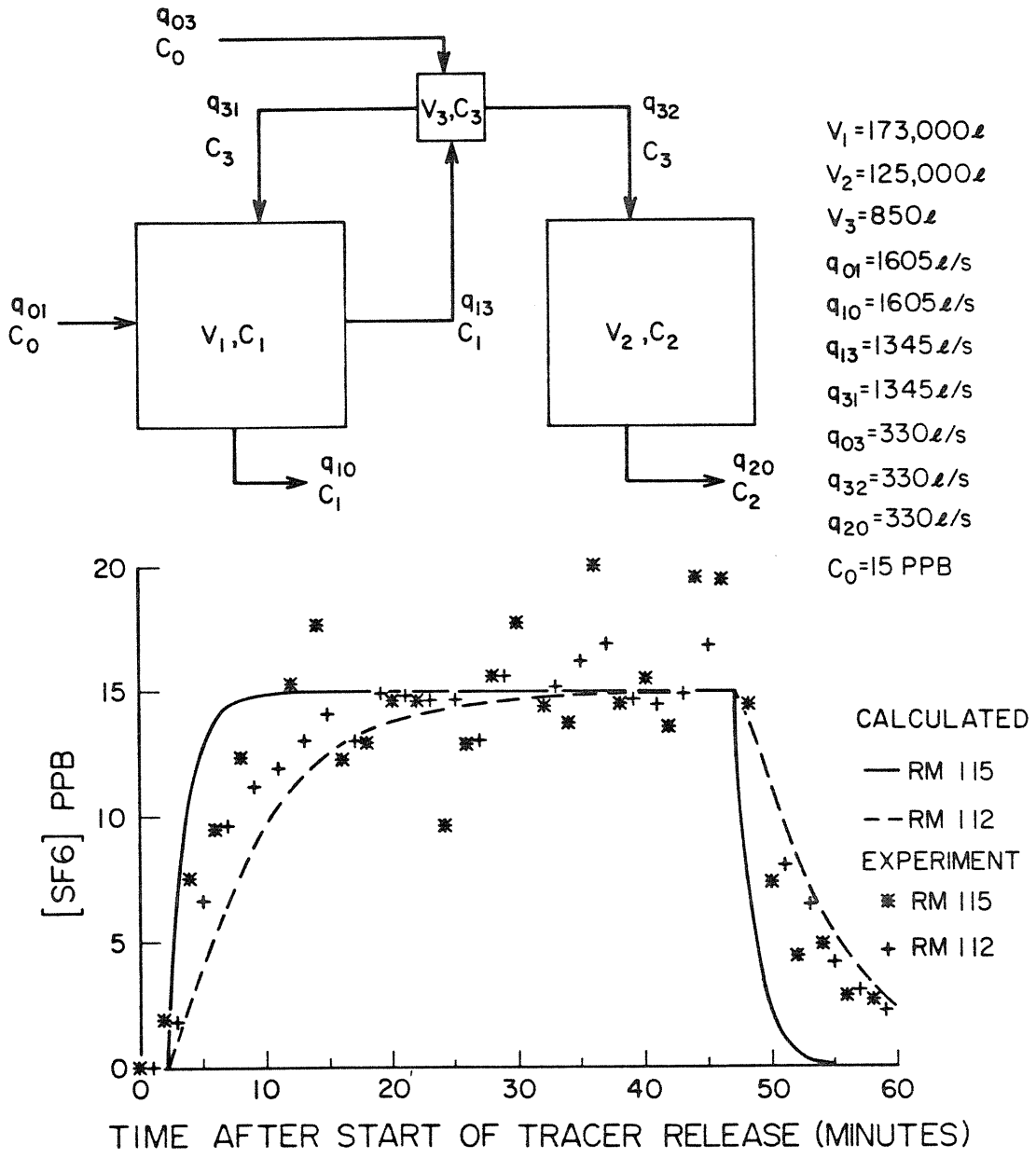

Figure 6 - Three compartment model and predicted concentration profiles. Three compartment model based upon ventilation system design.

Runge-Kutta numerical scheme. In each case, the steady-state concentration was chosen to fit the experimental data. In additon, since the models could not account for the observed time-lag between release start and detection, the time axis in each model was shifted accordingly. The room volumes and ventilation rates required for the models, however, were actual values. The figures indicate that the worst fit to the experimentally observed tracer concentrations among the three models was that model based upon the design of the ventilation system (Figure 6). The system design indicates that the only possible interaction between Rooms 115 and 112 occurs through the small air handler indicated as volume 3 in the figure. The predicted difference in unsteady-state concentration between the two rooms far exceeds the observed difference, although both curves lie within the scatter of the data at steady-state. This again indicates that the transport between Rooms 115 and 112 and between the rooms and the exterior was by infiltration and not through the ventilation system. This suggests that it is generally not possible to predict the machanism whereby pollutants are transported into an imbalanced ventilation system without some type of tracer experiment. Not surprisingly, the two compartment model (Figure 5) provides the best fit to the dynamics of the experimental data through the addition of an unconstrained adjustable parameter, the "wake" exchange rate (V/Q - wake volume/wake ventialtion rate). As shown in Figure 7, however, the predicted room concentrations are not a strong function of this parameter as long as the steady-state concentration is forced to

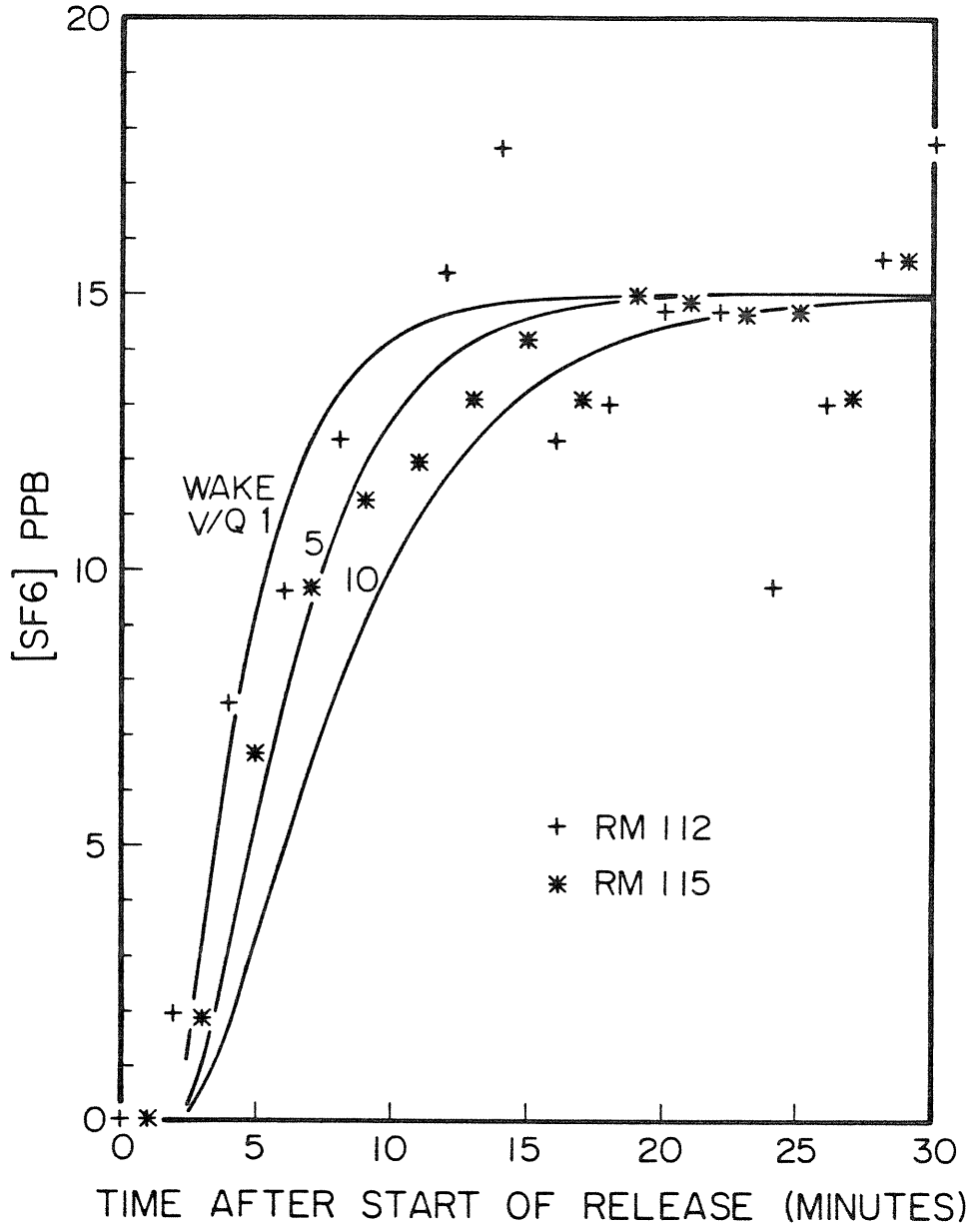

Figure 7 - Comparison of predicted and observed room concentrations using the two compartment model and different wake exchange rates.

remain constant. Note that the wake included in this model, is not the lee wake behind the building, but instead represents a small wake-like structure on the side of the building near the entrance through which SF_6 infiltrated to Rooms 115 and 112. The single compartment model does not incorporate any unconstrained adjustable parameters and while the two compartment model provided a better fit, it is difficult to justify the additional complexity of that model in view of the scatter of the data. In addition, the two compartment model postulates the existence of a wake-like structure that may have no physical basis. Due to these factors, the most satisfactory model of the dynamic impact in Rooms 115 and 112 was also the simplest.

Summary and Conclusions

In order to illustrate the potential for significant indoor air quality problems in an imbalanced ventilation system, a sulfur hexafluoride tracer study was conducted on such a building. Even though the building was in overall balance, excess exhaust capacity (over and above the intake capacity) in a single room led to a reentrained steady-state concentration of about 235 PPB/gr-mole released/hr due to a release in that room's fumehood. The problem was accentuated in this case by a flush side vent for the fumehood exhaust rather than a generally more effective vertical stack. Based upon sampling in the heavily impacted rooms and elsewhere in the building, about 10-11% of the released tracer was reentrained into the building. These data indicate that the ventilation system imbalance can lead to significant "short-circuiting" of a building's intake and exhaust systems.

Although the interior concentrations were clearly not uniform, small well-mixed zones composed of one or more rooms were observed. In an attempt to describe the dynamics of the air infiltration into the heavily impacted rooms, three stirred-tank models were developed. A three compartment model based upon the building ventilation system design provided the poorest fit to the data. While a two compartment model, with a single unconstrained adjustable parameter, provided the best fit to the data, a simple single compartment model, with no unconstrained adjustable parameters, also provided a reasonable fit within the scatter of the data. Due to the complexity of the reentrainment of the

exhausted tracer, realistic dynamic models of the indoor impact could only be developed after conducting a tracer experiment.

Acknowledgements

The authors appreciate the efforts of Paul Nielson, Anita Jakub and Henry Smith in assisting with the experiment and its analysis. Particularly appreciated was the encouragement and interest of Al Klascius, Glen Berry and Gary Weber of the Jet Propulsion Laboratory.

References

(1) Halitskey, J. Meteorology and Atomic Energy,1968, 221.

(2) Vincent , J.H. Atmospheric Environment, 1977,11, 765.

(3) Drivas, P.J., and Shair, F.H. Atmospheric Environment, 1974, 8, 1165.

(4) Sabersky, R.H.; Sinema, D.A.; Shair, F.H. Environmental Science and Technology, 1973, 7, 347.

(5) Shair, F.H.; Heitner, K.L. Environmental Science and Technology, 1974, 8, 5.

(6) Committee on Indoor Pollutants (1981). Indoor Pollutants, National Academy Press, Washington, DC.

(7) Drivas, P.J. Ph.D Thesis, California Institute of Technology, Pasadena, Ca., 1974.

(8) Lamb, B.K. Ph.D. Thesis, California Institute of Technology, Pasadena, Ca., 1978.

Chapter 3

The Transport and Dispersion of Airborne Contaminants in Boundary Layers over the Ocean and an Isolated Island Cape

by

D.D. Reible, F.H. Shair, R.J. Cayer, and D.W. Nelson

(Submitted to Boundary Layer Meteorology)

Abstract

A series of eighteen atmospheric tracer experiments using sulfur hexaflouride (SF_6) and chemical smoke were conducted to explore the transport of airborne contaminants in the boundary layer over the ocean surface and in the separating boundary layer over an isolated island cape. The immediate objective of the tests was to determine the impact of local pollutant sources on a background air quality sampling program conducted from elevated towers on the cape. In addition to satisfying this objective, the tests are of interest in that they illustrate the local behavior of pollutants in a complex natural atmospheric flow.

The tests indicated that the crosswind dispersion of pollutants over the ocean surface can be approximately modeled using the simple Gaussian plume model. The observed crosswind dispersion of the tracer corresponded to that expected under neutrally stable atmospheric conditions, consistent with the near equilibration of the ocean surface and air temperature. Tracer released into the wake downwind of the leading edge of the cape was found to mix relatively rapidly to a height of about 10 m above the surface (i.e. 35-40% of the cape height). Due to decoupling between the recirculating wake flow, and the freestream flow, however, very little of the tracer was observed above this height. This suggests that the impact of local pollutant sources (i.e. on the cape) would be minimized if the proposed sampling towers were elevated above a 10 m altitude.

INTRODUCTION

Much of what has been learned about the dispersion of airborne contaminants around surface mounted objects in a turbulent flow field has resulted from highly idealized wind and water tunnel studies. While these experiments have proved useful in exploring the basic structure of such flows, it is never quite clear how applicable such studies are to "real" systems. In order to quantitatively determine how pollutants are transported in a specific full-scale system, it is generally necessary to conduct atmospheric tracer experiments. In this work, a study of the local dispersion of pollutants around a cape at one end of an isolated island was conducted. This report serves to document the procedures used to solve a specific atmospheric transport problem in a real system as well as indicate the behavior of airborne contaminants in such a system.

The objective of this study was to determine the impact of local pollutant sources upon a sampling program conducted by SEAREX (Sea-Air Exchange Program) on American Samoa in the South Pacific. SEAREX is a marine air sampling program conducted by a consortium of universities and laboratories coordinated by the Graduate School of Oceanography of the University of Rhode Island. In American Samoa, SEAREX personel were attempting to measure the pollutant burden of the relatively pristine air at a remote site on Cape Matatula, Tutuila Island (see Figure 1). In order to limit the impact of local contaminants on the sampling program, it was proposed that all air sampling would be conducted from towers and in winds that were free from the contamination of upwind islands. Due to the sensitivity of the sampling apparatus employed, local crustal and organic contaminants from the land surface and vegetation could imperil the quality of the attempted measurements. The objectives of the current

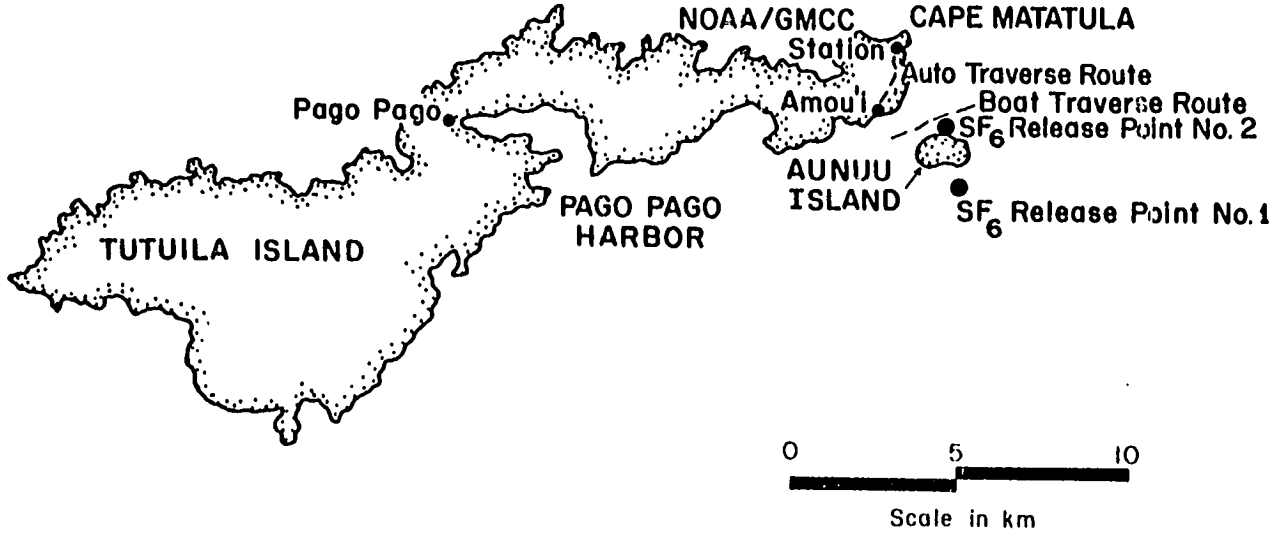

Figure 1 - Map of Tutuilla Island, American Samoa, showing Cape Matatula. Also shown are release and sampling locations for far-field experiments.

study was to determine the wind directions which would not be contaminated by upwind sources (specifically, Aunuu Island, approximately 5 km offshore) and the tower height necessary to negate the effect of crustal and organic sources below the sampling towers. Resolution of the former problem requires evaluation of the horizontal dispersion of pollutants over the ocean surface while the latter problem requires evaluation of the vertical dispersion of pollutants in the complex flow around Cape Matatula. The cape has a bluff southerly and northerly face indicating the importance of flow separation upon local vertical transport of pollutants in winds from those directions. Both problems were resolved in this study through atmospheric tracer experiments using chemical smoke and sulfur hexaflouride (SF_6). SF_6 is an inert, non-toxic gas that can be detected at concentrations as low as 1-10 parts SF_6 per trillion parts air. In addition to meeting the specific objectives of this work, the experiments provide some insight into the dispersion of pollutants over a smooth water surface and also the dispersion of pollutants in a separating boundary layer. Neither subject has been adequately investigated in the atmosphere.

EXPERIMENTAL PROCEDURE

A total of 18 atmospheric tracer experiments were conducted using smoke and sulfur hexafluoride (SF_6) to assess the possible contamination problems associated with sampling of the marine air on Cape Matatula, Tutuilla Island, American Samoa. Tests using chemical smoke involved releasing the smoke from a cannister or candle at a location of interest and visually monitoring the dispersion of the smoke plume. The experiments employing SF_6 as a tracer were very similar except that a quantitative observation of the tracer dispersion could be made. SF_6 can be detected at concentrations as low as 1-10 parts SF_6 per trillion parts air by electron capture gas chromatography. During each test, SF_6 was released continuously from a containment cylinder. The release rate was monitored with a calibrated rotameter. The release locations included various points on the cape (see Figure 2) and onboard a boat located close to Aunuu Island (see Figure 1).

All air samples were taken with 30 cm^3 plastic syringes. During near-field studies on Cape Matatula, grab samples were taken at various locations on the cape during walking traverses that were generally aligned perpendicular to the estimated path of the tracer plume. Additional samples were taken on the cape during these tests by remote sampling through long small diameter tubes. These sampling tubes were used to investigate the vertical distribution of tracer on masts raised to simulate the proposed sampling towers. They were also used to monitor concentrations at various heights on the upwind bluff face of the cape. During far-field experiments, in which the SF_6 was released from the vicinity of Aunuu Island, additional grab samples were taken onboard a boat traversing the channel between Aunuu and Cape Matatula and by automobile traverses along the coastline (see

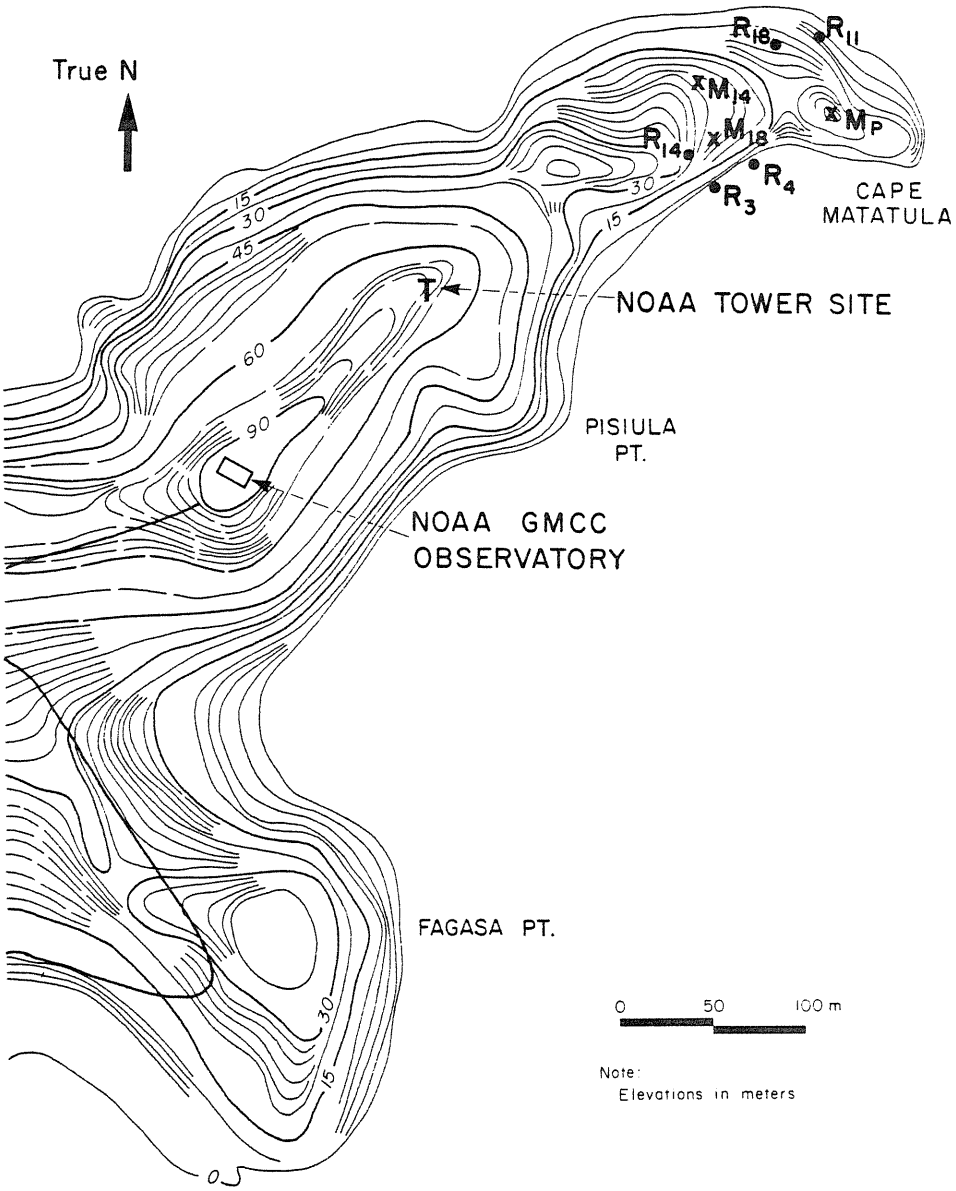

Figure 2 - Map of Cape Matatula showing temporary sampling masts (M_{14} and M_{18}) and release locations for each test (R_i = release for Test i).

Figure 1). During each tracer experiment, a portable gas chromatograph was used to provide real time feedback into the test plan by spot checking of samples. The balance of the collected samples were analyzed upon return to the laboratory at the California Institute of Technology. Prior tests had indicated that the time interval between collection and analysis of samples would not significantly alter the observed concentrations. A description of electron capture gas chromatography and the instrument calibration procedures can be found in Lamb (1978).

During all tests, wind speeds and directions were monitored by equipment located atop the plateau above the cape (see Figure 2). This monitoring station is part of the Global Monitoring for Climatic Change program of the National Oceanic and Atmospheric Administration. Additional wind speed and direction measurements were made on the cape in order to map the local flow field.

PRESENTATION AND DISCUSSION OF RESULTS

Far-field experiments

As mentioned previously, two SF_6 releases were made from a boat close to Aunuu Island (Figure 1). One release was conducted from a location upwind of Aunuu, approximately 4 km from the Tutuilla shoreline and about 6 km from Cape Matatula. The winds were southeasterly at 6-7 mps, as measured at Cape Matatula. A sharply peaked, essentially Gaussian, SF_6 concentration profile was detected downwind of the release during automobile and boat traverses. The automobile traverse data collected along the road indicated in Figure 1 is shown in Figure 3a. The transport and dispersion of atmospheric contaminants in a strong, uniform flow field is commonly modeled with the Gaussian plume model (Turner, 1970). Key parameters in this model are the width and depth of the plume as measured by the standard deviations in concentration in each direction. Turner has reported the value of these parameters as a function of downwind distance and atmospheric stability over flat terrain. Relatively few investigations of dispersion over bodies of water have been conducted, however, and it is interesting to compare the dispersion observed during the present study with that reported over land. For the traverse data presented in Figure 3a, the crosswind standard deviation in concentration was about 270 m, corrected for the 50-70^{o} angle between the road and the plume trajectory. Since the route traversed was approximately 4 km downwind of the source, this horizontal dispersion corresponds to that predicted by Turner (1970) for neutrally stable atmospheric conditions. Automobile traverses following the same route are shown in Figure 3b for the tracer release from downwind of Aunuu Island. The crosswind standard deviation in concentration during these traverses was about 90 m, again corrected for the 50-70^{o} angle

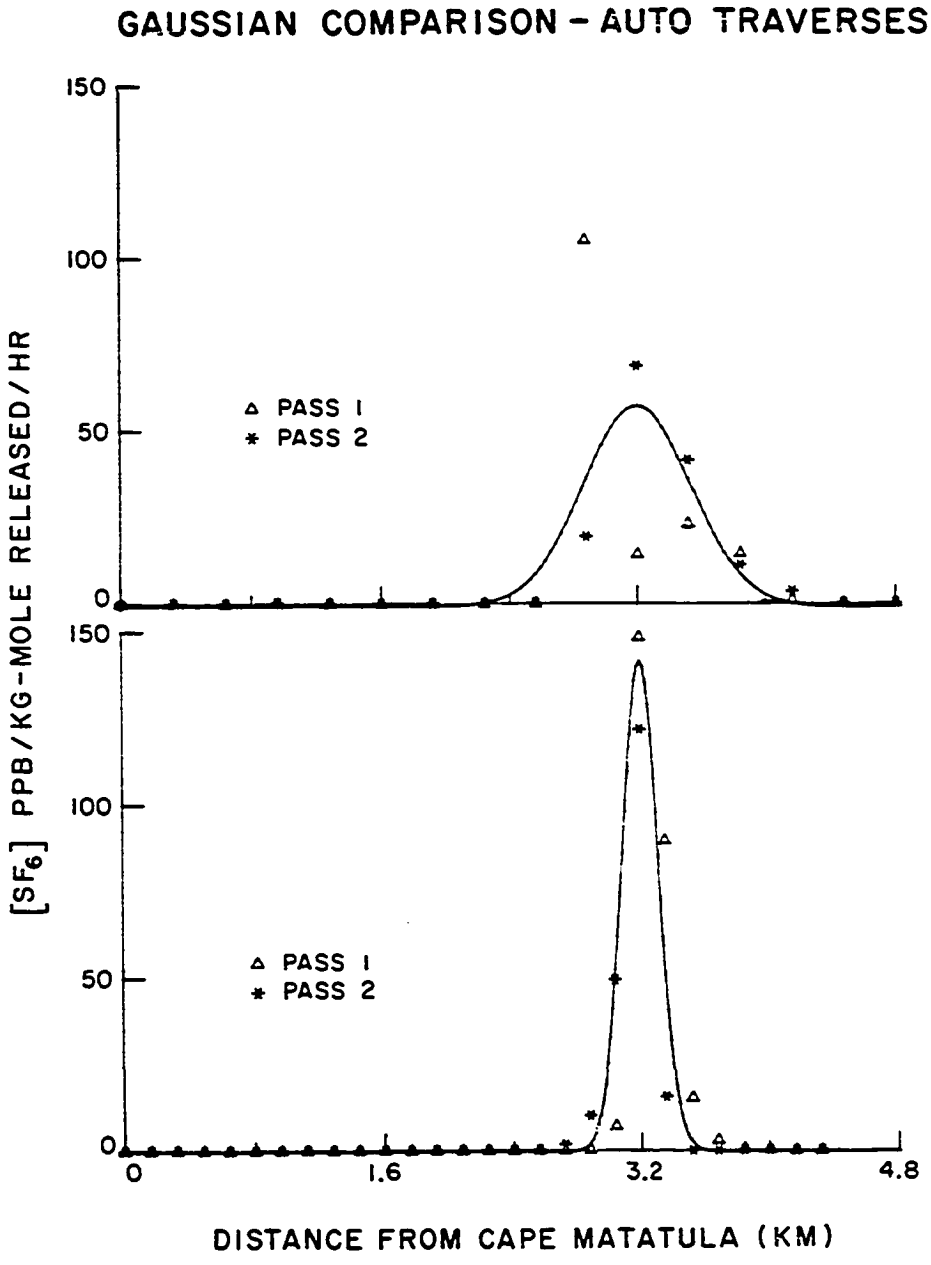

Figure 3 - (top) Automobile traverse data taken during SF_6 release from upwind of Aunuu Island. The Gaussian curve is a best-fit representation of the data.

(bottom) Automobile traverse data taken during SF_6 release from downwind of Aunuu Island. The Gaussian curve is a best-fit representation of the data.

between the plume trajectory and the traversed road. Since the tracer plume was detected about 1.5 km downwind of the release site during this test, the observed horizontal dispersion also corresponded to that expected during neutrally stable atmospheric conditions. The vertical temperature structure of the atmosphere was not measured during either test, making it impossible to correlate the observed tracer dispersion with the actual stability of the atmosphere. Neutral or slightly stable atmospheric conditions would be expected, however, due to the high wind speeds observed and the approximate equilibration between surface air and water temperatures. While two relatively simple experiments cannot hope to fully describe the horizontal dispersion of contaminants over the sea surface, these tests indicate that such dispersion can be predicted in much the same way that dispersion over flat terrain is predicted. Additional information on dispersion of pollutants over water surfaces (in this case a more stably stratified environment, the Santa Barbara Channel off southern California) can be found in Reible and Shair (1981).

Near-field experiments

As indicated previously, the primary objective of these studies was the evaluation of local pollutant sources on a proposed SEAREX sampling program at Cape Matatula. While the offshore releases described above allow evaluation of the impact of sources located some distance from the cape, a potentially more serious problem was contamination from sources on the cape. Due to the "bluffness" of the cape, the boundary layer flow observed over the ocean surface separated over the cape. Just as in turbulent flow over a surface mounted cube, a small upwind separated zone was observed as well as a larger, more encompassing downwind wake. Further complicating the flow was local surface roughness on the cape.

A complete description of the dispersion of pollutants in such a flow field was not possible. As shown in Figure 4, however, very little of the tracer released from locations on the cape was transported higher than about 10 m above the surface. The data included in Figure 4 were collected during 5 tests, each with a different release location (see Figure 2) and wind directions from 30^{o} to 140^{o}. The solid line connects the maximum concentrations detected at each height. The concentration data collected during each sampling period of each test is normalized with respect to the maximum concentration detected during that period (C_{*}). Based upon this data, a SEAREX sampling tower located at least 10 m above the surface would be relatively free from the influence of surface sources, at least during winds with an easterly component.

The sharp division in tracer concentration between the surface and the air aloft was apparently due to the structure of the lee wake of the cape. The rate of mixing between the wake and the freestream flow is generally about the same or less than the rate of mixing within the separated zone (Vincent, 1977 or Drivas and Shair, 1974), clearly suggesting that a sharp concentration gradient can exist between the separated zone and the free-stream. This phenomenon has been observed previously, but usually in the reverse context, during the determination of a stack height necessary to carry pollutants away from the influence of the wake of an object. Smith (1978) found that a stack height 30% higher than a building model was sufficient to reduce the downwind wake concentrations by an order of magnitude below that observed with a flush vent (i.e. pollutant source at building height). By comparison, the 10 m layer of the highest tracer concentrations, as indicated in Figure 4, was about 35-40% of the cape height at the sampling locations. Thus the vertical extent of the lee

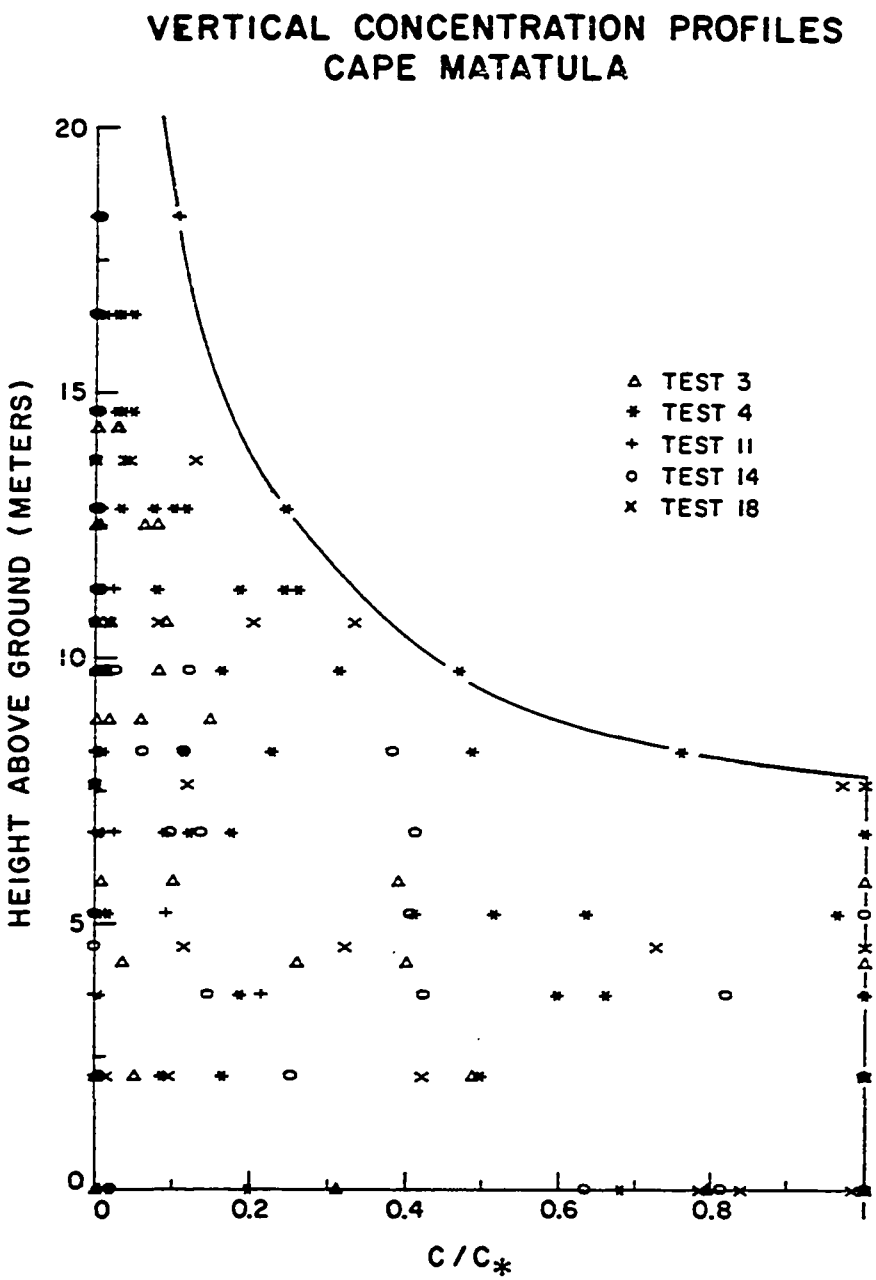

Figure 4 - Summary of vertical concentration profiles taken at temporary sampling masts during all 5 near-field SF_6 releases. Concentrations are shown as a fraction of the maximum concentration detected during each set of samples collected during each test.

wake above a surface mounted object was essentially the same whether the estimate was made by, (1) determining the release height necessary to eliminate significant transport into the wake, or by (2), determining the vertical influence of a pollutant source within the wake. The current study is one of the few that has explored such concepts in relation to natural geographical features. In addition to resolving the immediate problem of quantifying the impact of local pollutant sources upon the SEAREX sampling program, the results of this study provide some qualitative insights into the nature of a complex natural flow field and the resulting pollutant dispersion.

References

Drivas, P. J. and Shair, F. H. (1974). Probing the air flow within the wake downwind of a building by means of a tracer technique. Atmospheric Environment, 8 1165-1175.

Lamb, B. K. (1978). Development and application of dual atmospheric tracer techniques for the characterization of pollutant transport and dispersion. Ph.D. Thesis, California Institute of Technology, Pasadena, California 91125.

Reible, D. D., Shair, F. H., Cayer, R. J., and Nelson, D. W. (1980). Atmospheric tracer studies associated with the evaluation of the SEAREX atmospheric sampling site at the NOAA/GMCC station in American Samoa. Available from Dr. F. H. Shair, California Institute of Technology, Pasadena, California 91125.

Reible, D. D., and Shair, F. H. (1981). The transport and dispersion of airborne contaminants in the Santa Barbara Channel area of Southern California. Submitted to Atmospheric Environment.

Smith, D. G. (1978). Turbulent diffusion around a building in the natural wind and effluent reentry. Ph.D. Thesis, Harvard School of Public Health, Boston, Massachusetts.

Turner, D. B. (1970). Workbook of atmospheric dispersion estimates. Environmental Protection Agency, Office of Air Programs Publication AP-26, 84 pp.

Vincent, J. H. (1977). Model experiments on the nature of air pollution transport near buildings. Atmospheric Environment, 11, pp. 765-774.

Part II.

Pollutant Transport in Mountain-Valley and Coastal Regions of California

Chapter 4

Introduction

Statement of Problem

Although there have been attempts over the past few decades to reduce the quantity of pollutants emitted into the air, continued growth has led to a potential increase of emissions in many areas of the United States. The shift in population from urban centers to rural areas, coupled with the need to develop rural resources (such as energy sources), has led to indications that air pollution is no longer a problem limited to cities. At the same time, there has been increasing recognition that significant pollutant impacts can occur at large distances from their source. This problem has been linked, for example, to the acidity of the rainfall in Scandinavia (Bergstrom, et al., 1972), and the transport of visibility degrading pollutants into the southwest deserts of the United States (Trijonis, 1979). The transport of both sources and pollutants into more rural areas has resulted in an increasing need to predict the impact of industrial and urban development on air quality in areas that have faced comparatively little previous study. A prediction of air quality at a particular location requires knowledge of 1) the quantity and distribution of emissions of primary pollutants, 2) the transport and dispersion of the emitted pollutants by the applicable meteorological factors, and 3) the formation of secondary pollutants by reactions within the atmosphere. This research is devoted to acquiring an understanding of the second factor, the transport and dispersion of pollutants in the atmosphere.

The study was centered about the Great Central Valley of California (San Joaquin-Sacramento Valley) and the coastal regions of Southern California. The San Joaquin-Sacramento Valley is a rich agricultural region with an annual crop yield in excess of 4 billion dollars (Census of Agriculture, 1981). The valley faces significant industrial development in coming years to develop and process oil reserves. Additional industrial and urban development is expected due to the low cost of land when compared to the urban centers on the west coast of California. Because of the importance of the agricultural products of the Central Valley, the impact of even minor increases in air pollution can be significant. It has been estimated (CARB, 76-19-4, 1976), that the annual crop losses in the San Joaquin Valley due to oxidant damage currently exceed 30 million dollars annually.

In other regions, similar problems also occur. The Santa Barbara Channel area of Southern California, for example, faces more extensive development of oil reserves located offshore as well as the pressures of urban growth. Pt. Conception, at the western end of the Santa Barabara Channel has been suggested as a possible location for a major liquefied natural gas terminal. Concerns over the impact of development of these areas are compounded by the nearness of locations that currently exhibit comparatively pristine air quality. The Central Valley is bounded on the east by the California Coastal Mountains, on the north by the Cascades, on the east by the Sierra Nevada, and on the south by the Tehachapi Mounatins. The Cascades and the Sierra Nevada Mountains both contain National Parks, Forests and Recreation

Areas that are heavily used by the public and often protected by the Prevention of Significant Deterioration Policy of the Clean Air Act, as amended in 1977 (Council on Environmental Quality, 1978). The Mojave Desert, east of the southern San Joaquin Valley, exhibits generally good air quality that may have been deteriorating over the past few decades (Trijonis, 1979). The southern boundary of the Santa Barbara Channel is the ecologically fragile Channel Islands, some of which make up the Channel Islands National Monument. Thus the Central Valley, the surrounding mountainous areas, and the coastal region of Southern California are excellent examples of the often conflicting requirements currently being placed upon the air resources of rural areas.

This research will attempt to provide a sound basis for the technical evaluation of the impact of development on these areas, by developing an in-depth description of the flow field and the resulting transport and dispersion of pollutants. The specific objectives of this study can be stated in the following manner:

1) Determine the transport routes into, within, and out of the Central Valley of California, the surrounding mountainous areas, and the coastal areas of southern California.
2) In so doing, delineate the basic characteristics of the flow field important to the ventilation of these and other similar areas.
3) Determine the rates and mechanisms of air exchange between the flow structures, such as eddy and convergence zones, that characterize the wind field within the study areas.

While these investigations are necessarily site-specific, it is quite likely that the transport mechanisms observed will be applicable to other mountain-valley or coastal environments. At the very least, site-specific studies provide a foundation on which to base future investigations in other locales.

Meteorological Complexity of Mountain-Valley and Coastal Regions

The meteorology of rural, mountainous areas is generally not characterized to the degree of urban environments. Complex topography tends to modify the local wind field. Urban areas in flat terrain also exhibit local influences but the length scale of such influences is generally less than the length scales of interest in the prediction of pollutant dispersion. Thus the "roughness" and thermal effects of cities in flat terrain may simply enhance mixing processes in the atmosphere rather than modify the mean flow field (McElroy, 1969). The local effects of mountain-valley and coastal environments, however, both enhance the mixing of pollutants in the atmosphere and modify the mean flow field. Mixing is enhanced by mechanically induced turbulence and flow channeling can occur due to flow blockage by the terrain.

In addition to these more localized effects of terrain, diurnally varying winds are observed in mountain-valley and coastal environments due to differential heating of the earth's surface. During the day, enhanced heating of a mountain surface with respect to the valley floor, and of the land with respect to the adjacent sea surface, results in a density gradient, and thus

a driving force, for the development of an upslope or onshore flow. At night, the reverse flow develops due to more rapid cooling of the mountain slopes with respect to the valley floor and the land with respect to the sea surface. While the cause and the basic structure of these flows are known (e.g. Defant, 1951), such important meteorological parameters as the depth and strength of these flows have not been adequately characterized to predict the transport characteristics of a pollutant. In addition, the twice daily wind reversals are characterized by light and variable winds. The transport and dispersion of pollutants in such wind conditions are very difficult to predict due to the scarcity and inaccuracy of typical meteorological measurements. Because the depth of the diurnal winds in mountain-valley or coastal environments is limited to the height influenced by the diurnal surface temperature variations, a distinct layering can often be observed in the atmosphere. The air above the buoyancy driven surface flows is typically driven by the synoptic scale pressure gradients. The interaction of these layers introduces additional complexity to the transport of pollutants in mountain-valley and/or coastal areas.

In addition to the localized effects of complex terrain, such as channeling and mechanically induced turbulence, and the effects of intermediate scale, such as the diurnally varying winds, there exists the potential for very large scale flow modification by the terrain, due to the size of the systems under study. The Central Valley of California, for example, is approximately 700 km in length and averages about 80-100 km in width. In the Central

Valley, perhaps the best example of the large scale modification of the environment is the variation in climate between the west and east sides of the valley. The western side of the San Joaquin Valley is quite arid while the eastern side of the valley receives significantly more precipitation due primarily to the uplifting of air over the mountains that form the eastern boundary of the valley. The physical size of the mountain-valley and coastal environments of California represents possibly the greatest challenge to the investigator attempting to describe the transport and dispersion of pollutants in such a system.

Methods of Investigation

There are four basic methods of probing the transport and dispersion of pollutants in a complex flow field:

1) sufficiently detailed meteorological measurements to allow inference of the transport wind field,
2) numerical simulation based upon the application of the conservation equations to the atmosphere,
3) laboratory scale modeling of the physical system, and,
4) atmospheric tracer studies on the full-scale system.

Since airborne contaminants are transported and dispersed by the wind field, it would appear that the most direct means of describing the behavior of pollutants in the atmosphere is through meteorological measurements. In practice, however, because of the substantial spatial and temporal variations in the wind field typically observed in mountain-valley and coastal environments, it

is generally difficult to collect sufficient meteorological measurements to adequately characterize the behavior of pollutants. This is especially true in rural areas that have not benefited from detailed study over long periods of time.

Numerical simulation of the atmospheric system under study has the advantage of being easily modified for different conditions. In principle, the resolution of the numerical model could be as small as necessary to provide adequate results. Unfortunately, the flow field over complex terrain or in diurnally varying flows cannot generally be evaluated from first principles. Thus numerical models of transport in the atmosphere tend to be based upon a wind field developed from meteorological measurements. At best, such numerical models can be only as accurate as the input wind field. As indicated above, this can be a significant limit to the accuracy of these models in rural areas where the wind field is only poorly characterized. Benarie (1980) has reviewed the state of the art of air quality modeling. Benarie emphasized the difficulty in predicting the transport and dispersion of pollutants in wind speeds below 3 m/s, by indicating that only moderate to strong winds can be expected to follow an observable cause-and-effect relationship. At wind speeds much below 3 m/s, the lack of a well-defined wind field precludes accurate prediction. This indicates that the dispersion of a pollutant during a wind reversal may prove very difficult to predict. Throughout the book, Benarie reports varying degrees of success in modeling the air quality in urban areas. Numerical simulation of the behavior of a pollutant in the atmosphere can be

both accurate and useful given a sufficiently broad data base for validation. Because such a data base rarely exists, however, accurate models are generally available only for relatively specific locations or conditions. The Gaussian plume model (Turner, 1970), for example, has proven quite useful for predicting the concentration profile directly downwind of a continuous source in a strong, uniform wind field. Under less ideal conditions, however, the Gaussian plume model may at best be an order of magnitude estimate (see, for example, Chapter 5). In conclusion, numerical simulation of the transport and dispersion of pollutants in the mountain-valley and coastal locales of California does not appear to be a viable alternative at this time due to the lack of data about the wind field or the basic mechanisms of the ventilation of these areas.

The third means of establishing the transport characteristics of the rural air basins under study is through laboratory scale physical models. Just as in numerical models, however, physical models are applicable to certain specific problems of transport in complex flow situations, but the more general problem of the ventilation characteristics of a large air basin appear beyond its capabilities. Deardorff, et al. (1980), for example, conducted a laboratory experiment to investigate the rate of entrainment of a convectively mixed layer into a more stable layer above. But while such studies shed light on the mechanisms of mixed layer growth during the day, the results of the study are not directly applicable to a real atmosphere except in a limited sense. Cermak and Arya (1970) summarized the difficulties of the laboratory

simulation of atmospheric flows and many of their comments are still applicable. They considered the difficulty of accurately modeling 1) thermal stratification, 2) surface roughness, 3) the non-uniformity of the surface roughness or the temperature field, and 4) surface irregularities due to hilly or mountainous terrain. While concluding that similarity between the atmosphere and the laboratory models can be achieved, at least for specific flow situations, the authors pointed out the difficulty in achieving accurate laboratory representations of 3-dimensional flow fields. Compounding these problems is the difficulty of physically simulating dynamic atmospheric flows, such as the diurnally varying mountain-valley or land-sea breezes.

A fourth method of establishing the ventilation characteristics of a particular air basin is through atmospheric tracer techniques. A number of tracers have been used to indicate the movement of air masses, including pollutants such as ozone (Wolff, et al., 1977), meteorological tools such as tetroons (Angell, et al., 1972), and artificially introduced tracers such as flourescent particles (Hinds, 1970), and sulfur hexafluoride (Start, et al., 1974, Lamb, et al., 1978). Pollutant tracers suffer from the possibility of chemical conversion between source and receptor thus confusing the transport characteristics with the chemistry. It is also often difficult to unambiguously determine the source of a pollutant plume, especially after extensive dilution with time. Meteorological techniques, such as the use of tetroons, are easy to follow long distances, but cannot be used to determine the dispersion characteristics of the atmosphere.

Ballon trajectories also may not follow an air parcel trajectory due to the significant mass and buoyancy effects of the balloon. Fluorescent particles suffer from the same disadvantage in that they often indicate the transport and dispersion of small particles rather than that of a gaseous pollutant (Eggleton and Thompson, 1961). In addition, zinc-cadmium sulfide, a commonly used fluorescent particle tracer, is known to be toxic (Spomer, 1973).

Over the past decade, however, electron capture gas chromatography has been applied to the investigation of the transport and dispersion of pollutants in the atmosphere. Electron capture gas chromatography, originally developed by Lovelock and Lipsky (1960), allows the detection at very low concentrations of non-toxic gaseous compounds which have a high affinity for the absorption of electrons. Such compounds include sulfur hexafluoride, which can be measured at concentrations approaching 1 part in a trillion parts air (1 PPT), and bromo-trifluoromethane, which can be measured at concentrations approaching 10 PPT. The fact that these compounds are generally non-toxic, odorless, colorless, and stable in the atmosphere, makes them ideal atmospheric tracers. The use of such tracers allows a quantitative description of the atmospheric flow field and the associated transport and dispersion of pollutants. Tracer experiments have the disadvantage, however, in that their results are strictly applicable only to the meteorological conditions under study. Thus great care must be taken to ensure the representativeness of the field studies, by repetition of

experiments where possible, and by adequate characterization of the basic atmospheric conditions.

Most experiments employing these gaseous, ultra-sensitive tracers have been used to explore specific transport problems in the atmosphere. Many tracer experiments, for example, have been used for the sole purpose of determining the dispersion parameters associated with a particular model, such as the Gaussian plume model (Turner, 1970). While such studies are useful, they suffer from many of the same disadvantages as laboratory scale experiments, namely an a' priori determination of how the data are to be analyzed. In order to realize the full potential of these gaseous atmospheric tracers, it would seem that they should be used to probe the structure and mechanisms of the transport and dispersion of pollutants in the atmosphere, and not simply to provide experimental inputs for a preconceived model. In urban areas, where the pollutant behavior is generally somewhat better characterized, an a' priori specification of a model may prove fruitful in that a model may be based upon an adequate fundamental understanding of the problem. But while this may be true in many well studied urban areas, it is apparently not true in rural areas which exhibit the complicating factors of complex terrain. It seems clear that more basic research into the mechanisms and structure is needed before an adequate model of the transport and dispersion of pollutants in such areas can be formulated. It is this need that formed the basis of this work.

As indicated by this discussion, the use of ultra-sensitive atmospheric tracers such as sulfur hexafluoride appears to be the

best available means of achieving the specific purposes of the current research. In the following chapters, a series of atmospheric tracer experiments in the mountain-valley and coastal regions of California and their results are described. It is hoped that these studies will allow a more accurate estimation of the impact of development on the study areas and a more thorough understanding of the mechanisms of transport in complex terrain.

References

Angell, J.K., Pack, D.H., Machta, L., Dickson, C.R., and Hoecker, W.H. (1972). Three dimensional air trajectories determined from tetroon flights in the planetary boundary layer of the Los Angeles Basin. Journal of Applied Meteorology,11, 451-471.

Benarie, M.M. (1980). Urban Air Pollution Modeling. MIT Press, Cambridge, Mass., 405 pp.

Bergstrom, et al. (1972). A Method for the Determination of Long Range Transport of Atmospheric Sulfur. Proceedings of 4th UN International Conference on the Peaceful Uses of Atomic Energy, Geneva,1971, 14, 481-492.

CARB 76-19-4 (1976). California Air Resources Board Staff Report, PO Box 2815, Sacramento, CA 98512.

Census of Agriculture (1981). Vol 1, Part 5, Data for 1978. Available from the Superintendent of Documents, United States Government Printing Office, Washington, DC 20402.

Cermak, J.E., and Arya, S.P.S. (1970). Problems of atmospheric shear flows and their laboratory simulation. Boundary Layer Meteorology,1, 40-60.

Council on Environmental Quality (1978). Environmental Quality. For sale by the Superintendent of Documents, United States Government Printing Office, Washington, DC 20402.

Deardorff, J.W., Willis, G.E., and Stockton, B.H. (1980). Laboratory studies of the entrainment zone of a convectively mixed layer. Journal of Fluid Mechanics, 100, 1, 41-61.

Defant, F. (1951). Local Winds. Compendium of Meteorology. American Meteorological Society. Boston, Mass. 655-672.

Eggleton, A.E.J., and Thompson, N. (1961). Loss of fluorescent particles in atmospheric diffusion experiments by comparison with radioxenon tracer, Nature, 192, 935-936.

Hinds, W.T. (1970). Diffusion over coastal mountains of southern California. Atmospheric Environment, 4, 107-124.

Lamb, B.K., Shair, F.H., and Smith, T.B. (1978). Atmospheric dispersion and transport within coastal regions- Part II. Tracer study of industrial emissions in the California Delta region. Atmospheric Environment, 12, 2101-2118.

Lovelock, J.E., And Lipsky, S.R. (1960). Electron affinity spectroscopy- a new method for the identification of functional groups in chemical compounds separated by gas chromatography, Journal of the American Chemical Society, 82, 431-433.

McElroy, J.L. (1969). A comparative study of rural and urban dispersion. Journal of Applied Meteorology, 8, 19-31.

Spomer, L.A. (1973). Fluorescent particle atmospheric tracer: toxicity hazard. Atmospheric Environment, 7, 353-355.

Start, G.E., Dickson, C.R., and Ricks, N.R. (1974). Effluent dilutions over mountainous terrain and within mountainous canyons. Symposium on Atmospheric Diffusion and Air Pollution, American Meteorological Society, Boston, Mass.

Trijonis, J. (1979). Visibility in the Southwest- an exploration of the historical database. Atmospheric Environment, 13, 833-843.

Turner, D.B. (1970). Workbook of atmospheric dispersion estimates, Environmental Protection Agency. AP-26, 84 pp.

Wolff, G.T., Lioy, P.J., Wight, G.D., Meyers, R.E., Cederwall, R.T. (1977). An investigation of long-range transport of ozone across the midwestern and eastern United States. Atmospheric Environment, 11, 797-802.

Chapter 5

Plume Dispersion and Bifurcation in Directional Shear Flows in Complex Terrain

by

D.D. Reible, F.H. Shair and E. Kauper

(Published in Atmospheric Environment,15,7,1165-1172)

Atmospheric Environment. Vol. 15, No. 7, pp. 1165–1172, 1981
Printed in Great Britain.

0004–6981/81/071165–08 $02.00/0

PLUME DISPERSION AND BIFURCATION IN DIRECTIONAL SHEAR FLOWS ASSOCIATED WITH COMPLEX TERRAIN

DANNY D. REIBLE and FREDRICK H. SHAIR*
Department of Chemical Engineering, California Institute of Technology, Pasadena, California 91125, U.S.A.

and

ERWIN KAUPER
Metro Monitoring, Inc., 436 North Barranca Avenue, Covina, California 91723, U.S.A.

(*First received* 1 *August* 1980 *and in final form* 28 *October* 1980)

Abstract—The results of three atmospheric tracer studies involving winds in complex terrain are discussed. Winds above complex terrain frequently exhibit directional shear due to the presence of relatively shallow layers of air driven by surface heating and cooling. The three tracer tests were conducted to elucidate pollutant transport and dispersion in multi-directional flows in complex terrain.

During the first test, in the Lost Hills region of the San Joaquin Valley of California, the tracer (sulfur hexaflouride, SF_6) was split into two distinct plumes by wind directional shear. During the second test, conducted in the California coastal mountains near Clear Lake in northern California, under conditions approaching minimum wind directional shear, no plume bifurcation was detected. The tracer dispersion characteristics during this test could be accurately modeled using the Gaussian plume model using dispersion coefficients corresponding to "*D*" stability. The third test was also conducted from the Clear Lake area and during this test the SF_6 plume was again bifurcated due to the action of wind directional shear.

Estimates of the amount of tracer within each of the plumes were made for each test. These estimates accounted for essentially all of the tracer and showed that significant amounts of tracer (and thus airborne pollutants) can be transported by the winds aloft. Predictions of pollutant transport based on surface wind measurements cannot normally be expected to provide good results in complex terrain. The tracer experiments also showed that destabilization of the atmosphere by complex terrain can lead to efficient vertical transport of airborne pollutants through stable layers of air such as nocturnal ground-based inversions.

INTRODUCTION

Atmospheric pollutants are transported and dispersed by winds which can be grouped into three broad categories: macroscale, mesoscale and microscale phenomena, which occur over length scales of hundreds and thousands of km, of tens of km and less than 1–10 km respectively. Events dominated by macroscale phenomena are perhaps the easiest to predict or describe quantitatively (see e.g. Holton, 1972). Events that reflect mesoscale phenomena, however, such as pollutant transport by mountain–valley winds, have proven much more difficult to quantify. Unfortunately, the local meteorology and the resulting pollutant transport in complex terrain is often dominated by mesoscale phenomena especially during stable atmospheric conditions (Defant, 1951 and Hinds, 1970).

The meteorology and the pollutant transport and dispersion in complex terrain are influenced by mechanical effects and thermally induced buoyant effects. The mechanical effects include flow channeling due to valley or canyon walls and enhanced turbulence due to surface roughness. Daytime upslope flows and reversed nocturnal flows are examples of the mesoscale buoyancy effects. The basic theory and observations of the buoyancy driven mountain–valley circulation systems, caused by the diurnal heating and cooling of sloping surfaces, has been summarized by Defant (1951). The basic structure of such flows is outlined by the Eatontown Signal Laboratory Group, US Army Signal Corps (1945). During the generally stable nighttime conditions, the slope flow (in this case a downslope or drainage flow) is typically confined to a sharply defined layer close to the surface that is essentially decoupled from the air aloft (see e.g., Ayer, 1961). Because the synoptic flow is often directed differently than the slope flow, a layer of air with pronounced directional shear is quite common in mountain–valley systems during stable conditions.

In order to quantify the effect of the industrial, commercial and recreational requirements placed on mountainous terrain and its resources, a number of investigators have attempted to understand the characteristics of pollutant transport and dispersion in complex terrain. Egan (1975) has described the basic concepts of turbulent diffusion in complex terrain. He reviewed some of the available theoretical and exper-

* To whom all correspondence should be directed.

imental results. He also discussed the experimental modeling of flow over complex terrain involving wind and water tunnels. Hinds (1970) employed zinc sulfide particles as a tracer to study transport in the coastal mountains of southern California. He found that stable conditions maximized the meteorological effects of the terrain. Kao and Taylor (1977) followed an SO_2 plume from a copper smelter and found that the plume dilution was affected by two local wind effects; enhanced mechanical turbulence due to the terrain and wind directional shear. During some of the experiments, the SO_2 plume bifurcated. Due to insufficient meteorological data it was not possible to correlate the bifurcation with the wind structure. The investigators found that the plume dispersion was strongly influenced by wake effects on the lee side of a mountain range. Start *et al.* (1974) used SF_6 as a tracer in Utah and found that both mechanical turbulence due to the terrain and wind directional shear contributed to increased dilution of the plume, over and above that predicted for flat terrain. Whaley and Lee (1977) also found enhanced plume dilution in complex terrain during their study of an SO_2 plume emitted from a smelter. The crosswind dilution was limited, however, by steep valley walls that caused channeling of the flow. Whaley and Lee also found that the SO_2 dispersion was complicated by a shallow surface layer of air that caused transport upwind of the prevailing wind direction. Saffman (1962) and Csanady (1969) have developed theories for diffusion from an instantaneous point source in winds exhibiting speed and directional shear. Saffman used an eddy diffusivity approach to evaluate diffusion in both bounded and unbounded atmospheres with wind velocity shear. Using a dimensional analysis approach, Saffman also considered diffusion in an atmosphere exhibiting a general three dimensional power law velocity profile. Csanady theoretically investigated diffusion in an Ekman Layer. Both Saffman and Csanady used the method of moments (Aris, 1956) in their analysis. Due to the complexity of the problems, only the lower order moments of concentration could be derived. Both authors concluded that concentration distributions downwind of a source emitting into a wind exhibiting speed or directional shear were asymmetric. This can be compared to the symmetric concentration distributions predicted by the Gaussian diffusion model in which the velocity profile is characterized by an average speed and direction. Results similar to those of Saffman and Csanady have been reported in theoretical studies by Smith (1965) and Hogstrom (1963). Csanady (1972) semi-quantitatively analyzed some data which exhibited some effects of crosswind shear upon diffusion. He found that the lateral spread of a pollutant plume may be dominated by directional shear when the pollutant has mixed sufficiently within the shear layer. In qualitative agreement with theory, concentration profiles downwind of the tracer source were asymmetrical due to the directional shear. The data which Csanady analyzed indicated a bifurcation of the tracer plume during some tests. The experiments strongly influenced by directional shear were associated with moderate to strong temperature inversions in the atmosphere.

Due to the complexity of wind flow patterns in and around mountainous or hilly terrain, attempts to model pollutant transport and dispersion in such regions have generally been unsuccessful. Primarily because of its relative simplicity, the Gaussian plume model has been applied to many atmospheric diffusion problems. It is well known, however, that the Gaussian model and the values of its dispersion parameters, were developed from data collected over smooth terrain under relatively simple meteorological conditions (see e.g., Pasquill, 1974; Scorer, 1978). The extension of such a model to complex terrain and meteorology is not straightforward. As pointed out by Scorer (1978): "Many studies do not appreciate that it is easier to measure the distribution of pollution than to measure the eddy characteristics of the air motion and then predict the distribtion of pollution by means of some theory." Therefore, atmospheric tracer experiments are the most direct way to predict the impact of pollutant source in complex terrain or meteorology. Currently, the Environmental Protection Agency is supporting at least two studies of pollutant transport and dispersion on and around an isolated hill (Lamb and Drivas, personal communication). A third study of pollutant transport and dispersion in complex terrain is being conducted by the Department of Energy in the Geysers Area of California, wherein much of the current study was located (Dickerson, personal communication.)

The purpose of this work was to conduct atmospheric tracer experiments designed to characterize the transport and dispersion of gaseous pollutants emitted into a complex wind flow pattern which includes directional shear with altitude.

EXPERIMENTAL PROCEDURE

The first tracer test was conducted from Lost Hills in the western San Joaquin Valley of California. The San Joaquin Valley is the southern half of the great central valley of California. The valley is about 400 km long and 80 km wide, being bounded on the east by the Sierra Nevada mountains and on the west by the California coastal mountains. 285 kg of an inert, nontoxic tracer gas, sulfur hexaflouride (SF_6) was released continuously at ground level in Lost Hills between 1400 and 2030 PST on 8 December 1978.

The second and third tests were both conducted in Lake County, California, which lies in the coastal mountains of northern California. The second test was conducted from the Mcleskey geothermal well site close to a small ridge at 640 m above sea level and about 3 km southeast of the intersection of California Highways 175 and 29. The third test was conducted from the Wilson Well geothermal site, 5 km south of the same highway intersection, at 730 m above sea level. The release sites lay between Mt. Kinocti (1280 m

elevation) to the north and Mt. Hannah (1213 m) to the south. East–west ground level elevations decreased to 412 m at Kelseyville, about 10 km northwest of the release sites, and to 418 m at Lower Lake, about 13 km east of the release sites. During the second test, 41 kg of SF_6 were released continuously between 2100–2300 PDT on the night of 15 July 1979. After 2300 PDT, mechanical difficulties with the release system caused a rapid deterioration of the release rate. During the third test, 93 kg of SF_6 was released continuously between 2340 PDT on 19 July 1979 and 0540 PDT, 20 July 1979.

The SF_6 was released as a gas from cylinders containing about 45 kg of liquid SF_6. The cylinders were connected via 1.27 cm OD copper manifolding. The SF_6 flowrate was monitored with a high volume rotameter and verified by weighing the cylinders both before and after the release. The SF_6 was released from ground level during the San Joaquin Valley test. During the Lake County tests, the SF_6 was released at an altitude of 30 m above ground level by attaching the release tube to helium balloons.

During each of the tests, a series of automobile air sampling traverses was conducted using two person teams. During an automobile traverse, the passenger in each car took grab samples in 30 cm^3 plastic syringes. The distance between samples was dependent on the distance downwind of the release site and varied between 0.3 and 1.6 km. Traverse paths were determined during each experiment based upon real time wind data and spot checking of samples with a portable electron-capture gas chromatograph. During the Lake County tests, 30 cm^3 syringes were also used to collect air samples at 10 min intervals from 13 fixed locations.

Air samples were analyzed for SF_6 using electron-capture gas chromatography. Details of the analytical procedure are described by Drivas (1974) and Lamb (1977). The gas chromatographs were calibrated using the exponential dilution method and checked between calibrations by comparison to a known standard. Calibration results showed that concentrations as low as ten parts SF_6 per trillion parts air (10 ppt) could be detected within about 10%. Concentrations between 1 and 5 PPT could be detected within a factor of 2.

PRESENTATION AND DISCUSSION OF RESULTS

Test of 8 *December* 1978, *San Joaquin Valley*

SF_6 was released at a continuous rate of 47.5 kg h^{-1} from 1400 and 2030 PST on 8 December 1978 from Lost Hills in the San Joaquin Valley of California. During the first two hours of the release the surface winds were from the southeast at about 2 m s^{-1}. Throughout the rest of the release, however, the surface winds shifted counterclockwise until westerly winds at 2 m s^{-1} were measured at the end of the release. Winds above 150 m, however, were southeasterly (2–3 m s^{-1} at 100–130 deg. true) throughout the release. Figure 1 summarizes the grab sample data

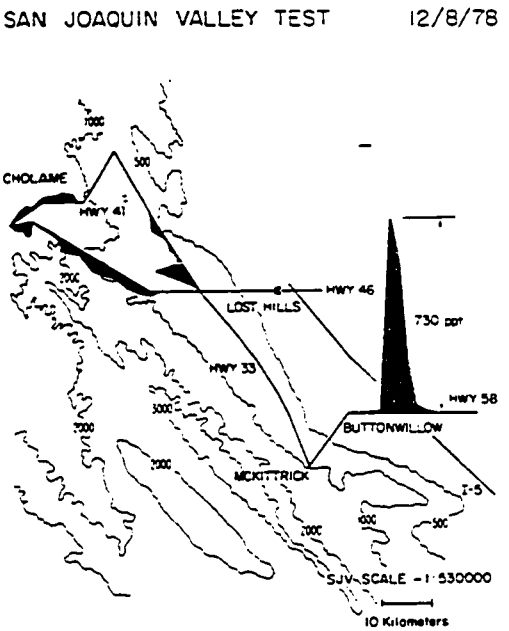

Fig. 1. SF_6 concentration as function of location. San Joaquin Valley Test, 12/8/78. Thickness of shaded region proportional to concentration (100 ppt/cm). Release point denoted by *.

from two automobile traverses conducted between 2030 and 2130 PST. During the afternoon, efficient mixing between the surface layer and the air aloft caused the tracer to be transported towards the northwest. As mixing between the surface layer and the air aloft decreased due to surface cooling during the later stages of the release, some tracer was transported towards the southeast. At least 75% of the tracer was estimated to have been transported towards the northwest where lower concentrations (but spread over a larger area) were detected. The directional shear between the surface and winds above 150 m measured throughout much of the experiment apparently had little effect on the direction of tracer transport until vertical mixing became limited near nightfall. A trajectory analysis based only on the surface winds suggested that the bulk of the tracer would lie southwest and southeast of the release site rather than northwest as detected. More detailed information on this test can be found in Reible *et al.* (1981).

Test of 15–16 *June* 1979, *Lake County*

During this period, the study area was influenced by a gradually deepening marine layer, with a persistent flow from the west being noted everywhere but the most sheltered locales. The stable marine air generally extended to the 1150 m elevation (about 500 m above release height). A secondary temperature inversion aloft based near 1000 m was observed. The synoptic flow was strong enough to dominate the local meteorology, minimizing the effects of topography. The surface winds at the release site were 3 m s^{-1} at

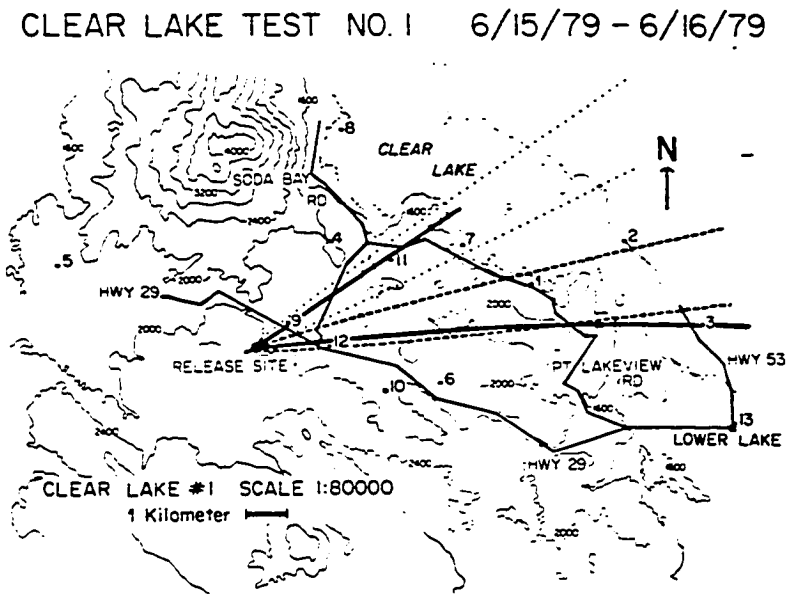

Fig. 2. Study area showing fixed sampling sites and traverse routes. Clear Lake County Test No. 1, 15–16 June 1979. Also included are 1 ppt (g mole h)$^{-1}$ concentration isopleths drawn from Gaussian plume calculation (. . . . surface winds and ——, 30 m pibal winds) and from experimental data (————).

240–280° while the 30 m winds were estimated by pilot balloon measurements to be 5–6 m s^{-1} at 260–280° true north. The meteorological conditions corresponded to Pasquill–Gifford stability class E (Turner, 1973).

A total of approximately 73 kg of SF_6 was released continuously from the Mclesky Well site between 2100 PDT, 15 June 1979 and 0200 PDT, 16 June 1979. The initial SF_6 flowrate was 20 kg h^{-1}. Between 2 and 3.5 h after the start of the release, the average release rate was 14 kg/hr. Between 3.5 and 5 h the average release rate was 7 kg h^{-1}.

Figure 2 displays the 13 fixed sampling sites for this test along with the roads that were sampled by automobile traverses. Figure 3 displays the SF_6 concentrations detected at each of the fixed sampling sites which showed an hourly average concentration of greater than 1 ppt (g mole/h)$^{-1}$. High concentration levels were detected only during the first 3 h of the test due to the significant drop in SF_6 release rate after 2 h. Using automobile traverse data obtained between 2300 PDT and 2330 PDT along Pt. Lakeview Rd. it was possible to estimate an SF_6 flowrate of approximately 23 kg h^{-1}. This mass flow estimate was obtained using the experimentally determined ground level SF_6 concentrations and ground level speed. The vertical distribution was calculated using Turner (1973). Whaley and Lee (1977) have suggested that vertical plume spread in complex terrain can be predicted reasonably well by Pasquill–Gifford stability criteria. In view of the uncertainties, the mass balance calculation appears reasonable and merely indicates that essentially all of the tracer was accounted for.

As mentioned above, the atmospheric conditions prevailing at the time of the test corresponded to class E stability (Turner, 1973). Figure 2 displays the 1 ppt (g mole h)$^{-1}$ isopleth calculated by the Gaussian plume model for E stability using both the surface winds (3 m s^{-1}, 240–280°) and the 30 m pibal winds (5–6 m s^{-1} at 260–280°). The solid line encloses the area where maximum hourly averaged fixed site concentrations of greater than 1 ppt (g mole/h)$^{-1}$ were detected. Grab samples taken during automobile traverses were used to aid in determination of the limits of

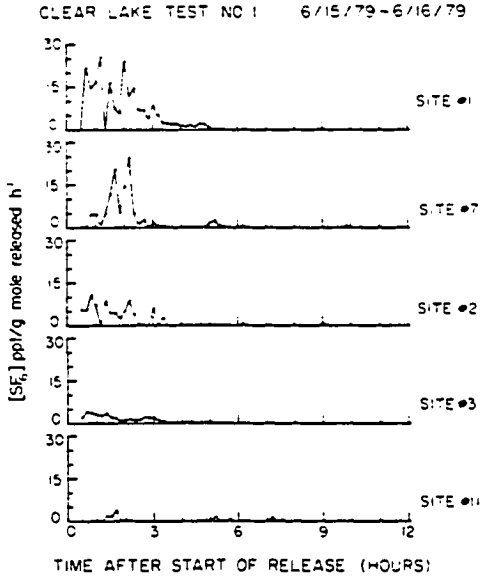

Fig. 3. Concentration vs. time at the fixed sampling sites where the maximum hourly averaged SF_6 concentration detected exceeded 1 ppt (g mole/h)$^{-1}$ during Clear Lake County Test No. 1, 15–16 June 1979.

Table 1. Comparison of experimental* and calculated plume centerline concentrations +

Location	Distance from release site (km)	Equivalent SF_6PPT/G-MOLE/H	
		Experimental (maximum)	Calculated (centerline)
Hwy. 29	1.6	119	100
Soda Bay Rd.	2.2	46.1	66.0
Pt. Lakeview Rd.	6.4	28.5	14.5

* Grab sample concentrations detected during automobile traverses on roads listed.

+ Calculations follow Turner (1973) using *D* stability and the average of the surface and 30 m pibal winds.

this area. The discrepancy between the predicted and actual crosswind dispersion could be due to topographically induced turbulence. It might, however, be a reflection of the slight directional shear with altitude. The cross wind standard deviation in concentration, σ_y, was estimated at two distances downwind of the release site using automobile traverse data. The crosswind dispersion of the tracer roughly corresponded to Pasquill stability class D. Urban plumes often exhibit dispersion rates characteristic of the next less stable classification than that predicted over flat terrain (McElroy, 1969). Table 1 compares the calculated SF_6 centerline concentrations based on D stability and the experimental concentration maxima. Even using experimentally determined σ_y valves (i.e. σ_y for *D* stability), the Gaussian model yielded results only within a factor of two of actual concentrations. This could be due to flow channeling or uncertainties in wind speed and/or vertical dispersion coefficient, σ_z. In the absence of tracer data, one must expect calculated results to be even less accurate.

Test of 19–20 *June* 1979, *Lake County*

During this period, the study area was influenced by a westerly flow similar to, but much weaker than, that encountered during the first test. Winds speeds at the surface and at 30 m elevation were about $2\,m\,s^{-1}$ throughout the entire region of interest. Localized topographical effects produced downslope (i.e., drainage) flows with similar velocities. Temperature soundings during the test indicated generally stable conditions to a height of 1150 m above sea level. Ground based radiational inversions were also evident during this test. The meteorological conditions corresponded to Pasquill–Gifford stability class *F* (Turner, 1973).

A total of 91 kg of SF_6 was released continuously from the Wilson Well site between 2340 PDT, 19 June 1979 and 0540 PDT, 20 June 1979. The release rate remained uniform throughout this period at about $15\,kg\,h^{-1}$. Throughout most of the test, a drainage condition (southerly flow) was found at the release site. The westerly synoptic flow was found at elevations greater than 90 m above the surface. Between the surface drainage layer and the synoptic flow existed a region containing both velocity and directional shear. The tracer was released at a height of 30 m into this region.

Figure 4 displays the 1 ppt(g mole/h)$^{-1}$ isopleth test along with the roads involved in the automobile traverses. The directional shear above the release site caused the tracer plume to split into two distinct sections as shown by a plot of an automobile traverse along Redhills Road and Hwy. 175 (Fig. 5). An estimate was made of the tracer mass flow in the eastern plume from automobile traverse sample concentrations plus the mean wind speed and by assuming a Gaussian concentration profile in the vertical (vertical distribution again calculated via Turner (1973)). This plume, which was driven by the synoptic scale winds, contained approximately 80% of the SF_6 released. Thus, about 20% of the SF_6 released followed the surface winds. This is in good agreement with an independent mass estimate on the northern plume, which suggested that 15% of the SF_6 was transported by the surface drainage flow.

Figure 6 displays the concentration data at each of the fixed sampling sites which showed an hourly average concentration of greater than 1 ppt(g mole/h)$^{-1}$. High SF_6 concentrations were detected at site 9 only between 5:00 and 8:00 a.m. This is presumably due to some shift in the wind direction during that time. Sites 13, 12, 8, 5, 7 and 6 lie northwest of the release point and thus were impacted by the surface drainage flow. Note the similar structure of the concentration profiles in Sites 5, 6, 7 and 8. The tracer was essentially well mixed over the entire area enclosed by these sites, suggesting that Gaussian modeling of the tracer transport and dispersion is not appropriate.

Figure 4 displays the 1 ppt(g mole/h)$^{-1}$ isopleth developed from the maximum hourly averaged concentrations detected at the fixed sampling sites (solid line). Automobile traverse grab samples were used to aid in determination of the isopleth location. Note that the experimental isopleths were extended towards the regions of lowest elevation (Lower Lake and Kelseyville) due to the action of drainage winds. The location of the isopleths that bound the region between the two plumes is not well defined due to the sparcity of experimental data in this region. The high morning concentrations detected at site 9 were apparently due to a shift in wind direction and were excluded from the

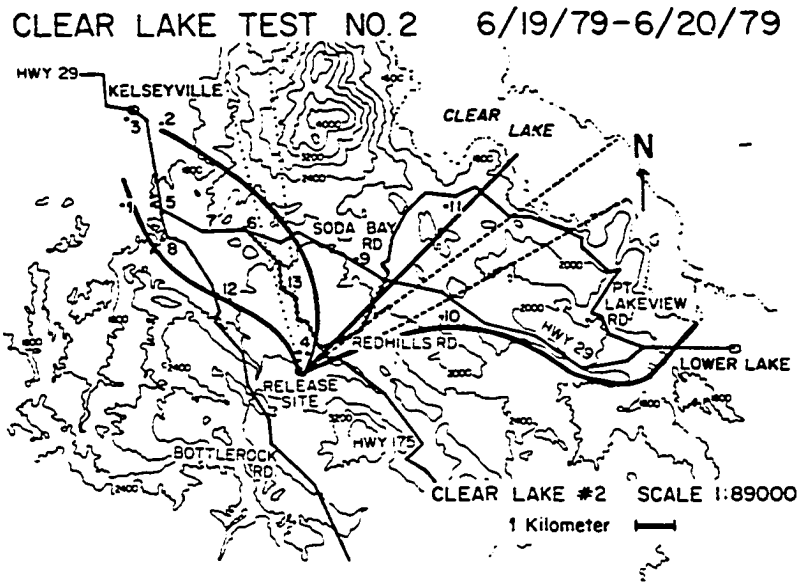

Fig. 4. Study area showing fixed sampling sites and traverse routes for Clear Lake County Test No. 2, 15–16 June 1979. Included is the route traversed in Fig. 5 (HHHHHH). Also included are 1 ppt (g mole/h)$^{-1}$ concentration isopleths drawn from a Gaussian plume calculation ..... surface winds and ----. 30 m pibal winds) and from experimental data (———).

isopleth determination. Also shown in the figure are 1 ppt (g mole·h)$^{-1}$ isopleths predicted using either the surface winds or 30 m pibal winds and stability class *F* (as suggested by Turner for the atmospheric conditions prevailing during the test). An attempt to apply a simple Gaussian plume model to the tracer transport would not predict the relatively large crosswind dispersion of the tracer nor the trajectory of either plume. In addition, there appears to be no way to accurately estimate, *a priori*, the amount of tracer transported by either the drainage or synoptic flow.

The maximum ground level tracer concentration in the eastern plume (driven by the winds aloft) occurred about 3 km east of the release point. The Gaussian plume model suggests that the maximum concen-

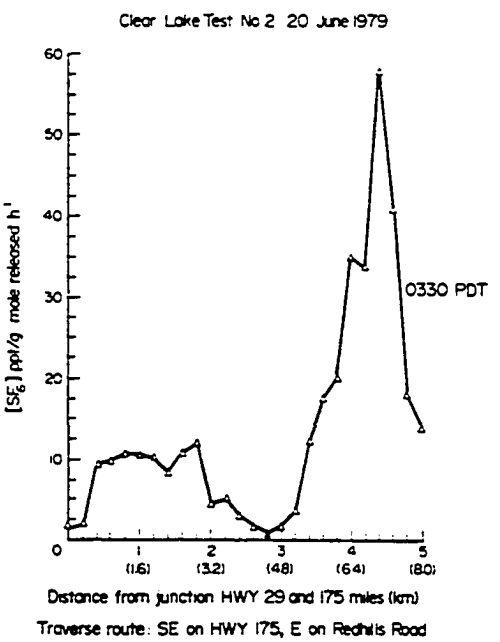

Fig. 5. Concentration vs. distance from the intersection of HWY 29 and HWY 175 at about 0330 PDT on 20 June 1979. Traverse followed HWY 175 and then turned east on Redhills Road.

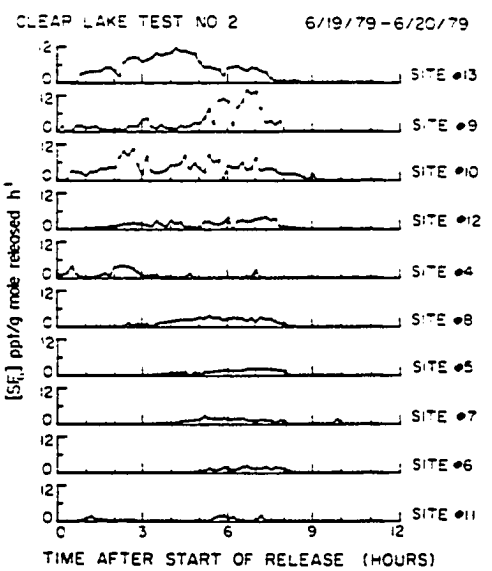

Fig. 6. Concentration vs. time at the fixed sampling sites where the maximum hourly averaged SF_6 concentration detected exceeded 1 ppt(g mole/h)$^{-1}$ for Clear Lake County Test No. 2, 15–16 June 1979.

tration should occur at half this distance downwind. Since complex terrain is generally believed to increase the vertical dispersion of pollutants, especially at small distances from the source, the discrepancy between the predicted and actual location of the maximum concentration is probably due to the strong directional shear between the release height and the ground. An air layer exhibiting strong direction shear is generally assumed to be a region of limited vertical mixing caused, for example, by the top of a temperature inversion. In this test, the limited vertical mixing reduced the average effective diffusivity to about half that predicted over flat terrain. Presumably, vertical mixing would be further reduced if it were not for the destabilizing effect of the complex terrain.

One way to model the rate of vertical mixing is to consider the directional shear layer as a turbulent mixing layer, which is frequently described with a relationship of the form

$$\mathscr{D}_e = c\Delta u l \tag{1}$$

where Δu represents the change in velocity across the width of the mixing layer, l. The quantity c is an empirical constant and is typically of value between 10^{-1} and 10^{-2} (Tennekes and Lumley, 1972). This relationship is based on dimensional arguments and assumes that the characteristic time for bulk transport ($t_t = L_c/u_c$) is approximately equal to the characteristic diffusion time ($t_D = L_c^2/D_e$). L_c and U_c are the characteristic length and velocity scales of the flow. In the current experiment, the directional shear between the surface ($2\,\mathrm{ms}^{-1}$@ 170°) and 30 m ($2\,\mathrm{ms}^{-1}$@ 240°) accounted for an "apparent" velocity change of $1.2\,\mathrm{ms}^{-1}$. The magnitude of the average effective diffusivity can be estimated by the relation

$$\mathscr{D}_e = l^2/t_D = l^2/t_t = l^2/(L/u) \tag{2}$$

with $l = 30\,\mathrm{m}$, $u = 2\,\mathrm{ms}^{-1}$ and $L = 3000\,\mathrm{m}$. The average effective diffusivity for the tracer detected at the location of maximum concentration is approxi- $6 \times 10^3\,\mathrm{cm}^2\,\mathrm{s}^{-1}$. Substitution into Equation (1) gives $c = 0.017$, the same order of magnitude as found in laboratory experiments on neutrally stratified mixing layers. This again suggests that the stability of the surface layer may be partially offset by the enhanced mechanical turbulence due to the terrain. More detailed information on the third test can be found in Reible *et al.* (1979).

The primary difficulty in predicting pollutant transport and dispersion in this or a similar meteorological condition, is the lack of knowledge about the three-dimensional flow field. When topography affects the local meteorology (as in the occurence of shallow drainage flows), then small variations in the effective stack height of the plume and/or location may give rise to significantly different transport paths and dispersion characteristics of the pollutants. Even though the Gaussian plume model is very popular, it should be used with caution especially when considering shallow drainage conditions. Since the air flows over complex terrain are often multidirectional, in most cases the Gaussian plume model will underestimate the dispersion of the plume. Consequently, the Gaussian plume model can provide an upper bound value for the level of maximum impact. The Gaussian plume model may not provide an upper bound to pollutant exposure levels, however, if the terrain limits horizontal dispersion (e.g., by canyon walls). It should also be noted that the location of the maximum impact generally cannot be determined from calculations based upon the Gaussian plume model wherein some average speed and direction is assumed to characterize the transport wind. This is particularly important when an elevated plume might impact surrounding higher terrain. If the transport wind is a buoyancy driven slope flow, the pollutant plume will move roughly perpendicular to the mean lines of constant elevation, providing an estimate of the location of maximum impact. In principle, only meteorological data (i.e., surface winds and winds aloft) could be used to estimate the location of the maximum impact zone; however, to do so, the distance between wind monitoring stations must be less than the distances over which changes in wind speed and direction occur due to local variations in terrain. For example, during Test 3 (conducted 19–20 June 1979) wind speeds and directions would be required at 30 m vertical intervals at sites separated by distances no greater than a few km throughout the total region of interest. Consequently, in order to economically determine the location of maximum impact either pollutant data and/or tracer data should be analyzed.

SUMMARY

(1) The influence of complex terrain on the transport and dispersion of pollutants has been reviewed. Emphasis was placed on pollutant transport in directional shear flows which often occur in complex terrain due to decoupling between suface air and the air aloft. Three atmospheric tracer tests were conducted. During the first test, a shallow surface layer of air transported some of the tracer upwind of the prevailing flow aloft. During the second test, the study area was influenced by a strong, essentially uniform, synoptic scale flow. In this test, the crosswind spread of the tracer plume was larger than would have been predicted over flat terrain, but only a single, essentially Gaussian, plume was observed. During the third test, the local meteorology was strongly influenced by nighttime drainage flows which caused strong wind directional shear with altitude. The tracer was split into two separate plumes. The crosswind spread of each of the plumes was more extensive than would have been predicted over flat terrain. The tracer driven by the winds aloft was quickly transported through the stable surface layer and detected at ground level within 3 km of the release point. The transport rate was similar to that found in laboratory experiments on neutrally stratified turbulent mixing layers, suggesting that the stability of the

surface layer was at least partially offset by the enhanced turbulence due to the terrain.

(2) No generally applicable model of pollutant transport in mountainous or hilly terrain is available. This is primarily due to the complex nature of the wind field in such terrain. Under conditions of generally uniform winds (little or no directional shear or channeling effects due to the terrain), the Gaussian model can be used to give a reasonable approximation to pollutant dispersion by employing empirical dispersion coefficients corresponding to more unstable conditions than would be predicted over flat terrain. It should be noted that even using experimentally determined horizontal dispersion coefficients, predicted pollutant concentrations cannot be expected to be more accurate than a factor of two.

(3) If there exist significant variations in the wind speed and direction, either with altitude or distance downwind, then a simple Gaussian model does not accurately predict pollutant transport and dispersion. Variations in wind direction with distance downwind can cause large uncertainties with respect to the location of the plume. Wind directional shear with altitude causes enhanced horizontal dispersion of pollutants and can lead to bifurcation of the plume. Since directional shear enhances plume dispersion, however, the Gaussian plume model can be used to provide an upper bound to the pollutant concentrations downwind of a source. If the vertical wind structure in the atmosphere can be represented by two or more layers each characterized by a single wind direction, an appropriate upper bound calculation should consider complete transport of the pollutant in each of the wind directions. If the pollutant plume is elevated, an appropriate upper bound calculation should consider the possibility of direct impingement of the plume at elevated points on the surrounding terrain. When using the Gaussian model for an upper bound calculation, flat terrain dispersion coefficients corresponding to the meteorological conditions under study should be used.

(4) In general, pollutant and/or tracer data should be analysed in order to accurately determine the levels and locations of impact associated with a pollutant source in complex terrain.

Acknowledgements—The assistance of Charles Bennett, Ross Kauper, John King, John Lawton, Kathy Lewis, Susanne Reible, Ray Reed, Henry Smith, and Sara Stage was greatly appreciated. This work was supported in part by grants from the Lake County Air Pollution Control District and the California Air Resources Board.

REFERENCES

Aris R. (1956) On the dispersion of a solute in a fluid flowing through a *tube. Proc. R. Soc. (London).* **A235,** 67–77.

Ayer H. S. (1961) On the dissipation of drainage wind systems in valleys in morning hours. *J. Met.* **18,** 560–563.

Csanady G. T. (1969) Diffusion in an Ekman layer. *J. Atmos. Sci.* **26,** 414–426.

Csanady G. T. (1972) Crosswind shear effects on atmospheric diffusion. *Atmospheric Environment* **6,** 221–232.

Defant F. (1951) Local winds. *Compendium of Meteorology,* American Meteorological Society, Boston, Mass., 655–672.

Dickerson M. H. (1980) Personal communication. Scientific Director, DOE-ASCOT Program, Box 808, Lawrence-Livermore Laboratory, Livermore, California 94550.

Drivas P. J. (1974) Investigation of atmospheric dispersion problems by means of a tracer technique. Ph.D. Thesis, California Institute of Technology, 16–26, Pasadena, California 91125.

Drivas P. J. (1980) Personal communication. Environmental Research and Technology, 696 Virginia Road, Concord, Mass. 01742.

Eatontown Signal Laboratory Group (1945) Local winds. Report No. 982, U.S. Army Signal Corps, Dugway Proving Grounds, Tooele, Utah, 50 pp.

Egan B. A. (1975) Turbulent diffusion in complex terrain, *Lectures on Air Pollution and Environmental Impact Analysis,* American Meteorological Society, Boston, Mass., 112–135.

Hinds W. T. (1970) Diffusion over coastal mountains of southern California. *Atmospheric Environment* **4,** 107–124.

Hogstrom U. (1964) An experimental study on atmospheric diffusion. *Tellus* **16,** 205–251.

Holton J. R. (1972) *An Introduction to Dynamic Meteorology.* Academic Press, New York, 319 pp.

Lamb B. K. (1978) Development and application of dual atmospheric tracer techniques for the characterization of pollutant transport and dispersion, Ph.D. Thesis, California Institute of Technology, 16–26, Pasadena, California 91125.

Lamb B. K. (1980) Personal communication. Air Pollution Research, Washington State University, 306 Dana, Pullman, Washington 99163.

McElroy J. L. (1969) A comparative study of urban and rural dispersion. *J. appl. Met.* **8,** 19–31.

Pasquill, F. (1974) *Atmospheric Diffusion,* 2nd ed., Ellis Horwood, Ltd.

Reible D. D., Shair F. H. and E. Kauper (1979) Atmospheric tracer tests conducted to determine the transport and dispersion of airborne pollutants emitted from the Red Hills geothermal area in Lake County, California. Final Report to Lake County Air Pollution Control District, Lakeport, California, 176 pp.

Reible D. D., Shair F. H. and T. B. Smith (1981) A study of the origin and fate of air pollutant's in California's central valley. Final report to California Air Resources Board, Sacramento, California.

Smith F. B. (1965) The role of wind shear in horizontal diffusion of ambient particles. *Q. Jl. R. met. Soc.* **91,** 318–329.

Start G. E., Dickson C. R. and Ricks N. R. (1974) Effluent dilutions over mountainous terrain and within mountain canyons. *Symposium on Atmospheric Diffusion and Air Pollution,* American Meteorological Society, Boston, Mass.

Tennekes H. and Lumley J. L. (1972) *A First Course in Turbulence.* MIT Press, Cambridge, Mass. 300 pp.

Turner D. B. (1973) *Workbook of Atmospheric Dispersion Estimates,* Environmental Protection Agency. AP-26, 84 pp.

Whaley H. and Lee G. K. (1977) Plume dispersion in a mountainous river valley during spring. *J. Air Pollut. Control Ass.* **27,** pp. 1001–1005.

Chapter 6

Uncertainties Associated with the Estimation of Mass Balances and Gaussian Parameters from Atmospheric Tracer Studies

by

P.A.Sackinger, D.D. Reible, and F.H. Shair

(Submitted to the Journal of the Air Pollution Control Association)

ABSTRACT

Data resulting from two atmospheric tracer experiments in the land-sea breeze winds in Los Angeles, California are used to compare the observed and released amounts of tracer (a mass balance). The mass balance calculation indicated that essentially all of the tracer transported to sea during the land breeze was transported back across the shore during the subsequent sea breeze. A methodology for calculating a mass balance and the associated uncertainties is presented. The experimental and calculation procedures presented allowed mass balance estimates with less uncertainty than is present in individual measurements of concentration or mixing height.

Similarly, a methodology for calculating dispersion parameters for the Gaussian plume model from tracer data is discussed and applied to the results of two atmospheric tracer studies conducted during the afternoon sea breeze in the Santa Barbara Channel of California. The method presented involves the integral definitions of the statistical quantities. By considering only tracer concentrations greater than 10% of the maximum concentration, and by considering sufficiently many data points, the uncertainty associated with the parameter estimation was again less than the relative uncertainties in any individual data point.

These studies were primarily designed to relate the uncertainties in estimates of mass balances and in estimations of Gaussian parameters to the uncertainties inherent within field data.

INTRODUCTION

Interest in atmospheric tracer studies has increased greatly during the last few years. Typically the results of such studies have been used to estimate empirical parameters of dispersion models, such as the Gaussian plume model (Turner, 1970)[4]. Also, to ensure the accuracy of the parameter estimation, or to accurately evaluate downwind impact, estimates of mass and/or flux balances are of great help. Unless a major portion of the tracer can be accounted for by means of such balances the associated field study results will be of limited value. The purpose of this paper is to demonstrate through example (1), a technique for estimating nominal values and uncertainties of mass balances incorporating field data and, (2), a technique for estimating nominal values and uncertainties of Gaussian dispersion parameters from field data.

PRESENTATION AND DISCUSSION OF RESULTS

MASS BALANCE ESTIMATES

Until recently, the application of mass balance calculations to atmospheric tracer studies had been limited due to the quality and quantity of available tracer and meterological data. However, the quantity of tracer and meteorological data has increased greatly during recent studies; additionally, the use of gaseous tracers (such as SF_6) has significantly improved the quality of data as compared to particle tracers, when used to tag specific masses of air (Lamb, 1978,[1] Reible, 1982[2]).

Two tracer studies conducted in July of 1977 were used to probe the transport of airborne pollutants in the land breeze-sea breeze system of the Los Angeles air basin. Sulfur hexafluoride was released from a power plant stack in El Segundo, California. The tracer was carried aloft and out to sea by the nocturnal land breeze. During midmorning the tracer mixed downward to the sea surface and was transported back across the shore during the daytime sea breeze. Further details concerning the tracer transport may be found in Shair, et al. (1981).[3] Our current study seeks to estimate the nominal value and the associated uncertainties in the amount of tracer returned across the shore during the sea breeze.

The total mass balance, for a system without sources, sinks or chemical reaction, may be written as an integral:

$$m_t = \iint_S c' \, \underline{u} \cdot \underline{n} \, dS \, dt \qquad (1)$$

where S is the surface of the control volume, c' is the mass concentration (kg/m^3), $\underline{u}$ is the tracer velocity (m/s), and $\underline{n}$ is a unit normal to the surface, S. In general, c' and $\underline{u}$ are functions of time and position, and the surface any reasonable simply connected region through which all tracer passes. Often the case with field studies, continuous data are not available and the integral is approximated by a discrete summation such as the trapezoidal rule. In this study, the control surface was the coastline between sea level and the mixing height. As indicated in Figure 1, this control surface was represented by 24 line segments. Consequently, equation (1) may be adequately approximated by

$$m_t = \sum_{i=1}^{I} \sum_{j=1}^{J} \sum_{k=1}^{K} \rho \, z_i \, u_{ij} \, c_{ijk} \left[l_{jk}^{(a)} \cos(\theta_{ij} - \phi_{jk}^{(a)}) + l_{jk}^{(b)} \cos(\theta_{ij} - \phi_{jk}^{(b)}) \right] \Delta t_i \qquad (2)$$

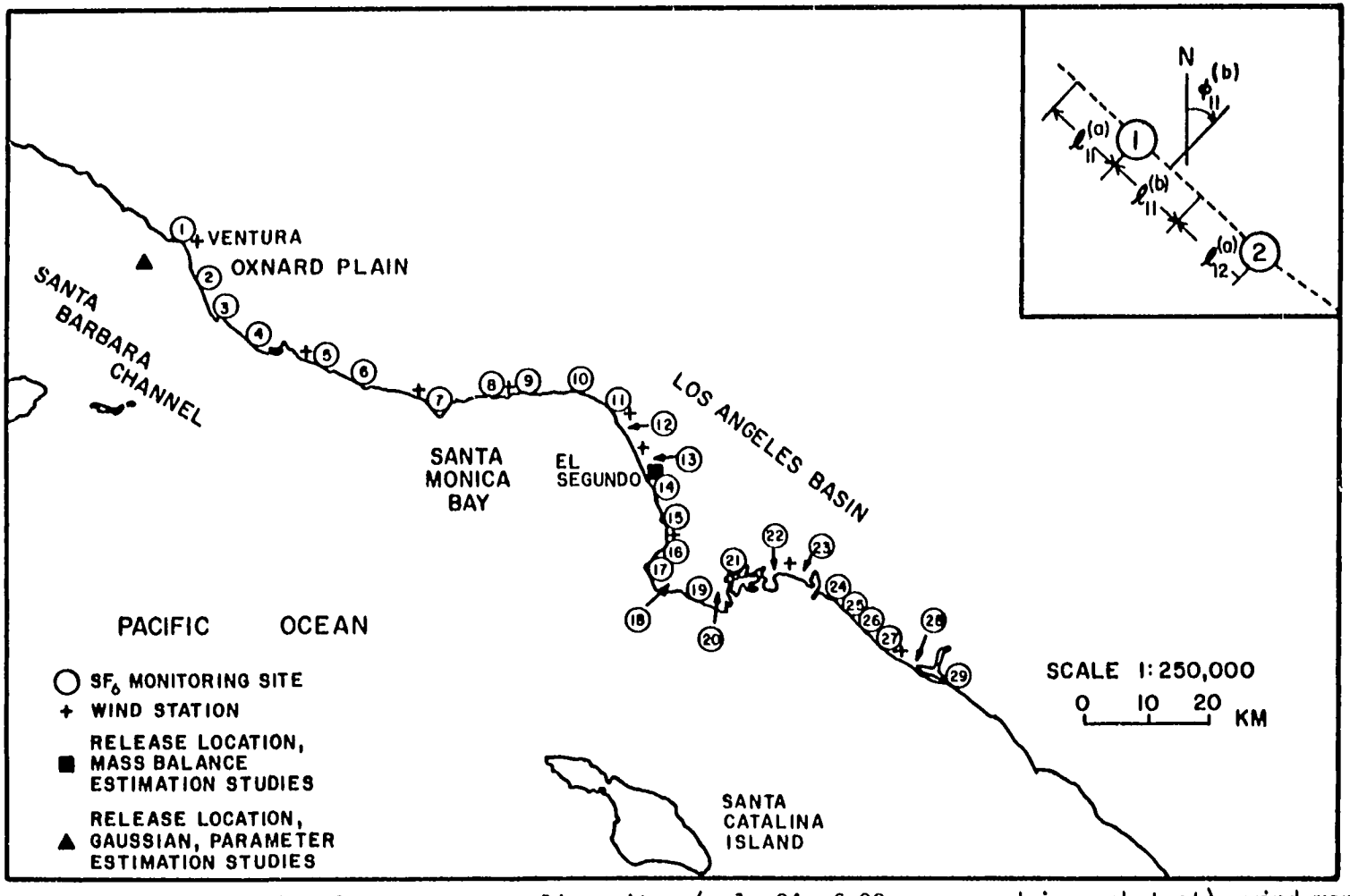

Figure 1 - Locations of hourly average sampling sites (only 24 of 29 were used in each test), wind monitoring stations, and the release point for the tests of the mass balance calculation. Also included is the location for the tests used in the Gaussian parameter estimation.

where ρ is the density of pure tracer, z_i is the mixing height, u_{ij} and θ_{ij} are, respectively, the estimated hourly averaged wind speed and direction across each segment, c_{ijk} is the hourly averaged concentration of tracer (assumed to be uniform throughout each segment), and l_{jk} and ϕ_{jk} are the length and normal angle associated with each segment defining the control surface. The time interval, Δt_i, is always one hour, i.e., hourly averaged concentrations were used. Figure 1 shows the locations of wind monitoring stations and air sampling sites. The dotted lines are the coastline segments forming the control surface. Summation is over three subscripts: i, indicates the hour, j, the wind station, and k, the air sampling site. Variables are subscripted as often as the measurements were made. Thus, for example, density was estimated once for the day from the observed average temperature and pressure, while wind velocities were measured every hour and at each of nine stations.

The results of the total mass balance calculations, for both example tests, are shown in Table 1. During both tests, essentially all of the tracer, initially transported out to sea, was returned across the shore on the day of the release. This conclusion agrees with independent calculations reported in Shair et al. (1981).[3] They used another method for constructing the control surface, as well as a different method of wind averaging. The two sets of results differ for this reason, but as will be seen, the discrepancies lie within the calculated uncertainties.

Table 1

Total Mass Balance and Uncertainty Analysis

Test Number	1	2
Date of Test	July 22, 1977	July 24, 1977
Amount SF_6 released (grams)	90,800	236,080
Amount SF_6 returned (grams)[a]	111,244	211,917
Percentage return[a]	123	90
Amount SF_6 returned (grams)[b]	95,490	244,569
Percentage return[b]	105	104
R-factors:		
R_ρ	1.000	1.000
R_z	0.165	0.165
R_c	0.038	0.034
R_u	0.067	0.080
R_ℓ	0.082	0.052
R_ϕ	0.013	0.026
R_θ	0.055	0.062
Estimated uncertainty in raw data:		
ρ - density (%)	5	
z - inversion height (%)	40	
c - SF_6 concentration (%)	30	
u - wind speed (%)	25	
ℓ - coastal length (%)	10	
ϕ - coastal angle (radians)	0.175	
θ - wind direction (radians)	0.698	
Calculated uncertainty in		
m_t - total mass returned (%)	25.4	25.5

[a](This calculation)

[b](Calculation of Shair, et al., 1981)

UNCERTAINTY ANALYSIS OF MASS BALANCE

For a function of several variables,

$$y = f(x_1, x_2, \ldots, x_n), \tag{3}$$

the uncertainty in the dependent variable is a function of the uncertainties in each of the independent variables (Bevington, 1969)[4]:

$$\sigma_y^2 = \sum_{i=1}^{n} \sigma_{x_i}^2 \left(\frac{\partial f}{\partial x_i}\right)^2 \tag{4}$$

The partial derivatives are to be evaluated for each variable which is a source of uncertainty. With the assumption that the dependent variables of the mass balance are independent of one another and are evenly and randomly distributed about the actual value of the variable, we may apply the formula to equation (2) for total mass returned to yield

$$\sigma^2_{m_t} = \left[\frac{\sigma_\rho}{\rho}\right]^2 \rho^2 \left(\frac{\partial m_t}{\partial \rho}\right)^2 + \sum_{i=1}^{I} \left(\frac{\sigma_{z_i}}{z_i}\right)^2 z_i^2 \left(\frac{\partial m_t}{\partial z_i}\right)^2$$

$$+ \sum_{i=1}^{I} \sum_{j=1}^{J} \left[\frac{\sigma_{u_{ij}}}{u_{ij}}\right]^2 u_{ij}^2 \left(\frac{\partial m_t}{\partial u_{ij}}\right)^2$$

$$+ \sum_{j=1}^{J} \sum_{k=1}^{K} \left\{ \left[\frac{\sigma_{\ell^{(a)}_{jk}}}{\ell^{(a)}_{jk}}\right]^2 \ell^{2(a)}_{jk} \left(\frac{\partial m_t}{\partial \ell^{(a)}_{jk}}\right)^2 \right.$$

$$\left. + \left[\frac{\sigma_{\ell^{(b)}_{jk}}}{\ell^{(b)}_{jk}}\right]^2 \ell^{2(b)}_{jk} \left(\frac{\partial m_t}{\partial \ell^{(b)}_{jk}}\right)^2 \right\}$$

$$+ \sum_{i=1}^{I} \sum_{j=1}^{J} \sum_{k=1}^{K} \left[\frac{\sigma_{c_{ijk}}}{c_{ijk}}\right]^2 c^2_{ijk} \left(\frac{\partial m_t}{\partial c_{ijk}}\right)^2$$

$$+ \sum_{j=1}^{J} \sum_{k=1}^{K} \left\{ \sigma^2_{\phi^{(a)}_{jk}} \left(\frac{\partial m_t}{\partial \phi^{(a)}_{jk}}\right)^2 + \sigma^2_{\phi^{(b)}_{jk}} \left(\frac{\partial m_t}{\partial \phi^{(b)}_{jk}}\right)^2 \right\}$$

$$+ \sum_{i=1}^{I} \sum_{j=1}^{J} \sigma^2_{\theta_{ij}} \left(\frac{\partial m_t}{\partial \theta_{ij}}\right)^2 \qquad (5)$$

For simplicity and convenience the following assumptions are made about the uncertainties for similar variables

$$\frac{\sigma_{z_1}}{z_1} = \frac{\sigma_{z_2}}{z_2} = \cdots = \frac{\sigma_{z_I}}{z_I} \tag{6}$$

$$\sigma_{\theta_{11}} = \sigma_{\theta_{12}} = \cdots = \sigma_{\theta_{IJ}} \tag{7}$$

etc.

The advantage of these assumptions is that constant factors (here designated by R_α) relate uncertainty in the dependent variables to that in the independent variable. Factoring the like terms outside the various sums results in a compact equation involving each R_α.

$$\sigma_{m_t}^2 = \left[\frac{\sigma_\rho}{\rho}\right]^2 R_\rho + \left[\frac{\sigma_z}{z}\right]^2 R_z + \left[\frac{\sigma_c}{c}\right]^2 R_c + \left[\frac{\sigma_u}{u}\right]^2 R_u$$

$$+ \left[\frac{\sigma_\ell}{\ell}\right]^2 R_\ell + \sigma_\phi^2 R_\phi + \sigma_\theta^2 R_\theta \tag{8}$$

For example, R_z and R_θ are:

$$R_z = \rho^2 \sum_{i=1}^{I} z_i^2 \left\{ \sum_{j=1}^{J} \sum_{k=1}^{K} u_{ij}\, c_{ijk} \right.$$

$$\left[\ell_{jk}^{(a)} \cos\left(\theta_{ij} - \phi_{jk}^{(a)}\right) \right.$$

$$\left. \left. + \ell_{jk}^{(b)} \cos\left(\theta_{ij} - \phi_{jk}^{(b)}\right) \right] \right\}^2 \qquad (9)$$

$$R_\theta = \rho^2 \sum_{i=1}^{I} \sum_{j=1}^{J} \left[z_i u_{ij} \left(\sin\theta_{ij} \Sigma_{ij}^{(c)} - \cos\theta_{ij} \Sigma_{ij}^{(s)} \right) \right]^2 \qquad (10)$$

where:

$$\Sigma_{ij}^{(c)} = \sum_{k=1}^{K} c_{ijk} \left[\ell_{jk}^{(a)} \cos\phi_{jk}^{(a)} + \ell_{jk}^{(b)} \cos\phi_{jk}^{(b)} \right] \qquad (11)$$

$$\Sigma_{ij}^{(s)} = \sum_{k=1}^{K} c_{ijk} \left[\ell_{jk}^{(a)} \sin\phi_{jk}^{(a)} + \ell_{jk}^{(b)} \sin\phi_{jk}^{(b)} \right] \qquad (12)$$

The R factors, which are independent of the uncertainties in the input data, are calculated but once for each test; the uncertainty in the dependent variable is then found from a relatively simple expression. The best estimates for the input variable uncertainties for the two example tests are presented in Table 1, along with the corresponding value of uncertainty in the total mass.

The overall uncertainties, 25% for both tests, reward the effort to include as many data points as possible. Some uncertainty was foreshadowed insofar as the mass balance calculation occasionally showed over a 100% return. In view of the uncertainties there is no catastrophe in finding a nominal value of mass returned slightly above 100%. The interpretation is that essentially all of the tracer passed through the control surface. The calculated uncertainties provide an upper bound as to what constitutes a reasonable and probable total mass return.

The variations in the coefficients of Table 1 merit inspection. As expected from statistics, R_u is smaller than R_ρ because wind speed was measured more frequently than was density. Also, as the number of significant (nontrivial) data points included in the computation increases, the contribution to the uncertainty is softened. Thus, for

example, a very narrow plume would contribute few significant data points and would be characterized by larger R values; uncertainty in the final result would be more sensitive to uncertainties in the input data. For the two example tests, both of which were characterized by broad returning plumes, the R factors were of comparable size. The effect on R values and overall uncertainty due to the number of significant data points contained in a plume will be seen later in the context of Gaussian parameter estimation.

Estimates of the independent variable uncertainties listed in Table 1 came from two sources: observations of random fluctuations due to measurement at a data point, and experiential knowledge of uncertainties brought about by the trapezoidal integral approximations. In particular, uncertainties in wind speed and direction were assigned from average deviations between two adjacent wind stations over a period of time, each assumed to be influenced by the same winds. The contribution to the uncertainty from tracer concentration measurement uncertainty can be estimated from prior experiments. Of less certitude is the accurate assessment of uncertainty contributions brought about by assuming the tracer to be well mixed over the convection layer and over the width of the sampling interval. Knowledge of the plume dispersion history is a guide for estimating such uncertainties.

GAUSSIAN PARAMETER ESTIMATE

Emissions from a point source in a uniform wind field are often distributed downwind in approximate agreement with the Gaussian model, in which the height and width of the concentration profile are correlated with atmospherice stability (Turner, 1970).[5] Under such conditions the tracer data can easily be reduced and the results compared to the predictions of the Gaussian model with the aid of integral identities for the plume parameters. The Gaussian parameters to be estimated are the horizontal standard deviation in concentration, σ_y, the plume centerline, y_o, and the centerline concentration, c_{max}. From these parameters it is possible to estimate either the vertical standard deviation in concentration, σ_z, (or, alternately, the well mixed depth of the tracer plume), or, if the vertical distribution is also measured, a mass flux balance (a comparison between observed and released tracer fluxes).

The horizontal distribution of tracer for a Gaussian plume may be described by

$$c(y) = c_{max}\, e^{-\frac{(y-y_o)^2}{2\sigma_y^2}} \qquad (13)$$

where the parameters are the same as those defined above. By standard statistical techniques, the Gaussian plume parameters can be determined from the zeroeth, first, and second moment integrals of the continuous concentration distribution,

$$I_0 = \int_{-\infty}^{\infty} c(y)\, dy \tag{14}$$

$$I_1 = \int_{-\infty}^{\infty} yc(y)\, dy \tag{15}$$

$$I_2 = \int_{-\infty}^{\infty} y^2 c(y)\, dy \tag{16}$$

The appropriate formulae for the plume centerline location, crosswind standard deviation in concentration, and the centerline maximum concentrations are:

$$y_0 = I_1/I_0 \tag{17}$$

$$\sigma_y^2 = I_2/I_0 - y_0^2 \tag{18}$$

$$c_{max} = I_0/\sqrt{2\pi}\sigma_y \tag{19}$$

For sampling traverses which are not straight, or oriented precisely crosswind, suitable average correction factors can be applied, or the traverse data projected, point by point, onto a straight line segment which is orthogonal to the wind. In order to limit the influence of low concentrations far from the plume centerline, where, presumably, the tracer detection technique is less accurate, the integration interval is contracted, excluding concentrations less than 10% of the maximum. The neglected integral area can be included by applying a correction factor for neglected area under a suitably normalized exact Gaussian curve. The normalization procedure includes choosing an exact Gaussian distribution with the same centerline maximum concentration and standard deviation in concentration, σ_y, and by shifting the abscissa of the experimental data to align the origin with the plume centerline. This normalization procedure gives the following relations between the complete (I) and contracted integrals (I'):

$$I_0 = k_0 I_0' \tag{20}$$

$$I_1 = k_1 I_1' \tag{21}$$

$$I_2 = k_2 I_2' \tag{22}$$

where

$$k_0 = 1.032925 \tag{23}$$

$$k_1 = 1.032925 \tag{24}$$

$$k_2 = 1.254861 \tag{25}$$

The algorithm used here for estimating the appropriate Gaussian parameters is:

(1) Evaluate plume centerline location using all data, including data points extending past concentrations less than 10% of the observed maximum.

(2) Shift the position coordinate axis so that the plume centerline, calculated above, coincides with the origin.

(3) Evaluate the horizontal dispersion coefficient, σ_y, and the plume centerline concentration, c_{max}, using the fully extended limits of integration as in step 1.

(4) By interpolating (linearly or otherwise) between appropriate points, find the location corresponding to 10% of the centerline concentration as calculated in step 3.

(5) Recalculate the best fit Gaussian parameters by evaluating the appropriate integrals between the limits specified in step 4.

(6) If necessary, repeat steps 4 and 5 until the limits of integration are at 10% of the recalculated maximum concentration.

Additionally, as was done for the total mass balance, the trapezoidal rule is used to approximate the integrals to accommodate discrete sampling. For four data points equidistant in the integration interval (interval defined as the region between the locations corresponding to 10% of the maximum concentration), the errors introduced by the trapezoidal approximation are no more than 4%: plume centerline location calculations are affected least by the approximation. Fewer data points lead to significantly larger errors in the parameter estimation. A rule of thumb is, therefore, to have at least one data point every horizontal standard deviation, σ_y, across the plume, since the 10% limits encompass about a 4.3 σ_y distance in the plume.

Two SF_6 releases in the Santa Barbara Channel conducted on September 24 and 28, 1980, under stable transport conditions gave rise to concentration profiles suitable for comparison to the

Gaussian model (Reible, 1981)[6]. The tracer was released from 9 km offshore, as indicated in Figure 1. Grab samples were gathered by automobile teams traversing along the coastline between hourly-averaged sampling locations 1 and 2 in Figure 1. The observed concentration profiles are indicated in Figure 2. Using the formulae developed above for finding Gaussian plume parameters, concentration versus distance data for the three traverses were reduced; the results are contained in Table 2. In all instances the calculated horizontal dispersion parameter indicated greater stability than might be anticipated from the vertical temperature profile. It should be noted, however, that the automobile traverse data represent short time averages (between 3 and 10 minutes). As the sample averaging time increases, the observed plume generally becomes flatter and broader due to meandering of the wind (Reible, 1981)[6]. This could account for the difference between the observed atmospheric stability and that indicated by the tracer data.

UNCERTAINTY ANALYSIS OF GAUSSIAN PARAMETER ESTIMATES

Analogous to the procedure used for the total mass balance calculation, equation (4) may be applied to the formulae for the Gaussian plume parameters. We collect terms assuming the same uncertainty in similar variable, i.e., assuming

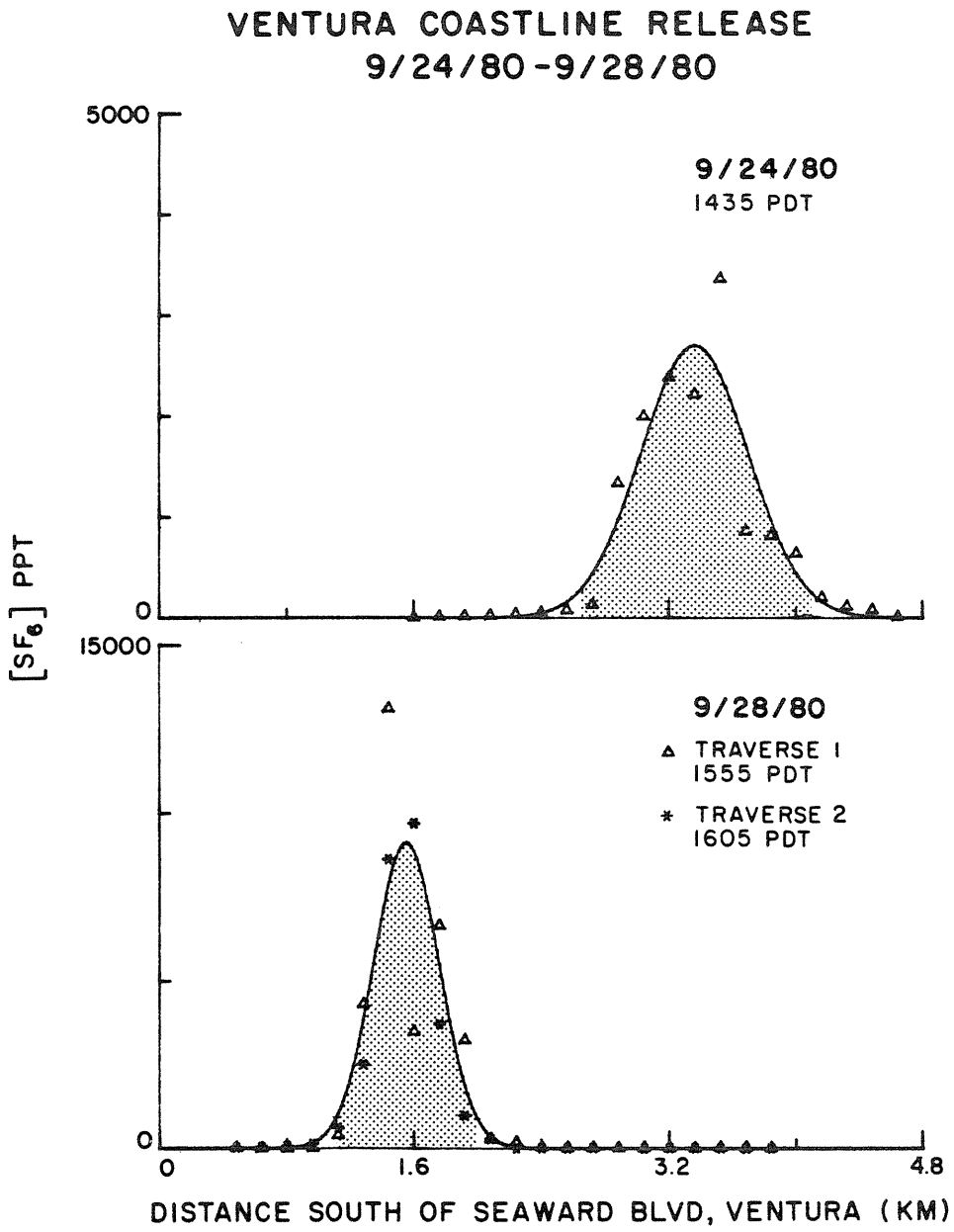

Figure 2 - Concentration profiles from automobile traverses. Gaussians are fit to three traverses; the last two traverses were of the same plume and the fitted curve combines both data sets. The shaded region indicates the limits of the integration for the curve fitting procedure.

Table 2

Gaussian Plume Parameters and Uncertainty Analysis

Traverse number	1	2*	3*
Date of test	9/24/80	9/28/80	9/28/80
Plume parameters			
y_o (km)	3.38	1.56	1.54
σ_y (km)	0.38	0.23	0.18
c_{max} (PPT)	2730	9150	9410
R-factors:			
$R_c^{(y_o)}$	0.0033	0.0027	0.0013
$R_c^{(\sigma_y)}$	0.032	0.040	0.052
$R_c^{(c_{max})}$	0.25	0.40	0.51
$R_y^{(y_o)}$	0.05	0.10	0.06
$R_y^{(\sigma_y)}$	0.040	1.14	0.60
$R_y^{(c_{max})}$	0.92	2.92	1.99
Estimated uncertainty in raw data:			
c - concentration (%)	30		
y - distance crosswind (km)	0.16		
Calculated uncertainty in			
y_o (km)	0.06	0.08	0.06
σ_y (%)	11.5	18.2	14.2
c_{max} (%)	21.5	33.4	31.2

*These traverses were within one hour of one another, during the same release.

$$\sigma_{y_1} = \sigma_{y_2} = \cdots = \sigma_{y_n} \tag{26}$$

$$\frac{\sigma_{c_1}}{c_1} = \frac{\sigma_{c_2}}{c_2} = \cdots = \frac{\sigma_{c_n}}{c_n} \tag{27}$$

we obtain

$$\sigma_{y_0} = \sigma_y^2 R_y^{(y_0)} + \left[\frac{\sigma_c}{c}\right]^2 R_c^{(y_0)} \tag{28}$$

$$\sigma_{\sigma_y} = \sigma_y^2 R_y^{(\sigma_y)} + \left[\frac{\sigma_c}{c}\right]^2 R_c^{(\sigma_y)} \tag{29}$$

$$\sigma_{c_{max}} = \sigma_y^2 R_y^{(c_{max})} + \left[\frac{\sigma_c}{c}\right]^2 R_c^{(c_{max})} \tag{30}$$

Equations 28-30 simply describe the dependence of the uncertainty in the various plume parameters upon uncertainty in position and uncertainty in concentration. Estimates for the uncertainty in postion and concentration, the R factors for equations 28-30, and the final results of the calculations are shown in Table 2. Note the

lesser uncertainty for Test 1, with its wider plume: more significant data points are included in the determination of the Gaussian parameters.

Distinct from the issue of input data uncertainty is whether a Gaussian model accurately depicts the physical situation. Using a standard statistical technique, the so-called chi-squared test, the deviations of the experimental data from the fitted Gaussian curves indicate that the parent distribution of tracer is not Gaussian (Bevington, 1969).[4] Due to nonuniformities in the mean and turbulent wind field, the assumption that the tracer is normally distributed crosswind is but a crude approximation. It is, however, a level of approximation consistent with the current state of knowledge on dispersion in the atmosphere, and, for plumes such as those of Figure 2, a very useful approximation.

SUMMARY AND CONCLUSIONS

A method for estimating nominal values and uncertainties associated with mass balances has been demonstrated by way of example. For the cases studied the nominal values of mass returned across the shore were in good agreement with that known to have been released into the land breeze; that is, essentially all of the tracer returned across the control surface. In these cases the total uncertainties in the nominal values (about 25%) were actually less than the uncertainty in any individual measurement of concentration or mixing height (30%-40%). This is simply a reflection of the effect of statistical cancellation of errors distributed randomly about the actual value of the measured variables, but, nonetheless, clearly demonstrates that a complicated calculation such as the tracer mass balance may be subject to less uncertainty than might otherwise be expected.

A technique for fitting data to the Gaussian plume model was also demonstrated, using the integral definitions of the Gaussian dispersion parameters. The technique presented was relatively insensitive to uncertainties in the data; relative uncertainty in plume centerline location and horizontal standard deviation in concentration were much less than the relative uncertainties in individual measurements of concentration or location. However, to ensure good results at least four approximately equidistant sampling points must lie between the locations corresponding to 10% of the

maximum concentration, i.e., data points should be spaced no farther than one σ_y apart.

References

1 Lamb, B. K., "Development and Application of Dual Atmospheric Tracer Techniques for the Characterization of Pollutant Transport and Dispersion," Ph.D. Thesis, California Institute of Technology, 16-26, Pasadena, CA, 1978.

2 Reible, D. D., "An investigation of the Transport and Dispersion of Atmospheric Contaminants in the Mountain-Valley and Coastal Regions of California," Ph.D. Thesis, California Institute of Technology, 16-26, Pasadena, CA, 1982.

3 Shair, F. H., Sasaki, E. J., Carlan, D. E., Cass, G. R., Goodin, W. R., Edinger, J. G., and Schacher, G. E., "Transport and Dispersion of Airborne Contaminants in the Santa Barbara Channel Area of Southern California," in press, Atmospheric Environment, (1981).

4 Bevington, P. R., Data Reduction and Error Analysis for the Physical Sciences, McGraw-Hill, New York, pp. 56-60, 1969.

5 Turner, B., "Workbook of Atmosperic Dispersion Estimates," U.S. Environmental Protection Agency, Research Triangle Park, North Carolina, 1970.

6 Reible, D. D., and Shair, F. H., "The Transport and Dispersion of Airborne Contaminants in the Santa Barbara Channel Area of Southern California," submitted to Atmospheric Environment, (1982).

Chapter 7

The Origin and Fate of Air Pollutants in California's San Joaquin Valley

I. Winter

by

D.D. Reible, F.H. Shair, T.B. Smith, and D.E. Lehrman

(Submitted to Atmospheric Environment)

Abstract

A series of 19 atmospheric tracer experiments, 7 during the winter of 1978-1979 and 12 during the summer of 1979, were conducted to determine the transport route of pollutants into, within, and out of the San Joaquin Valley of central California. In this, the first of two papers reporting the results of the study, the ventilation characteristics of the valley during wintertime conditions are discussed.

During the winter, the San Joaquin Valley is characterized by very stable atmospheric conditions. The 24 hr average air flow at the northern mouth of the valley is directed towards the north and out of the valley. Based upon the calculated flux out of the valley during this period, the average residence time of air within the valley was about 8-12 days. The actual residence time of pollutants within the valley is generally much shorter, however, due to the effective ventilating action of the passage of low pressure troughs which occur with an average period of about 6 days. The tracer experiments confirmed the relatively low ventilation rates within the valley in that essentially all of the tracer was accounted for within the valley on days subsequent to its release. During one experiment, even after four days, mass balance estimates indicated that half of the tracer remained in the valley. Releases in the southern part of the valley indicated that the tracer, and thus any air pollutant, was effectively mixed throughout the southern part of the valley

within 24-48 hours after its release. This cross-valley mixing could not be explained on the basis of meteorological observations, even though the normally available wind sampling network was supplemented with pilot balloon observations.

Because of the low ventilation rates in the San Joaquin Valley there is a great potential for air pollution during the winter months. Also, between frontal passages, the stable atmospheric conditions lead to extensive periods of dense fog which have an, as yet unkown, effect upon the heterogeneous conversion of SO_2 to sulfate in the atmosphere.

Introduction

As the demands man has placed upon his environment have become increasingly more stringent, there has been more and more concern with the efficient allocation of the world's resources. It has proved exceedingly difficult to balance the often conflicting pressures posed by the need to retain land for agricultural and urban uses, develop mineral and energy reserves, and to retain uncontaminated air and water resources. The objective of this work is to evaluate the potential for air quality degradation in the San Joaquin Valley of central California due to agricultural, industrial and urban development.

The San Joaquin Valley is a large inland valley about 380 km in length and 80 km in width. Bounding the fairly level and featureless valley floor are the Sierra Nevada Mountains to the east (peak heights in excess of 4000 m), the Tehachapi Mountains to the south (peak heights of 1500-2000 m), and the California coastal mountains to the west (peak heights of 1000-1500 m). The general topography of the valley is indicated in Figure 1. Primarily due to the presence of a semi-permanent subtropical high pressure belt off the California coast, the climate of the San Joaquin Valley is essentially Mediterranean, with hot, dry summers and cool, rainy winters. Much of the local meteorology is controlled by the interaction of the prevailing pressure gradient from the coast to the inland desert areas of the United States and the mountain-valley breezes that develop due to differential

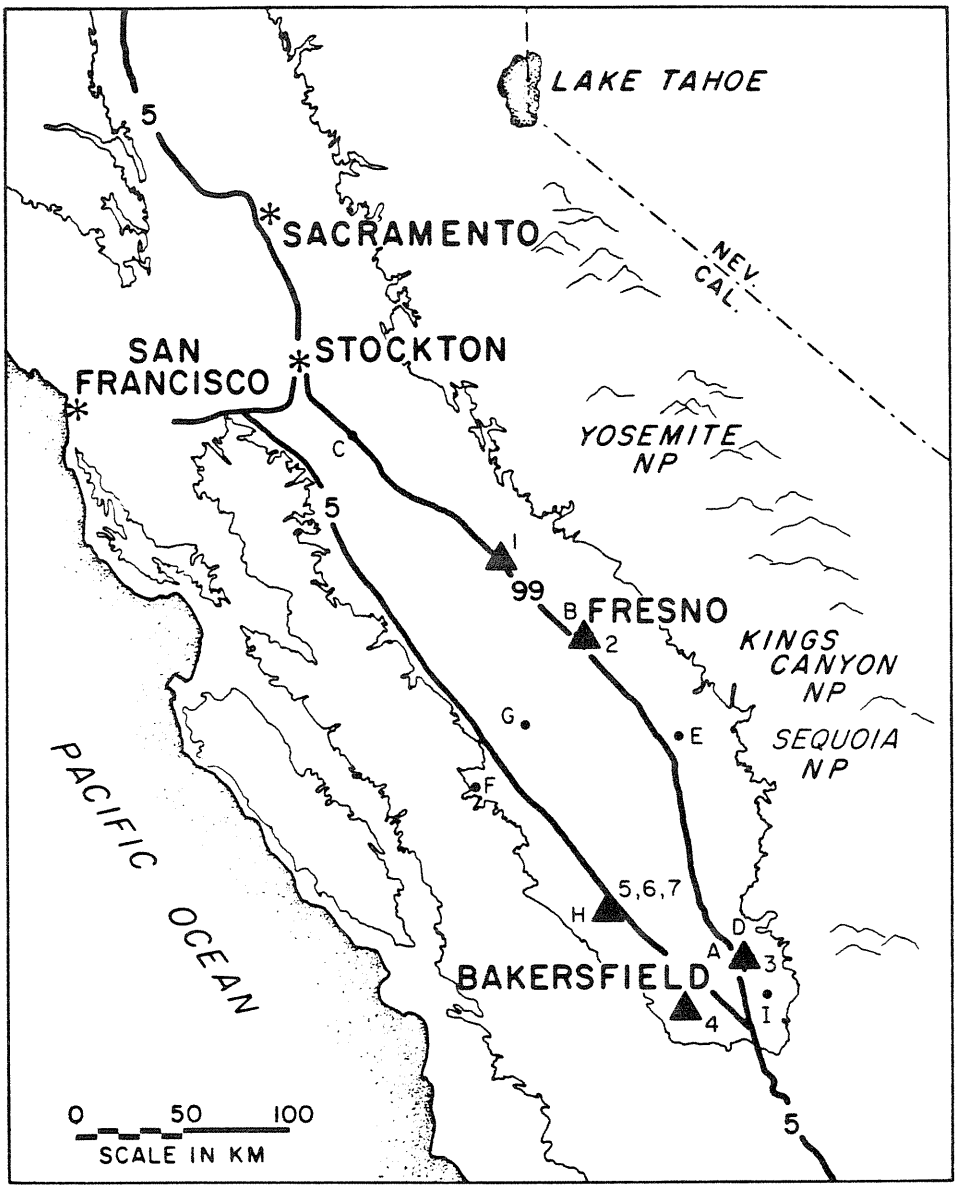

Figure 1 - Map of the San Joaquin Valley indicating release locations for each test (▲), and pollutant monitoring sites reported in Table 2 (•).

heating between the sloping surfaces and the valley floor. Due to a normally long growing season and sufficient mountain runoff water for irrigation, the valley has developed into a major agricultural producer, with a crop value in excess of 4 billion dollars annually (Census of Agriculture, 1981). In addition, almost 200 million barrels of oil and 4.1 billion liters (at standard conditions) of natural gas are produced annually (California Abstracts, 1980). This production rate can be expected to rise as the value of the oil increases. Also, the valley faces significant urbanization in the coming years with a 17% population growth between 1970 and 1978 (World Almanac, 1972 and World Almanac, 1981). These conflicting environmental pressures have already caused some air pollution problems. A California Air Resources Board staff report (CARB 76-19-4, 1976) estimates that annual crop losses may have reached $32,000,000 per year as a result of ozone and other airborne contaminants. In addition, mid-day visibility within the San Joaquin Valley is less than that specified in the California ambient air quality standard (i.e., less than 10 miles when the relative humidity is less than 70%) about a third of the time (Duckworth and Kinney, 1978). It is clear that in order to efficiently allocate the finite amount of available resources equitably among the potential users it is necessary to evaluate the negative air quality impact of each use in addition to its potential economic or social benefits. It was this need that formed the impetus for the current study.

The specific objectives of this study were threefold.

1. Identify the transport routes into, within and out of the San Joaquin Valley.
2. Determine the chemical composition of the particulate matter in the valley and trace the sources of this material.
3. Acquire an aerometric data base that can be used in air quality model simulation of the photochemical formation and transport in the valley.

In view of the comprehensive and complex nature of the study, it was conducted as a cooperative effort by four organizations, Meteorology Research, Inc. (Altadena, Ca.), the California Institute of Technology (Pasadena, Ca.), the Rockwell Air Monitoring Center (Woodbury Park, Ca.), and Environmental Research and Technology (Westlake Village, Ca.). The results of the study embody a report to the California Air Resources Board (Smith, et al., 1981). The current paper will emphasize the findings of the study with respect to the first objective, the identification of the transport routes into, within, and out of the San Joaquin Valley. This aspect of the study involved extensive meteorological and pollutant measurements as well as atmospheric tracer experiments. The study was broken into two basic meteorological regimes, winter and summer, and for clarity, the current paper describes only the transport and dispersion of pollutants in the San Joaquin Valley during the winter. A separate paper will describe the behavior of pollutants in the valley during summer atmospheric conditions (Reible, et al., 1982).

Experimental Procedure

The study consisted of three intensive field programs, each of about three weeks duration. Field programs were carried out in November-December, 1978, and in July and September, 1979, in order to examine seasonal variations in the valley characteristics. During the November-December field program, 5 releases of the atmospheric tracer, sulfur hexafluoride (SF_6), were conducted with the support of extensive meteorological and air quality measurements. In addition, two other tracer releases were conducted during February and March, 1979, but with limited meterological support.

The meteorological observations during the first 5 winter tests included a surface wind network which included existing, as well as supplemental, stations. During the November-December, 1978, program, the winds aloft were measured via pilot balloons at 3 and occasionally 4 locations within the valley. An acoustic sounder was used to assist in the estimation of the vertical mixing height. The vertical mixing height was also inferred from vertical pollutant and temperature distributions measured by aircraft. In addition, pibal measurements were used as an indicator of layering in the atmosphere since the interface between layers typically exhibits significant wind speed and directional shear.

Air quality measurements included airborne observations by Meteorology Research, Inc., of sulfur dioxide, ozone, oxides of nitrogen, and light scattering coefficient. The aircraft used to make these observations typically traversed particular sections of the San Joaquin Valley during each tracer release. Some traverses were designed to transect pollutant plumes from significant source areas while others were designed to measure the regional background pollutant levels. The airplane was also used to observe the vertical distribution of pollutants at specific locations through spirals. In addition to the mobile airborne pollutant sampling, similar measurements were made at ground level in three vans operated by Rockwell. Also located at the Rockwell vans were filter samplers for particulates that were later analyzed by Environmental Research and Technology (ERT). The ERT analysis consisted of speciation of the collected particulates and source determination by the chemical element balance method (Friedlander, 1973 and Watson, 1979).

The atmospheric tracer releases were conducted by the California Institute of Technology. The tracer employed for these studies was sulfur hexafluoride (SF_6). SF_6 is a non-toxic, colorless, odorless gas that can be detected by electron capture gas chromatography at concentrations as low as 1-10 parts SF_6 per trillion parts air (PPT). The analytical procedure, as well as instrument accuracy and calibration procedures, has been described by Lamb (1978). A gaseous atmospheric tracer provides a true measure of the tranport winds from a particular release site.

Because the grid over which tracer concentrations can be measured is typically much finer than it is feasible to measure the wind field, it is sometimes easier to infer the wind field from tracer measurements than from direct wind observations. All air samples for tracer concentrations were collected in 30 cm^3 plastic syringes. During airplane or automobile traverses, grab samples were collected at regular time or distance intervals from a specified start point. In addition, automatic samplers were used to determine hourly-averaged concentrations at specified fixed sites. The automatic samplers pull a 30 cm^3 syringe over the course of an hour, at the end of which the syringe is sealed and the subsequent syringe started. Generally, automatic sampling continued for 24 hours during a given experiment, although sampling periods as long as 96 hours were employed during some tests.

The tracer release locations were chosen to meet the specific objectives of a particular test. In most cases, this meant that the tracer was being used to tag a particular source region. During some experiments, however, the objective of a particular test was to evaluate the transport and dispersion of pollutants in a particular flow structure observed within the valley. A summary of the late fall and winter tracer experiments are included in Table 1. The locations of these releases are shown in Figure 1.

Table 1

Fall and Winter Tracer Releases

Test 1 - Release of 45 kg SF_6 per hour between 1100 and 1600 PST, 11/15/78, from Chowchilla

Test 2 - Release of 43 kg SF_6 per hour between 1300 and 1700 PST, 11/18/78, from Fresno

Test 3 - Release of 25 kg SF_6 per hour between 1200 and 1700 PST, 11/35/78, from Bakersfield

Test 4 - Release of 38 kg SF_6 per hour between 1300 and 1700 PST, 11/28/78, from Valley Acres in the Elk Hills

Test 5 - Release of 44 kg SF_6 per hour between 1400 and 2030 PST, 12/8/78, from Lost Hills

Test 6 - Release of 24 kg SF_6 per hour between 2000 PST, 2/6/79, and 0800 PST, 2/7/79, from Lost Hills

Test 7 - Release of 27 kg SF_6 per hour between 2030 PST, 3/6/79, and 0800 PST, 3/7/79, from Lost Hills

Presentation and Discussion of Results

Overall Valley Ventilation

As mentioned previously, the valley winds are normally dominated by the interaction of the pressure gradient from the coast to the inland deserts and the local terrain influences of the mountains surrounding the valley. The coastal-inland pressure gradient is lowest during the winter. For example, the pressure difference between San Francisco and Las Vegas during January of 1975, for example, averaged only 1.1 mbs, about 15% of the average pressure difference detected during June of the same year. An analysis of the wind velocities at the northern mouth of the San Joaquin Valley (as measured at the surface at Stockton) during the same year indicates that there is a weak net flow out of the valley during January and February. The 24-hour net velocity during these months was less than 1 mps, which can be compared to a net 24-hour velocity in excess of 3 mps into the valley throughout most of the summer. Assuming that the efflux at the northern mouth of the valley during the winter is the only significant exit from the valley during the stagant winter conditions, it is possible to estimate the mean residence time of an air parcel within the valley. The average out-of-valley wind speed observed at Stockton during January, 1975, was 0.36 mps, and 0.52 mps during February, 1975. Assuming that these are typical values, and assuming a typical mixing height of about

500 m (validated during the current test program), and an 80 km valley width, these wind velocities correspond to a volumetric flow of about 50 km^3/hour during January and 75 km^3/hour during February. Since the valley is 380 km long and 80 km wide, and again assuming 500 m deep, the average residence time of an air parcel within the valley is approximately 8-12 days during these winter months.

A second means of transport across the valley borders involves the thermally driven slope flows on the surrounding mountains. During the summer, extensive slope heating leads to strong afternoon flows directed upslope. During the winter, however, the limited afternoon heating weakens the upslope flow with respect to the corresponding nighttime drainage flow which is driven by surface cooling of the slopes. This results in a relatively limited 24 hour net flow either in or out of the valley. Also, due to the apparently limited vertical mixing within the valley during cool, stable winter conditions, very little air is transported aloft and out of the valley during the winter.

Due to the influence of synoptic pressure upsets (i.e., passage of frontal movements through the valley), the actual residence time of an air parcel is frequently less than that suggested from the previous discussion (8-12 days). The enhanced vertical mixing and higher wind speeds observed during frontal passages rapidly reduce pollutant levels giving rise to a rapid increase in visibility. The observation of visibilities in excess

of 16 km can be used as a rough indicator of the occurrence of frontal system passages. Between 1967 and 1977, visibilities in excess of 16 km were detected at Fresno an average of 10-11 days in December and January and 19 days in February. Assuming that each frontal system passage efficiently ventilates the valley for 2 days, these data suggest that the average length of stable, low visibility conditions during December and January was 4 days. Thus, on average, frontal system passage accounts for a more rapid ventilation of the valley than the efflux of air at the valley mouth. Clearly, however, an extended period without frontal system passage can lead to a significant buildup of valley pollutants due to inadequate ventilation.

Pollutant dispersion within the valley

The previous section described the overall ventilation characteristics of the San Joaquin Valley by considering the volumetric flow balance at the borders of the valley. The current section, however, will describe the implications of the overall ventilation characteristics on the internal distribution of pollutants in the valley, as observed during the test program. As mentioned in the preceding section, in the absence of frontal system passage, the volume of air transported across the borders of the valley during each day was estimated to be only about 1/8 or 1/12 of the total volume of the surface layer of the valley. As expected from this statistic, wind speeds within the valley were generally light and variable. Between storm fronts, the

valley atmosphere was extremely stable and moisture from winter rainfall and extensive irrigation led to persistent fogs. During each January, an average of 10 days of fog was observed between 1970 and 1979, and in at least one case fog was observed for 21 consecutive days. Visibility during these foggy periods was reported as less than 3.2 km. The importance of the fog from the air pollution standpoint is the probable participation of the water in the heterogeneous conversion of SO_2 to sulfate. Peak sulfate measurements in Bakersfield in 1978-1979 occurred in December to February during the months when fog or high humidities were most present. Bakersfield is located in Kern County, in which about 274 tons of SOx is emitted daily (Technical Services Division, California Air Resources Board, 1979). Of this, 230 tons per day, or 84%, were emitted during the combustion of fossil fuels by the petroleum industry. The highest 24 hour average aerosol sulfate concentration to date in California, 80 $\mu g/cm^3$, was found near Bakersfield in December, 1978 (Duckworth and Crowe, 1979). These figures are expected to increase as the oil reserves in the southern San Joaquin Valley are developed further.

During the November-December field program, as in the preceding 11 year period, stagnant conditions were broken by occasional intrusions of cold air troughs. As shown in Figure 2, a negative correlation existed between the visibility at Bakersfield and the temperature at the 850 mb pressure level. Stagnant conditions, as measured by a visibility of less than 16 km at Bakersfield, persisted during periods of from 2 to 8 days.

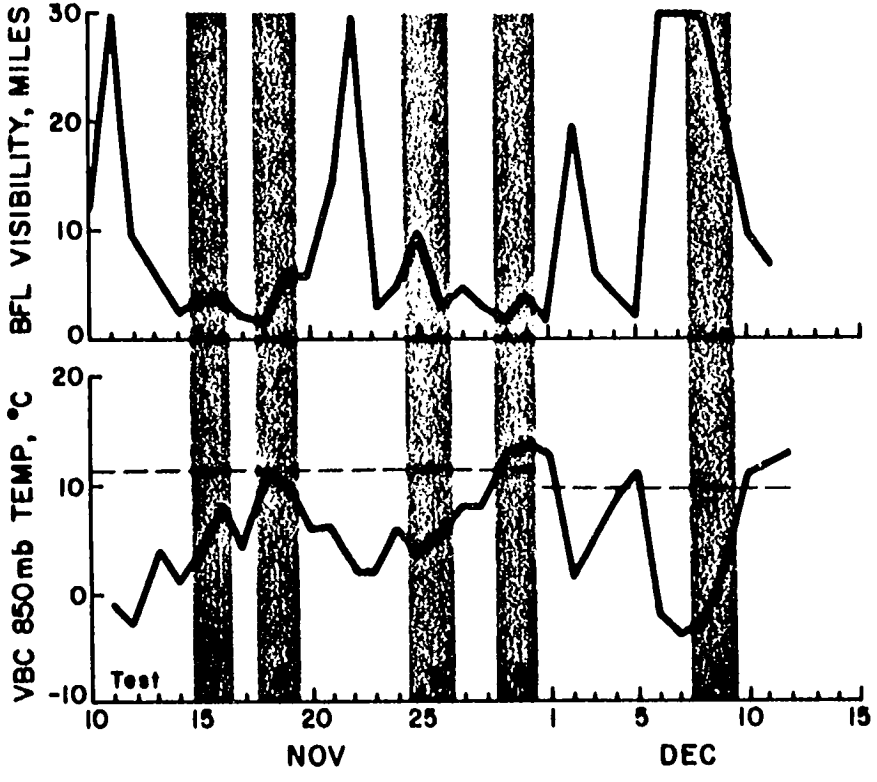

Figure 2 - Comparison of visibility at Bakersfield and the air temperature at the 850 mb pressure level during the November-December, 1978, test period. The shaded regions indicate the individual tracer release periods.

The first five atmospheric tracer experiments were conducted during stable periods as shown in the figure. As expected from the previous discussion, the dispersion of the tracer during these stable conditions was extremely limited. The tracer concentrations observed almost 30 hours after the start of the first release, for example, are shown in Figure 3. Assuming that the average concentration of 50 PPT SF_6 detected during this traverse was well-mixed to an altitude of 500 m within the rectangle outlined in the figure, about 90% of the released tracer was within 110 km of the release site. This release, from Chowchilla on the eastern side of the valley, was conducted in light southerly winds that later reversed. During both releases from the northern half of the valley (Test 1 and 2), most of the SF_6 was limited to a relatively narrow band along the eastern side of the valley. This differs from the subsequent 5 experiments conducted at the southern end of the valley. During each of these experiments, the tracer was mixed, over a period of days, throughout the southern end of the valley. This phenomenon discloses a great deal about the flow patterns in the southern valley, and thus merits closer consideration.

In that part of the San Joaquin Valley south of Fresno, the nighttime drainage flows from the surrounding mountain slopes form a convergence zone near the center of the valley. It was not known prior to the experiments what effect the convergence would have on the cross-valley transport of the tracer. During Test 4

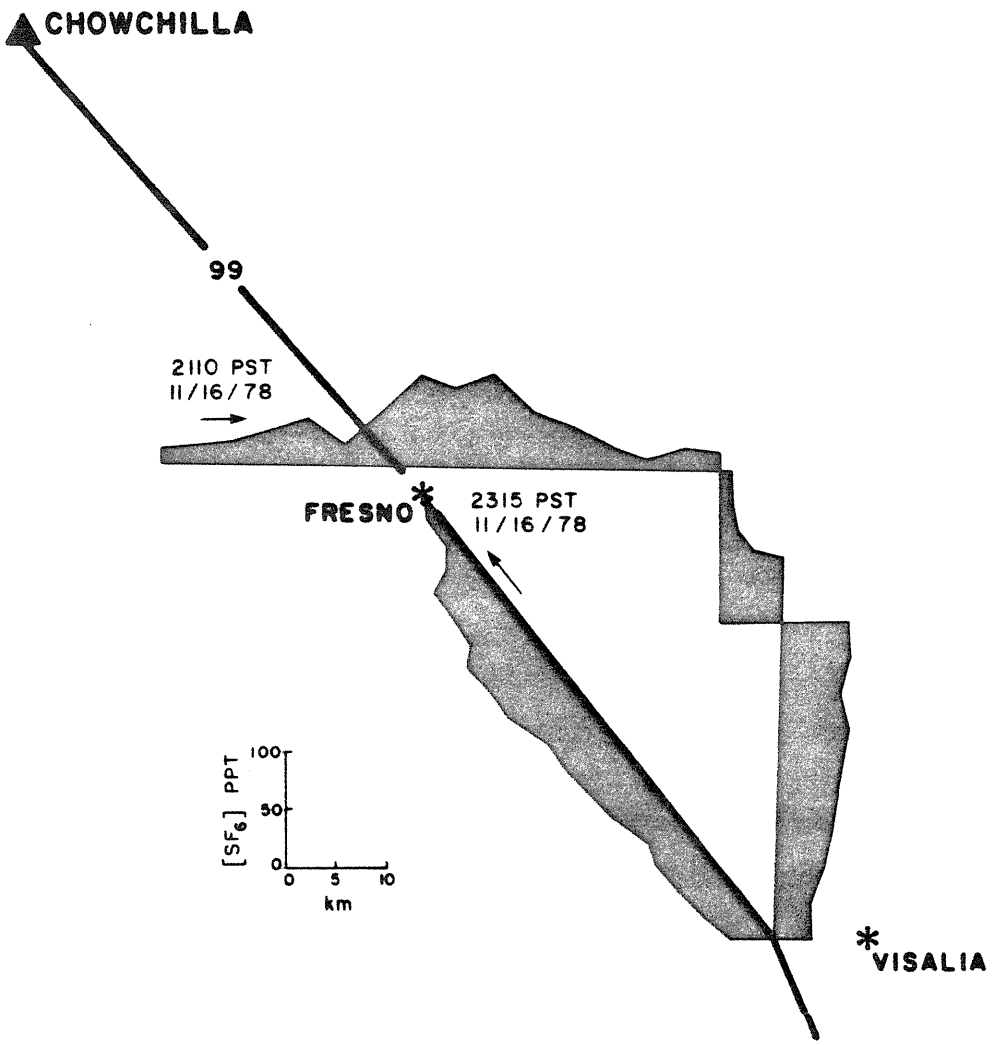

Figure 3 - SF_6 concentrations observed during an automobile traverse conducted between 2110 and 2315 PST, 11/16/78. Release was conducted at Chowchilla between 1100 and 1600 PST the previous day.

SF_6 was released during the early aftenoon from the Elk Hills in the southwestern valley. This region is near large oil fields which are significant pollutant sources in the San Joaquin Valley. Figure 4 depicts surface wind streamlines at 13 and 22 PST, 29 November and at 10 PST, 30 November, respectively. At 13 PST and at 10 PST on the following day, generally light, upslope winds were noted in most locations. At 22 PST on the day of the release, however, the nighttime downslope, or drainage, flow had led to the development of a convergence zone in mid-valley. The experimentally determined hourly-averaged tracer concentrations at fixed sampling sites is shown in Figure 5. As shown by the figure, when the initial easterly winds reversed shortly after nightfall, the tracer was apparently split into two plumes, one transported more northward and later observed at Delano and Richgrove, and one transported directly eastward and later observed at Greenfield and Lamont. A wind reversal is a complex meteorological phenomenon and even with the extensive wind monitoring network established for this test program it was not possible to predict the plume trajectory during the wind reversal. The effect of the wind reversal was to spread the tracer over a wide area, although in this case, apparently not uniformly. The reversed winds transported the tracer towards the predicted location of the flow convergence zone near the center of the valley. The flow convergence probably slowed the eastward movement of the tracer but by early the next morning the SF_6 was detected east of the presumed location of the convergence zone.

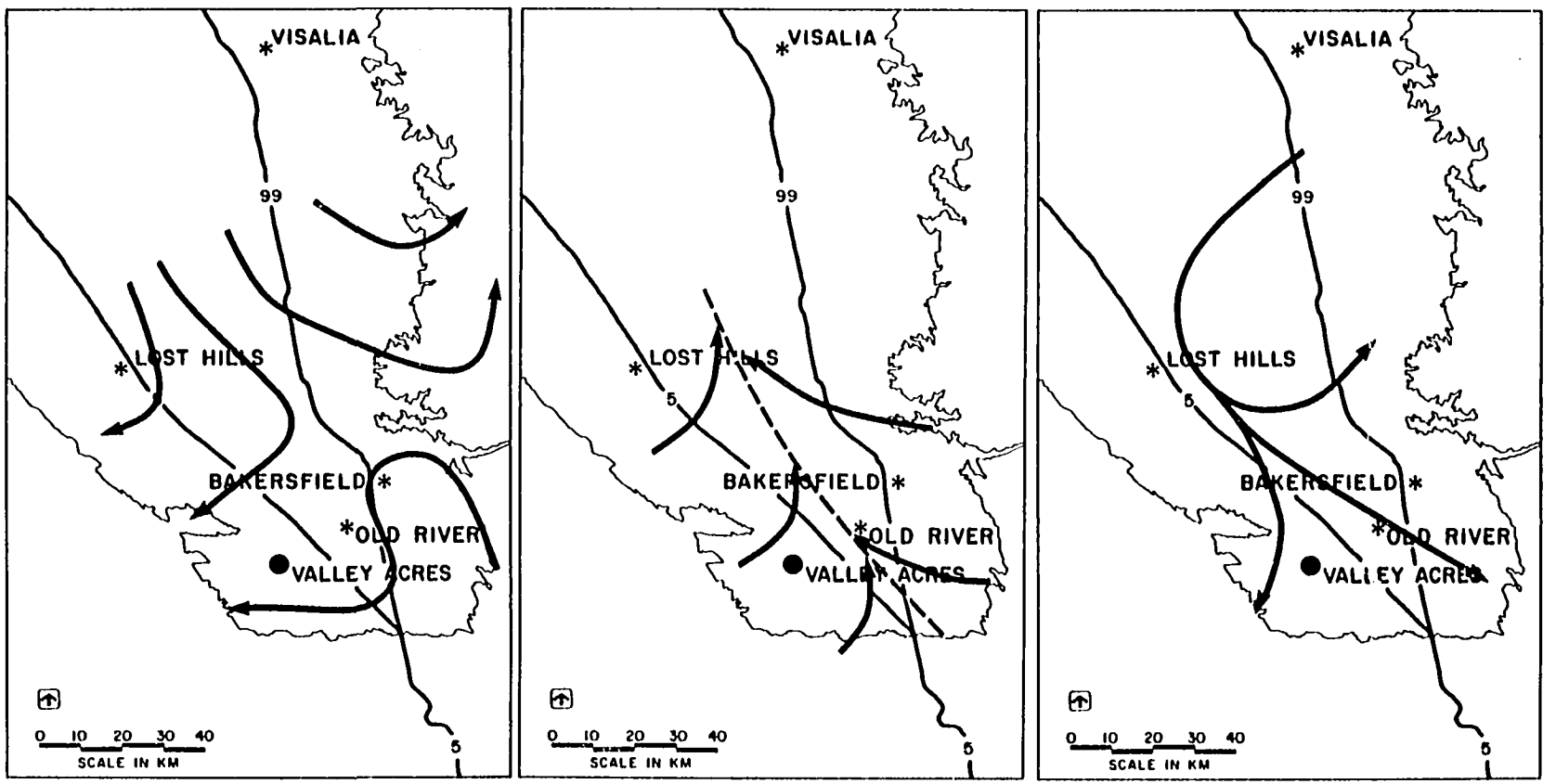

Figure 4 - Surface wind streamlines observed in the southern San Joaquin Valley during the fourth tracer test. SF_6 was released from Valley Acres, in the Elk Hills, between 1300 and 1700 PST, 11/29/78.

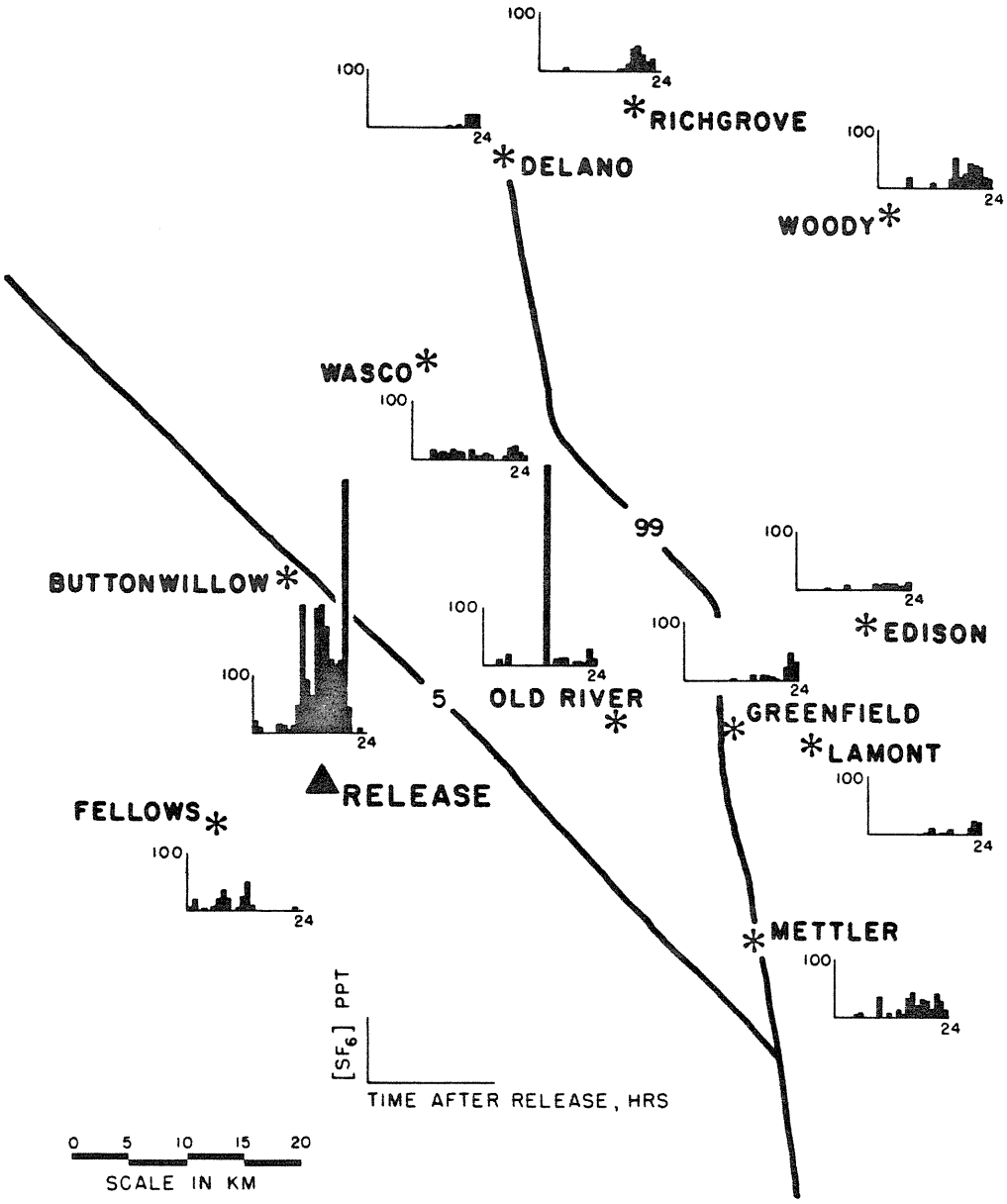

Figure 5 - Hourly-averaged tracer concentrations observed after the release of tracer from Valley Acres between 1300 and 1700 PST, 11/29/78.

Cross-valley transport was clearly noted in all 5 tracer experiments conducted in the southern valley during the winter. During this particular test, a maximum hourly-averaged concentration of about 200 PPT per kg-mole of SF_6 released per hour was detected on the east side of the valley by mid-morning on the day following the release. As shown in the figure, the southern tracer plume was continually transported eastward throughout the afternoon on the day after the release and was apparently transported into the Tehachapi Mountains east of Bakersfield.

Efficient cross-valley mixing in the southern valley was also indicated during the final winter tracer experiment in which SF_6 was released throughout the night of March 6, 1979, from Lost Hills on the western side of the valley. By the second day after the start of the release, essentially all of the tracer was uniformly mixed over the entire southern end of the valley. This test also indicated the significance of pollutant carryover into days subsequent to their release. The hourly-averaged tracer concentrations detected at Wasco and Old River during the experiment are shown in Figure 6. Although the concentrations observed at these sites varied with the local diurnal wind patterns, the concentration levels on March 7 and later were remarkably consistent between the sites and from day to day. The degree of mixing in the southern valley was also indicated by an automobile traverse conducted during the afternoon of March 8, 1979. As indicated in Figure 7, SF_6 concentrations as

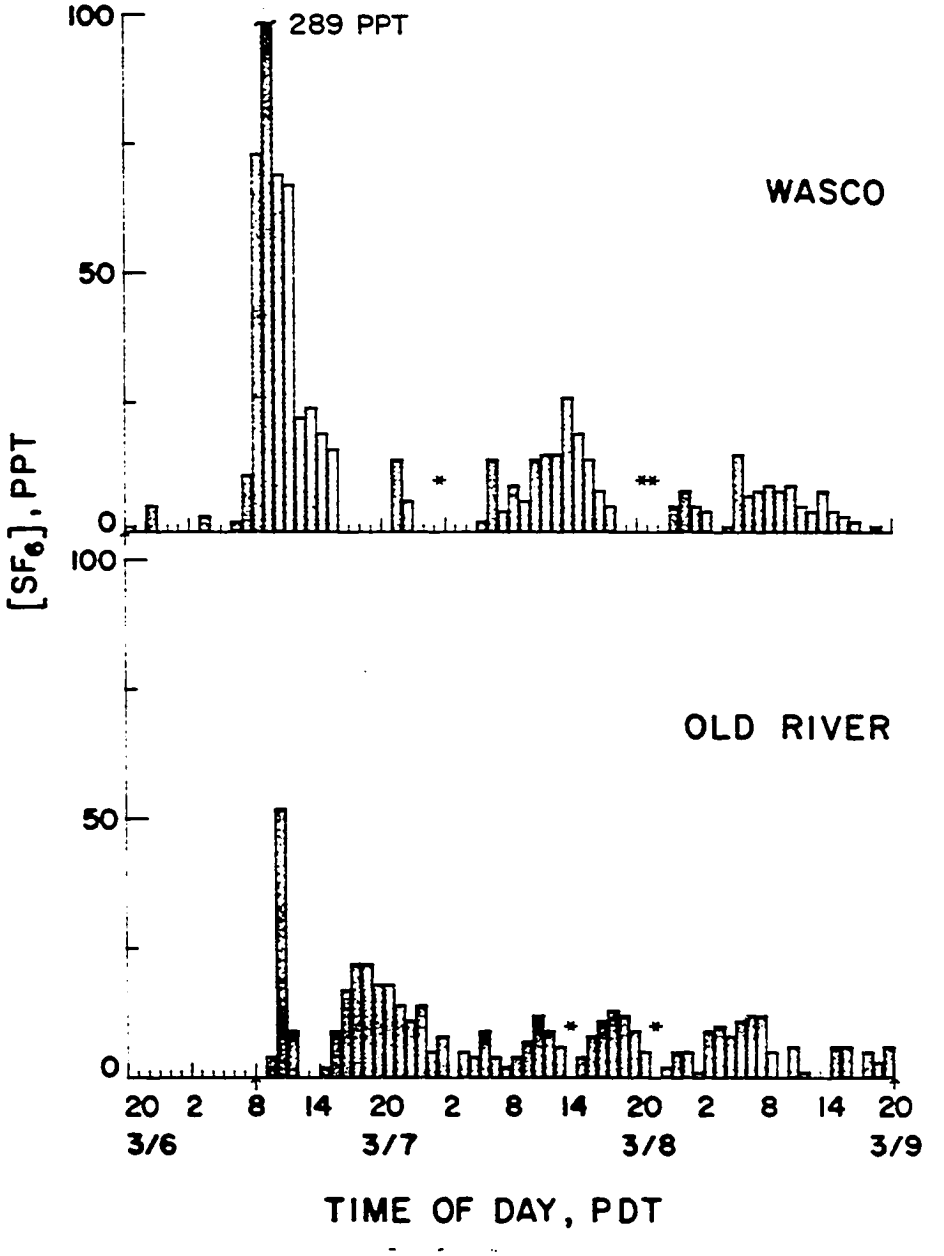

Figure 6 - Hourly-averaged tracer concentrations observed at Wasco and Old River during the last winter test, during which SF_6 was released from Lost Hills between 2030 PST, 3/6/79, and 0800 PST, 3/7/79.

high as about 25 PPT were observed over much of the valley south of Wasco. Assuming that the tracer concentrations observed at Old River on the evening of March 9 applied to the entire valley south of Wasco (~4500 km^2), and that the tracer was mixed up to 1200 m (maximum afternoon mixing height measured at Fresno), accounted for about 50% of the tracer released. An independent mass balance estimate made in the same manner using automobile traverse data also indicated about 50% of the tracer remained within the southern valley on March 9. Modeling the southern San Joaquin Valley as a well-mixed stirred tank, this loss rate corresponded to a mean residence time of about 4 days. Due to the inherent uncertainty in the mass balance calculation, the estimated mean residence time might have been as short as 2 days and as long as 8 days for this experiment. This can be compared to the estimate of 8-12 days based upon the averaged measured efflux from the valley's northern mouth during stable winter conditions in 1975. Note that the assumption that the southern end of the valley is well-mixed does not apply to pollutants less than 24 hours after their release. A significant fraction of the pollutants emitted from near the edge of the valley during the afternoon upslope flow, for example, might be transported out of the valley prior to becoming well-mixed.

Based upon the severely limited ventilation of the valley, it might be expected that pollutant levels would approach episodic levels on a region-wide basis. This was not observed during the field study. As shown in Table 2, carbon monoxide and oxides

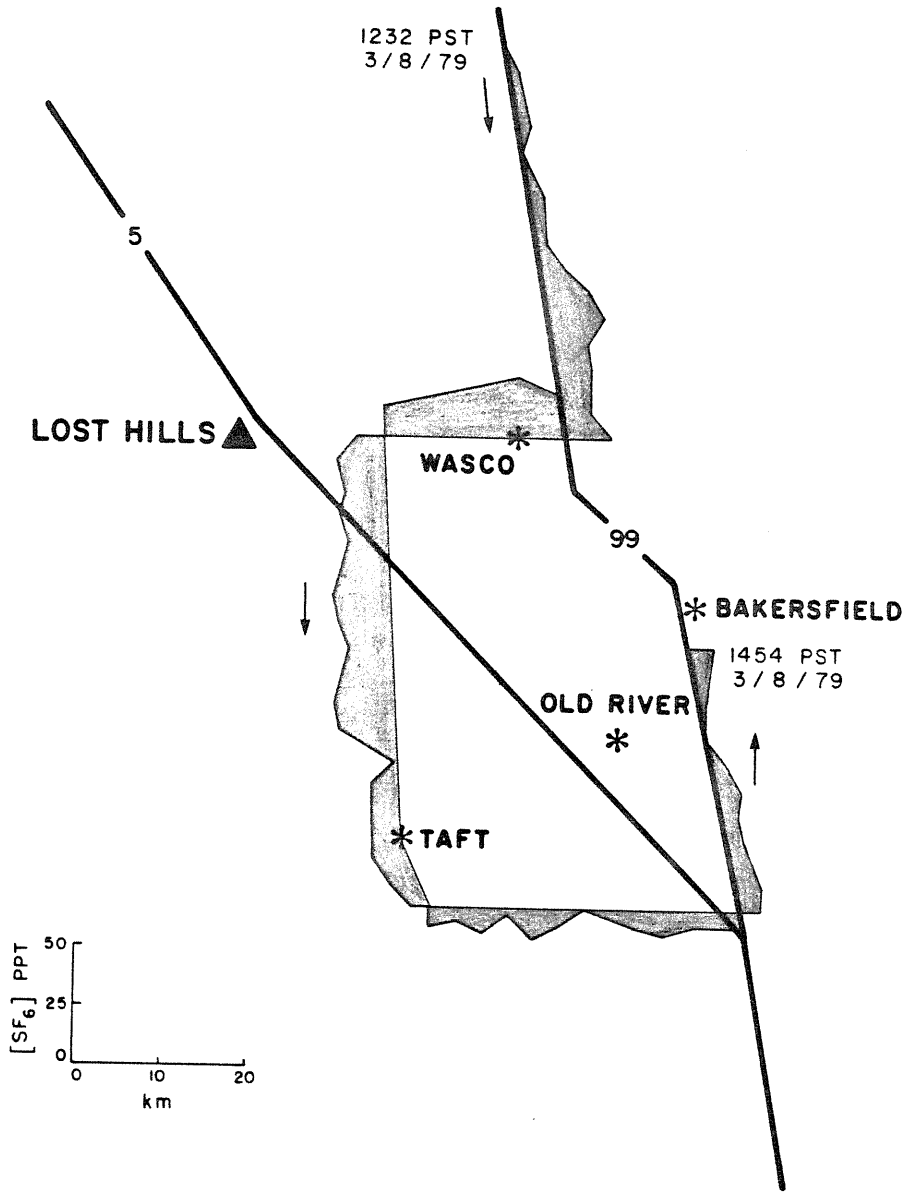

Figure 7 - SF_6 concentrations observed during an automobile traverse conducted between 1232 and 1454 PST, 11/16/78. Release was conducted from Lost Hills between 2030 PST, 3/6/79, and 0800 PST, 3/7/79.

Table 2

Maximum Hourly Pollutant Concentrations

November-December, 1978

	Pollutant Concentration (PPM)			
Location	Ozone	CO	NOx	SO_2
I. Urban Sites				
A Bakersfield	0.06	16	0.9	0.05
B Fresno-Olive St.	0.05	18	0.88	0.04
C Modesto	0.03	13	0.62	0.03
D Oildale	0.05			0.15
E Visalia	0.07	11	0.55	
II. Rural Sites				
F Coalinga	0.06	4	0.09	
G Five Points	0.06	5		0.03
H Lost Hills	0.07		0.18	0.005
I Radome	0.07		0.13	0.01

of nitrogen showed the marked influence of urban areas and the sulfur dioxide measurements indicated the strong source area near Oildale, alluded to earlier. As emission levels within the valley increase, however, the impact of pollutant sources will probably tend to become less localized.

Summary and Conclusions

During this study, the San Joaquin Valley was shown to have a significant air pollution potential during the winter due to stagnation of the surface layer of the atmosphere. Mean residence times of an air parcel within the valley can be as long as 8-12 days if no frontal passages occur. It appears that the frequency of frontal passages is such that they provide the most significant mechanism for cleansing of the valley of airborne contaminants during the winter. During stable periods between frontal passages, the generally slow ventilation rate of the valley tends to well-mix aged pollutants, especially in the southern valley. That is, the characteristic time for transport out of the valley (8-12) days is generally greater than the characteristic time for mixing within the southern valley (1-2 days). In the northern valley (Fresno and north), cross-valley mixing was slower during the two experiments conducted in this area due to the generally north-south orientation of the winds.

While the stable wintertime conditions pose a significant air pollution potential, at the present time pollutant impacts are generally localized. Valley wide hazards are limited, apparently due to the relatively low present source density within the valley. A potential problem area for the valley, however, is the production of sulfate in the southern valley during stagnant fog conditions. Sulfur dioxide sources (primarily oil field combustors) are located in the southern valley and increased

emissions are likely in the coming years. The effect of such increases on sulfate levels and the fog in the southern valley is not known and worthy of additional study.

Although the results of this experimental program strictly pertain only to the San Joaquin Valley, the phenomenological behavior is undoubtedly repeated elsewhere. The results of this study may have some application to any mountain-valley system where the transport and dispersion of pollutants might be controlled by complex flows resulting from the interaction of the local thermally-driven and diurnally varying slope flows and the synoptic scale flow. It appears clear, also, that approaching a complex natural flow system from a volumetric balance point of view can be instructive in elucidating the basic behavior of pollutants within the system as well as allowing an understanding of how the system breathes.

References

CARB 76-19-4 (1976). California Air Resources Board Staff Report, P.O. Box 2815, Sacramento, CA 98512.

California Statistical Abstracts (1980). Available from the State of California, Documents Section, P.O. Box 1015, North Highlands, CA 95660.

Census of Agriculture (1981). Vol. 1, Part 5 - California Data for 1978. Available from the Superintendent of Documents, United States Government Printing Office, Washington, D.C. 20402

Duckworth, S., and Crowe, D. (1979). Sulfur dioxide and sulfate trends - Bakersfield, 1977-1978. Technical Services Division, California Air Resources Board, P.O. Box 2815, Sacramento, CA 98512.

Duckworth, S. and Kinney, J. J. R. (1978). Visibility trends in the great central valley of California, 1958-1977. Technical Services Division, California Air Resources Board, P.O. Box 2815, Sacramento, CA 98512.

Friedlander, S. K. (1973). Chemical element balances and identification of air pollution sources. Envir. Sci. and Tech., 7, 235-240.

Lamb, B. K. (1978). Development and application of dual atmospheric tracer techniques for the characterization of pollutant transport and dispersion. Ph.D. Thesis, California Institute of Technology, Pasadena, CA 91125.

Reible, D. D., Shair, F. H., Smith, T. B., and Lehrman, D. E. (1982). The origin and fate of air pollutants in California'a San Joaquin Valley, II. Summer. Submitted to Atmospheric Environment.

Smith, T. B., Lehrman, D. E., Reible, D. D., and Shair, F. H. (1981). The origin and fate of airborne pollutants within the San Joaquin Valley. Final report to the California Air Resources Board, P.O. Box 2815, Sacramento, CA 98512.

Technical Services Division, CARB (1979). Emission inventory, 1976. California Air Resources Board, P.O. Box 2815, Sacramento, CA 98512.

Watson, J. G. (1979). Chemical element balance receptor model methodology for assessing the sources of fine and total suspended particulate matter in Portland, Oregon. Ph.D. Thesis, Oregon Graduate Center.

World Almanac (1972). The World Almanac and Book of Facts. Newspaper Enterprise Association, 200 Park Ave., New York, NY 10166.

World Almanac (1981). The World Almanac and Book of Facts. Newspaper Enterprise Association, 200 Park Ave., New York, NY 10166.

Chapter 8

The Origin and Fate of Air Pollutants in California's San Joaquin Valley

II. Summer

by

D.D. Reible, F.H. Shair, T.B. Smith, and D.E. Lehrman

(Submitted to Atmospheric Environment)

Abstract

In this, the second of two papers on the ventilation characteristics of the San Joaquin Valley of Central California, summer conditions are discussed.

During the summer, the San Joaquin Valley is characterized by sunny, warm days that result in strong low-level mixing, and in afternoon upslope flows along the mountains that bound the valley. A strong influx of air at the northern mouth of the valley is balanced during the day by the upslope flows and the efflux from the southern end of the valley. Tracer released near the mouth of the valley was rapidly transported towards Bakersfield in an essentially Gaussian plume. Tracer released near the foothills of the Sierra Nevada indicated that valley pollutants result in a significant impact upslope both during the afternoon and during stable nighttime conditions. Tracer released at the southern end of the valley indicated that San Joaquin Valley pollutants have a significant impact upon the Mojave desert during the late afternoon. At night, stabilization of the low-level air limits the ventilation of the valley and an eddy develops in the southern valley. The continued influx of air at the mouth of the valley leads to acceleration of the air above a 300 m altitude and growth of the eddy. During most days the eddy influenced locations as far north as Fresno by mid-morning, hence its more common name, the Fresno Eddy. Tracer experiments indicated that the nocturnal jet can rapidly transport pollutants from the northern valley towards the south and that the eddy can transport pollutants both

cross-valley and from the south towards the north. These complex dynamic structures must be included in any realistic air pollution model of the San Joaquin Valley.

Introduction

As described in the previous paper in this series (Reible, et al., 1982a), the San Joaquin Valley of central California faces considerable agricultural, industrial and urban development in the coming years. In order to balance the often conflicting pressures of such development, an accurate technicological assessment of the the impact of this development on the valley is required. The current study evaluated the potential for air quality degradation in the San Joaquin Valley in the coming years.

The San Joaquin Valley is a large inland valley about 380 km in length and 80 km wide, bounded on the east by the Sierra Nevada Mountains, on the south by the Tehachapi Mountains, and on the west by the California Coastal Ranges. The general topography of the valley is indicated in Figure 1. The climate of the San Joaquin Valley is essentially Mediterranean with hot, dry summers and cool, rainy winters. Much of the local meteorology is controlled by the interaction of the prevailing pressure gradient from the coast to the inland desert areas of the United States and the mountain-valley breezes that develop due to differential heating between the sloping surfaces and the valley floor. As described in the preceding paper (Reible, et al., 1982a), the San Joaquin Valley faces the conflicting environmental pressures posed by large agricultural and oil producing industries combined with rapid population growth. It is clear that in order to efficiently allocate the finite amount of available resources equitably among the potential users it is necessary to evaluate the negative air quality impact of each use in addition to its potential economic

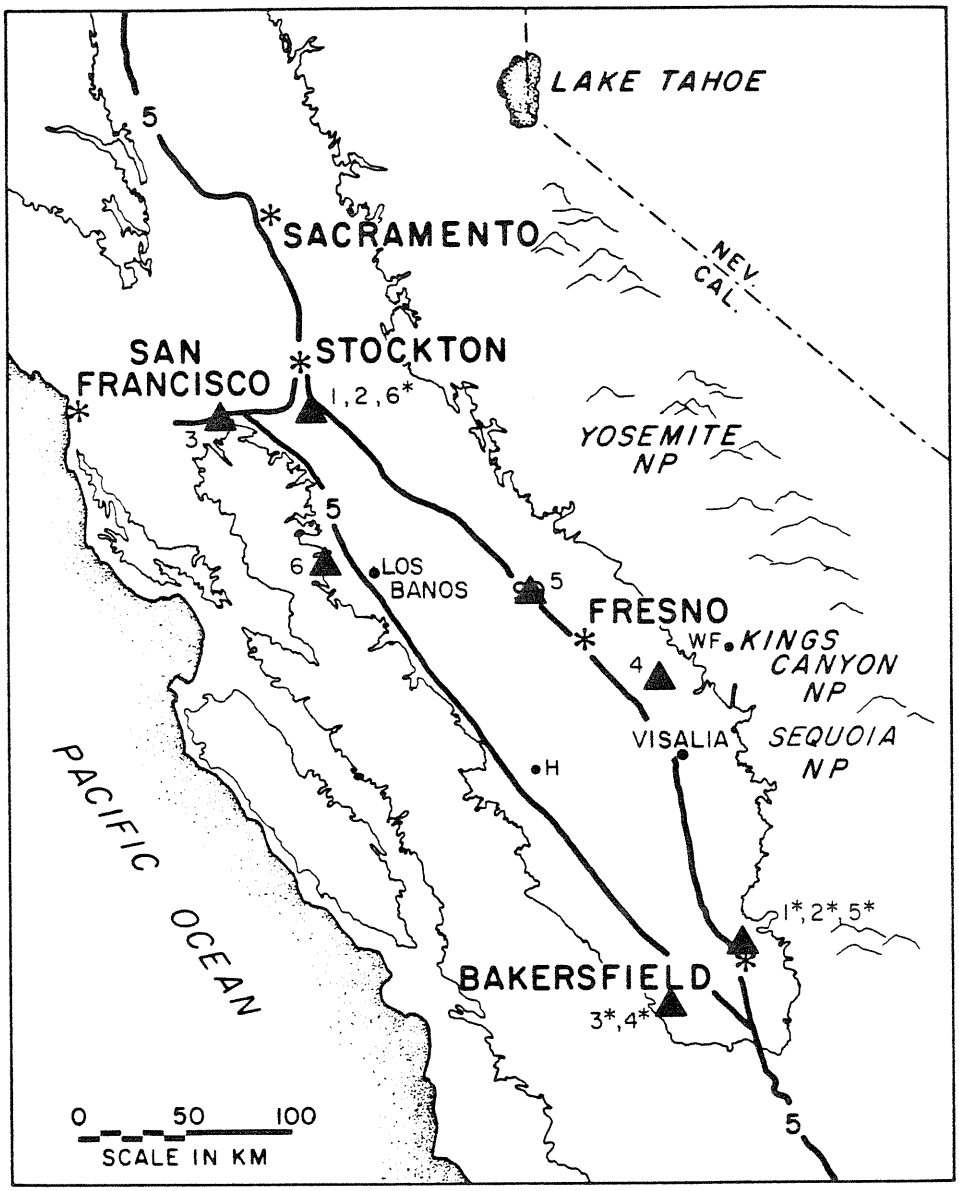

Figure 1 - Map of the San Joaquin Valley, indicating release sites and test numbers (▲). September, 1979 releases are denoted by an asterisked number. WF denotes Whitaker Forest and H, Huron. 300 m elevations are shown.

or social benefits. It was this need that formed the impetus for this study.

The specific objectives of this study were threefold.

1. Identify the transport routes into, within and out of the San Joaquin Valley.
2. Determine the chemical composition of the particulate matter in the valley and trace the sources of this material.
3. Acquire an aerometric data base that can be used in air quality model simulation of the photochemical formation and transport in the valley.

In view of the comprehensive and complex nature of the study, it was conducted as a cooperative effort by four organizations, Meteorology Research, Inc. (Altadena, Ca.), the California Institute of Technology (Pasadena, Ca.), the Rockwell Air Monitoring Center (Newbury Park, Ca.), and Environmental Research and Technology (Westlake Village, Ca.). The complete results of the study embody a report to the California Air Resources Board (Smith, et al., 1981). The current paper will emphasize the findings of the study with respect to the first objective, the identification of the transport routes into, within and out of the San Joaquin Valley. This aspect of the study involved extensive meteorological and pollutant measurements as well as atmospheric tracer experiments. The study was broken into two basic meteorological regimes, winter and summer, and for clarity, the current paper describes only the transport and dispersion of pollutants in the San Joaquin Valley during the summer. The behavior of pollutants in the valley during winter atmospheric

conditions is described in a separate paper (Reible, et al., 1982a).

Experimental Procedures

The study consisted of three intensive field programs, each of about three weeks duration. Field programs were carried out in November-December, 1978, and in July and September, 1979, in order to examine seasonal variations in the valley characteristics. The July and September field programs included extensive meteorological and air quality measurements, and a total of 12 releases of an atmospheric tracer, sulfur hexafluoride (SF_6).

The meteorological observations included pilot balloon measurements of the winds aloft at 7 locations as well as surface wind measurements at a number of existing and supplemental locations. Air quality measurements included airborne observations by Meteorology Research, Inc., of sulfur dioxide, ozone, oxides of nitrogen, and light scattering coefficient. In addition to the mobile airborne pollutant sampling, similar measurements were made at fixed surface sites in three vans operated by Rockwell. Also located at the Rockwell vans were filter samplers for particulates that were later analyzed by Environmental Research and Technology (ERT). The atmospheric tracer releases were conducted by the California Institute of Technology, using sulfur hexafluoride (SF_6). SF_6 is a non-toxic, colorless, odorless gas that can be detected by electron capture gas chromatography at concentrations as low as 1-10 parts SF_6 per trillion parts air (PPT). The analytical procedure, as well as instrument accuracy and calibration procedures, are described by Lamb (1978). A summary of the tracer experiments conducted during

the summer field programs are included in Table 1. The locations of these releases are shown in Figure 1. The reader is referred to the preceding paper (Reible, et al., 1982a) for a more detailed description of the experimental procedures employed.

Table 1 - Summer Tracer Releases

July 1979

Test 1 - Release of 47 kg SF_6 per hour between 0700 and 1300 PDT, 7/13/79, from Manteca

Test 2 - Release of 47 kg SF_6 per hour between 1300 and 1900 PDT, 7/16/79, from Manteca

Test 3 - Release of 46 kg SF_6 per hour between 1510 and 2030 PDT, 7/18/79, from Livermore

Test 4 - Release of 44 kg SF_6 per hour between 1200 and 1700 PDT, 7/25/79, from Reedley

Test 5 - Release of 30 kg SF_6 per hour between 2300 PDT, 7/27/79 and 0215 PDT, 7/28/79 from between Chowchilla and Fresno. Release made at altitude of about 300 m from circling airplane.

Test 6 - Release of 45 kg SF_6 per hour between 1200 and 1725 PDT, 7/30/79, from Los Banos

September, 1979

Test 1 - Release of 49 kg SF_6 per hour between 0700 and 1200 PDT, 9/5/79, from Oildale

Test 2 - Release of 48 kg SF_6 per hour between 0200 and 0700 PDT, 9/8/79, from Oildale

Test 3 - Release of 49 kg SF_6 per hour between 0700 and 1200 PDT, 9/11/79, from Fellows

Test 4 - Release of 49 kg SF_6 per hour between 0107 and 0647 PDT, 9/14/79, from Fellows

Test 5 - Release of 48 kg SF_6 per hour between 2200 PDT, 9/16/79 and 0337 PDT, 9/17/79, from Oildale

Test 6 - Release of 44 kg SF_6 per hour between 0900 and 1400 PDT, 9/21/79, from Manteca

Presentation and Discussion of Results

Overall Valley Ventilation

The bulk of the air transported into the valley apparently results from a single mechanism, the intrusion of marine air from the San Francisco Bay area due to the normal pressure gradient from the coast to the inland deserts of the southwestern United States. As shown in Table 2, the 24 hr average surface winds at Stockton during 1975, for example, were directed into the valley during all months of the year except January and February. This was borne out during the more extensive meteorological measurements collected during the current study. Perhaps the clearest means of illustrating the ventilation budget of the valley during the test program is an analysis of the winds at 5 locations along the axis of the valley. Pibal observations were taken at 05, 09, 13, 17 and 21 PDT daily at Stockton, Los Banos, Fresno, Visalia and Bakersfield during the July field program (see Figure 1 for locations of these sites). The average wind profiles during the entire month at 05, 09 and 17 PDT are shown for each location in Figure 2. Only the components of the winds along the valley axis are shown in the figure. The average profiles for 17 PDT were similar for all stations, indicating relatively uniform transport from the northwest throughout the valley. During the afternoon, the influx of air at the valley's northern mouth was apparently in approximate balance with the efflux at the southern end. At 05 PDT, however, the winds in the lower 1000 to 1500 m were considerable weaker at Bakersfield and southerly winds were observed at Visalia. This profile was created by terrain blocking

Table 2 - 1975 Stockton Surface Winds

Along valley component (mps)*

	Time (PST)			
Month	03	09	15	21
January	-0.86	-0.35	0.58	-0.81
February	-0.41	-1.01	-0.29	-0.38
March	0.06	0.08	1.79	1.50
April	0.32	1.94	4.09	2.02
May	2.46	3.52	5.12	3.38
June	2.37	3.78	4.52	3.50
July	2.02	2.71	3.89	3.50
August	1.81	2.26	3.61	3.30
September	1.26	2.58	4.25	3.11
October	0.50	0.76	2.91	1.84
November	0.43	0.82	2.01	0.68
December	-0.28	-0.47	2.06	-0.03

* Positive values indicate flow into the valley from Stockton towards Bakersfield

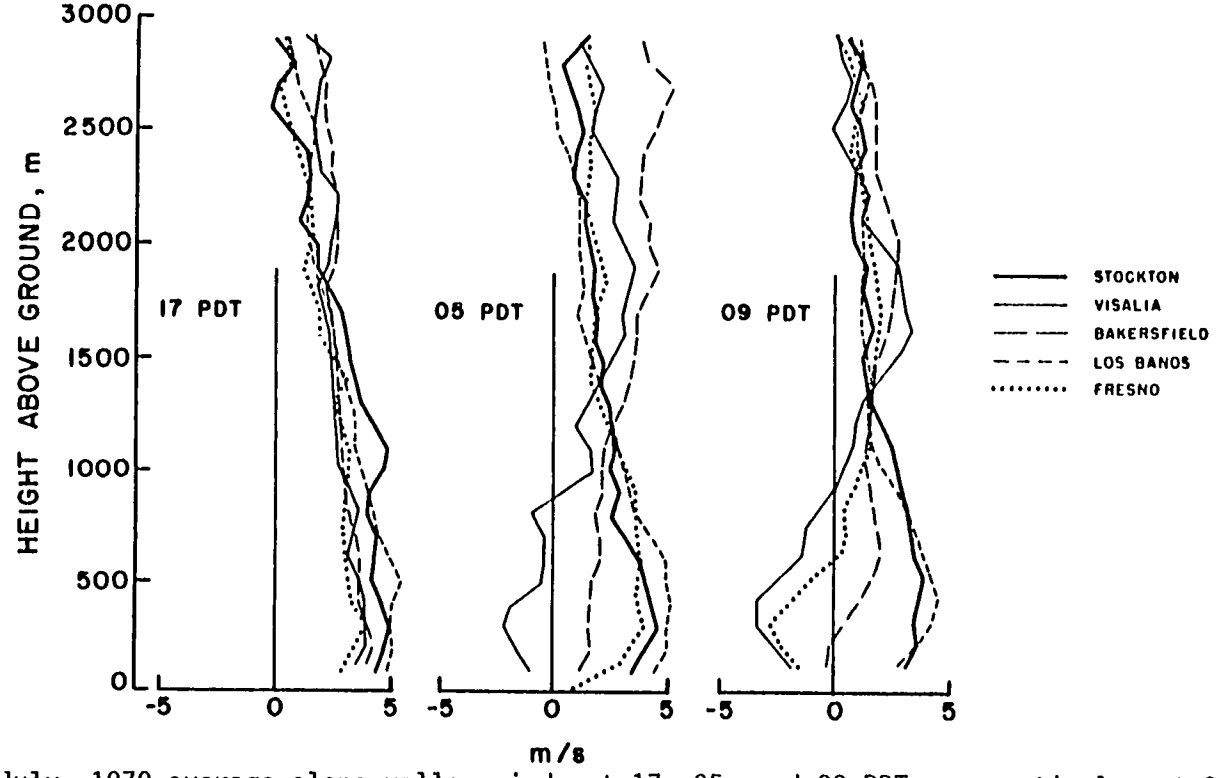

Figure 2 - The July, 1979 average along valley winds at 17, 05, and 09 PDT, respectively, at Stockton, Fresno , Los Banos , Visalia , and Bakersfield . Positive velocities indicate flow from Stockton towards Bakersfield.

of the northwesterly flow when nocturnal stability began to inhibit the free transport of low-level air over the Tehachapi mountains at the southern end of the valley. At the same time the increased flow aloft at Bakersfield and Visalia (above 1000-1500 m) served to balance part of the air still being transported into the valley by the winds at its northern mouth. By 09 PDT, the terrain blocking was felt as far north as Fresno. The presence of a southerly morning wind at Fresno has been termed the Fresno Eddy. From the above discussion, however, it is clear that the Fresno Eddy is really the mid-morning influence of a southern valley eddy. During the July field program, a morning southerly or easterly wind was observed at Fresno on 18 of 22 days for which data existed. During the September program, the eddy winds were observed at Fresno on 17 of 22 days. Figure 3 indicates the typical diurnal behavior of the eddy. The early morning streamlines differ markedly from those during the afternoon due to the existence of the eddy. The eddy grows throughout the night as more and more air is transported into it, only to break up as the unstable daytime conditions begin to prevail. The primary importance of the eddy from an air pollution standpoint lies in its ability to redistribute pollutants, primarily throughout the southern part of the valley.

It is apparent from the above discussion that air above about 1200 m moved readily out of the valley to the southeast on a mean flow basis during July. This indicates that only the lower 1200 m is of concern in terms of the ventilation of the valley. Mean velocities for the lowest 1200 m were calculated at each of the

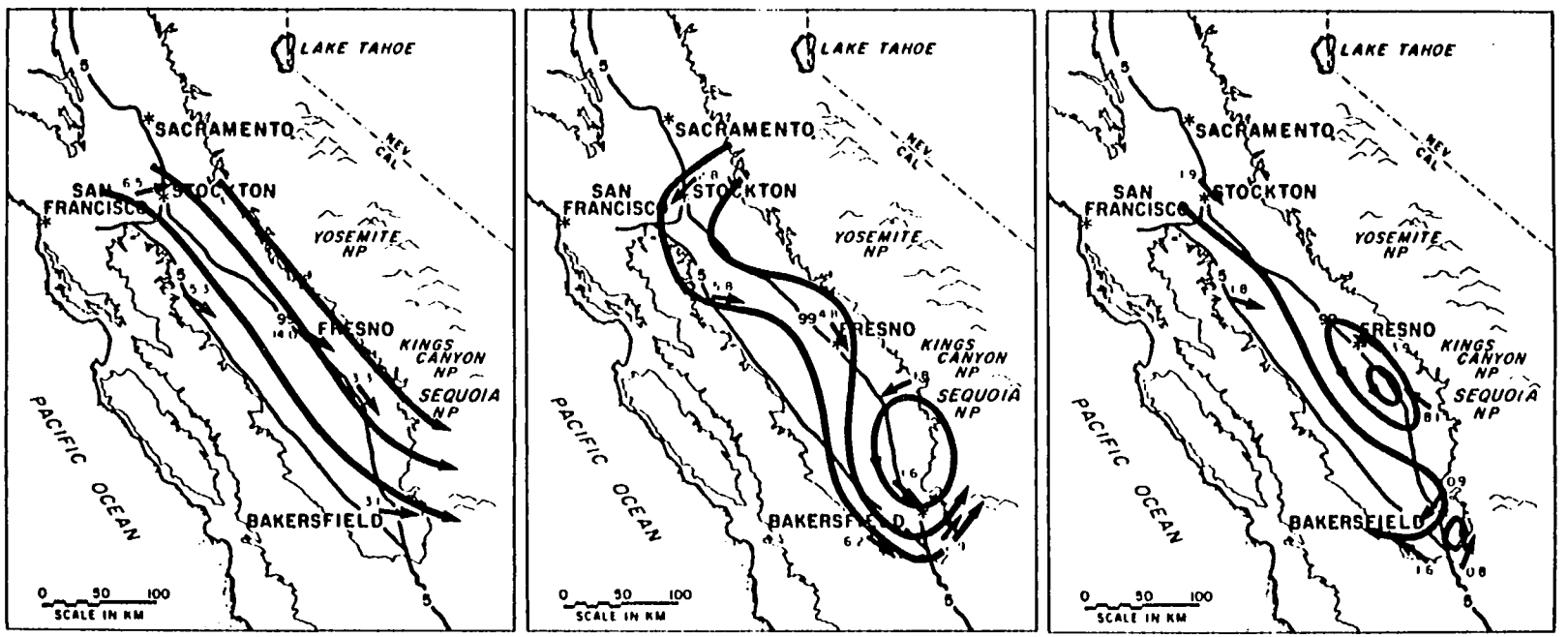

Figure 3 - Typical behavior of the southern valley eddy during the nighttime hours. Shown are the 300 m wind streamlines at 21 PDT, 9/16/79 and at 01 and 09 PDT, 9/17/79, respectively. Wind speeds are in mps.

pibal locations for the July period. By assuming that the airflow is uniform across the valley at the average velocity of the pibal observations it is possible to make an estimate of the volume flux of air as a function of distance along the valley. The assumption of lateral uniformity appears to be reasonable during the afternoon when a northwesterly flow sweeps the entire valley and throughout the day in the northern part of the valley. Table 3 gives the calculated fluxes at each location as a function of time of day. The average flux at Stockton is 1.3 X 10^{12} m^3/hr. The total volume of the valley below 1200 m is about 3.9 X 10^{13} m^3, indicating that about 30 hours would be necessary to replace the layer of air below 1200 m in the valley during July. As mentioned previously, no other mechanism for a significant transport of air into the valley was found during the test program, suggesting that the average residence time of air within the valley is about 30 hours during the summer.

Average fluxes can also be used to indicate the transport routes out of the valley. In the northern part of the valley, the flux estimates at the three observational locations (Stockton, Los Banos and Fresno) were quite similar with the exception of the morning fluxes at Fresno. Given this uniformity, there is apparently little air transported out of the valley between Stockton and Fresno. From Fresno southward, however, there were indications of a significant decrease in air flux. At 17 PDT, when the most uniform flow exists throughout the valley, the flux estimated at Bakersfield was about 0.5 X 10^{12} m^3/hr less than that estimated at Fresno. This was most likely due to the transport of

Table 3 - Estimated Along Valley Air Flux

July 1979 winds averaged over lower 1200 m

Time	Flux ($10^{12} m^3$/hr)				
(PDT)	Stockton	Los Banos	Fresno	Visalia	Bakersfield
17	1.59	1.63	1.44	1.27	0.95
21	1.54	2.16	2.44	1.61	0.71
05	1.15	1.42	1.37	-.18	0.47
09	1.10	1.12	-.14	-.50	0.26
13	1.00	1.10	0.50	0.47	0.45

air out of the valley by the afternoon upslope flows. The balance of the air flow, about 1 X 10^{12} m^3/hr, must be transported out of the southern end of the valley.

The ventilation balance during the night and early morning is not as well understood. As mentioned earlier, as the air on the slopes stabilizes and begins to move downslope during the evening, the air influx at the northern end of the valley cannot be balanced by the surface layer flow. There is, however, a net increase in the wind velocities above 1200 m at Bakersfield, possibly leading to transport of the elevated layers out of the valley. This excess flux (compared to Fresno) amounts to about 0.7 X 10^{12} m^3/hr within the layer from 1200 m to 2740 m and represents about half of the total flux below 1200 m at Fresno. The balance of the flux into Fresno apparently causes the region influenced by the terrain blockage to grow during the night. As described previously, the southerly winds typically observed at Fresno during the morning are the result of the growth of this region.

Pollutant dispersion within the valley

As described above, the overall ventilation rate of the San Joaquin Valley is considerably greater during the summer than during the winter in that the mean residence time of air is of the order of 1 day as opposed to the mean residence time of 8-12 days estimated for the stable winter conditions (Reible, et al., 1982a). In the case of photochemically reactive pollutants, however, the apparently good overall ventilation of the valley was more than offset by the warmer temperatures observed during the

summer. Ozone concentrations in excess of the California Air Quality Standard (0.10 PPM) were observed at a number of sites during the summer test program. Figure 4 shows the maximum hourly-averaged ozone concentrations observed within the San Joaquin Valley during the first test of the July field program (July 13, 1979). Two observations can be made upon examination of this figure; 1) the maximum ozone concentrations on the east side of the valley generally exceed those measured on the west, and 2) the maximum ozone concentrations on the western slopes of the Sierra Nevada Mountains (east side of the valley) can equal or exceed the ozone concentrations measured on the valley floor. Both of these observations were further explored with atmospheric tracer experiments.

Four tracer releases (Tests 1, 2 and 3 during July and Test 6 during September) near the northern mouth of the valley were used to evaluate the impact of pollutants entering the San Joaquin Valley. Sources of the pollutants contained within this air include the San Francisco Bay area, the Livermore Valley and the California Delta region (Lamb, et al., 1978). As indicated in Figure 5, tracer released from Manteca during the afternoon (Test 2, July) was found during automobile traverses to preferentially impact the western side and center of the San Joaquin Valley. The sharply peaked concentration profiles shown in Figure 5 can be compared to predictions of the Gaussian plume model (Turner, 1970). As shown in Figure 6, the horizontal and vertical dispersion of the tracer corresponded closely to that expected in neutral or slightly unstable atmospheric conditions. The figure

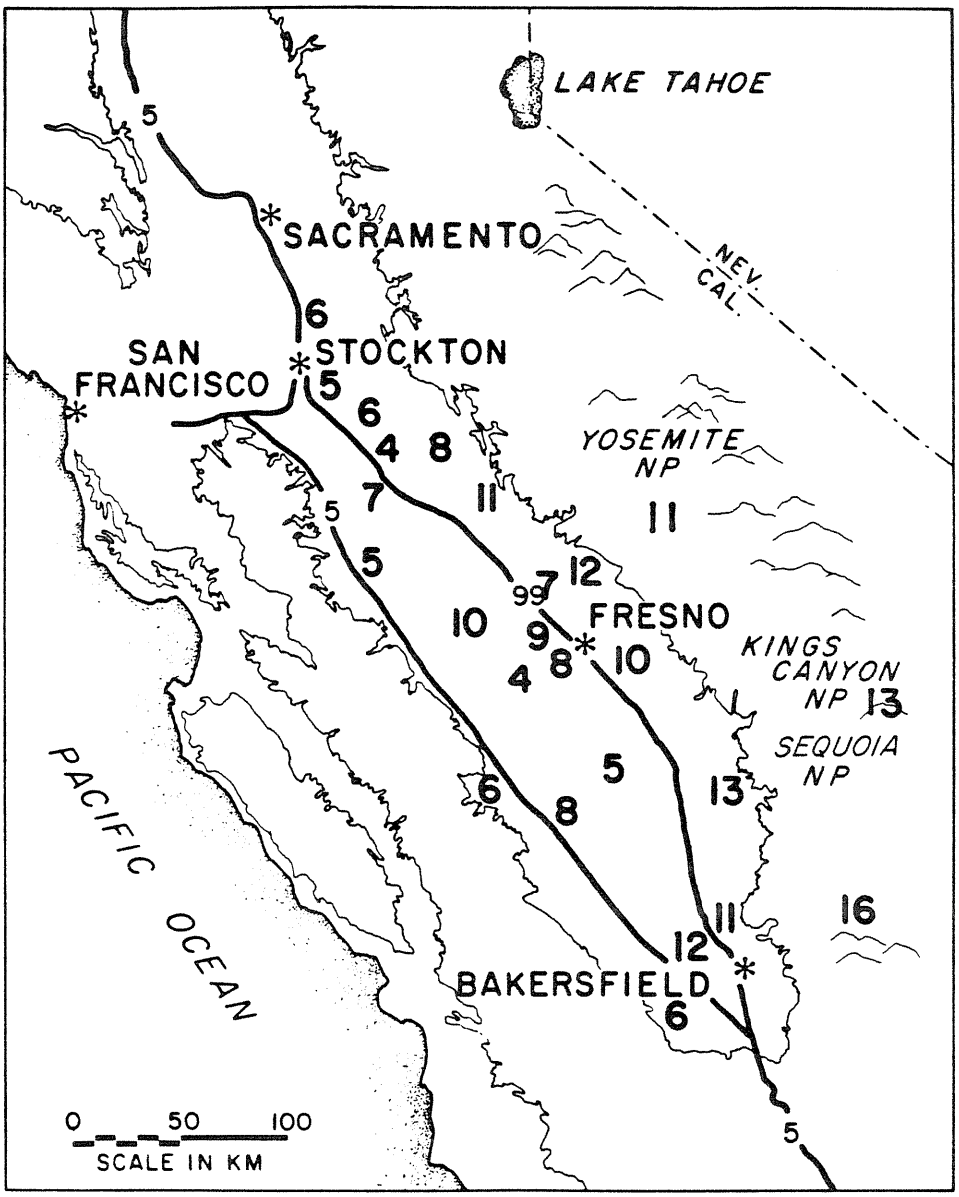

Figure 4 - Maximum hourly-averaged ozone concentrations observed at various sites within the San Joaquin Valley on 7/13/79.

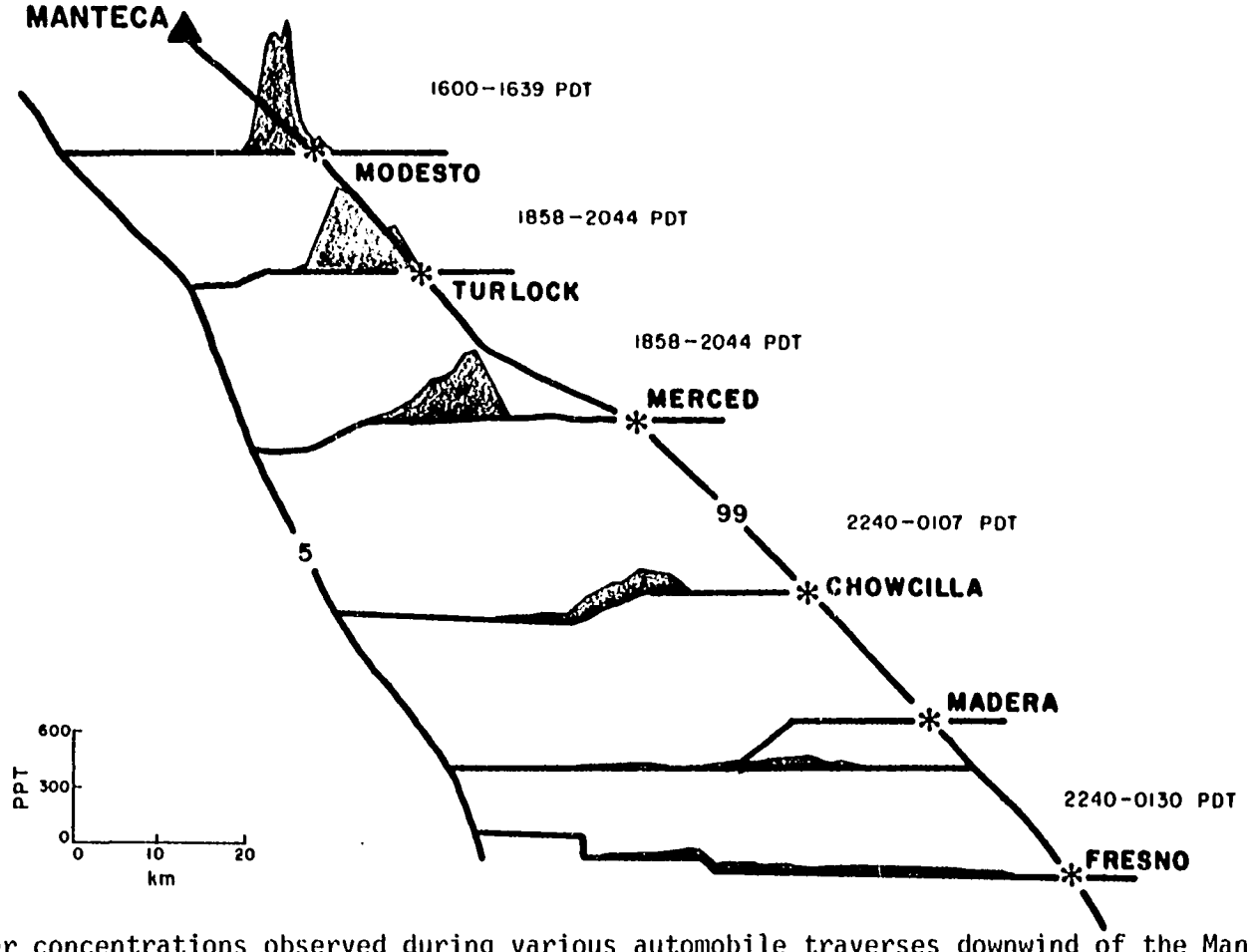

Figure 5 - Tracer concentrations observed during various automobile traverses downwind of the Manteca release site on 7/16/79 (Test 2, July). Height of shaded regions correspond to the observed concentrations.

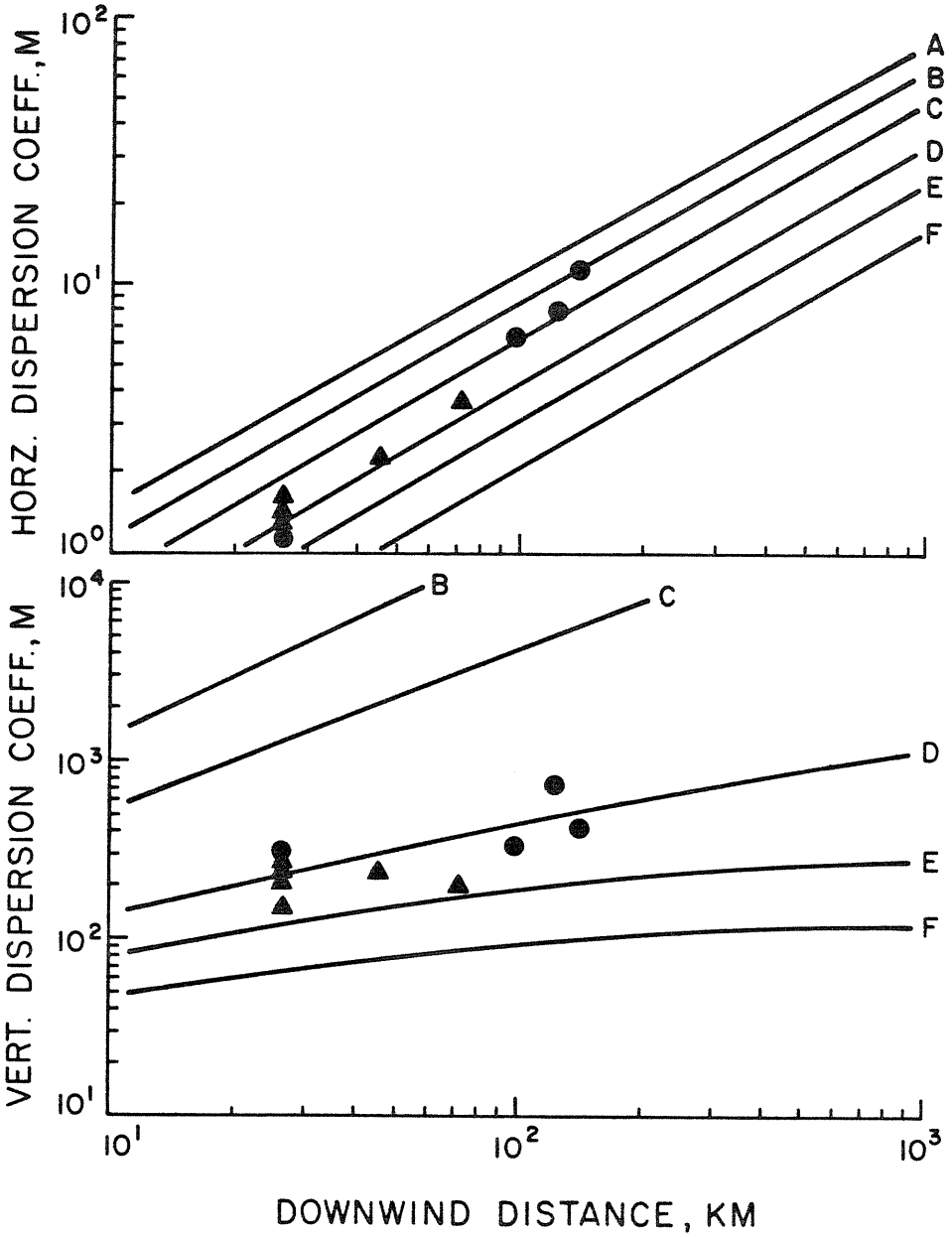

Figure 6 - Best-fit Gaussian parameters for all traverse data on day of second Manteca release (Test 2, July). Shaded circles represent traverses conducted after the end of the release.

suggests that the Gaussian plume model can be a useful modeling tool in a uniform flow field even at distances in excess of 100 km downwind. The basic results of this test were verified during the three other tracer releases conducted near the northern mouth of the valley. Thus most of the large influx of air at the northern end of the valley probably does not serve to directly ventilate the urban, eastern side of the valley, where the highest ozone concentrations are observed (as indicated in Figure 4). The western and central valley impact of the tracer during these releases, when coupled with the lower ozone concentrations observed on the western side of the valley, indicate that transport of ozone and precursors into the valley is generally overshadowed, at least in terms of maximum resulting concentrations, by sources within the valley. The limited transport of air from the mouth of the valley to its urban, eastern side is consistent with the apparently small daytime flux up the slopes north of Fresno.

As indicated by the average along valley air flux, however, the afternoon upslope winds in the mountains south of Fresno appear to be a significant ventilation mechanism for the valley. As was shown in Figure 4, the maximum hourly-averaged ozone concentrations on the slopes can be equal to or higher than the concentrations on the valley floor. The effectiveness of upslope transport of pollutants was evaluated during a tracer experiment during the July field program. The tracer release was conducted during the afternoon of 25 July, 1979 from Reedley, about 25 km southeast of Fresno. Westerly, upslope winds during the release carried the tracer into the National Forest and Park areas east of

the release site. As shown in Figure 7, a maximum hourly-averaged concentration of 65 PPT (215 PPT/kg-mole SF_6 released/hr) was detected at Whitaker Forest (WF in Figure 1), about 50 km east of the release site. The arrival of SF_6 at Whitaker Forest by 1800 PDT suggested that the mean transport speed of the upslope wind was just over 2 mps. Grab sample concentrations of up to 90-95 PPT were observed during automobile and airplane traverses near Whitaker Forest. Both the maximum observed concentrations and the width of the essentially Gaussian tracer concentration profiles detected during these traverses were consistent with very unstable atmospheric conditions (approximately Pasquill-Gifford Stability Class A) and a mixing depth of about 600 m. This mixing depth is approximately equal to the typical slope flow depth over the Sierra Nevada (Reible, et al. 1982b) and that observed by Reible, et al. (1981) over the geographically similar Tehachapi Mountains (southern boundary of the valley), and the San Gabriel Mountains (northern boundary of the Los Angeles Air Basin). A more complete description of this and other experiments designed to evaluate the air quality impact of pollutant transport into the western slopes of the Sierra Nevada can be found in Reible, et al. (1982b).

In addition to the direct upslope impact of valley pollutant sources during the afternoon, a significant carryover of pollutants into the following day can occur. As shown in Figure 7, the 5 hour tracer release on 25 July led to the observation of tracer concentrations greater than 10 PPT for 18 consecutive hours at Whitaker Forest. The carryover of ozone precursors into days

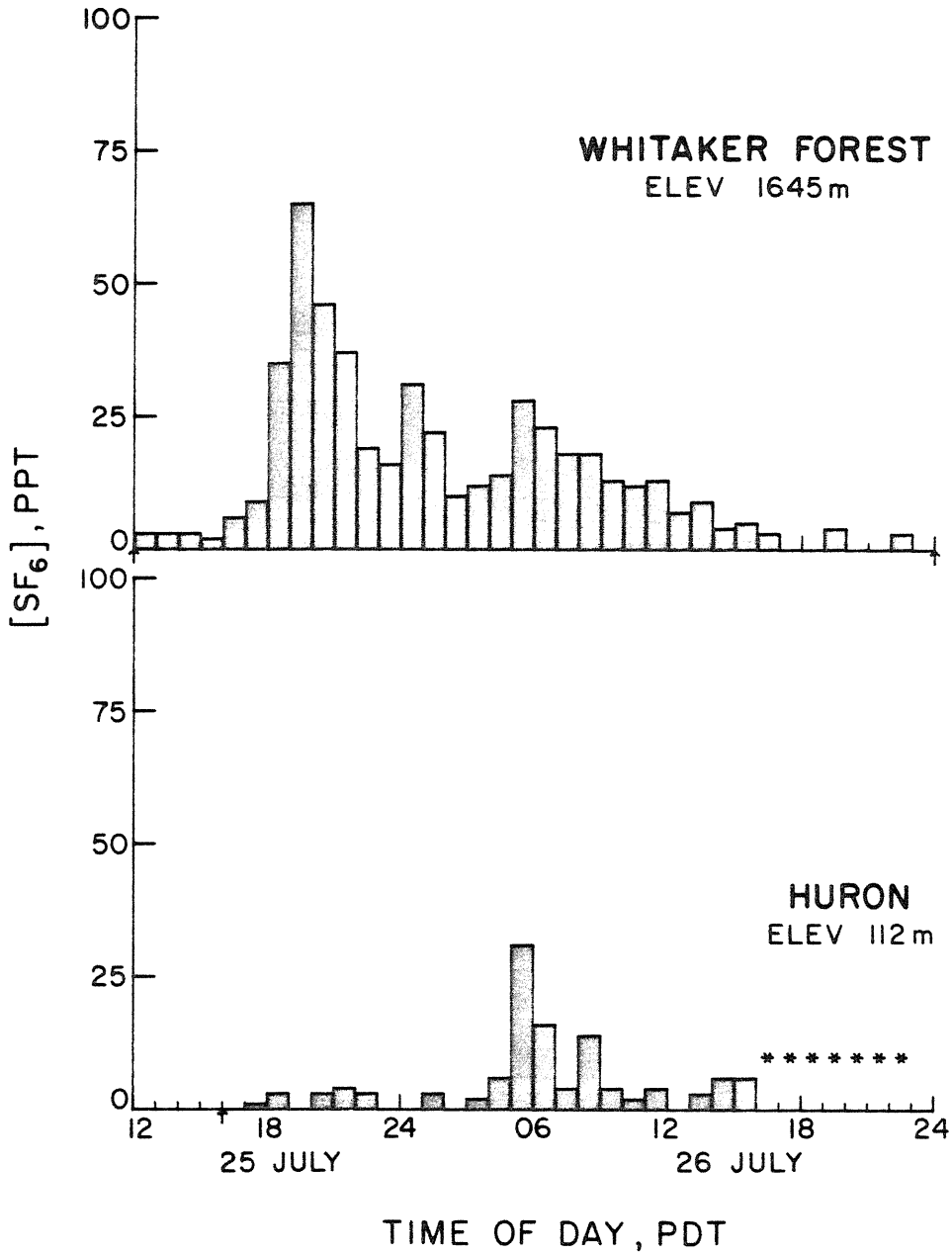

Figure 7 - Hourly averaged tracer concentrations observed at Whitaker Forest, near Kings Canyon National Park, and Huron, on the western side of the San Joaquin Valley, during the upslope flow test of 7/25/79 (Test 4, July).

subsequent to their release may help explain the relatively high ozone concentrations observed during night and morning hours on the slopes southeast of Fresno (Miller,et al., 1972, Pronos, et al., 1978, and Reible, et al., 1982b) as well as the high daytime maxima illustrated in Figure 4. The nighttime drainage flow can also transport pollutants back to the valley floor, further limiting effectiveness of the daytime upslope flow for ventilating the valley. As shown in Figure 7, tracer concentrations about 50% of the maximum detected upslope (at Whitaker Forest) were observed at Huron (H in Figure 1), on the western side of the valley by the morning following the release.

As described above, slope flows on the western slopes of the Sierra Nevada Mountains can result in a significant pollutant impact in the mountains. At the southern end of the San Joaquin Valley, however, the slope flows also lead to significant transport out of the valley and pollutant impacts on the northern Mojave Desert. As indicated by the average flux estimates, the main daytime exit path for air entering the valley is through its southern end. Two tracer releases conducted from Oildale during September, 1979 indicated the ventilating action of the afternoon winds over the the Tehachapi Mountains and the southern tip of the Sierra Nevada. During both of these experiments, the tracer was initially transported toward the center of the valley by the early morning drainage winds. As indicated in Figure 8, for the first Oildale release, however, the SF_6 was transported out of the valley and into the Mojave Desert during the afternoon. During the first experiment of the September field program, average

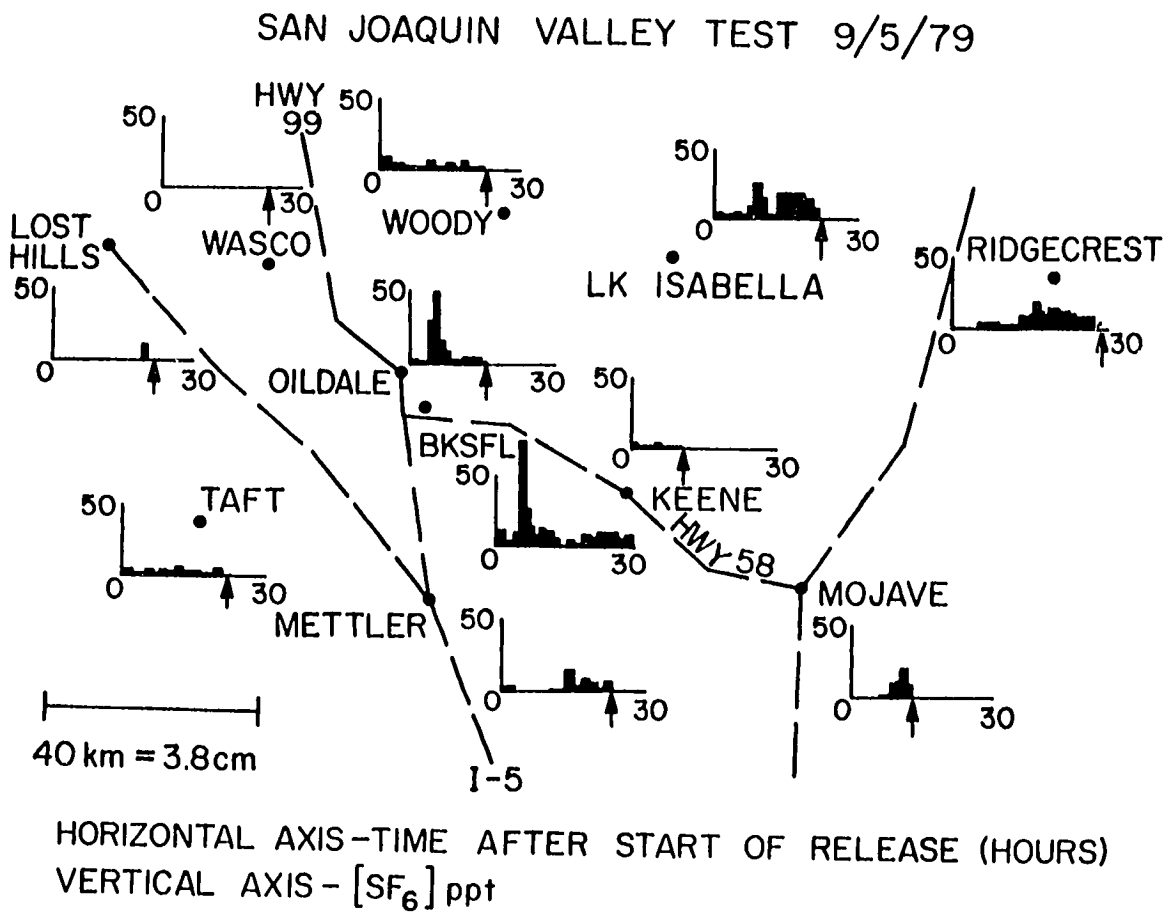

Figure 8 - Hourly averaged tracer concentrations observed during the first Oildale release (Test 1, Sept), indicating transport into the Mojave Desert sites of Mojave and Ridgecrest.

concentrations on the east side of the mountains were only about a factor of 3 lower than those observed on the western side of the mountains. During this test, automobile traverses indicated that about 85% of the tracer was transported into the Mojave Desert on the day of the release. The results of these tests are described in detail in Reible, et al., 1981. As described in that paper, the transport of San Joaquin Valley pollutants apparently causes a rapid degradation in visibility in the northern Mojave Desert during the evening (see also Ouimette, 1981). Pollutant sources on the southwestern side of the San Joaquin Valley can also impact the Mojave Desert during the afternoon and evening hours. During the fourth release of the September, 1979 field program, tracer released during the early morning hours at Fellows was transported at least as far east as Keene by late afternoon on the day following the release. The hourly-averaged concentrations detected at fixed sampling sites during this test are shown in Figure 9. These data indicate that the entire southern end of the valley is efficiently ventilated by the afternoon northwesterly flow. This observation is consistent with the earlier estimate that a volume equal to about 2/3 of the afternoon influx of air at the valley's northern mouth is transported over the Tehachapi Mountains.

The interaction of the buoyant slope winds and the marine air intrusion at the valley's northern mouth also lead to the development of the Fresno Eddy and the nocturnal jet. These dynamic flow structures greatly complicate the transport of pollutants within the valley. As described previously,

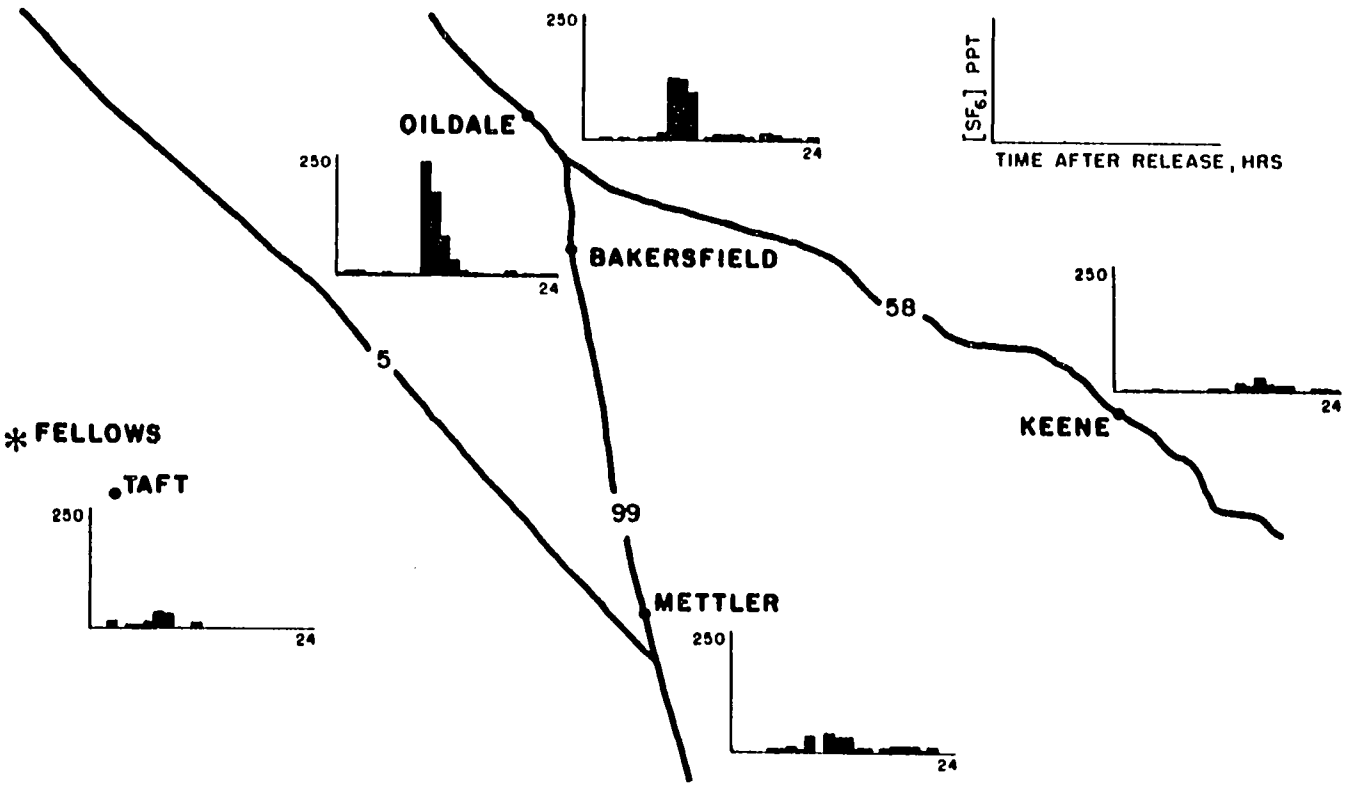

Figure 9 - Hourly averaged tracer concentrations observed during second Fellows release (Test 4, Sept), indicating efficient cross-valley transport.

stabilization of the low level air in the southern end of the valley during the night leads to the development of a counterclockwise eddy motion in the southern valley, the so-called Fresno Eddy. At about the same time the stabilization and decoupling of the surface layer from the air aloft leads to the development of the nocturnal jet, a high velocity layer from 300 m to 1-2000 m altitude.

Because of the extensive length of the valley, the Fresno Eddy can only transport air through about half of the valley length before it breaks up. Consequently, a thorough horizontal mixing process is not possible but significant transport can occur. Due to the dynamic behavior of the eddy, a numerical model of such transport appears difficult. The potential for cross-valley transport within the eddy was demonstrated during the fourth test of the September, 1979 series, in which SF_6 was released during the early morning hours from Fellows, on the southwestern edge of the valley. As previously shown in Figure 9, the tracer was transported into Bakersfield and Oildale on the eastern side of the valley by late morning. Hourly-averaged concentrations as high as 770 PPT/kg-mole released/hr were detected at Bakersfield, on the opposite side of the valley from the release. Clearly, pollutant sources on the southwestern side of the valley must be considered in evaluating the air quality on its southeastern side. The eddy can also transport pollutants from the southern end of the valley towards the north. During the fifth test of the September field program, tracer released at Oilale during the night and early morning hours (2200, 9/16/79 to

0337, 9/17/79) was transported towards the northwest. As indicated in Figure 10, the tracer impacted locations at least as far away as Richgrove, about 50 km north, by mid-afternoon.

While the Fresno Eddy can transport pollutants in the surface layer northward, as well as laterally in the southern valley, the nocturnal jet can transport pollutants that have mixed upward during the afternoon towards the south. During the night, the surface layer of air stabilizes and tends to decouple from the air aloft. The lack of frictional drag at the surface leads to acceleration of the essentially decoupled air aloft. This jet has a peak velocity often in excess of 10 mps at 300 m above the ground. A noticeable jet occurred on between 80 and 90% of the nights during the July and September field programs. While other investigators have reported the frequency and basic structure of the nocturnal jet (Willis and Williams, 1972 and Morgan, 1974), during this study it was possible to directly evaluate the jet's potential for transporting pollutants in the valley. During the fifth test of the July program, SF_6 was released via aircraft directly into the zone exhibiting peak jet velocities. Essentially none of the tracer released during this test was detected at ground level on the night of the release. During late morning on the following day, however, tracer concentrations as high as about 200 PPT/kg-mole released/hr were found at an altitude of about 300 m by airplane traverses throughout the southern end of the valley. Presumably, this material could be transported to the surface as the mixing layer deepened during the afternoon. Thus the nocturnal jet can serve to transport

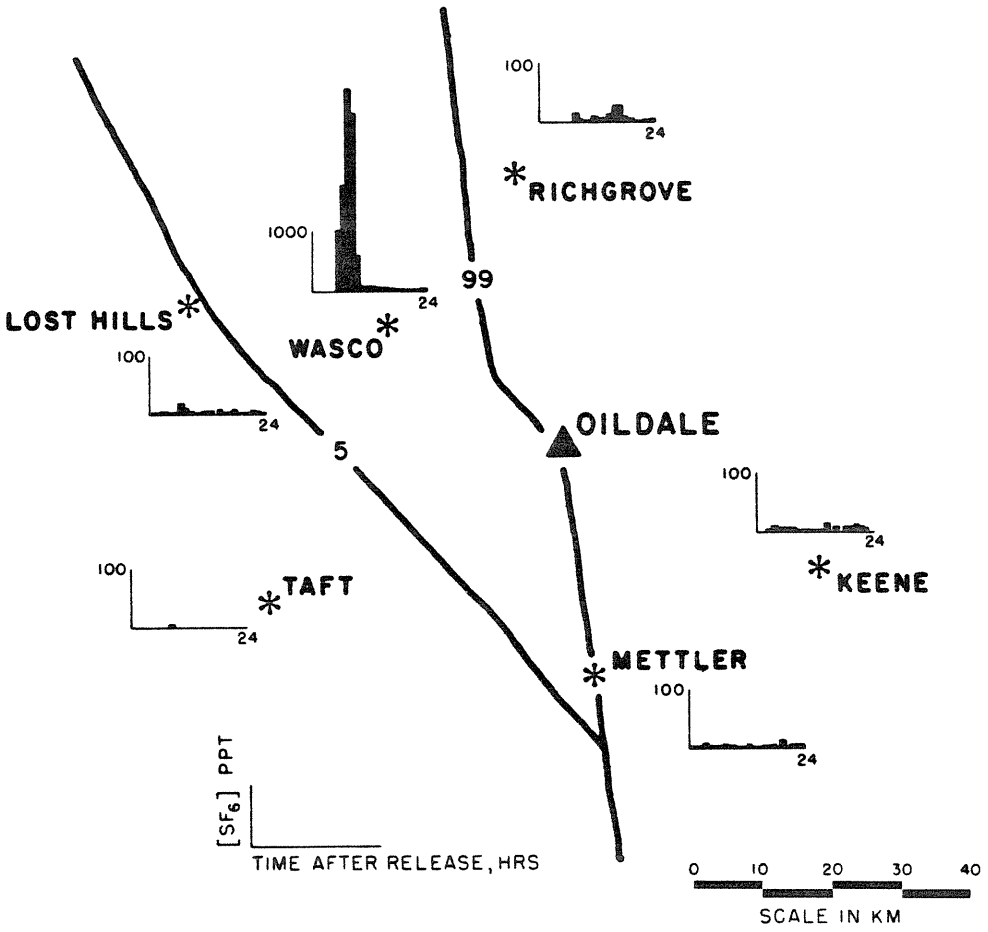

Figure 10 - Hourly averaged tracer concentrations observed during third release from Oildale (Test 5, Sept), indicating transport northward during early morning.

pollutants to the southern end of the valley, even though vertical mixing during the time that the jet exists appears to be limited. During the final tracer test of the September program, tracer released at Manteca, in the extreme northern end of the valley, was detected at Bakersfield about 25 hours later. The hourly-averaged tracer concentrations at Merced and Bakersfield are included in Figure 11. The average transport speed of 4.2 mps could only be explained if the transport was aided by the nocturnal jet winds. Concentrations as high as 90 PPT/kg-mole released/hr were detected at Bakersfield during this experiment.

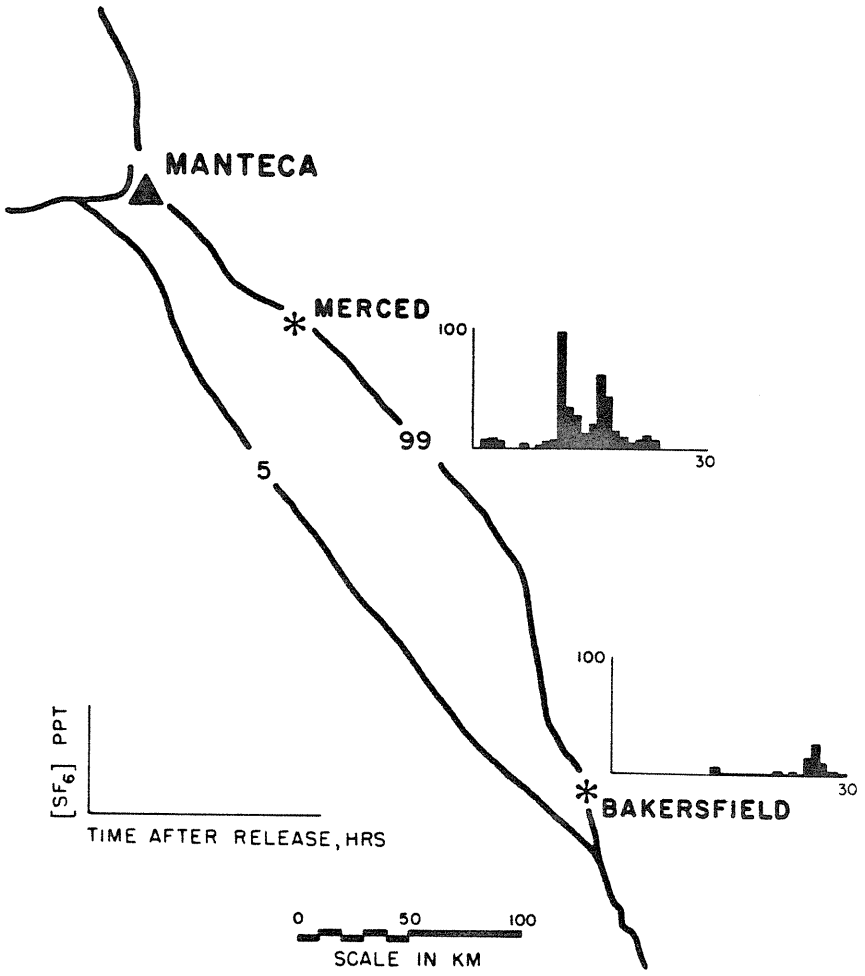

Figure 11 - Hourly averaged tracer concentrations observed at Merced and Bakersfield during third release from Manteca (Test 6, Sept), indicating rapid transport into Bakersfield.

Summary and Conclusions

It is clear that the air pollution meteorology of the San Joaquin Valley is complex, but apparently reproducible from day to day. It was possible to describe through a combination of meteorological and tracer data, the basic, dynamic structure of the flow within the valley. The flow is typically controlled by the interaction of the influx of air at the northern mouth of the valley and the buoyant slope flows along its boundaries. During the afternoon, when these driving forces are oriented in the same direction, the influx of air at the valley's northern mouth is balanced by a corresponding efflux at its southern end. Some valley air is also transported up the western slopes of the Sierra Nevada Mountains during the afternoon, leading to significant pollutant impacts on the National Forest and Park areas. At night, however, the efflux of air in the surface layer at the southern end of the valley is limited by the nighttime low-level stabilization. This leads to the development of a counterclockwise eddy motion in the southern valley that under typical conditions grows to include about half of the valley by mid-morning. This flow structure can lead to significant lateral transport across the valley as well as transport from the south towards the north. Also during the nighttime hours, pollutants that have mixed upward during the day can be transported from the northern end of the valley towards the south by the nocturnal jet, a high-velocity layer between 300 m and 1-2000 m altitude. While very little of the air in the nocturnal jet can impact the surface during the stable nighttime conditions, such impacts can occur

during the following afternoon as vertical mixing increases.

These studies have indicated that potential air pollution problems during summer atmospheric conditions appear most serious along the western slopes of the Sierra Nevada Mountains where significant carryover of valley pollutants may occur from day to day, and in the southeastern San Joaquin Valley, through which the bulk of the valley air must pass (effectively making this area downwind of the all pollutant sources in the San Joaquin Valley). In a like manner, further development in the San Joaquin Valley will undoubtedly lead to further degradation of the air quality in the northern Mojave Desert which typically lies downwind of the valley.

References

Lamb, B.K. (1978). Development and application of dual atmospheric tracer techniques for the characterization of pollutant transport and dispersion. Ph.D. Thesis, California Institute of Technology, Pasadena, Ca.

Lamb, B.K., Shair, F.H., and Smith, T.B. (1978). Atmospheric dispersion and transport within coastal regions- Part II, tracer study of industrial emissions in the California Delta Region. Atmospheric Environment, 12, 2101-2118.

Miller, P.R., McCutchan, M.H., and Milligan, H.P. (1972). Oxidant air pollution in the Central Valley, Sierra Nevada foothills, and Mineral King Valley of California. Atmospheric Environment, 6, 623-633.

Morgan, D.L. (1974). Jet winds in the San Joaquin Valley. Final report to the USDA Forest Service, Berkeley, Ca.

Ouimette, J.R. (1981). Aerosol chemical species contributions to the extinction coefficient. Ph.D. Thesis, California Institute of Technology, Pasadena, Ca.

Pronos, J., Vogler, D.R., and Smith, R.S. (1978). An evaluation of ozone injury to pines in the southern Sierra Nevada. USDA

Forest Service Report No. 78-1, San Francisco, Ca.

Reible, D.D, Ouimette, J.R., and Shair, F.H. (1981). Atmospheric transport of visibility degrading pollutants into the California Mojave Desert. To appear in Atmospheric Environment.

Reible, D.D., Shair, F.H., Smith, T.B., and Lehrman, D.E. (1982a). The origin and fate of air pollutants in California's San Joaquin Valley. Submitted to Atmospheric Environment.

Reible, D.D., Shair, F.H., Smith, T.B., and Lehrman, D.E. (1982b). The transport of airborne contaminants via buoyant slope flows in the Sierra Nevada Mountains of California. Submitted to Journal of Applied Meteorology.

Smith, T.B., Lehrman, D.E., Reible, D.D., and Shair, F.H. (1981). The origin and fate of airborne pollutants within the San Joaquin Valley. Final report to the California Air Resources Board, Sacramento, Ca.

Turner, D.B. (1970). Workbook of Atmospheric Dispersion Estimates. Environmental Protection Agency. Publication AP-26.

Willis, R.A., and Williams, P. (1972). A study of the low-level jet stream of the San Joaquin Valley (Project Lo-Jet). NOAA Western Region Tech Memo No. 75.

Chapter 9

Atmospheric Transport of Visibility Degrading Pollutants into the California Mojave Desert

by

D.D. Reible, J.R. Ouimette, and F.H. Shair

(In Press, Atmospheric Environment)

ABSTRACT

Three atmospheric tracer experiments using SF_6 and fine aerosol measurements were conducted in California to determine the relative impact of pollutant sources in the San Fernando Valley area of Los Angeles and the southern San Joaquin Valley on visibility in a portion of the Mojave Desert. Dilution ratios calculated for SF_6 and various gaseous and aerosol chemical species were used to indicate atmospheric transformation processes between source and receptor. The evolution of the aerosol sulfur mass distribution resulting from transport and transformation was measured. The SF_6 data were compared to predictions based upon the Gaussian dispersion model.

SF_6 released in the San Fernando Valley was found to impact the southern Mojave Desert including the towns of Palmdale and Adelanto during a test on July 20, 1978. SF_6 released at Oildale in the southern San Joaquin Valley was found to directly impact the northern Mojave Desert including the towns of Mojave and China Lake. Some SF_6 released in the San Joaquin Valley was also detected in the southern Mojave Desert. SF_6 was found to be diluted by factors of only 2 to 3 during passage over the mountains separating the source and receptor areas. The SF_6 dispersion during the San Fernando Valley experiment could be modeled with the Gaussian plume model if the experimentally determined mixing height, transport speed and plume trajectory were used, and the stability class was chosen to give good agreement with the data. A simple Gaussian plume model could not provide an adequate description of the San Joaquin Valley test because of the complexities of the wind reversal thatoccurred during the transition from morning to afternoon flow conditions during this test.

Dilution ratios for conserved fine aerosols between Oildale and China Lake were found to be about 3, in excellent agreement with the SF_6 data.

The timing of the diurnal degradation in visibility at China Lake was found to coincide with the arrival of SF_6, thus indicating that the southern San Joaquin Valley was the source of visibility degrading aerosol. The aerosol sulfur mass distribution was found to be essentially conserved between Oildale and China Lake and substantially different from Los Angeles-Palm Springs sulfur mass distributions.

Our data indicate that pollutants from both the southern San Joaquin Valley and the Los Angeles Basin can impact the Mojave Desert during their transport eastward by the predominantly westerly summertime winds; consequently, both "plumes" should be taken into account when considering the impact of southern California pollutants upon the southwestern United States.

INTRODUCTION

It has become apparent in recent years that air pollution is not only a localized problem. Some aspects of air pollution have become regional and even global in scope. For example, emissions from urban sources can lower the pH of rain in rural areas downwind. Liljestrand (1979) concluded that more than half of the acids and bases released within the Los Angeles area are advected out into the California Desert. In addition to contributing to the acid rain problem, the long range transport of pollutants has been implicated in the visibility degradation in the southwestern United States.

The Mojave Desert of California (see Figure 1) appears to be a transition region between the heavily populated California coast and the sparsely populated Southwest. Although visibility in the arid Southwest is currently excellent in most locations, Trojinis (1979a) has noted a 10-30% deterioration in visibility at some locations within this region from the middle 1950's to the early 1970's. Visibility degradation throughout the Mojave Desert appears to be associated with fine particles of anthropogenic origin (Charlson et al., 1978; Macias et al., 1979; Trijonis, 1979a and Ouimette et al., 1980). Macias, et al. (1980) and Hering, et al. (1980) have found that pollutant sources in southern California contribute to the regional haze in the southwestern United States.

Substantial variations in the particle light scattering coefficient, b_{sp}, as measured with an integrating nephelometer, may take place both seasonally and diurnally at China Lake, California in the northern Mojave Desert (Ouimette, 1980). Afternoon visibility during summer and early fall is often as high as 160 km. During the late evening and night-time hours, however, the visibility is typically reduced to about 50-80 km. There are no significant local sources of pollutants that could cause this visibility reduction

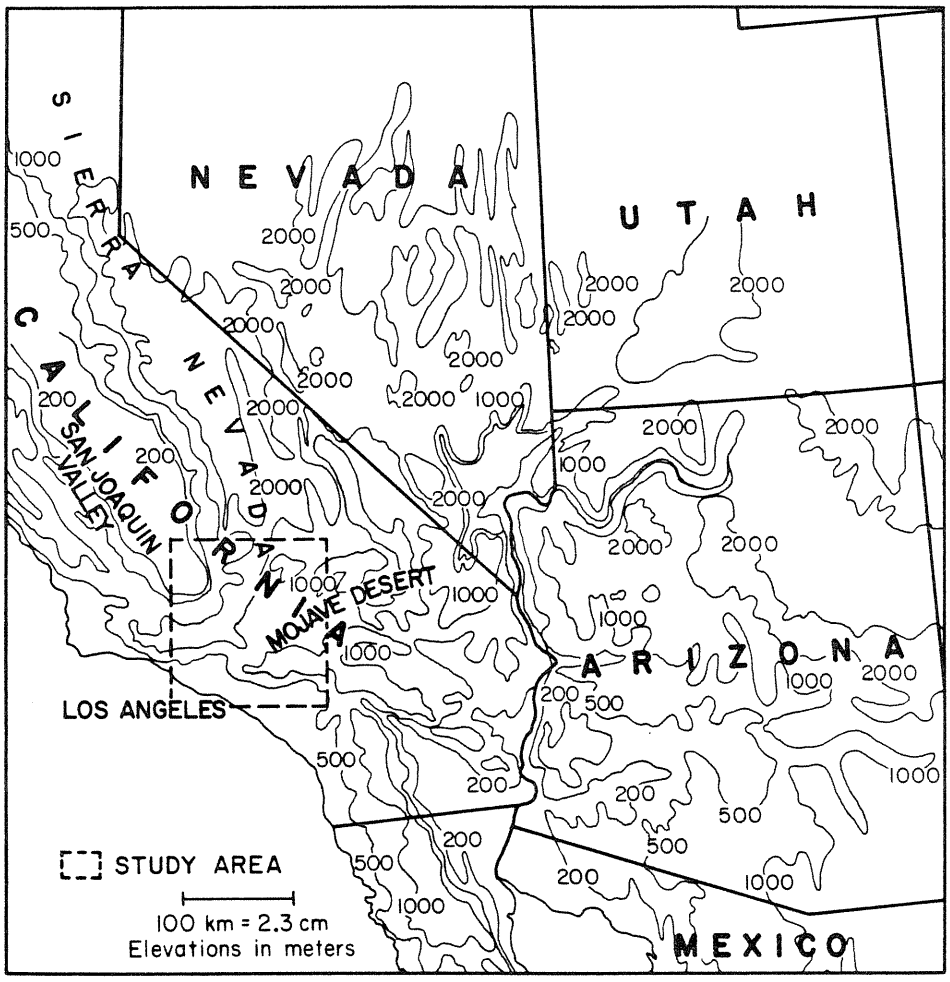

Figure 1 - Map of southwestern United States showing the region of study and its relationship to the surrounding area.

(Ouimette, 1974). Based on typical wind flow patterns in California, the two most likely sources of airborne contaminants detected at China Lake are the western end of the Los Angeles air basin (e.g. the San Fernando Valley) and the southern San Joaquin Valley. The Los Angeles air basin is a large, densely populated urban area that is well known for its air pollution problems. The southern San Joaquin Valley is less densely populated but the area has a number of significant agricultural and industrial pollution sources. In 1976, 275 tons per day of SO_2 were emitted in the Kern County portion of the San Joaquin Valley (Duckworth and Crowe, 1979). The highest 24 hour average aerosol sulfate concentration to date in California, 80 $\mu g/m^3$, was found at Oildale in Kern County in 1978 (Duckworth and Crowe, 1979). It should be noted that the Mojave Desert is within the Southeast Desert Air Basin while the two suspected source areas are within separate air basins. The "air basin" is the basic organization of air pollution regulation and control in California.

The purpose of the present work was to determine the transport and dispersion of visibility-degrading pollutants from the San Fernando Valley area of the Los Angeles air basin and the Oildale-Bakersfield area of the San Joaquin Valley to the Mojave Desert, including China Lake, under typical summer conditions. The complexities of the pollutant transport and dispersion in complex terrain are such that no existing model can be expected to provide accurate estimates with the necessarily limited meteorological data available. For this reason, this work involved the use of atmospheric tracers to quantify the impact of the San Fernando Valley and the San Joaquin Valley on the Mojave Desert. The transport and dispersion of pollutants from the San Fernando Valley was investigated by employing sulfur hexafluoride (SF_6) as an atmospheric tracer. Fine aerosols of less than 2 micrometers (μm) diameter

and SF_6 were relied upon as quantitative tracers for the investigation into the impact of the San Joaquin Valley on the Mojave Desert.

EXPERIMENTAL PROCEDURE

A. Atmospheric tracer studies

During the first tracer test, 245 kg of an inert, non-toxic gas, sulfur hexafluoride (SF_6), were released continuously from Whiteman Airport in the San Fernando Valley of Los Angeles, California. The release took place on July 20, 1978 between 1030 and 1607 PDT (continuous release rate of 44 kg SF_6/hr). The San Fernando Valley is a densely populated region north of central Los Angeles. The release point was east of the San Fernando convergence zone described by Edinger and Helvey (1961). Based on average wind trajectories (Demarrais et al., 1965), pollutant sources in this region can have an impact on the western Mojave Desert. As shown in Figure 1, 1-2 km peaks (San Gabriel Mountains) separate the valley from the desert. The second tracer test involved a continuous release of 245 kg of SF_6 from Oildale in the San Joaquin Valley of California between 0700 and 1200 PDT on September 5, 1979 (49 kg SF_6/hr). In a third test, 240 kg of SF_6 were released continuously from Oildale between 0200 and 0700 PDT on September 9, 1979 (48 kg SF_6/hr). The San Joaquin Valley is a large inland valley (400 km long by 80 km wide) bounded on the west by the California Coastal Mountains (elevations from 0.3 to 1.2 km), on the south by the Tehachapi Mountains (elevations of 1-2.5 km) and on the east by the Sierra Nevadas (elevations of 2 to 4 km). The Oildale area is a significant source of airborne pollutants in the southern San Joaquin Valley. Bakersfield, an urban area with a population in excess of 80,000, lies immediately to the south of Oildale, and a large oilfield lies north and east. During all tracer tests, the gaseous SF_6 was released at a constant rate from 6 cylinders, each containing about 45 kg of liquid SF_6. The cylinders were connected via 1.3 cm OD (1/2") copper manifolding. The SF_6 flowrate was

monitored with a high volume rotameter and verified by weighing the cylinders both before and after each release.

During each test, a series of automobile air sampling traverses were conducted using two person teams. During the automobile traverse, the passenger in each car took grab samples in 30 cm^3 plastic syringes. Samples were typically taken at 1.6 km intervals (1 mile) but during some traverses that passed close to the release site, the sampling interval was 0.8 km (0.5 miles). During the San Joaquin Valley release an airplane was used to obtain additional grab samples. Airplane traverse samples were generally taken every minute (every 3.2 km-2 miles). In addition, the vertical distribution of SF_6 was investigated by airplane spirals in which samples were taken at altitude intervals of about 150 m. Both airplane and automobile traverse paths were determined in the field based upon real time wind data and spot checking of samples with a portable electron capture gas chromatograph. Hourly averaged air samples were obtained during each test by automatic samplers at fixed locations. The samplers uniformly fill a 30 cm^3 syringe each hour for 12 hours. Two or more samplers were deployed at each location to provide continuous coverage for at least 24 hours. The locations of the hourly averaged sampling stations for the San Fernando release are shown in Figure 2. Also included are some of the hourly averaged sampling stations used during the San Joaquin Valley releases (a complete display of these sites is shown in Figure 7) and the major traverse routes for each test.

Air samples were analyzed for SF_6 using electron capture gas chromatography. Details of the analytical procedure and the experimental apparatus are described by Drivas (1975) and Lamb (1978). The gas chromatographs were calibrated using the exponential dilution method and checked between calibrations by comparison to a known standard. Calibration results showed that

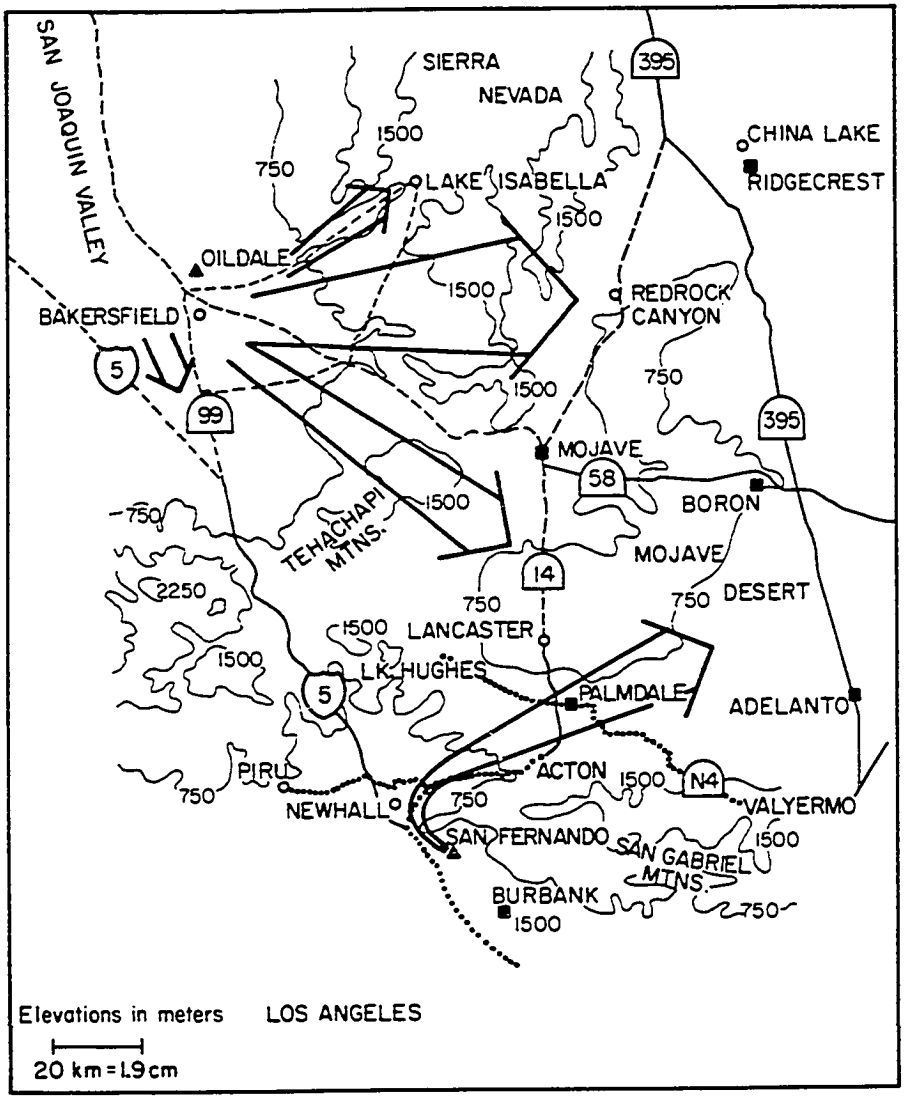

Figure 2 - Map of study area including SF_6 release points (▲), SF_6 fixed site sample locations (■), and main automobile traverse routes (...) for the San Fernando Valley release and the main automobile traverse routes (--) for the San Joaquin Valley release. Also included are arrows indicating the general direction(s) of SF_6 transport during each test. The width of the arrows for the San Joaquin Valley test is a qualitative indicator of the amount of mass transported in each direction and does not represent the width of the plume.

concentrations as low as 10 parts SF_6 per trillion parts air (10 PPT) could be detected within about 20%. Concentrations between 1 and 5 PPT could be detected within a factor of two.

B. Aerosols

San Fernando Valley SF_6 Release of July 20, 1978:

During the San Fernando Valley test, the aerosol measurements were limited to continuously monitoring the particle light scattering coefficient, b_{sp}, at China Lake with a Meteorology Research Inc. (MRI) Model 1561 integrating nephelometer.

Oildale SF_6 Release of September 5, 1979:

Aerosol measurements were more complete during the Oildale-San Joaquin Valley test. The aerosol analysis was, however, limited to fine particles. This mode is linked closely to human influence, dominates light extinction through particle scattering and absorption, and is transported over long distances (Friedlander, 1977). To estimate aerosol dilution from source to receptor, fine aerosol was sampled at the Oildale SF_6 release site on September 5, 1979 from 0850-1302 PST. Similarly, aerosol was sampled at China Lake from 1000 PST September 5, 1979 to 1800 PST September 7, 1979.

At the Oildale site, the aerosol was sampled from a roof at a height of about 3 meters above the ground which was located about 20 meters from the SF_6 release point and about 10 meters from a monitoring trailer operated by the California Air Resources Board (CARB). Two calibrated cyclone separators were operated at a flowrate of about 23 liters per minute. These removed coarse particles from the airstream with efficiencies of 50% for 2 μm and 98% for 6 μm aerodynamic diameter (John and Reichl, 1978). The fine particle airstream from each cyclone was sampled by a total filter and a low pressure

impactor (LPI) operating in parallel. The calibrated LPI segregates aerosol into eight stages having 50% efficiency aerodynamic diameters of 4.0, 2.0, 1.0, 0.50, 0.26, 0.12, 0.075, and 0.05 μm respectively (Hering, et al., 1978 and Hering, et al., 1979). Immediately after collection, all samples were placed in petri dishes, sealed with parafilm, wrapped in a sealed ziplock bag, and placed in an ice chest or refrigerator. This was to prevent contamination and loss of volatile species.

The fine aerosol from cyclone #1 was collected by a Pallflex Tissuequartz filter which had been baked at 900 ^{o}C for 1 hour. The Tissuequartz filters were subsequently analyzed for total carbon by proton induced gamma ray emissions (Macias et al., 1978) and graphitic carbon (soot) by optical reflectance at Washington University (Delumyea, et al., 1980). In parallel to the Tissuequartz filter, a LPI collected aerosol on vaseline coated stainless steel strips to determine sulfur mass distributions by the technique of flash volatization and flame photometric detection (Roberts and Friedlander, 1976).

The fine aerosol from cyclone #2 was collected by a 0.4 μm pore size Nuclepore polycarbonate filter. After determination of the average fine particle mass concentration by gravimetric analysis, the filters were cut into pieces for separate additional analyses. The time average particle absorption coefficient, b_{ap}, at a wavelength of 0.63 μm was measured with an He-Ne laser and phototransister using the opal glass technique (Lin, et al., 1973). Aerosol sulfate, nitrate, phosphate and ammonium ion mass concentrations were determined by liquid ion chromatography and calorimetry at Environmental Research and Technology, Inc. (ERT), Westlake Village, California. Elemental mass concentrations were determined by particle induced X-ray emissions (PIXE) at Crocker Nuclear Laboratory, U.C. Davis, California (Cahill, 1975) and Florida State University.

To obtain time averaged gas phase HNO_3 and NH_3 concentrations, ambient air was filtered through, in succession, a Millipore 1 μm pore size teflon filter, a prewashed Ghia nylon filter, and 2 oxalic acid impregnated glass fiber filters. It was assumed that the HNO_3 and NH_3 would pass through the teflon filter and would be collected with 100% efficiency by the nylon and oxalic acid impregnated filters, respectively (Spicer, 1979; Richards, 1979). The average HNO_3 concentration was determined from the NO_3^- extracted from the nylon filter and analyzed by liquid ion chromatography at ERT. The NH_3 concentration was determined from the NH_4^+ extracted from the oxalic acid filters by Rockwell International, Thousand Oaks, California and analyzed using colorimetry.

Aerosol at China Lake was sampled at about 3 meters above ground on top of an air-conditioned air monitoring trailer operated by the U.S. Naval Weapons Center, China Lake, California. The trailer was located about 5 miles north of Ridgecrest on restricted land away from any significant local sources. Aerosol sampling and analyses were accomplished for China Lake in a manner similar to that of Oildale. In addition, the aerosol scattering coefficient, b_{sp}, was continuously measured with two MRI Model 1561 nephelometers modified by Alan Waggoner at the University of Washington to provide automatic daily zeroing and an accuracy of $\pm$ 2.5 (10^{-6}) m^{-1} from 0 to 250 (10^{-6}) m^{-1}. The submicron aerosol size distribution was obtained from a Thermo Systems Model 3030 Electrical Aerosol Analyzer. Temperature, dew point, solar intensity, wind speed, and direction were also continuously monitored.

PRESENTATION AND DISCUSSION OF RESULTS

San Fernando Valley Release of July 20, 1978

As described previously, 245 kg of SF_6 were released continuously from Whiteman Airport in the San Fernando Valley between 1030 and 1607 PDT on July 20, 1978. During the release period, winds in the eastern San Fernando Valley were generally from the southeast at 3 mps. Typical July wind flow patterns persisted in the San Fernando Valley throughout the test (Demarrais,et al., 1965). Winds measured at Newhall (3 mps @ 130-170^{o}), north of the release site, and in the Mojave Desert (7-9 mps @ 220-250^{o} at Palmdale) also corresponded to typical July wind flow patterns. Demarrais,et al. (1965) found, for example, that July afternoon winds at Palmdale average about 6 mps and are from the southwest quadrant 83% of the time.

Figure 3 shows the time variation in the light scattering coefficient due to particles, b_{sp}, on July 20 and 21, 1978 at China Lake. Comparing this to the July composite average $\pm$ one standard deviation for 1978-1979 on the same figure, it is seen that b_{sp} levels during this period were slightly higher than normal although a typical diurnal variation was observed (Ouimette, 1980). None of the SF_6 released in the San Fernando Valley was detected at China Lake during the sampling period (1300 PDT, July 20 to 1300 PDT, July 21, 1979). This would indicate that either the San Fernando Valley was not a significant source of visibility degrading aerosol at China Lake during this period, or that its plume was too dilute to detect by SF_6, but still optically significant.

Two main automobile traverse routes were followed during the test. These are shown as dotted lines in Figure 2. The arrow drawn from the San Fernando Valley release point in Figure 2 is a qualitative depiction of the experimentally determined tracer plume transport path. This line connects the locations of

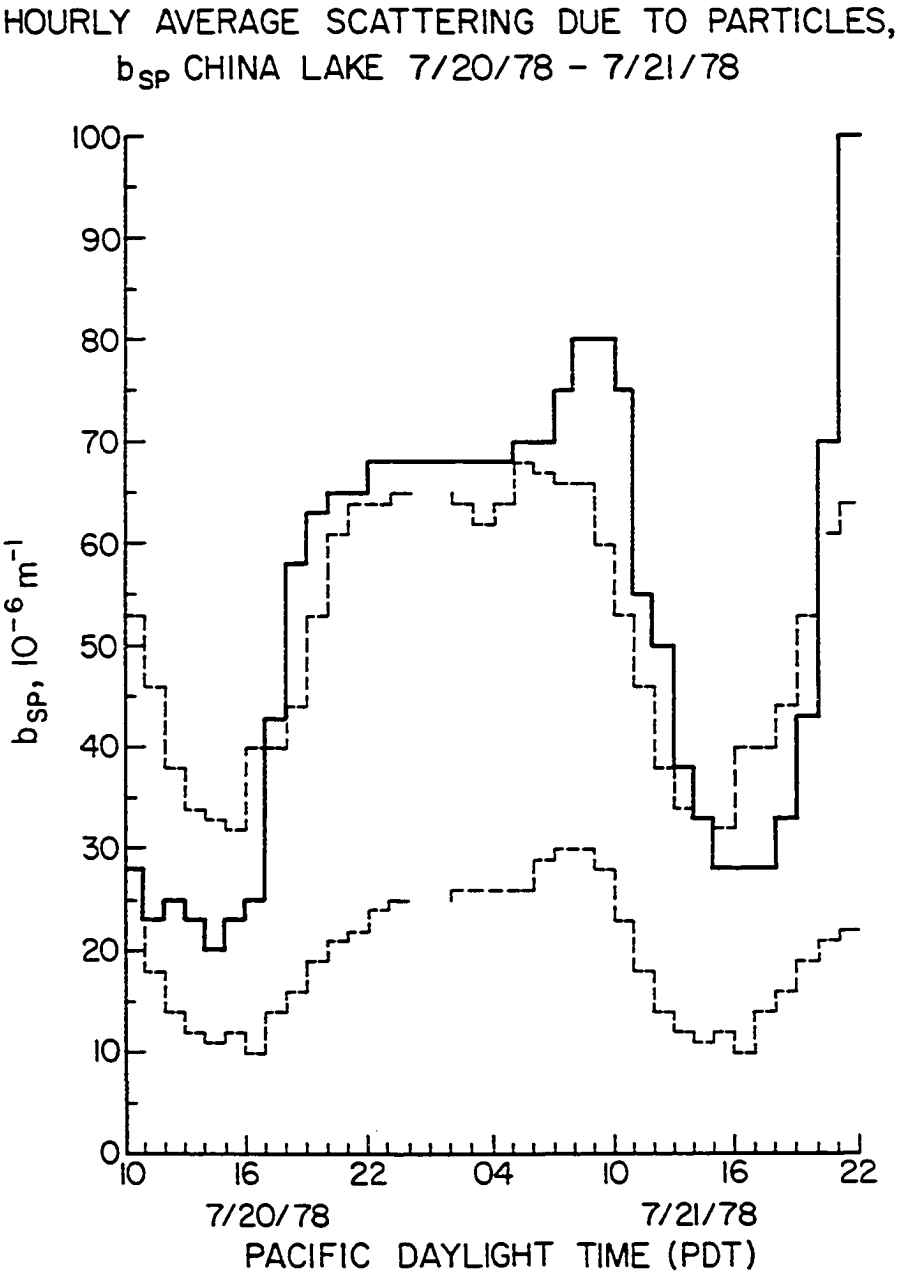

Figure 3 - Hourly average scattering due to particles, b_{sp}, at China Lake on July 20 and 21, 1978 (—). Also shown are the b_{sp} levels within one standard deviation of the 1978, 1979 July composite mean b_{sp} at China Lake (--).

the maximum traverse concentrations. A third traverse route showed that apparently none of the tracer was transported south or west of the release site.

Beginning at 1004 PDT on the day of the release, automobile traverse samples were taken along California Highway 126 and the Soledad Canyon Road between Piru and Acton (shown as a dotted line in Figure 2). This route lies about 19 km downwind of the release site. By traveling back and forth between the end points, this traverse was sampled six times between 1004 PDT and 1820 PDT. These traverses were designated as Traverses 1-1 through 1-6. The experimentally determined SF_6 concentration profiles for these traverses are shown in Figure 4. The first two traverses found essentially no SF_6. The third traverse, which began at the eastern end of the route, found a very sharply defined SF_6 plume spread over 12-16 km. Traverses 1-4 and 1-5 encountered SF_6 plumes of about the same width and location. During all three traverses the peak SF_6 concentration was between 250 and 320 PPT. The arrival of SF_6 occurred about 2 hours after the start of the release suggesting a transport speed of about 2.5 mps for the plume. Traverse 1-6, which began about 1-1/2 hours after the end of the release, found essentially no SF_6.

The second traverse route was sampled nine times between 1318 and 2227 PDT. As shown in Figure 2, this route followed the eastern edge of the San Gabriel Mountains between Lake Hughes and Valyermo (shown as a dotted line in Figure 2). The experimental concentration profiles found during the second through the ninth traverse are shown in Figure 5. An SF_6 plume was found in the vicinity of Palmdale during Traverses 2-3 through 2-7. The peak SF_6 concentrations for Traverses 2-3 through 2-6 were between 100 and 200 PPT. The lower SF_6 concentrations measured during Traverse 2-7 imply that essentially all of the SF_6 had passed through the area by about 1900 PDT. Between 1500 and 1800 PDT (Traverses 2-4 through 2-6), the location of the maximum SF_6 concentration shifted

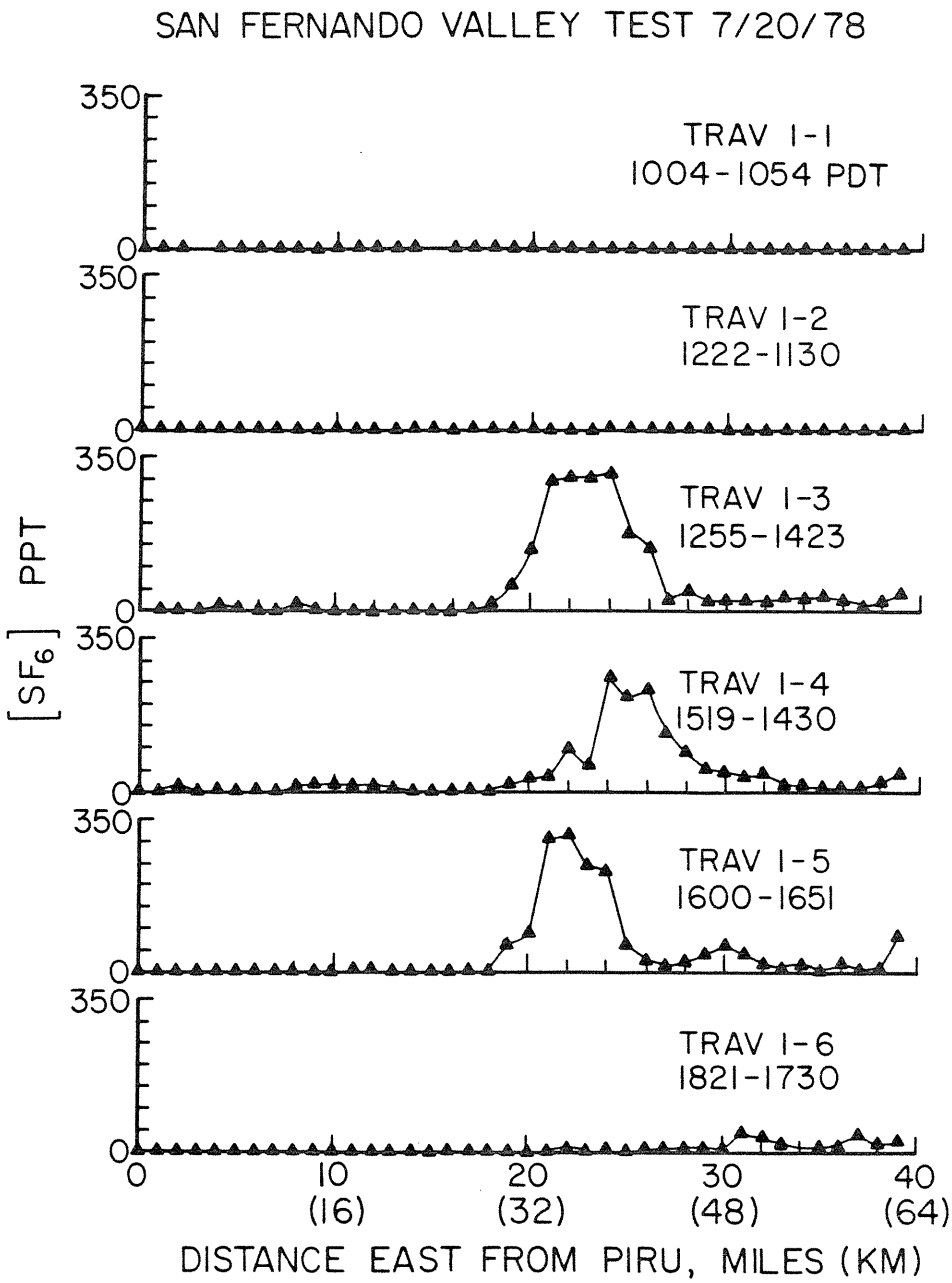

Figure 4 - SF_6 concentrations detected during automobile traverses between Piru and Action on the west side of the San Gabriel Mountains during the San Fernando Valley release.

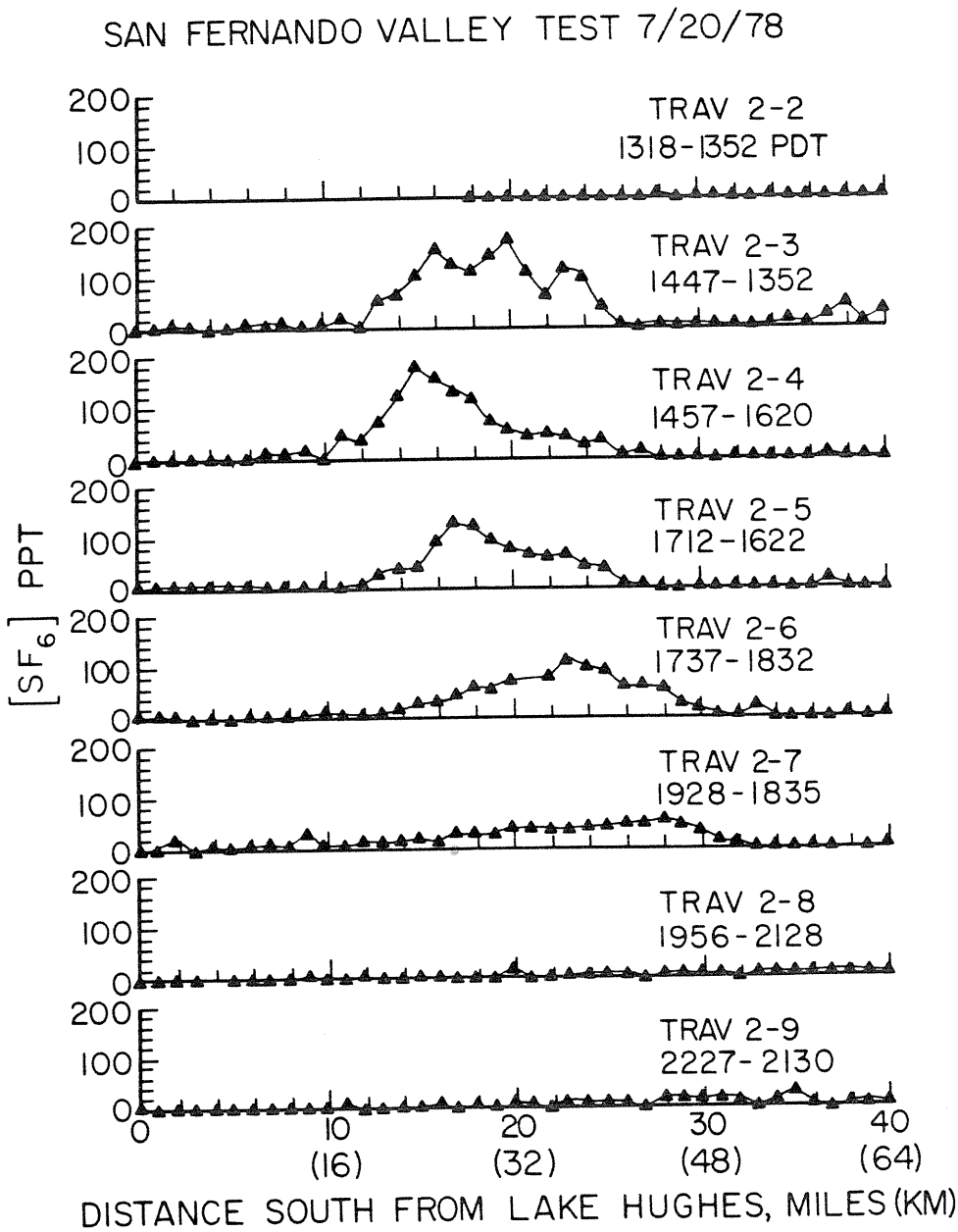

Figure 5 - SF_6 concentrations detected during automobile traverses between Lake Hughes and Valermo on the east side of the San Gabriel Mountains during the San Fernando Valley release.

towards the southeast. This was presumably due to a slow shift in the prevailing wind direction. This conclusion could not be verified because of insufficient wind data. The detection of the plume at Palmdale suggested a transport speed of about 3 mps (65 km, 5.5-6 hours).

The automobile traverse data summarized above were used to estimate the vertical dispersion of the tracer in the slope flow over the San Gabriel mountains. In the absence of airborne sampling, it was assumed that the tracer was well-mixed over the height of the slope flow layer since this flow is typically only weakly coupled with the synoptic scale flow aloft (i.e. the flow above the slope flow layer). As mentioned previously, an automobile traverse showed that essentially no SF_6 was transported south or west of the release point. It was thus assumed that essentially all of the released SF_6 was in the plumes detected near Newhall and Palmdale. The height of the well-mixed layer above the surface can be estimated from the mean transport wind speed, the density of the air and the crosswind integrated tracer concentration:

$$H = \frac{q}{U_c \rho f_{rd} \cos\theta \int_{\ell} C(\ell) d\ell}$$

where,

H = height of the well mixed layer

q = tracer release rate per unit time (45 kg SF_6/hr)

U_c = mean transport wind speed

ρ = air density at sampling position (5.6 kg/m^3)

C = experimentally determined SF_6 concentration

f_{rd} = the ratio of the straight-line and along road distance between the points representing the limits of the integration ($f_{rd} \sim 0.85$ for both Trav Rt 1 and Trav Rt 2)

θ = the average angle between the road and the tracer plume centerline (i.e. the mean wind direction). Together with f_{rd}, this term corrects for the fact that the road is not straight nor crosswind to the plume ($\theta \sim 45^o$ for both Trav Rt 1 and Trav Rt 2)

ℓ = distance coordinate along road traversed

The integral in this equation was evaluated using the experimental concentration data and the trapezoidal rule. The calculated mixing height was 600 ± 100 m using Traverses 1-3, 4, 5 and 2-3, 4, 5. Thus, the average value of about 600 m appears to be a reasonable estimate of the slope flow depth above the San Gabriel Mountains on the test day.

The automobile traverse data were also compared to predictions of the Gaussian plume model. Traverses 1-3, 1-4 and 1-5 on the west side of the San Gabriel Mountains were fit to a Gaussian curve. The best-fitted curves had a peak of 300 ± 70 PPT and a crosswind standard deviation in concentration of 1.9 ± 0.3 km. The curve-fitting technique employed was that described by Sackinger, et al. (1981). This technique involves evaluating the integral definitions of the necessary statistical quantities (such as the standard deviation). Because of the sensitivity of the standard deviation to the "tail" of the concentration data, the integrals are evaluated between the locations corresponding to 10% of the maximum detected concentration and then corrected for the neglected area under an exact Gaussian curve. The calculated standard deviations in concentration were corrected for crosswind distance along the traversed road (i.e. the crosswind distance was estimated to be about 60% of the along-road distance). Assuming stability class C, and by employing the calculated mixing height and mean transport wind speed, the Gaussian model predicts a centerline concentration of 380 PPT and a crosswind standard deviation in concentration of 1.5 km at this distance downwind (19 km). A similar curve fitting procedure for data from Traverses 2-3, 2-4, and 2-5, estimated a peak concentration of 135 ± 25 PPT with a crosswind standard deviation in concentration of 3.4 ± 1.0 km. The standard deviation was corrected for the fact that the crosswind distance was again about 60% of the along-road distance. Assuming stability class C, the Gaussian model

predicts a centerline concentration of 72 PPT and a crosswind standard deviation of about 4 km at this distance downwind (65 km). The downwind distances used in these calculations are along the plume trajectory as defined by the automobile traverse data. These calculations suggest that it is possible to describe the observed horizontal dispersion with a Gaussian model once the mean wind speed, the vertical mixing height, stability class, and trajectory have been accurately determined. Because of the complexities of pollutant transport and dispersion in mountainous terrain, the Gaussian plume model may at times be the most cost-effective modeling approach, especially when experimental tracer data are available. However, Gaussian modeling in complex terrain cannot be relied upon to provide much more than an order of magnitude type of analysis, especially if experimental data are not available. Reible et al. (1981b) have outlined the use of the Gaussian plume model in worst case analyses of pollutant transport and dispersion in complex terrain.

Comparison of the average concentrations within the plume on the west and east sides of the San Gabriel Mountains shows that this value decreased by a factor of about 2.0 $\pm$ 0.5. The limits of the plume were again defined as the locations corresponding to SF_6 concentrations 10% of the peak concentration. Thus the tracer plume was diluted only by a factor of two during passage over about 50 km of mountainous terrain. This suggests that the boundaries normally used to separate various regulatory airsheds (e.g. mountains) are <u>not</u> barriers to significant pollutant transport under certain conditions, in that the dilution over these mountains can be relatively small.

The fixed site hourly averaged data shows the same basic tracer transport and dispersion as the grab sample automobile traverse data. Palmdale was the most highly impacted of the sites sampled (maximum SF_6 concentration - 65 PPT).

Good agreement between grab and hourly averaged concentrations was found in that the average ratio of the hourly averaged concentration to the corresponding traverse concentration was 0.77. This ratio is substantially higher than would be predicted by the Hino correction, (see Hino, 1968). The only other sampling site that showed a significant SF_6 concentration was the southern Mojave Desert sampling site of Adelanto in which three consecutive samples (1900-2200 PDT) showed SF_6 levels of about 10 PPT. For the purposes of this study, the southern Mojave Desert was defined as that part of the desert south of Highway 58 (as shown in Figure 2). Essentially no SF_6 was transported to the northern Mojave Desert sampling sites of Mojave, Ridgecrest and Boron. This suggests that airborne pollutants emitted in the eastern San Fernando Valley primarily impact the southern Mojave Desert under the meteorological conditions prevailing during this tracer test. It should be remembered, however, that typical wind flow patterns were observed throughout the study area (Demarrais, et al.1965) and that the visibility at China Lake, as measured by b_{sp}, also showed typical diurnal variations (Ouimette, 1980).

San Joaquin Valley Release of September 5, 1979

During the second test, 245 kg of SF_6 were released continuously from Oildale, within the San Joaquin Valley of California, between the hours of 0700 and 1200 PDT on September 5, 1979. Southeasterly drainage winds predominated throughout most of the release period, transporting the SF_6 to the northwest at 2 mps. At about 1100 PDT, 4 mps westerly winds developed due to daytime heating of the surrounding mountain slopes and the resulting upslope flow. This upslope flow in the Bakersfield area persisted until about 1900 PDT. These conditions are typical late-summer wind flow patterns (Schultz, 1975).

Figure 6 shows the temporal b_{sp} variation at China Lake on September 5 and 6, 1979. Comparison with the September composite average $\pm$ one standard deviation for 1978-1979 shows that b_{sp} levels observed during this period were typical in both magnitude and diurnal variation. In contrast to the San Fernando Valley release, however, the SF_6 released from Oildale was detected in significant quantities at Ridgecrest, about 8 km south of the aerosol sampling location. The SF_6 levels detected at Ridgecrest are also included in Figure 6. It is clear that the temporal variation in SF_6 and b_{sp} at China Lake were similar, indicating that the SF_6 adequately tagged the source of visibility degrading aerosol.

Automobile traverses during the first Oildale tracer release covered a very large area both within the San Joaquin Valley and in the Mojave Desert to the east of the release site. Initially the traverses showed the expected transport of the tracer via drainage winds to the northwest. Later traverses found SF_6 south and east of Bakersfield due to transport via the afternoon upslope winds. Airplane traverses at about 450 m (agl) showed similar concentration peaks at the same locations. An overview of the tracer transport is depicted in Figure 7 in which the hourly averaged fixed sampler data are shown. The Oildale and Bakersfield samplers did not show large SF_6 concentrations until after the upslope flow began in the early afternoon. Most of the SF_6 detected at these sites is thus the diluted reversed plume. The wind reversal caused the SF_6 to be spread over a large area as evidenced by its detection in Mettler, south of the release site, and Lake Isabella to the northeast. By midnight on the day of the release, an automobile traverse showed that SF_6 was well-mixed in the area south and east of Bakersfield at a concentration of about 14 $\pm$ 4 PPT. An area of approximately 370 sq km was

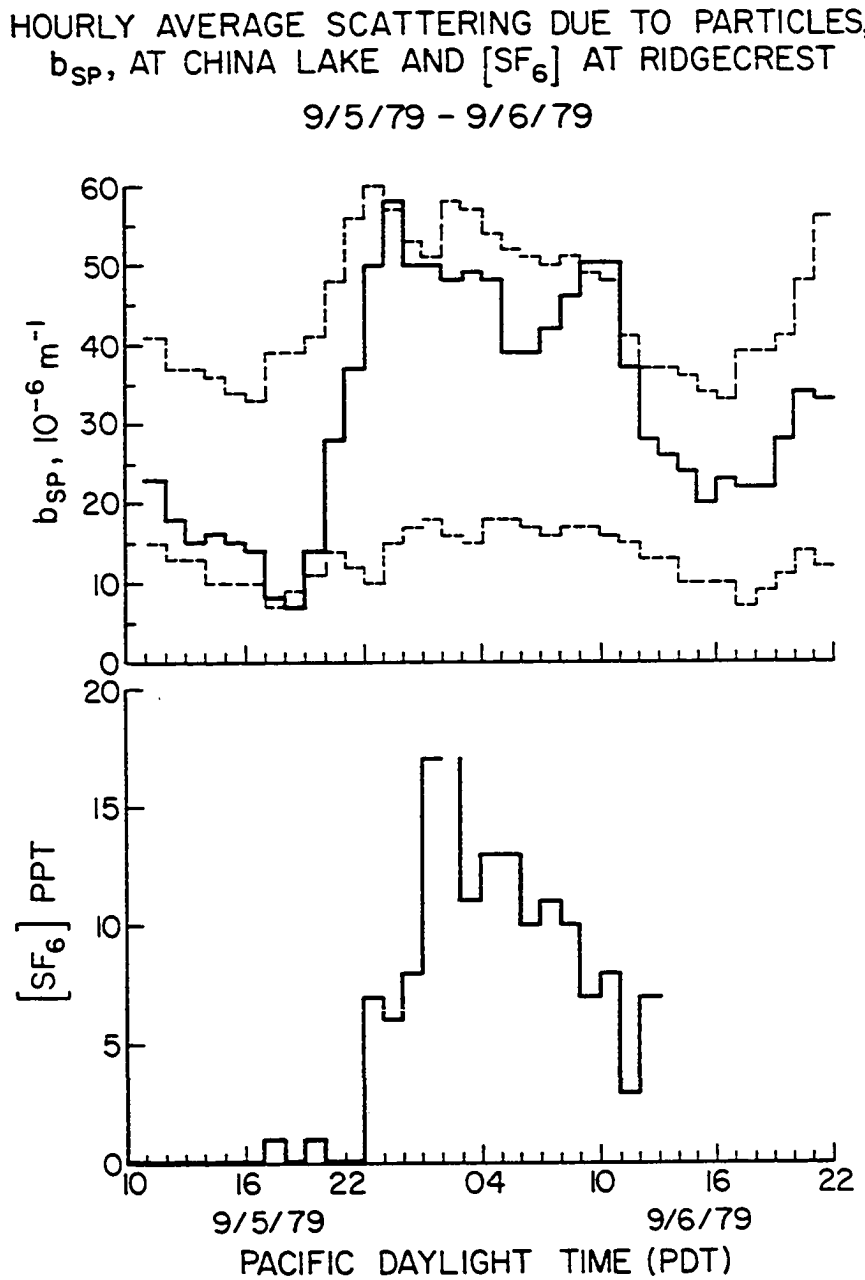

Figure 6 - Hourly average scattering due to particles, b_{sp}, at China Lake on September 5 and 6, 1979 (—). The SF_6 levels detected at Ridgecrest are shown in the bottom figure for comparison (—). Also shown are the b_{sp} levels within one standard deviation of the 1978, 1979 September composite mean b_{sp} at China Lake (--).

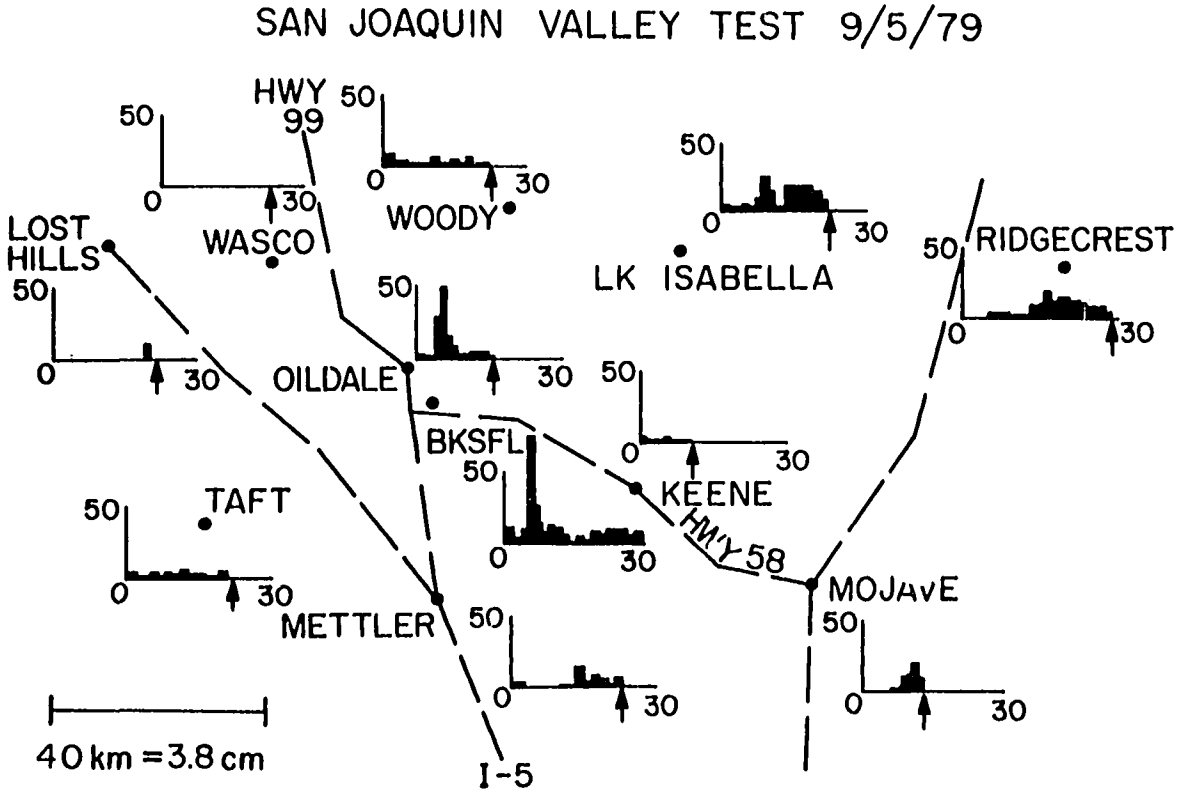

Figure 7 - Overview of SF_6 transport during San Joaquin Valley tests as shown by fixed site sample concentrations. Arrows denote end of sampling period.

enclosed by this traverse. A 1200 m (agl) maximum mixing height over Bakersfield on the test day can be inferred from airplane traverse spirals. Assuming that the SF_6 was well-mixed over the entire volume and assuming a pure SF_6 density of about 5.9 kg/m^3, suggests that about 15% of the total SF_6 emitted could still be detected within the valley on the night following the release. Traverses on the first and second day after the release showed that the mass of SF_6 within the valley continued to decrease. On the second day after the release (9/7/79) a similar calculation on automobile traverse data showed that only about 5% of the SF_6 originally released could be accounted for within the San Joaquin Valley.

The balance of the tracer material was transported over the Tehachapi Mountains and the southern tip of the Sierra Nevada's into the Mojave Desert. This is clearly shown in Figure 7 by the SF_6 levels detected at the Mojave Desert hourly averaged sampling sites of Mojave and Ridgecrest. Maximum SF_6 concentrations measured at Ridgecrest were a factor of 3.1 lower than the early afternoon concentrations measured at Bakersfield and Oildale. The estimated dilution ratio was calculated by comparing the 1200-1600 PDT averages at Bakersfield and Oildale with the average resulting from three different averaging periods at Ridgecrest (2200, 7/20 - 0300, 7/21; 2200, 7/20 - 0900, 7/21; and 0100 - 0900, 7/21). The different averaging periods all gave dilution ratios within 30% of 3.1. SF_6 arrived at Mojave and Ridgecrest between 11 and 15 hours after the start of the release. The arrival times at the fixed sampling sites are in good agreement with arrival times suggested by the automobile traverses depicted in Figure 8. These automobile traverses sampled along California HWY 14 on the western edge of the Mojave Desert (shown as broken line in Figure 2). These traverses each consisted of three passes between Lancaster and the intersection of HWY 14 with HWY 395 on the night following the release. No SF_6 was detected until the sampling run begun at

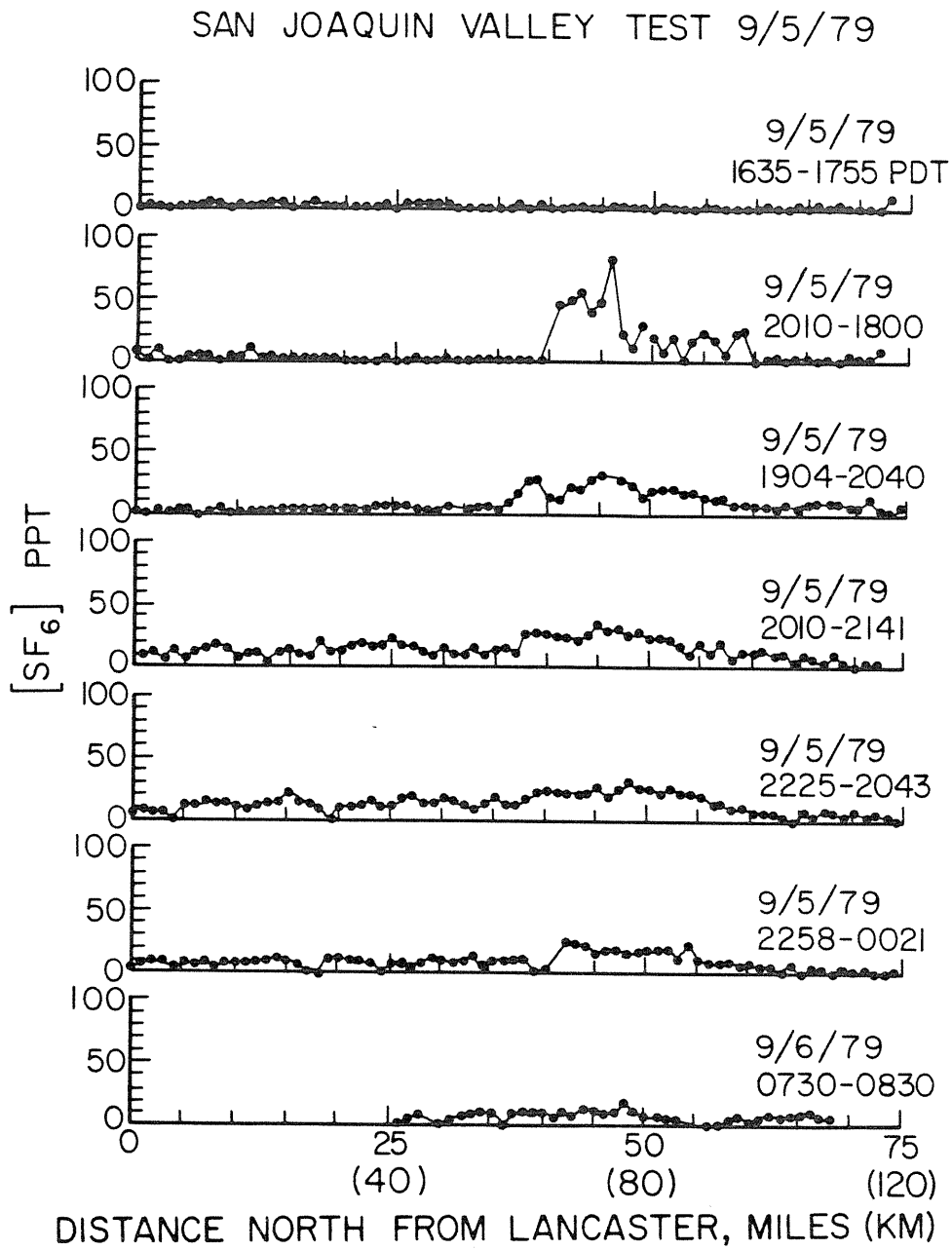

Figure 8 - SF_6 concentrations detected during automobile traverses between Lancaster and the intersection of CA Hwy's 14 and 395 in the Mojave Desert during the San Joaquin Valley test.

1800 PDT at the HWY 395 intersection. During this traverse, a maximum of 81 PPT SF_6 was detected in the vicinity of Red Rock Canyon State Recreation Area, directly east of Bakersfield. The average SF_6 concentration within this 30 km wide plume was about 27 PPT. The boundaries of the plume were defined as the locations where SF_6 levels corresponded to 10% or less of the measured maximum SF_6 level. This can be compared to an average of 68 PPT detected in a plume about 12 km wide in the San Joaquin Valley near Edison during an earlier traverse. The SF_6 detected near Edison was assumed to be the same material later encountered in the Red Rock Canyon Area. The ratio of the average concentrations within the plumes gives a dilution factor of 2.5 during passage over the mountains separating the Mojave Desert and the San Joaquin Valley. A traverse along a road near the ridgeline of the mountains encountered an SF_6 plume with an average concentration of 46 PPT over about 16 km (about 24 km as measured along the road). This gives a dilution factor for half of the distance over the mountains as roughly half the calculated dilution factor for the entire distance. During the traverse beginning at 2010 PDT from Lancaster, SF_6 was detected over the entire traverse route. The SF_6 encountered during the southern half of the traverse probably corresponds to SF_6 detected earlier in the southeastern San Joaquin Valley. Comparison of the average concentrations within the two plumes suggests a dilution factor of 2.1 for this distance. The detection of SF_6 throughout much of the western end of the Mojave Desert suggests that air pollutants from the San Joaquin Valley and those from the San Fernando Valley can jointly impact the eastern Mojave Desert and southern Nevada and Arizona. Our data suggest that both "plumes" should be taken into account when considering the impact of southern California pollutants upon the southwestern United States.

Table 1 summarizes the aerosol mass concentrations averaged over the times of the SF_6 release at Oildale and SF_6 detection at China Lake. Since b_{sp} was not measured at Oildale, it was estimated from average 1 pm July-September visual range data by Barone et al., (1978) and Trijonis (1979b), corrected for measured particle absorption. The table is divided into those species which may, in the absence of additional sources, be conserved, and those species which may undergo conversion. The amount of fine aerosol dilution from Oildale to China Lake may be estimated from the conserved chemical species data. The average dilution, from the ratios of Oildale to China Lake conserved species concentrations, is 3.0 ± 0.6. The fine aerosol dilution value compares favorably with that estimated from SF_6 dilution, 2.5-3.1. Just as in the San Fernando Valley release, the transport of tracer and/or pollutants over a mountain range does not result in dilution by a factor of much more than 2 to 3.

The effects of conversion and loss of aerosols during transport may be examined by comparing the dilution values of the unconserved species to 3.0. The sulfate and ammonium ratios are slightly less than average, and indicate the possibility of additional ammonium sulfate aerosol being produced enroute from Oildale to China Lake. Aerosol nitrate concentrations for both locations were close to, or within, the standard deviation of the Nuclepore filter blank (NO_3^-). Thus the nitrate ratio is the least precise of the values. In fact, at the temperatures sampled, the gas phase ammonia and nitric acid data indicate that no pure NH_4NO_3 should be in the aerosol phase (Stelson, et al., 1979). The small quantity of nitrate aerosol at Oildale was evidently volatized into its gaseous precursors by the time the air parcel reached China Lake. The lower dilution ratio for NH_3 indicates the possibility of a large area source for ammonia in addition to Oildale. The anomolously high value of the

TABLE 1 - TIME AVERAGED FINE AEROSOL AND SELECTED GASEOUS CONCENTRATIONS

A. Conserved Species

Species	Mass Concentration, $\mu g/m^3$ Oildale	China Lake	Ratio
Total Carbon	18.6	5.6	3.3
Soot	4.2	1.1	3.8
Al	0.68	0.21	3.2
Si	1.36	0.64	2.1
K	0.20	0.08	2.4
Ca	0.50	0.18	2.8
Fe	0.64	0.19	3.3
$b_{ap}, 10^{-6}m^{-1}$	29.	8.8	3.3
			average = 3.0 ± 0.6

B. Other Species

Species	Mass Concentration, $\mu g/m^3$ Oildale	China Lake	Ratio
SO_4^-	8.47	4.24	2.0
NO_3^-	1.81	0.44	4.1
NH_4^+	2.67	1.43	1.9
$NH_3(g)$	2.45	1.9	1.3
$HNO_3(g)$	10.1	1.2	8.4
Total Mass	44.9	19.7	2.3
$b_{sp}, 10^{-6}m^{-1}$	150.(est.)	49.	3.1 (est.)

Oildale average for 0951-1402 PDT, 9/5/79

China Lake average for 2210-0600 PDT, 9/5/79-9/6/79

HNO_3 dilution indicates that loss of HNO_3 likely took place enroute. Possible routes could include dry deposition to alkaline soil or by diffusion and adsorption on coarse alkaline aerosol which was not sampled.

The effect of transport on the distribution of aerosol sulfur with respect to aerodynamic diameter can be seen in Figure 9. Aerosol size was segregated by low pressure impactor (LPI) (Hering, et al., 1979) and analyzed by flash volatization and flame photometric detection (Roberts and Friedlander, 1976). Histograms are inverted distributions obtained from LPI calibration data and Twomey (1975) inversion algorithm (Ouimette, 1980). The Oildale sulfur aerosol mass was preferentially distributed between 0.1 and 0.2 μm diameter, consistent with the gas phase homogeneous oxidation of SO_2 to H_2SO_4 aerosol (Gelbard and Seinfeld, 1979; McMurry and Friedlander, 1978).

Earlier work by Drivas and Shair (1974), showed that under typical meteorological conditions, Palm Springs may be the recipient of polluted air from the Los Angeles Basin. Typical aerosol sulfur mass distributions at Palm Springs and Pasadena are plotted in Figure 10 (Hering, 1980 and Friedlander, 1978). It is seen that the sulfur distribution very likely preserves its shape in transit from the Los Angeles Basin to Palm Springs. However, in this case the sulfur is preferentially distributed at about 0.6 μm diameter, substantially larger than the Oildale-China Lake distribution. The larger Los Angeles sulfur aerosol is consistent with particle growth by heterogeneous droplet phase conversion of SO_2 (Friedlander, 1978; Friedlander, 1977). Mie calculations indicate that the Los Angeles-Palm Springs sulfate is distributed optimally for light scattering whereas the Oildale-China Lake sulfate is not, due to its distribution in smaller sizes (Ouimette, 1980). Because the Los Angeles and Oildale sulfur distributions are typical (Hering et al., 1980; Friedlander,

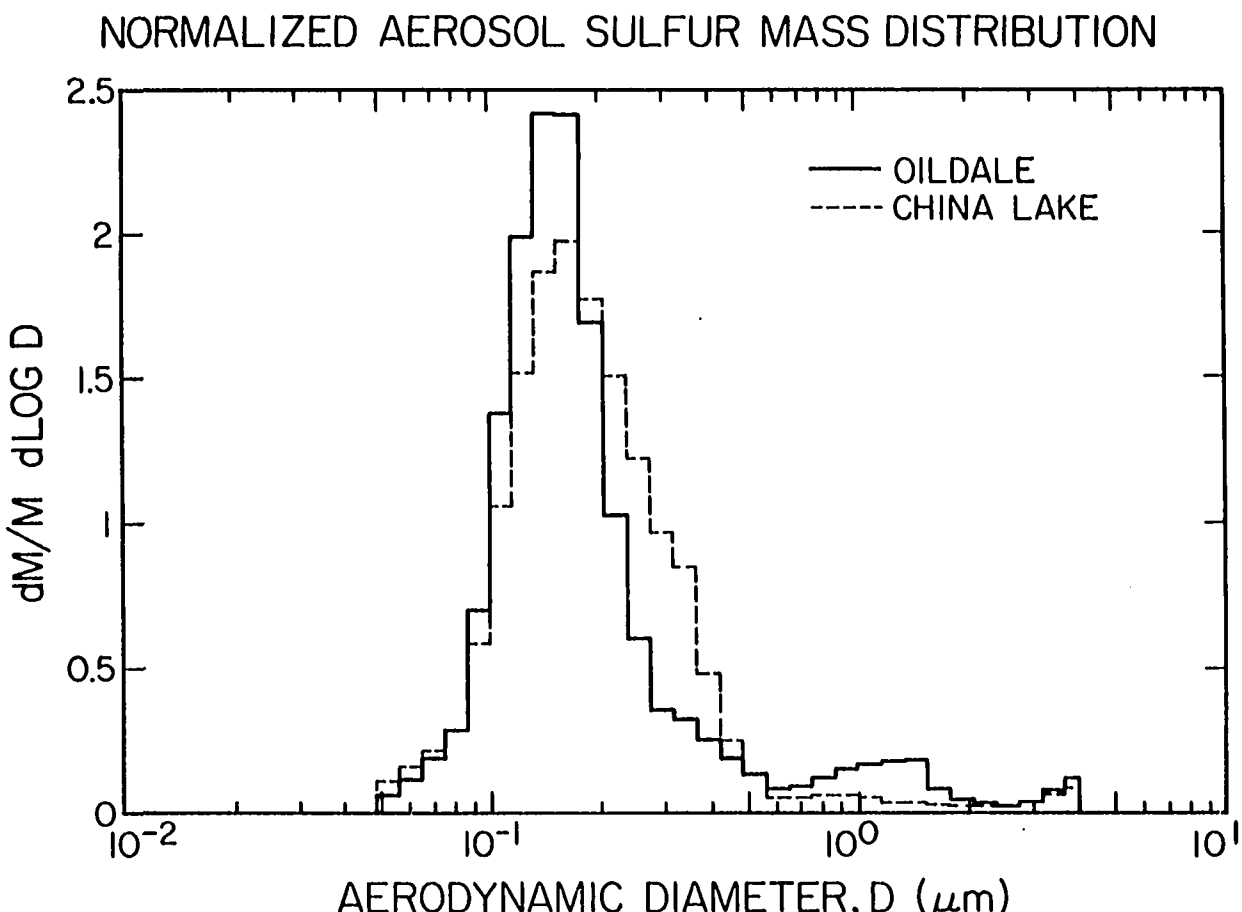

Figure 9 - Normalized ambient aerosol sulfur mass distributions. Oildale - 1127-1215 PDT, 9/9/79; M=3.48 $\mu g/m^3$. China Lake - 2200-0130 PDT, 9/9/79-9/10/79; M=1.15 $\mu g/m^3$.

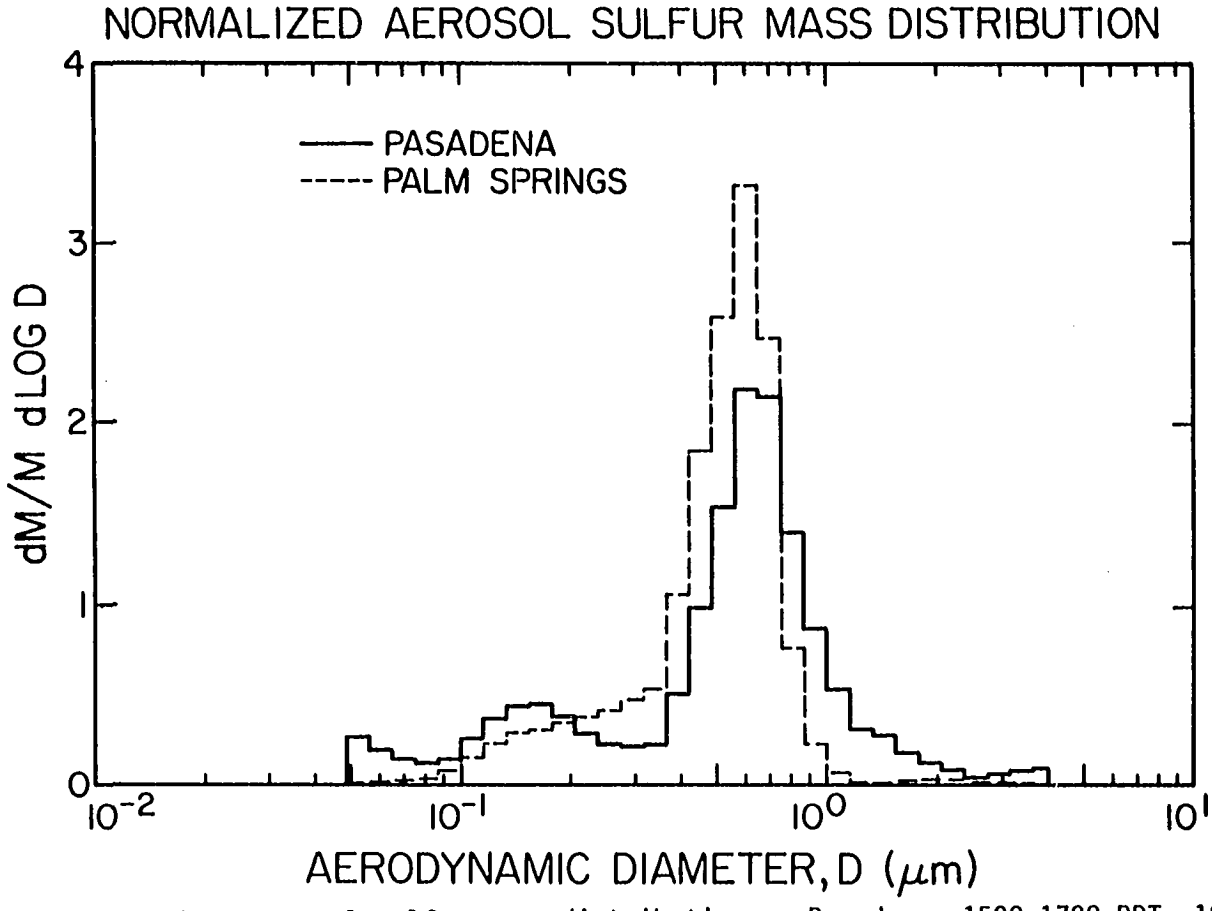

Figure 10 - Normalized ambient aerosol sulfur mass distributions. Pasadena, 1528-1728 PDT, 12/26/78; M=10.6 μg/m^3. Palm Springs, 1730-1830 PDT, 08/03/79; M=2.1 μg/m^3.

1978; Barone, et al., 1978) they may be used as qualitative aerosol tracers of each source in the absence of other sources in the Mojave Desert.

To ensure that the bulk of the tracer and pollutants from Oildale were transported to and detected in the Mojave Desert, a mass balance calculation on the tracer data was attempted. An airplane spiral during the afternoon on the day of the release above Caliente on the eastern edge of the San Joaquin Valley showed that SF_6 was relatively well-mixed to a height of about 1400 m (asl). Caliente lies in a small basin that has an average elevation around 6-800 m. Thus the mixing height above the mountain slopes is about 6-800 m (agl). This was roughly the mixing height calculated during the analysis of transport over the similar San Gabriel Mountain range during the first test. The mixing height on the desert side of the mountains was not measured. The travel time between Bakersfield and the Mojave Desert was about 6-8 hours which corresponds to a mean transport speed of about 4-5 mps. A mass balance calculation using the experimental concentration profiles, a 600 m mixing height and a 4.5 mps wind speed suggests that 70-80% of the SF_6 released at Oildale was transported eastward over the southern end of the Sierra Nevada Mountains into the northern Mojave Desert. About 10-20% of the SF_6 was transported to the southeast over the Tehachapi Mountains into the southern Mojave Desert. The town of Mojave appeared to be roughly the point separating the two transport paths and was used to separate the northern and southern Mojave Desert. For the mass balance calculations, a mass flowrate was calculated from each of the traverse passes and then multiplied by the time interval until the next traverse pass. Due to the uncertainty in vertical mixing height, the mass balance can merely suggest that most of the tracer not accounted for within the San Joaquin Valley on the night following the release was detected in the Mojave Desert.

Because of the complexity of the flow reversal during the transition from downslope to upslope flow at the release site, a simple Gaussian model cannot hope to provide a complete description of the tracer transport and dispersion during this test. The tracer was spread over a large area and significant amounts could be found throughout the western edge of the Mojave Desert and in the San Joaquin Valley. As described previously, however, the bulk of the tracer was transported directly east of the release point after the onset of the afternoon upslope winds. The peak concentrations within this plume, as measured by automobile on the western edge of the Mojave Desert, varied between 81 and 26 PPT. Assuming stability class C, the Gaussian model predicts a centerline concentration between 33 and 50 PPT, depending on whether the downwind distance is calculated along the reversed tracer trajectory or on a straightline from the release point. The concentration profiles along these traverses, however, are not Gaussian in shape and the crosswind spread of the tracer plume is not well described by the Gaussian model.

San Joaquin Valley Release of September 9, 1979

The results of the September 5, 1979 tracer study suggest that airborne pollutants released in and around Bakersfield and Oildale have a strong impact upon the northern Mojave Desert. The only effective mechanism of pollutant transport out of the southern San Joaquin Valley during summer and early fall appears to be afternoon upslope flows (Reible and Shair, 1981). Thus pollutants released at different times during the day from the industrial, agricultural and urban sources in the San Joaquin Valley probably impact the Mojave Desert at about the same time. Partially to test this hypothesis, an additional tracer study was conducted from Oildale involving the release of 240 kg of SF_6 between 0200 and 0700 PDT on September 9, 1979. The wind flow patterns during this test were

virtually indistinguishable from the first Oildale release. This test was primarily intended to detail transport within the San Joaquin Valley but one automobile traverse along the Tehachapi Mountains was extended into the town of Mojave. SF_6 levels around 20 PPT were detected in the vicinity of Mojave and 29 PPT were detected within the town at 2100 PDT. These can be compared to the 2000-2100 PPT hourly averaged SF_6 concentration of 20 PPT detected at Mojave during the first Oildale release (Figure 7). There thus appears to be little difference between the two Oildale releases in terms of impact on the Mojave Desert. No aerosol data were available, however, for an Oildale-China Lake comparison as in the first Oildale test.

SUMMARY AND CONCLUSIONS

Three atmospheric tracer experiments using SF_6 and fine aerosol measurements were conducted in California to determine the relative impact of pollutant sources in the San Fernando Valley area of Los Angeles and the southern San Joaquin Valley on visibility in a portion of the Mojave Desert. Dilution ratios calculated for SF_6 and various gaseous and aerosol chemical species were used to indicate atmospheric transformation processes between source and receptor. The evolution of the aerosol sulfur mass distribution resulting from transport and transformation was measured. The SF_6 data were compared to predictions based upon the Gaussian dispersion model.

CONCLUSIONS OF TRACER TEST FROM THE LOS ANGELES AIR BASIN

1) During a test conducted under apparently typical summer meteorological conditions, little or no impact of a tracer released in the San Fernando Valley of the Los Angeles air basin was detected in the China Lake area of the northwestern Mojave Desert.

2) SF_6 released from a location east of the San Fernando convergence zone of the Los Angeles air basin was found to be transported towards the north and then transported eastward into Palmdale and the southern Mojave Desert.

3) The average concentrations within the tracer plume were reduced by a factor of 2 during passage over the San Gabriel Mountains, between Newhall and Palmdale, clearly demonstrating that these mountains are <u>not</u> barriers to significant pollutant transport.

4) Good agreement was found between the experimental concentration profiles and those predicted by the Gaussian plume model

(using experimental inputs) for the tracer transport and dispersion from the San Fernando Valley.

CONCLUSIONS OF TRACER TESTS FROM THE SAN JOAQUIN VALLEY

1) During apparently typical summer meteorological conditions, airborne pollutants released at Oildale in the southern San Joaquin Valley clearly impact the northern Mojave Desert. This conclusion is based upon a number of independent indicators:

    a) SF_6 tracer released at Oildale during mid-morning was detected in Ridgecrest (near China Lake) that night. The tracer transport path was verified by automobile traverses both in the San Joaquin Valley and in the Mojave Desert.

    b) Coincident with the detection of SF_6 at Ridgecrest, the visibility, as measured by b_{sp} at China Lake, decreased from almost 200 km at 1600-1800 PDT to less than 60 km between 2200-2300 PDT.

    c) Both conserved fine aerosols and SF_6 levels detected in the Mojave Desert were a factor of 3 lower than the corresponding levels detected at Oildale.

    d) The aerosol sulfur mass distributions at Oildale and China Lake were quite similar, and both differed markedly from typical Los Angeles-Palm Springs sulfur mass distributions.

2) The average SF_6 concentration in the plume on the east side of the Tehachapi and Sierra Nevada Mountains was about 2.3 ± 0.2 lower than the average concentration in the plume on the west side of these mountains. When coupled with the dilution of aerosols and SF_6 between Oildale and China Lake, this again shows that mountains do not necessarily pose a barrier to significant pollutant transport.

3) Because of the wind reversal between drainage and upslope flow during the first SF_6 release from Oildale, the tracer plume was spread over a large area and was apparently bifurcated. The simple Gaussian plume model is inadequate to describe the asymmetry of the tracer plume, or even provide a rough estimate of its spread.

4) Because of the diurnal mountain-valley wind cycle, the maximum impact of sources in the southern San Joaquin Valley upon the Mojave Desert occurs during evening and night-time hours, apparently independent of the time of the release.

5) Even during relatively good ventilation of the San Joaquin Valley, carry-over of pollutants into the day following their release can be significant. During the first test from Oildale, at least 15% of the SF_6 released in the morning remained in the valley throughout the night.

6) There is indication that aerosol sulfate was created during transport between Oildale and China Lake, but that aerosol and gaseous nitrates were scavenged enroute.

7) The tracer data suggested that air pollutants released in the San Fernando Valley area of Los Angeles and the San Joaquin Valley can impact southern Nevada and Arizona.

ACKNOWLEDGEMENTS

It is a pleasure to acknowledge the contributions by C. Bennett and J. Suder of the California Air Resources Board, T. Smith and D. Lehrman of M.R.I., T. Dodson, A. Kelso, and T. van Curen of the U. S. Naval Weapons Center at China Lake; A. Leslie of Florida State University; G. Colovos of the Rockwell International Environmental Monitoring Center; B. Croes, P. Kezios, J. King, R. Reed, H. Smith and R. Flagan of Caltech; the Fire Departments of Kern, Los Angeles, and San Bernardino counties; and the airport personnel of Palmdale, Mojave and Lancaster. The majority of this work was sponsored under the California Air Resources Board Agreement A7-171-30.

REFERENCES

Barone, J. B., Cahill, T. C., Eldred, R. A., Flocchinig, R. G., Shadoan, D. J., Dietz, T. M. (1978). A Multivariate Statistical Analysis of Visibility Degradation at Four California Cities. Atmospheric Environment 12: 2213-2221.

Cahill, T. A. (1975). Environmental Analysis of Environmental Samples, in New Uses of Ion Accelerators, J. Ziegler, Ed., 1-75, Plenum Press, NY.

Charlson, R. J., Waggoner, A. P., and Thielke, J. F. (1978). Visibility Protection for Class I Areas: The Technical Basis. Report to Council on Environmental Quality, August, 1978. Available from the National Technical Information Service. PB-288-842.

Delumyea, R. G., Chu, L.-C., and Macias, E. S. (1980). Determination of Elemental Carbon Component of Soot in Ambient Aerosol Samples. Atmospheric Environment, 14, 647-652.

Demarrais, G. A., Holzworth, G. C., and Hosler, C. R. (1965). Meteorological summaries pertinent to atmospheric transport and dispersion over southern California. U.S. Weather Bureau, Technical Paper # 54.

Drivas, P. J. (1975). Investigation of Atmospheric Dispersion Problems by Means of a Tracer Technique, Ph.D. Thesis, California Institute of Technology.

Drivas, P. J. and F. H. Shair (1974). A Tracer Study of Pollutant Transport and Dispersion in the Los Angeles Area. Atmospheric Environment, 8, pp. 1155-1163.

Duckworth, S. and D. Crowe (1979). Sulfur Dioxide and Sulfate Survey - Bakersfield, California Air Resources Board, Technical Services Division.

Edinger, J. G., and Helvey, R. A. (1961). San Fernando convergence zone. Bull. Amer. Meteor. Soc., 42, 626-635.

Friedlander, S. K. (1977). Smoke, Dust and Haze: Fundamentals of Aerosol Behavior. Wiley-Interscience, New York.

Friedlander, S. K. (1978). A Review of the Dynamics of Sulfate Containing Aerosols. Atmospheric Environment 12: 187.

Gelbard, F. and Seinfeld, J. H. (1979). The General Dynamic Equation for Aerosols. J. Colloid and Interface Science, 68: 363.

Hering, S. V., Flagan, R. C., and Friedlander, S. K. (1978). Design and Evaluation of a New Low-Pressure Impactor. 1. Environmental Science and Technology, 12: 667.

Hering, S. V., Friedlander, S. K., Collins, J. J., and Richards, L. W. (1979). Design and Evaluation of a New Low-Pressure Impactor. 2. Environmental Science and Technology, 13: 184.

Hering, S. V., and Friedlander, S. K. (1980). Submicron Aerosol Sulfur Size Distributions in the Los Angeles Basin, Presented at Thirteenth Aerosol Technology Meeting, Boston, MA, August 24-26, 1980.

Hering, S. V., Bowen, J. L., Wengert, J. G., and Richards, L. W. (1980). Characterization of the Regional Haze in the Southwestern United States. Presented at Grand Canyon Conference on Plumes and Visibility, November 10-14, 1980.

Hino, M. (1968). Maximum Ground-level Concentrations and Sampling Times, Atmos. Environ., 2, 149-165.

John, W. and Reischl. G. (1978). A Cyclone for Size-Selective Sampling of Ambient Air. AIHL Report No. 187, Air and Industrial Hygiene Laboratory, 2151 Berkeley Way, Berkeley, California 94704.

Lamb, B. K. (1978). Development and Application of Dual Atmospheric Tracer Techniques for the Characterization of Pollutant Transport and Dispersion, Ph.D. Thesis, California Institute of Technology, Pasadena, California 91125.

Liljestrand, H. M. (1979). Atmospheric Transport of Acidity in Southern California by Wet and Dry Mechanisms, Ph.D. Thesis, California Institute of Technology, Pasadena, California 91125.

Lin, C., Baker, M., and Charlson, R. J. (1973). Absorption Coefficient of Atmospheric Aerosol: A Method of Measurement. J. Applied Optics, 12, 1356.

Macias, E. S., Blumenthal, D. L., Anderson, J. A., and Cantrell, B. K. (1979). Characterization of Visibility-Reducing Aerosols in the Southwestern United States: Interim Report of Project VISTTA, MRI 78-IR-1585.

Macias, E. S., Radcliff, C. D., Lewis, C. W., and Sowicki, C. R. (1978). Proton Induced γ-Ray Analysis of Atmospheric Aerosols for Carbon, Nitrogen, and Sulfur Composition. Anal. Chem. 50: 1120-1124.

Macias, E. S., Zwicker, J. O. and White, W. H. (1980). Regional Haze in the Southwestern U.S.: II. Source Contributions. Presented at the Grand Canyon Conference on Plumes and Visibility, November 10-14, 1980.

McMurry, P. H. and Friedlander, S. K. (1979). New Particle Formation in the Presence of an Aerosol. Atmospheric Environment, 13: 1635.

Ouimette, J. R. (1974). Survey and Evaluation of the Environmental Impact of Naval Weapon Center Activities. TM 2426, U.S. Naval Weapons Center. Available from National Technical Information Service.

Ouimette, J. R. (1980). Aerosol Chemical Species Contributions to the Extinction Coefficient. Ph.D. Thesis. California Institute of Technology, Pasadena, California 91125.

Ouimette, J. R., Flagan, R. C., Kelso, A. R., (1980). Chemical Species Contribution to Light Scattering by Aerosols at a Remote Arid Site: Comparison of Statistical and Theoretical Results, presented at the Symposium on Chemical Composition of Atmospheric Aerosols: Source/Air Quality Relationships, Second Chemical Congress of the North American Continental, Las Vegas, Nevada, August, 1980.

Reible, D. D., Shair, F. H., and Kauper, E. (1981-b). Plume Dispersion and Bifurcation Associated with Directional Shear Flows in Complex Terrain, in press, Atmospheric Environment.

Reible, D. D., and Shair, F. H. (1981). Tracer Investigations of the Pollutant Transport and Dispersion Into, Within and Out of the San Joaquin Valley. Final report to California Air Resources Board.

Richards, L. W. (1979). Ammonia and Sulfate Aerosol Study, Final Report. Prepared for Coordinating Research Council, Inc., by Rockwell International, Environmental Monitoring and Services Center.

Roberts, P. T. and Friedlander, S. K. (1976). Analysis of Sulfur in Deposited Aerosol Particles by Vaporization and Flame Photometric Detection. Atmospheric Environment, 10: 403.

Sackinger, P. A., Reible, D. D., and Shair, F. H. (1981). Uncertainties Associated with the Calculation of Mass Fluxes and Gaussian Parameters from Atmospheric Tracer Data, to be submitted to the Journal of the Air Pollution Control Assn.

Schultz, H. B. (1975). Meso-climatic wind patterns and their application for abatement of air pollution in the central California valley. Final report to the California Air Resources Board, Project No. 111.

Spicer, C. W. (1979). Measurement of Gaseous HNO_3 by Electrochemistry and Chemiluminescence in Current Methods to Measure Atmospheric Nitric Acid and Nitrate Arifacts, R. K. Stevens, Ed. EPA-600/2-79-051, Environmental Protection Agency.

Stelson, A. W., Friedlander, S. K., and Seinfeld, J. H. (1979). A Note on the Equilibrium Relationship between Ammonia and Nitric Acid and Particulate Ammonium Nitrate. Atmospheric Environment, 13: 369.

Trijonis, J. (1979a). Visibility in California, First Interim Report. Technology Service Corporation. ARB Contract No. A7-181-30, January, 1979.

Trijonis, J. (1979b). Visibility in the Southwest - An Exploration of the Historical Data Base. Atmospheric Environment, 13, pp. 833-843, 1979.

Twomey, S. (1975). Comparison of Constrained Linear Inversion and Interactive Nonlinear Algorithm Applied to the Indirect Estimation of Particle Size Distributions. J. Comp. Phys., 18: 188.

Chapter 10

The Transport of Airborne Contaminants via Buoyant Slope Flows in the Sierra Nevada Mountains of California

by

D.D. Reible, F.H. Shair, T.B. Smith, and D.E. Lehrman

(Submitted to Journal of Applied Meteorology)

Abstract

Three atmospheric tracer experiments were conducted to investigate the transport and dispersion of airborne contaminants associated with the afternoon upslope flows on the western slope of the Sierra Nevada Mountains of California. The tracer experiments were supported with a network of air quality and meteorological observations in order to determine the slope impact of pollutant sources in the San Joaquin Valley and the basic structure of the slope flows. The afternoon slope flow layer appeared to generally be a well-defined layer about 2-600 m in depth. A return flow directed towards the valley was observed above the upslope flow layer. The depth and speed of the slope flow layer tended to increase with altitude suggesting that air from elevated layers and not just the surface, make up the slope flow layer. The tracer results indicated that the tracer was typicallly well-mixed over the depth of the slope flow layer, and that apparently none of the tracer was returned to the valley by the return flow aloft.

The atmospheric tracer experiments also indicated that the dispersion of a pollutant plume could be approximately modeled with the Gaussian plume model. During these experiments the horizontal dispersion of the tracer corresponded to that expected in very unstable atmospheric conditions (A stability). While the maximum slope concentrations were observed during the afternoon, the stabilization of the atmosphere and corresponding drainage flow into the valley tended to return contaminated air to the

slope receptor zones. During one test, a 5 hour tracer release led to the detection of tracer for at least 18 hours at a site located about 1645 m above the valley floor. The return of contaminated air after wind reversals may provide a significant background inventory of pollutants for the next day's photochemical activity. This may explain, in part, the relatively high ozone concentrations detected 24 hours a day at slope receptor sites.

INTRODUCTION

The transport of pollutants in mountainous terrain is often controlled by the locally induced, diurnally varying buoyant winds. During the day, surface heating of the mountains produces a layer of air directed upslope while at night, surface cooling leads to a drainage layer of air directed downslope. While the basic qualitative structure of these flows has been reported elsewhere (see e.g. Eatontown Signal Laboratory Group, 1945 or Defant, 1951), through the use of ultra-sensitive tracer techniques it has only recently become possible to directly evaluate this flow structure with respect to the transport and dilution of pollutants. In the current studies, the transport of pollutants by the slope flows in the Sierra Nevada Mountains of California was investigated through atmospheric tracer experiments supported by extensive meteorological measurements. The emphasis of these studies was upon the evaluation of the influence of the upslope flow on air quality, and upon understanding the importance of the diurnal character of the slope flows.

The Sierra Nevada Mountains of California contain some of the highest mountain peaks in the United States, with many peaks exceeding 4000 m in altitude. As shown in Figure 1, several National Forests and National Parks are included within the mountain range. Much of this region is designated as wilderness and closed to natural resource exploitation. These areas are Class I regions under the United States Clean Air Act, as amended in 1977, and as such any use that leads to significant

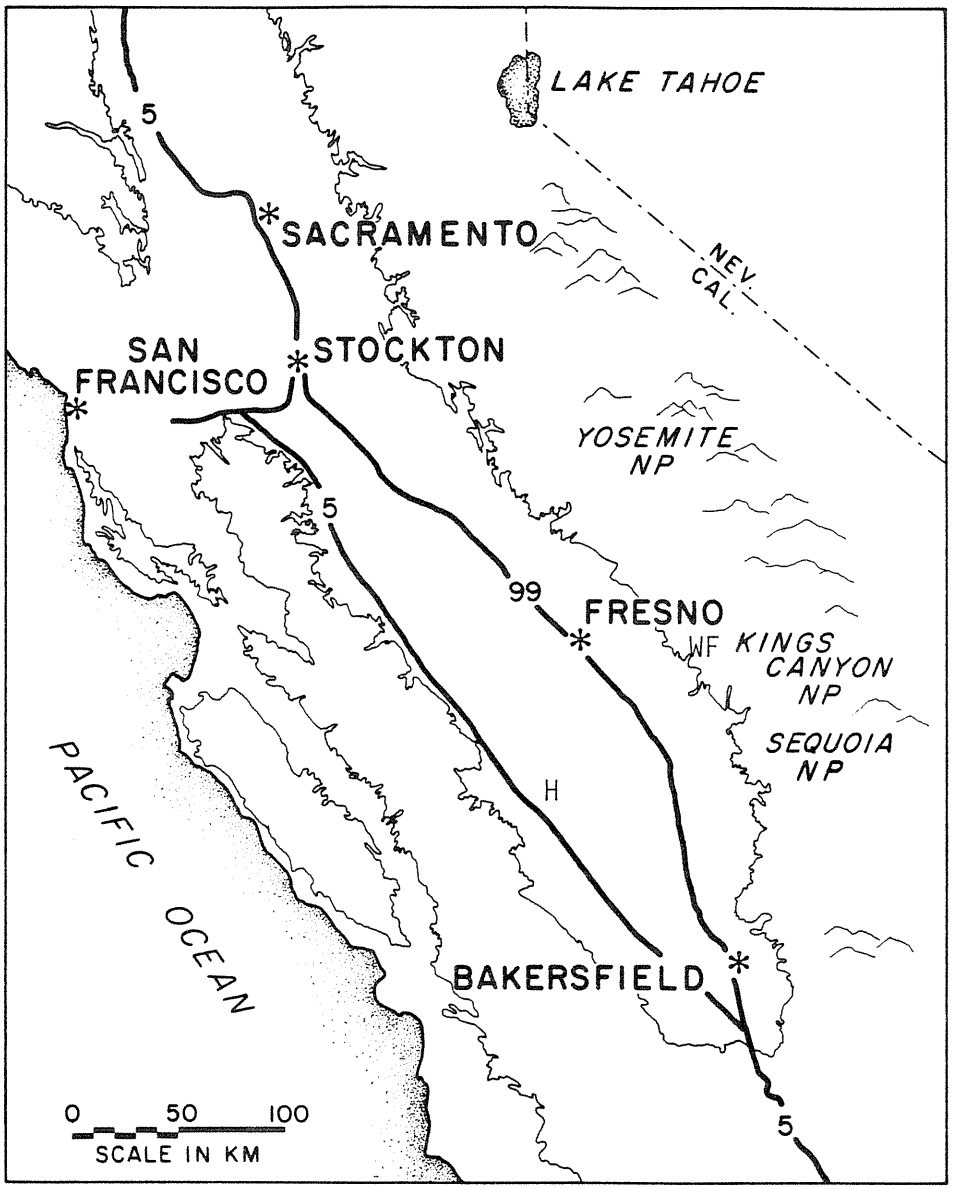

Figure 1 - Map of the San Joaquin Valley of California, indicating the National Parks on the western slopes of the Sierra Nevada.

deterioration of air quality is outlawed. Miller, et al. (1972), however, indicated that ozone formed from precursors emitted in the San Joaquin Valley was transported onto the western slopes of the Sierra Nevada by the afternoon upslope winds. Williams, et al. (1977) and Pronos, et al. (1978) observed significant oxidant damage to sensitive tree species in the National Forest and Park Areas. Maximum ozone concentrations in the mountain slopes often occurred during late afternoon, consistent with transport from distant source locations. Similarly, the highest ozone concentrations downwind of Sacramento, a large urban area in the northern half of the California Central Valley, were observed in excess of 30 km northeast of the city, in the foothills of the Sierra Nevada Mountains. More directly, recent atmospheric tracer studies in the San Joaquin Valley also indicated that pollutant sources in the valley may have a significant impact upon the surrounding mountains (Reible, et al., 1982a and b). The current work was designed to understand the structure of the slope flows that led to these observations and to correlate, through tracer techniques, high slope ozone concentrations with specific source areas or causal mechanisms. A major objective of the current work was the delineation of pollutant transport mechanisms that may occur in other mountain-valley environments.

EXPERIMENTAL PROCEDURE

The experimental program consisted of a total of 3 atmospheric tracer releases employing sulfur hexafluoride (SF_6) during July and August of 1979 in the region east of Fresno. A listing of the tracer releases can be found in Table 1, and the locations of the releases are shown in Figure 2. The first experiment was conducted by the California Institute of Technology (Pasadena, California) as part of an extensive study, supported by the California Air Resources Board, of the transport routes into, within, and out of the San Joaquin Valley (Smith, et al., 1981; Reible, et al., 1982a and b). This release was conducted during the afternoon of 25 July 1979 from Reedley southeast of Fresno. Two subsequent releases were conducted as part of a separate study supported by the U.S. Forest Service by Meteorology Research, Inc. (Altadena, California) on 25 and 28 August 1979 from the Friant Dam east of Fresno (Lehrman, et al., 1980). As shown in Table 2 and Figure 2, the tracer releases were supported by meteorological and air quality measurements at various sites in the mountain receptor areas throughout the late summer and early fall. The air quality measurements were limited to visibilty, as measured by the light scattering coefficient due to particles, and ozone concentrations. These measurements were supplemented during the release periods by air quality monitoring via aircraft.

Tracer concentrations were measured by analysis of air samples by electron capture gas chromatography. This technique allows detection of sulfur hexafluoride at concentrations as low

Table 1 - Tracer Releases

Test 1 - Release of 44 kg SF_6 per hour between 1200 and 1700 PDT, 7/25/79, from Reedley

Test 2 - Release of 36 kg SF_6 per hour between 1215 and 1530 PDT, 8/25/79 from Friant Dam

Test 3 - Release of 35 kg SF_6 per hour between 1230 and 1549 PDT, 8/28/79, from Friant Dam

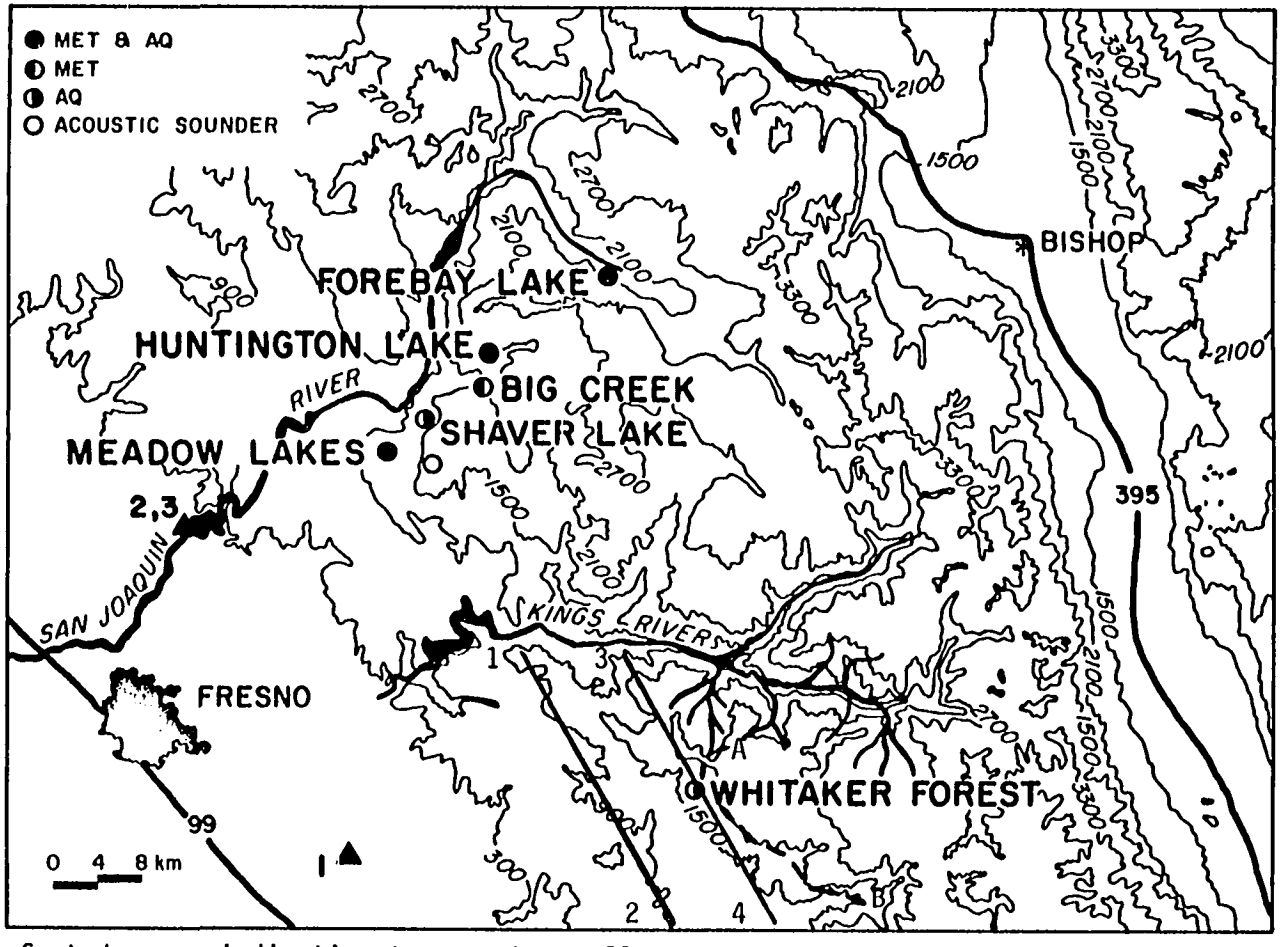

Figure 2 - Map of study area indicating topography, pollutant and meteorological sampling sites (●, ◑, ○) and tracer release sites (▲). Also included are airplane traverse routes (solid line between numbered points) and automobile traverse route (broken line between lettered points) for the test of 25 July (Reedley release).

TABLE 2

UPPER SAN JOAQUIN RIVER VALLEY

SURFACE METEOROLOGICAL AND AIR QUALITY MONITORING

Location	Elevation (m-msl)	Parameters Measured	Period of Sampling
Meadow Lakes	1366	O_3 (1), b_{scat} (2), Temperature, Wind	Met 24 July-19 Oct 1979
			AQ 26 July-1 Nov 1979
Big Creek	1530	Temperature, Wind	Met 21 July-23 Aug 1979
Huntington Lake	2133	O_3 (1), b_{scat} (3), Temperature, Wind	Met 21 July-28 Oct 1979
			AQ 23 July-1 Nov 1979
Forebay Lake	2195	b_{scat} (3), Temperature, Wind	Met 24 Aug-20 Oct 1979
			AQ 24 Aug-14 Oct 1979
Shaver Lake	1677	Atmospheric Stability	10 Aug-18 Oct 1979

(1) Manufacturer - Dasibi -- Method-ultraviolet absorption photometry.

(2) Manufacturer - MRI, Model 1550 -- Single wavelength integrating nephelometer.

(3) Manufacturer - MRI, Model 1569 -- Multiwavelength, high sensitivity integrating nephelometer.

as 1 part-per-trillion (PPT). All tracer air samples were collected in 30 cm^3 plastic syringes. Essentially instantaneous grab samples were collected during automobile and airplane traverses and at fixed sampling sites. In addition, hourly averaged samples were collected at various sites during the tracer experiment of 25 July. Details of the procedures for release, collection and analysis of the tracer can be found in Lamb (1978) or Reible (1982).

PRESENTATION AND DISCUSSION OF RESULTS

Basic Structure of the Slope Flow

Typical time-height cross sections of the upslope flow at two mountain locations are shown in Figure 3. As noted in the figure, the shaded region indicates downslope flow. On the day shown in the figure (27 July 1979), the speed of the upslope flow peaked at between 2 and 4 mps during mid-afternoon with larger velocities observed at the higher elevation site, Huntington Lake (elev. 2133 m). Upslope components existed to a maximum depth of about 600 m at both locations. Note that a reversed flow existed aloft, above the upslope component winds. An upslope directed flow was typically observed by 1200 PDT and persisted until about 2100 PDT at the sites indicated in Figure 2. Table 3 contains the observed depth of the slope flow layer at Huntington, Meadow and Millerton Lakes during the experimental program. Note that the depth of the layer is typically of about the same magnitude as found on 27 July (Figure 3). The depth of the upslope flow layer at Millerton Lake tended to deviate from this, presumably due to its close proximity to the valley floor. The mixing height over the flat valley floor was generally deeper than that observed over the mountain slopes.

Not shown in Figure 3 is the reverse flow directed downslope during the nighttime hours. The nighttime drainage flow was typically limited to a shallower, lower velocity layer than the corresponding daytime upslope flow. The timing of the start and end of the nocturnal drainage flow at several sites during the

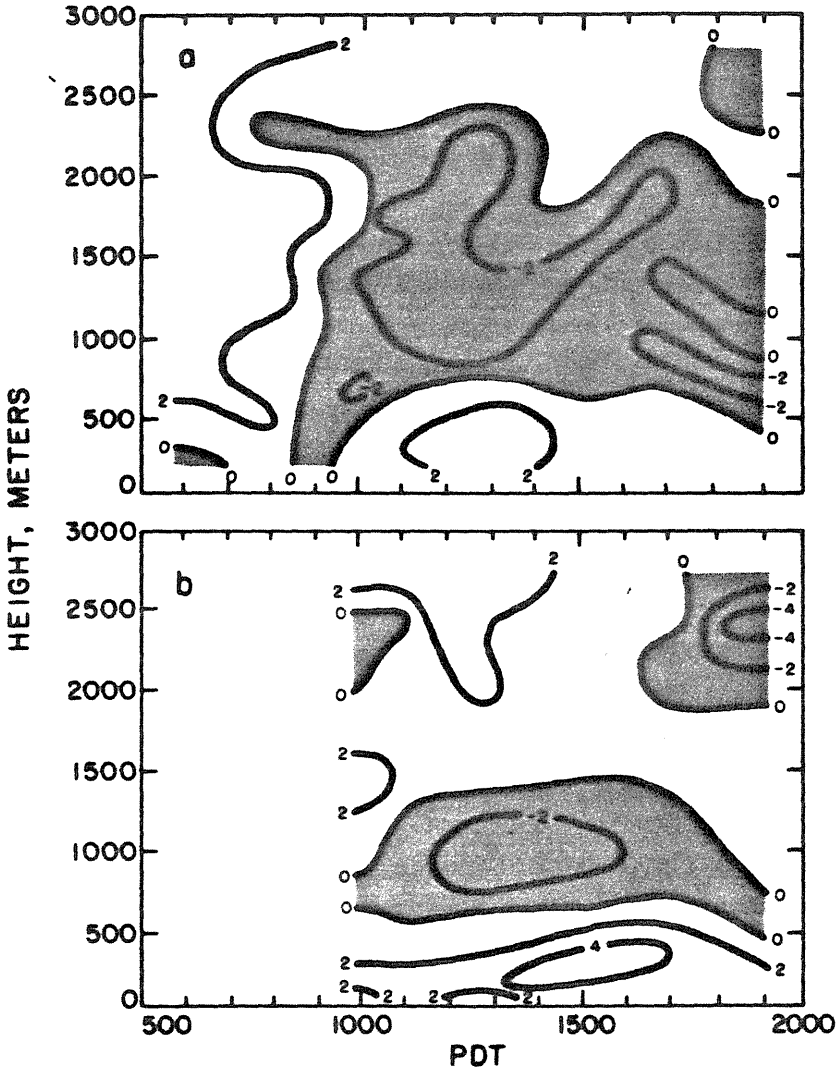

Figure 3 - Time-height cross section of upslope component of wind (mps), 27 July 1979, at Meadow Lakes (a - elev. 1366m) and Huntington Lake (b - elev. 2133m). Shaded areas represent downslope winds.

TABLE 3

PIBAL MIXING LAYER DEPTHS (m)

(Above Ground Level)

Time (PDT)	7/26	7/27	8/25	8/26	8/27	8/28	8/29	9/23
				Huntington Lake				
13	415	610	415	310		415	310	
15	610	610	415	415	310	210	210	415
17	515	610	515	415	415	310		415
19	415	515	<110	515	415	415		610
				Meadow Lakes				
13	210	310						
15	310	310						
17	515	610						
19	515	415						
				Millerton Lake				
13			710	515	310	610		
15			710	990	210	900	210	
17			515	1080	310	710	210	
19			990	900	900	610		

test program is indicated in Table 4. Typical wind speeds in the drainage flow were about 2 mps.

The depth and strength of the afternoon upslope flow indicated that it may be a significant ventilation mechanism for the San Joaquin Valley. During the parallel study of the transport of pollutants into, within, and out of the San Joaquin Valley, it was estimated that about 0.5×10^{12} m^3/hr of air was transported upslope during the afternoon between Fresno and Bakersfield (Reible, et al., 1982b). This estimate was based upon the difference in average estimated afternoon flux in the surface layer during July, 1979 between Fresno and Bakersfield. The total volume of the surface layer within the valley, assuming a 1200 m average depth (as suggested in that paper) is about 3.89×10^{13} m^3 of air. Thus the afternoon flow may transport about a tenth of the total valley air into the mountains during an 8 hour upslope flow.

The upslope flux can also be estimated from the depth and strength of the observed winds in the mountains. On 26 July, 1979, the hourly average flux per unit width of the upslope flow was about 1000 m^3/s at Meadow Lakes, and about 2000 m^3/s at Huntington Lake. On 27 July, the corresponding flux was about 565 m^3/s at Meadow Lakes and 1200 m^3/s at Huntington Lake. Thus the depth and total volume of air transported by the upslope flow appeared to increase with the altitude of the observing station. These data suggest that increased heat and buoyancy is contributed by the slope as the air moves upward to higher elevations. Air to satisfy the mass continuity must be drawn in laterally from layers

TABLE 4

DRAINAGE FLOW TEMPORAL CHARACTERISTICS (PDT)

	July	August	September	October
Big Creek				
Drainage Start	2100-2400	2000-2200		
Drainage End	0700-0800	0600-0900		
Huntington Lake				
Drainage Start	2000-2300	2300-0100	2000-0100	1900-0100
Drainage End	0800-0900	0800-1000	0800-1000	0800-1100
Forebay Lake				
Drainage Start	2000-2100	1900-2000	1800-2300	
Drainage End	0700-0800	0800-0900	0800-0900	

above the valley floor. This may limit the effectiveness of the upslope flow for ventilating the surface layer of air in the valley. Assuming that the flux estimated at Meadow Lakes is typical and that it is more representative of the air flow from the surface layer of the valley than the corresponding estimate at Huntington Lake, about 500-1000 m^3/s of air is drawn into the mountains for each m width of the slopes. This suggests that about 0.3 to 0.5 X 10^{12} m^3/hr of air from the valley floor could be moving upslope over the 150 km distance between Fresno and Bakersfield during the afternoon, in good agreement with the previous estimate based upon the flux deficit between Fresno and Bakersfield.

Transport and dispersion of the tracer during the slope flows

As mentioned previously, three atmospheric tracer experiments were conducted to quantitatively determine the transport and dispersion of pollutants in the slope flows. The first tracer experiment was conducted from Reedley, during the afternoon of 25 July, 1979. Within an hour after the start of the release (i.e. by 1300 PDT), the westerly upslope winds typically observed at Reedley were fully developed. As shown in Figure 4, the tracer was detected at Whitaker Forest in the King's Canyon National Park by 1800 PDT. This corresponded to a mean transport wind speed of about 2.2 mps, which compares favorably to the average afternoon surface wind speed at the release site of 2.5 mps. A maximum hourly-averaged concentration of 65 PPT (about 220 PPT/kg-mole SF_6

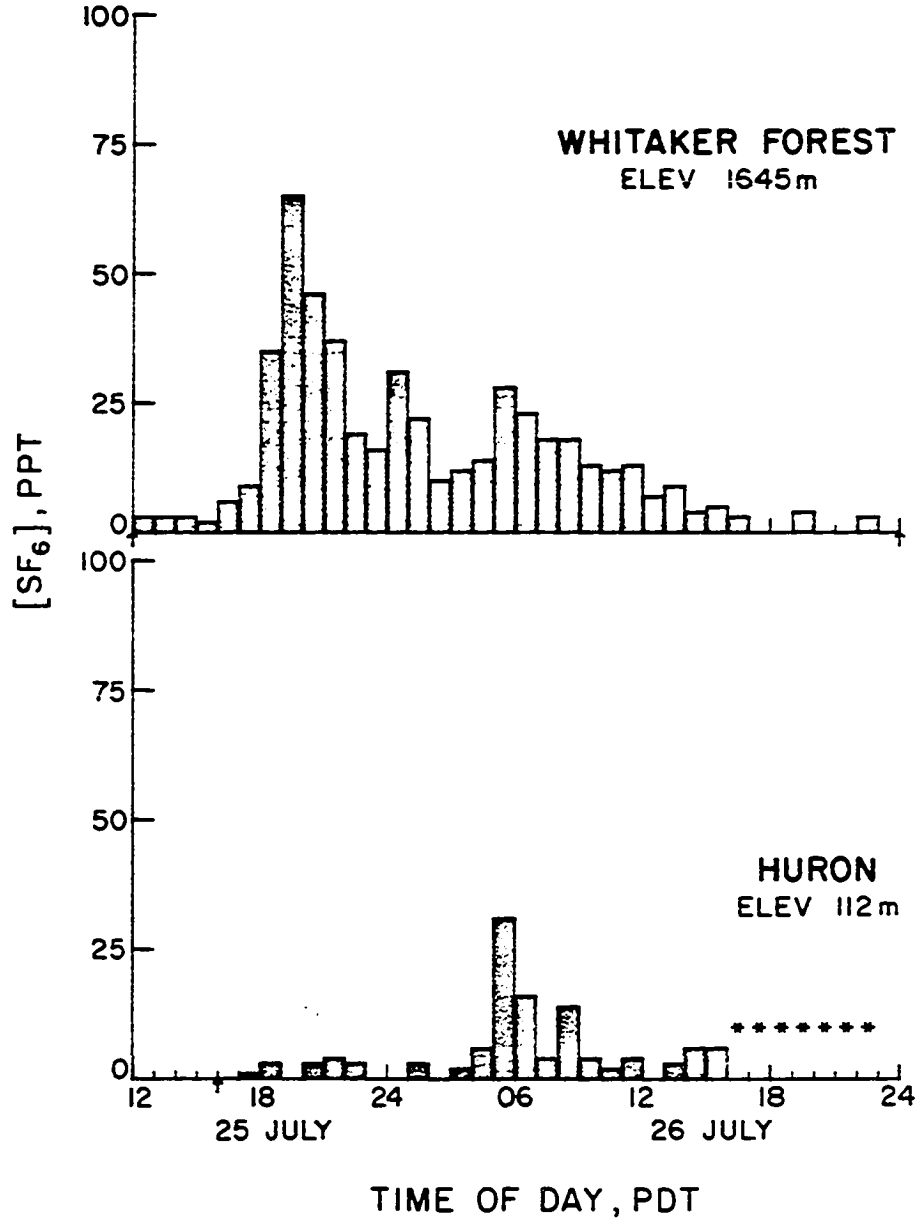

Figure 4: Hourly-Averaged Tracer Concentrations Observed at Whitaker Forest and Huron during Test of 25 July (Reedley Release).

released/hr) was detected at Whitaker Forest between 1900 and 2000 PDT.

The tracer plume was also detected by grab sampling traverses during the early evening on the day of the release. Figure 5 includes data collected by airplane and automobile traverses at two distances downwind of the release. Airplane traverse data collected about 35 km downwind is shown in the top figure. The solid line is the predicted concentration profile using the Gaussian plume model (Turner, 1970), assuming a wind speed of 2.5 mps (based on the arrival of SF_6 at Whitaker Forest), and very unstable atmospheric conditions (Pasquill-Gifford Stability Class A). To account for 100% of the mass flux from the release site, a 600 m mixing depth was also assumed. The bottom graph in Figure 5 shows data collected during one airplane and two automobile traverses located approximately 50 km downwind of the release site. The relatively good agreement between the ground-level and elevated measurements indicate that the tracer was well-mixed over some height. Due to the variation in the terrain height, it was not possible to accurately describe the height of the airplane above the ground. Assuming the mixing depth suggested by the previous airplane traverse, the observed transport wind speed and A stability class, the Gaussian plume model predicts the concentration profile included in the figure. The good agreement between the predicted and observed concentration profile suggests that the Gaussian model can be a useful tool in estimating the direct downwind impact of pollutant sources, even in complex terrain.

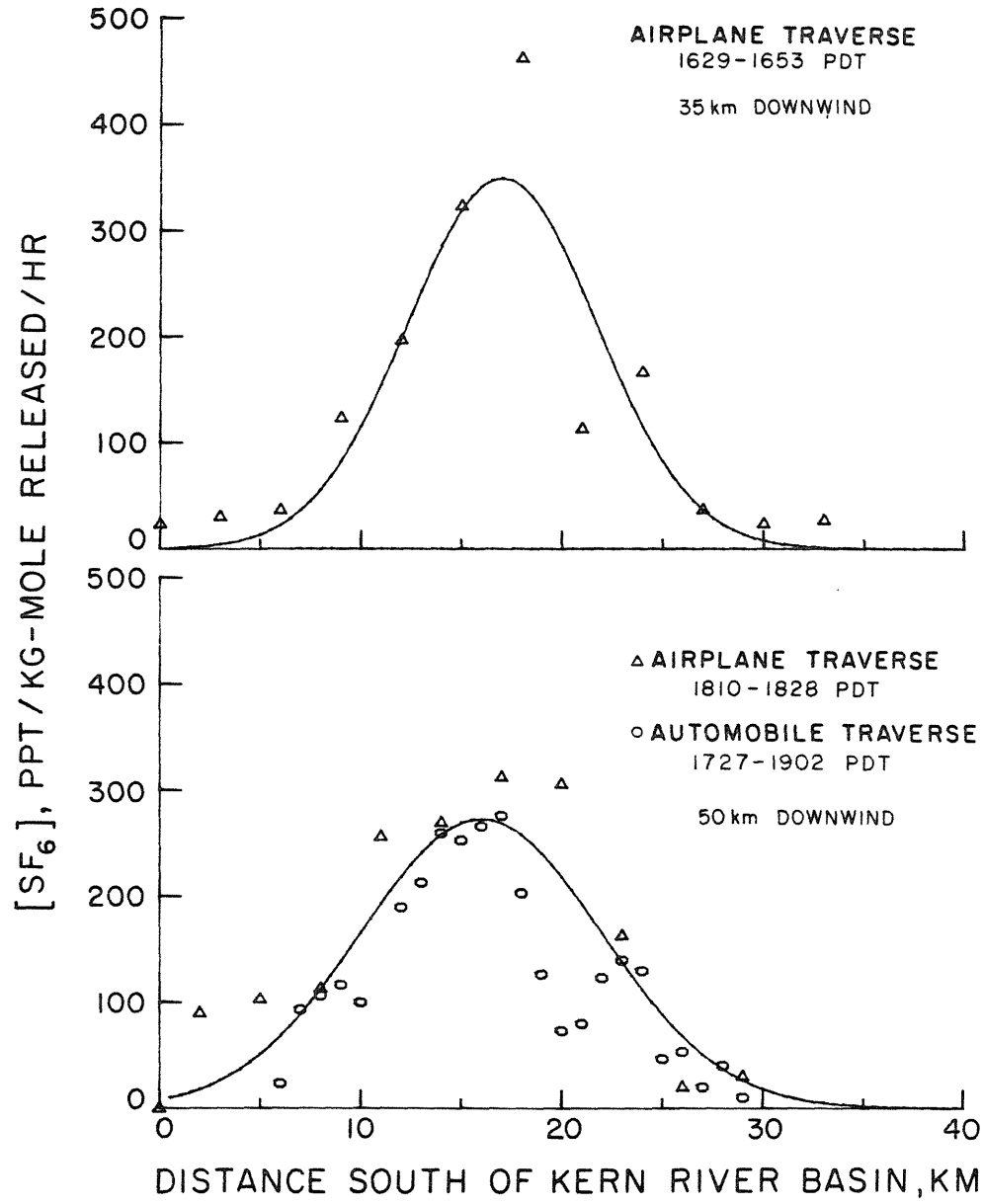

Figure 5 - Comparison of the tracer concentrations observed during airplane and automobile traverses on 25 July (Reedley release) and concentration profiles predicted via the Gaussian plume model, assuming "A" stability, 2.5 mps wind speed and 600 m mixing depth.

Shortly after the detection of the tracer at mountain sites, the nighttime drainage winds began to develop. This flow arrested the upslope movement of the tracer. As shown in Figure 4, the 5 hour tracer release led to a detectable impact of at least 18 hours at Whitaker Forest (WF in Figure 1). Thus ozone precursors, for example, can be retained overnight at mountain sites and available for photochemical reactions as the sun rises on the following day. The nighttime drainage flow also served to return at least some air to the valley basin. As indicated in Figure 4, SF_6 concentrations as high as 31 PPT were detected at Huron (H in Figure 1) on the western side of the valley between 0500 and 0900 PDT on the day following the release. It is unlikely that the nighttime drainage winds were sufficiently strong to transport the tracer from the mountains to this location. The drainage winds apparently transported the tracer to the valley floor where the typical recirculating flow in the southern valley (Reible, et al., 1982b) was responsible for the transport to the western side of the valley. Thus a significant amount of the tracer remained in the San Joaquin Valley into at least the day after its release. Although the net transport direction of the slope flows is out of the valley, due to the strength and depth of the upslope flow when compared to the nighttime drainage flow, these data indicate that transport out of the valley during any given day can occur only during a relatively narrow time window, apparently much shorter than the 5 hour period of the release.

The second and third tracer releases were conducted on the

afternoons of 25 and 28 August, 1979 from Friant Dam, northeast of Fresno (see Figure 2). These tracer releases were designed to determine the impact of pollutant transport into the Upper San Joaquin River Basin. Tracer sampling was conducted by airplane and automobile as well as fixed site grab sampling. As shown in Figure 6, the transport path of the tracer was similar between the two tests. The tracer generaly followed the Upper San Joaquin River Valley Basin during transport to higher elevations but plume separation was observed due to local terrain influences. Figure 7 shows the tracer data collected during an automobile traverse conducted during each test. The traverse route was about 15 km downwind of the release site and is shown as a broken line in Figure 6. While the locations of the maximum tracer concentrations differed somewhat between the two tests, the main tracer plumes (bounded by the broken lines in the figure), were remarkably similar in both concentration and width. Lower concentrations of tracer were also observed outside of the main tracer plume during both tests, presumably due to local terrain influences. As shown in Table 5, a mass flux estimate indicates that during both tests, in excess of 80% of the released tracer can be accounted for within the main tracer plume (again, as bounded by the broken lines in the figure). These mass flux estimates were made assuming that the tracer was well-mixed vertically at the average afternoon upslope flow depth at Huntington Lake, and that the applicable wind speed was that measured in the surface layer of the release site at 15 PDT. The width of the tracer plume was also corrected for the fact that the

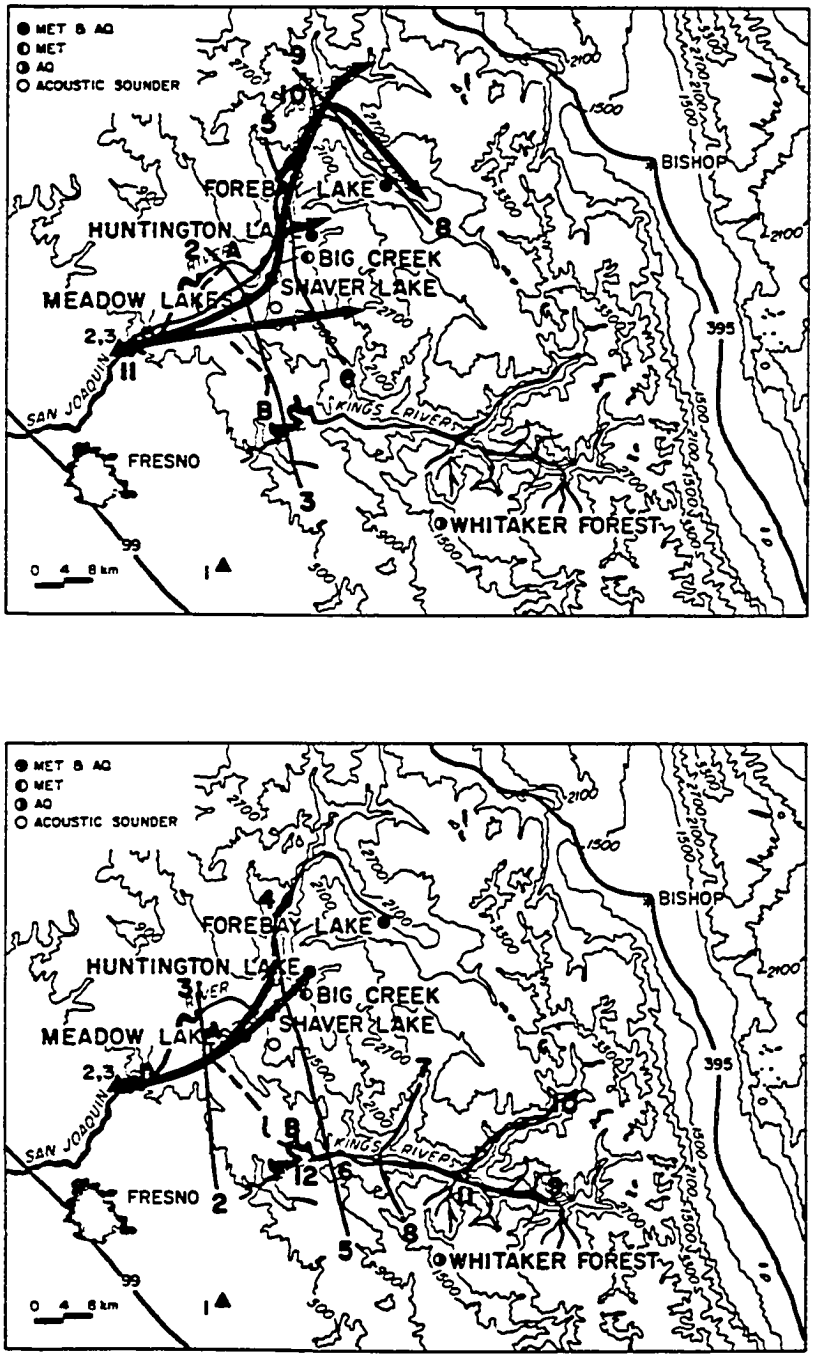

Figure 6 - Tracer trajectories during tests of 25 August (top) and 28 August 1979 (bottom). Also included are airplane traverse routes (solid lines between numbered points) and automobile traverse routes (broken lines between lettered points).

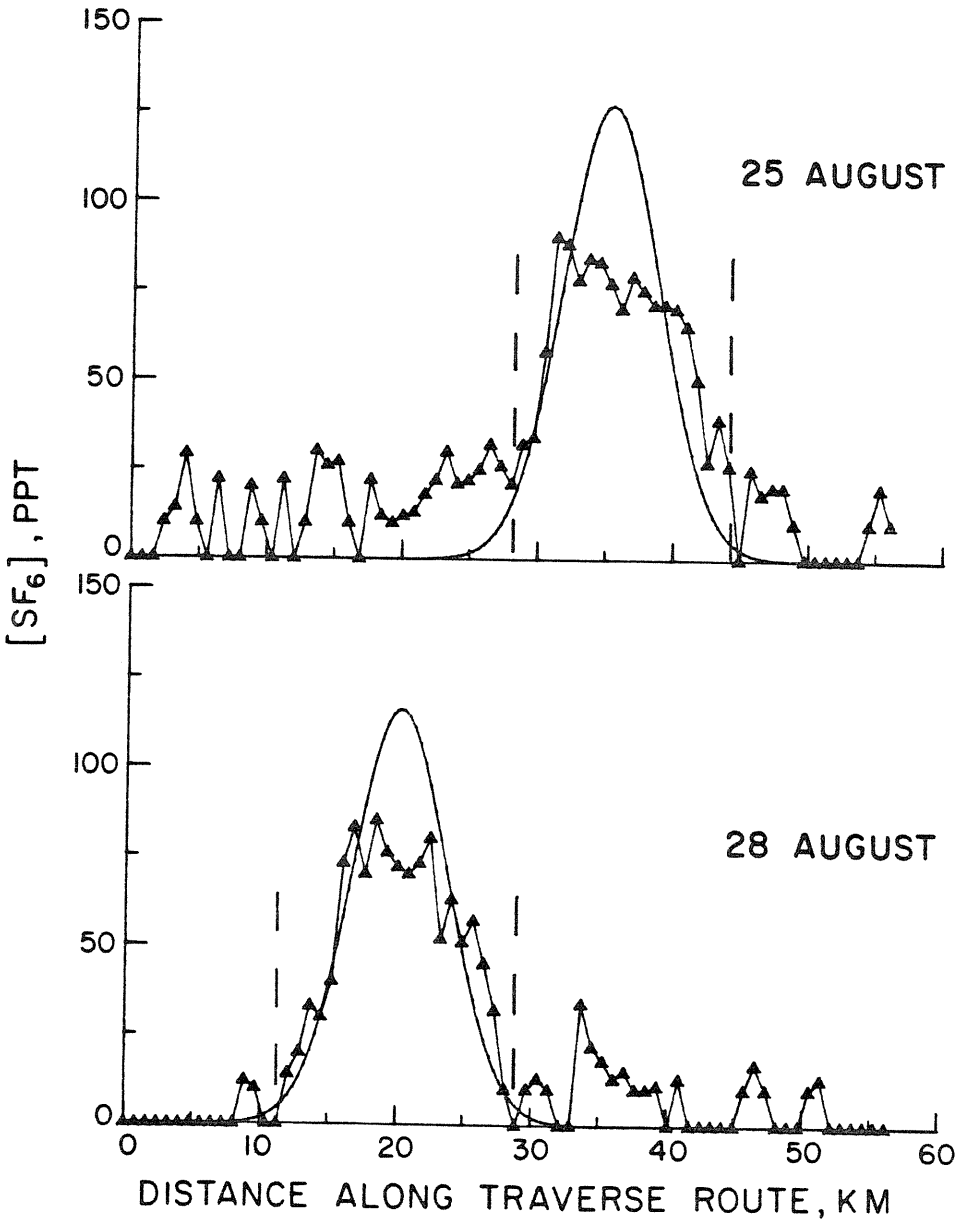

Figure 7 - Comparison of the tracer concentrations observed during automobile traverses conducted 15 km downwind of release site during test of 25 August (top) and 28 August (bottom), and concentration profiles predicted via the Gaussian plume model, assuming "A" stability, and the wind speeds and mixing depths indicated in Table 5.

distance along the traverse was about 56 km, while the straightline (and approximately crosswind) distance between the endpoints was only 32 km.

The main tracer plume, which, as described above, constitutes most of the released tracer, can be modeled with the Gaussian plume model (Turner, 1970). The results are also shown in Table 5, assuming A stability class (highly unstable conditions), and the wind speeds employed for the mass flux balances. For completeness, the results of the model comparison to the test of 25 July are also included in Table 5. Considering the uncertainties involved and the inhomogeneities of flow over complex terrain, the agreement between the model and experiment is quite good. While the simple Gaussian plume model cannot hope to predict the details of the tracer transport and dispersion, it appears, based on the three atmospheric tracer tests conducted, to be a reasonable approach to estimating direct downwind impacts of valley pollutant sources on mountain receptors. The dispersion of the main body of tracer during these experiments corresponded most closely to that expected during highly unstable atmospheric conditions (A stability), presumably due to the influence of terrain enhanced turbulence. Based strictly upon meteorological inputs a more stable atmosphere would be expected (stability class B or C). As noted in Reible, et al. (1981), the Gaussian model can be used to develop a worst case analysis of transport and dispersion in complex terrain in that actual dispersion will generally be greater than the meteorological conditions would suggest. It should be noted, however, that, without experimental

TABLE 5

MASS FLUX ESTIMATES AND GAUSSIAN COMPARISONS FOR TRAVERSE DATA

Parameter	Test			
	25 July		25 August	28 August
	1	2		
Downwind Distance-km	35	50	15	15
Wind Speed-mps	2.5	2.5	5	7
Mixing Depth-m	600	600	450	340
SF_6 observed				
max.-PPT	139	94	90	85
σ_y - m	5.0	5.3-6.5	2.7	2.2
SF_6 predicted				
max.-PPT	106	80	127	116
σ_y - m	4.7	6.0	2.2	2.2
% Mass Flux	-	-	88	81

data, it is difficult to predict a trajectory for a pollutant plume in a complex wind field. Also, as indicated by the tracer experiment of 25 July, a significant impact of pollutants on mountain receptors may occur long after the end of the daytime upslope flow. The concept of a plume, and thus the Gaussian plume model, may be meaningless after a wind reversal (see e.g. Reible and Shair, 1982)

Slope flow and pollutant impacts

As expected from the tracer experiments, the air quality measurements at the Upper San Joaquin River Valley sites reflected transport from valley pollutant sources. As shown in Figure 8, the median ozone concentrations at Meadow Lakes, Shaver Lake and Huntington Lake occur about 15 PDT, 14-16 PDT, and 18 PDT, respectively. If the ozone was primarily the result of local pollutant sources, the maxima would occur near the time of peak solar insolation, between 12 and 14 PDT. Note also that the ozone levels remained high throughout the night. In areas with significant local sources, the lack of photochemical activity during the night generally allows depletion of ozone through scavenging by oxides of nitrogen. This behavior is observed, for example, at Fresno and Reedley, as indicated in Figure 9. Also included in Figure 9 is the July to October median ozone concentrations observed at Whitaker Forest, which was shown to be downwind of Reedley during the first tracer experiment. The average time of maximum ozone at Reedley, 16-17 PDT, is consistent

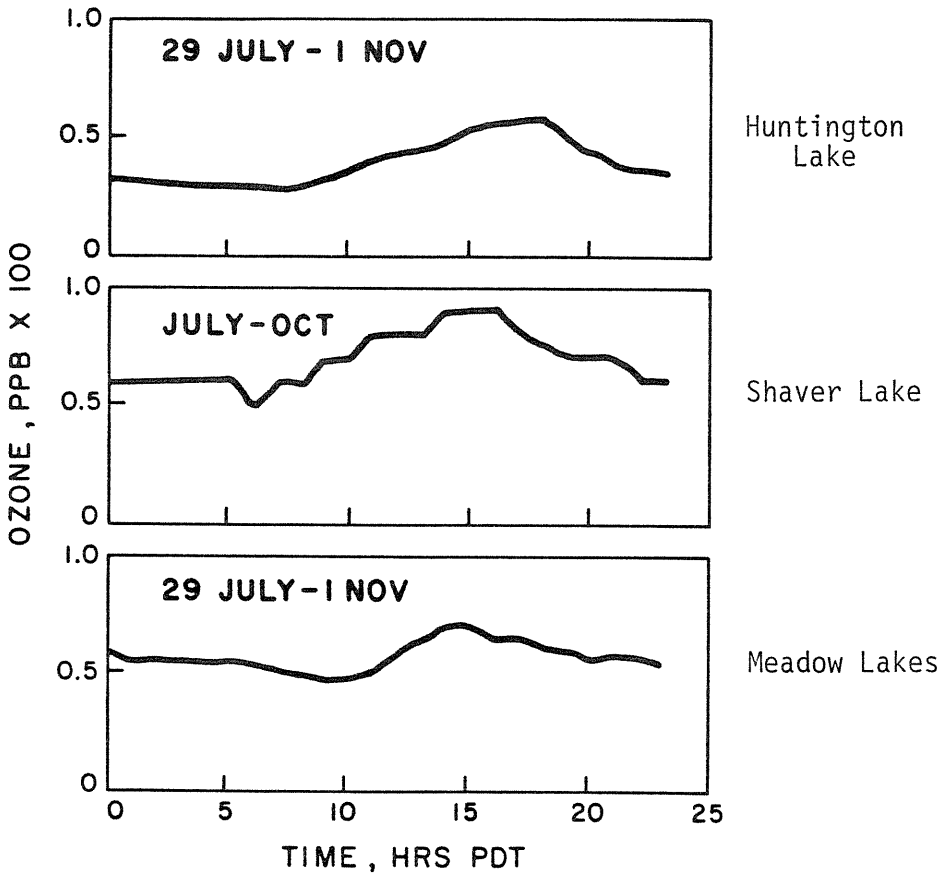

Figure 8 - Median ozone concentrations observed at Upper San Joaquin River Valley sites as a function of time of day. Averaging periods are as indicated in each figure.

with transport from upwind sources such as Fresno, but the ozone maximum at Whitaker Forest apparently occurs too early to be due to transport, at least from Fresno, 65-70 km away. Based on the essentially constant tracer concentrations detected at Whitaker Forest during 18 hours of the first tracer experiment, and the uniform ozone concentration detected at this location during the night (as shown in Figure 9), much of the ozone maximum at Whitaker Forest is probably due to the upslope transport of precursors on the previous day. Because of pollutant carryover through the night, the time-integrated ozone concentration, or dosage, at Whitaker Forest during the July through October period was 20% higher than that observed at Fresno and Reedley. In a similar manner, the ozone dosage at the Upper San Joaquin Valley River Basin sites of Shaver and Meadow Lakes was also 20-40% higher than that at the valley floor sites. At Huntington Lake, however, at an altitude in excess of 2000m and at least 50 km from Fresno, the ozone dosage during the test period was about 20% lower than the valley sites. These data indicate that the upslope impact of valley pollutant sources can exceed their local impact (i.e. close to the source). At the present time, however, very little is known about the flux of pollutants from natural sources in the mountain areas. The flux of hydrocarbons from vegetation, for example, could conceivably be a contributor to the high ozone levels typically detected during the night at the mountain locations.

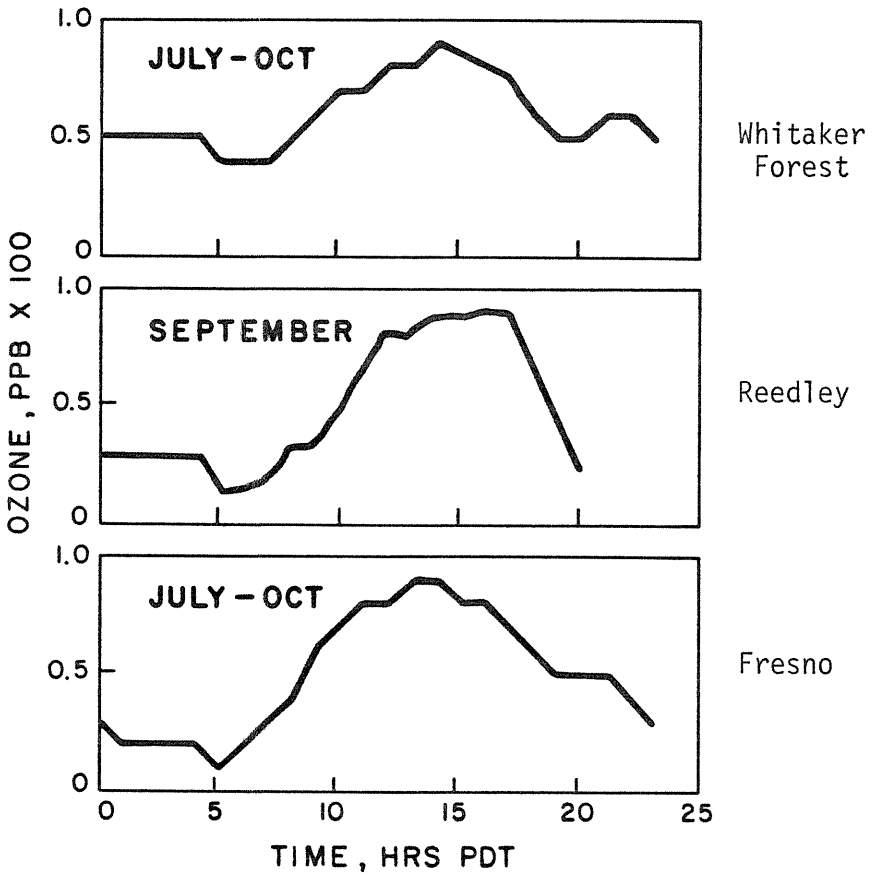

Figure 9 - Median ozone concentrations observed at Fresno and Reedley, within the San Joaquin Valley, and at Whitaker Forest, at an altitude of 2100 m, as a function of time of day. Averaging periods are as indicated in each figure.

SUMMARY AND CONCLUSIONS

These studies have indicated that pollutants can indeed be transported upslope during the afternoon mountain-valley winds. The slope flow layer over the western slopes of the Sierra Nevada Mountains is generally between 400 and 600 m in depth, a depth which may increase with altitude due to the entrainment of elevated air from the valley. The afternoon wind speeds are generally between 2-5 mps, with a late afternoon peak of 5-7 mps. The strength and depth of these flows is such that about 10% of the valley air can be transported up the slopes between Fresno and Bakersfield during a single afternoon. Pollutants drawn upslope tend to be well-mixed over the depth of the layer and their lateral dispersion can be approximately modeled with the Gaussian plume model by assuming less stable atmospheric conditions than are observed. During three atmospheric tracer studies, dispersion parameters corresponding to "A" atmospheric stability were applicable. This procedure cannot completely describe the dispersion of a pollutant, however, due to the inhomogeneity of the flow field over the complex terrain. Also, due to atmospheric cooling and stabilization during the night, and the subsequent development of a drainage flow to lower elevations, pollutants transported upslope can lead to significant next day impacts both within the mountains and in the valley below. Because of this, the ozone dosage at mountain sites can be larger than ozone dosages in pollutant source areas in the San Joaquin Valley. As the San Joaquin Valley faces continued development in the coming

years, this study indicates that the mountain slopes may face a significant degradation in air quality.

References

Defant, F. (1951). Local winds. Compendium of Meteorology, American Meteorology Society, Boston, Mass., 655-672.

Duckworth, S. and Crowe, D. (1979). Ozone patterns on the western Sierra slope. California Air Resources Board, Technical Services Division.

Eatontown Signal Laboratory Group (1945). Local winds. U.S. Army Signal Corps, Dugway Proving Grounds, Tooele, Utah, Report No. 982, 50 pp.

Lamb, B.K. (1978). Development and application of dual atmospheric tracer techniques for the characterization of pollutant transport and dispersion. Ph.D. Thesis, California Institute of Technology, 16-26, Pasadena, Ca. 91125.

Lehrman, D.E., Smith, T.B., and Gouze, S. (1980). Upper San Joaquin River Valley impact study. Final report to U.S. Forest Service, 630 Sansome Street, San Francisco, Ca. 94111.

Miller, P.R., McCutchan, M.H., and Milligam, H.P. (1972). Oxidant air pollution in the Central Valley, Sierra Nevada foothills,

and Mineral King Valley of California. Atmospheric Environment,6, 622-633.

Pronos, J., Vogler, D.R., and Smith, R.S. (1978). An evaluation of ozone injury to pines in the southern Sierra Nevada. Forest Insect and Disease Management, 630 Sansome St., San Francisco, Ca. 94111, Report No. 78-1.

Reible, D.D., Shair, F.H., Smith, T.B., and Lehrman, D.E. (1982a). The origin and fate of air pollutants in California's San Joaquin Valley, I.Winter. Submitted to Atmospheric Environment.

Reible, D.D., Shair, F.H., Smith, T.B., and Lehrman, D.E. (1982b). The origin and fate of air pollutants in California's San Joaquin Valley, II. Summer. Submitted to Atmospheric Environment.

Smith, T.B., Lehrman, D.E., Reible, D.D., and Shair, F.H. (1981). The origin and fate of airborne pollutants within the San Joaquin Valley. Final report to the California Air Resources Board, Sacramento, Ca.

Turner, D.B. (1970). Workbook of Atmospheric Dispersion Estimates. Environmental Protection Agency. AP-26, 84 pp.

Williams, W.T., Brady, M., and Willison, S.C. (1977). Air pollution damage to the forests of the Sierra Nevada Mountains of California. Journal of the Air Pollution Control Association,27, 3, 230-234.

Chapter 11

The Transport of Airborne Pollutants into, within, and out of the Sacramento Valley of California

by

D.D. Reible and F.H. Shair

(Submitted to Atmospheric Environment)

Abstract

A series of six tracer experiments was conducted in the Sacramento Valley of central California to determine the transport routes of pollutants into, within, and out of the valley. Individual tracer releases were conducted to explore the impact of San Francisco Bay area sources on the Sacramento Valley and to determine the downwind impact of the Sacramento urban plume at different times and under different atmospheric conditions. In addition, one tracer experiment was conducted to explore the influence of the Schultz Eddy on the air quality in the Sacramento Valley.

The tracer experiments indicated that transport from the San Francisco Bay area into the Sacramento Valley is generally limited to a short period during the afternoon. Most of the air passing through the Carquinez Straights, southwest of Sacramento, apparently impacts the San Joaquin Valley. The major source area within the valley, Sacramento, can impact receptor zones in the northern valley as well as the slopes to the northeast, depending on the timing and location of the particular source with respect to the flow divergence over the city. The Shultz Eddy, characterized by a northerly morning flow on the west side of the valley, can be a significant mechanism for the recirculation of valley pollutants, especially those released near Sacramento during the night. Pollutants can also be retained in the valley air basin during days subsequent to their release by transport, and subsequent entrapment, aloft. During the only test in which

airborne sampling was conducted on the day after a tracer release, significant tracer concentrations were observed between 450 and 750 m above sea level, a layer that is typically incorporated into the mixing layer during the afternoon. This mechanism may result in pollutant impacts, such as high ozone concentrations, that cannot otherwise be correlated with local sources or transport from distant sources.

Introduction

With the development during the last decade of ultra-sensitive tracer techniques employing inert gases that can be detected by electron-capture gas chromatography, it has become possible to probe the macroscale structure of large-scale atmospheric flows (length scales of greater than 100 km). Atmospheric tracer experiments have generally been limited to relatively small-scale studies designed, for example, to allow determination of dispersion model parameters or plume trajectories from particular source locations. Probes of the structure of the transport wind field of an entire air basin, on the other hand, have tended to be based upon meteorological measurements (e.g. Demarrais, et al.,1965). Pollutant transport in flow divergence or convergence zones, in large scale eddy structures, or in diurnally varying flows, however, is difficult to accurately predict based upon the limited meteorological data normally available. Unfortunately, this imposes an inherent limit to the accuracy of any numerical model of pollutant transport and dispersion, which must rely on the accuracy of the input wind field. As indicated in Reible and Shair (1982) and Reible, et al. (1982a and b), however, atmospheric tracer experiments, when supported with sufficient meteorological data to characterize the basic flow structure, can provide a more detailed and accurate description of the transport wind field and, specifically, the degree of interaction between large scale flow structures. Such studies can be used to develop conceptual models of the overall

ventilation of a large air basin as well as quantitative information on the behavior of pollutants within the system.

The above discussion indicates that atmospheric tracer studies can prove most useful to air basins that exhibit complex but consistent flow patterns. One such area is the Sacramento Valley of central California. The Sacramento Valley, shown in Figure 1, is about 250 km long and 50-100 km wide. It is bounded on the east by the Sierra Nevada Mountains, on the north by the Cascades, and on the west by the northern California Coastal Mountains. The surrounding mountains exhibit diurnally varying slope flows due to differential heating between the slopes and the valley floor. At the open southern end of the valley, a marine intrusion from the San Francisco Bay area is often noted during the afternoon. The marine air from San Francisco passes through the Carquinez Straits, south of Vallejo, after which the flow diverges, with some of the marine air being diverted north into the Sacramento Valley and the remainder south into the San Joaquin Valley. Without atmospheric tracer studies it is difficult to assess the relative fluxes of air into each valley, a potentially important question in that San Francisco is a significant pollutant source. Further complicating the flow of air at the southern end of the Sacramento Valley is the presence of the so-called "Schultz Eddy", a counter-clockwise eddy observed on the western side of the valley on many summer mornings. A companion feature of the Schultz Eddy is a flow divergence over the city of Sacramento, which at mid-day is characterized by southeasterly winds in eastern Sacramento and southwesterly winds in western

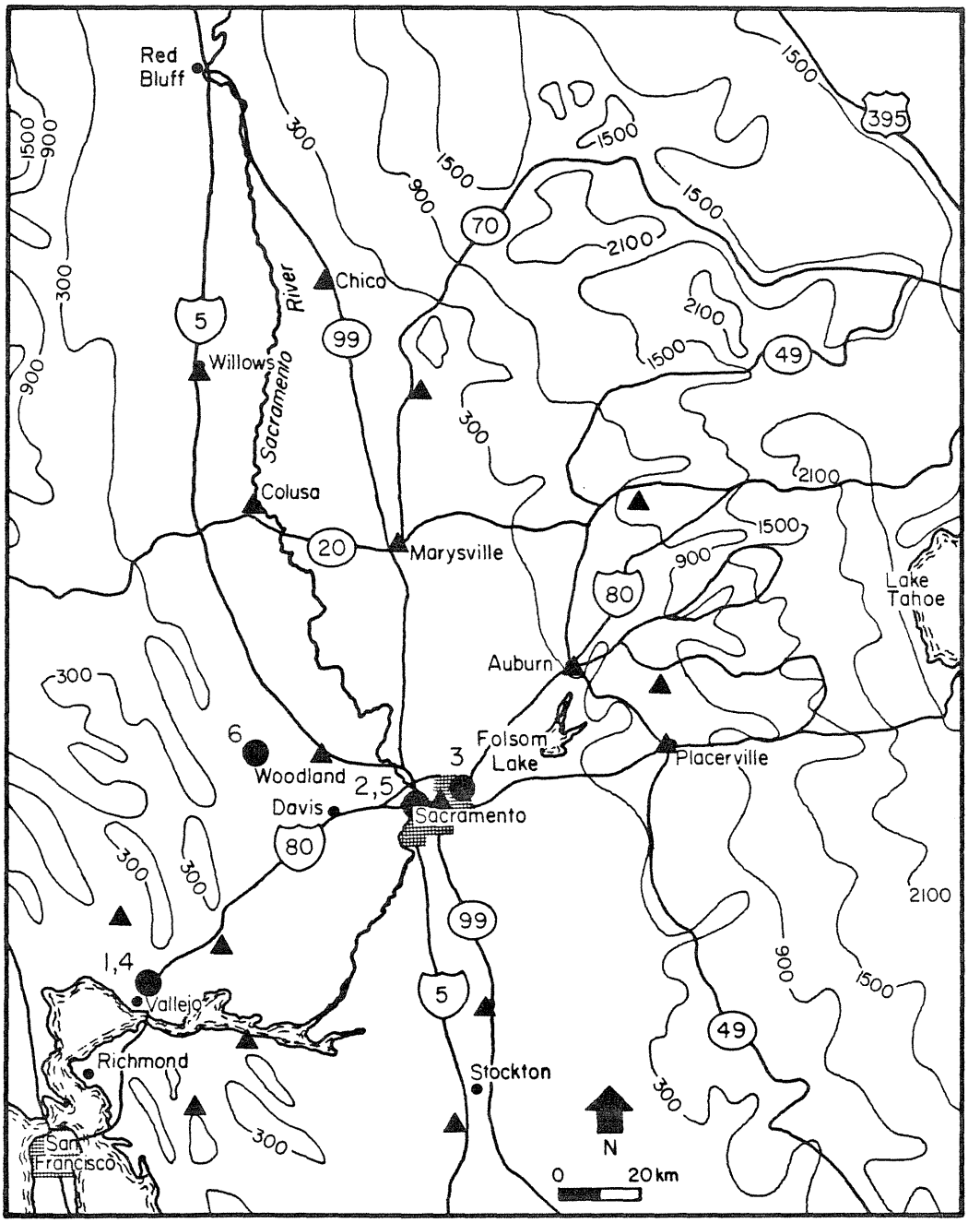

Figure 1 - Map of the southern Sacramento Valley and the surrounding area. Also included are tracer release sites (●), and hourly-averaged sampling sites (▲).

Sacramento. The existence of these flow structures was first established by wind observations (e.g. Shultz, 1975), but as described above, a finite wind network alone cannot adequately describe the structure of the flow field in sufficient detail to predict the transport path of pollutants. The purpose of the current work was to investigate, through atmospheric tracer studies, the structure of these flows and their impact on the distribution of pollutants in the Sacramento Valley.

Experimental Procedure

The study consisted of a three week intensive field program during which six atmospheric tracer experiments were conducted. Sulfur hexafluoride (SF_6) was employed as the tracer since it can be detected at concentrations as low as 1-10 parts-per-trillion (PPT) by electron capture gas chromatography. Air samples were collected by hourly-averaged and instantaneous grab samples at fixed sites, and by grab samples during automobile and airplane traverses. All air samples were collected in 30 cm^3 disposable plastic syringes and analyzed after return to the laboratory at the California Institute of Technology. During an experiment, a portable electron capture gas chromatograph was used to determine the tracer transport path to assist in the determination of traverse routes. The analytical procedure, as well as instrument accuracy and calibration procedures, are described by Lamb (1978). The locations of the tracer releases for all six tests are included in Table 1 and also in Figure 1. As indicated in the introduction, the tracer release locations were chosen to: 1) determine the impact of pollutants passing through the Carquinez Straits on the Sacramento Valley, 2) determine the impact of the Sacramento urban plume, and 3) determine the influence of the Schultz Eddy on pollutant transport in the southern Sacramento Valley.

All tracer experiments were supported with extensive meteorological and air quality measurements. In addition to the normal wind network, pilot balloon observations of the winds aloft

Table 1 - Sacramento Valley Tracer Releases

Test 1 - Release of 41 kg SF_6 per hour between 0620 and 1120 PDT, 8/9/80, from 6 km NE of Vallejo.

Test 2 - Release of 47 kg SF_6 per hour between 0600 and 1100 PDT, 8/13/80, from 15th and R St., Sacramento.

Test 3 - Release of 40 kg SF_6 per hour between 1500 and 1900 PDT, 8/20/80, from Auburn & Watt St., Sacramento.

Test 4 - Release of 43 kg SF_6 per hour between 1500 and 1900 PDT, 8/23/80, from 6 km NE of Vallejo.

Test 5 - Release of 49 kg SF_6 per hour between 0700 and 1100 PDT, 8/25/80, from 15th and R St., Sacramento.

Test 6 - Release of 26 kg SF_6 per hour between 0600 and 1000 PDT, 8/28/80, from Woodland Airport.

were made from 2-3 locations during each test by Meteorology Research Inc. (MRI), Altadena, Ca. Air quality measurements aloft were also made by MRI. These méasurements included sulfur dioxide, ozone, oxides of nitrogen, and light scattering coefficient.

Presentation and Discussion of Results

During the first and the fourth tracer experiments, the impact of sources upwind of the Sacramento Valley were evaluated. During both tests, SF_6 was released from near Vallejo, northeast of the Carquinez Straits and San Francisco. This release site essentially represents the northern boundary of air passing through the Carquinez Straits and thus a release from this area was most likely to be transported into the Sacramento Valley. In view of the flow divergence through the Carquinez Straits, an attempt to tag the northern boundary of the flow appeared to be the most satisfactory means of determining the Sacramento Valley impact of pollutants passing through the divergence. Other release locations separated by just a few kilometers could result in vastly different downwind impact zones.

As indicated in Table 1, SF_6 was released between 0620 and 1120 PDT of 8/9/80 during the first test. As expected from the divergence through the Carquinez Straits, the generally westerly winds in the area had a southerly component at the release site. The tracer was thus transported in the direction of Sacramento, towards the northeast. Sampling at locations downwind indicated, however, that the bulk of the tracer was not eventually transported into the Sacramento Valley. The tracer was instead transported into Lodi, directly east of the release site, by 1100-1200 PDT. An average of 33+/-25 PPT (0.12 PPB/kg-mole released/hr) was detected at Lodi between 1100 and 1900 PDT. The eastward transport of the tracer is indicated by the automobile

traverse data included in Figure 2. On Interstate 5 near Lodi, an average concentration of 40+/-17 PPT (0.14 PPB/kg-mole released/hr) was observed about 1630 PDT, in good agreement with the aforementioned hourly-averaged concentrations. As indicated in Figure 2, some tracer was also observed about 25 km northeast of the release site. No significant tracer concentrations were detected further to the north or in the Sacramento Valley, however, indicating that the tracer observed in this area represented only a small part (presumably the latter part) of the release.

The observation that the latter part of the SF_6 released was transported towards the Sacramento Valley, suggested that late morning or afternoon conditions might be more favorable for transport from the Carquinez Straits into the Sacramento Valley. During the fourth tracer test, SF_6 was released from the same location as in Test 1, but between 1500 and 1900 PDT, 8/23/80. As in the first test, the tracer was initially transported towards the northeast. The crosswind dispersion of the tracer was initially Gaussian and corresponded to that expected in neutral or slightly stable atmospheric conditions (Turner, 1970), in general accord with the actual atmospheric stability. The atmosphere was destabilized by high wind speeds (5 mps) and significant solar insolation, but stabilized by the cool marine air intrusion which was transporting the tracer. Unlike the first test, the bulk of the tracer did not turn southward upon reaching the middle of the California Delta which separates the Sacramento and San Joaquin Valleys. Instead the tracer was transported into Sacramento,

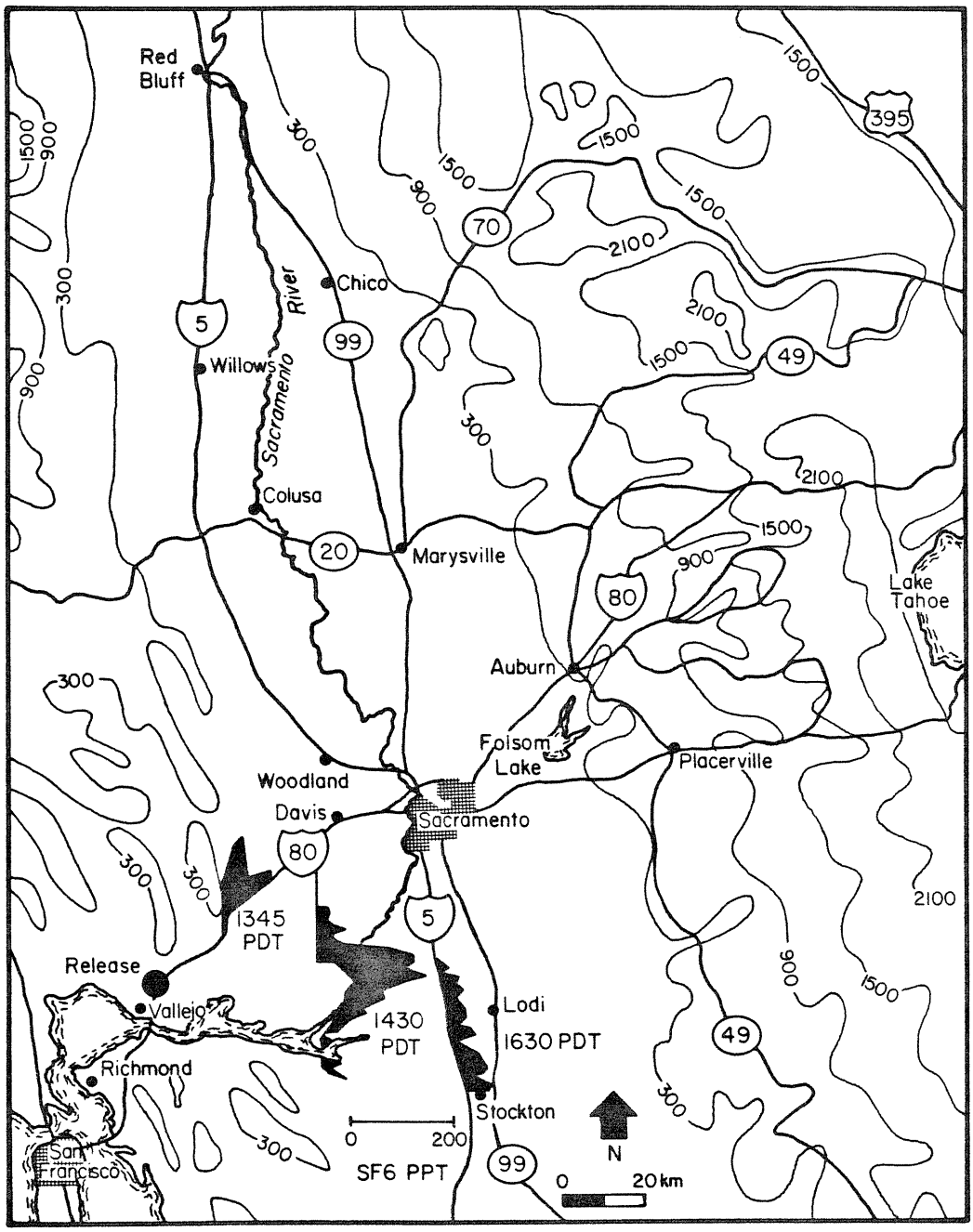

Figure 2 - Map of Sacramento Valley indicating the tracer concentrations observed during selected automobile traverses downwind of the first Vallejo release (Test 1, 8/9/80). The height of the shaded area is proportional to concentration.

where an average of 185+/-22 PPT (0.63 PPB/kg-mole released/hr) was observed between 1900 and 2100 PDT. Automobile and airplane traverses verified that the bulk of the tracer was transported into the Sacramento Valley. As indicated in Figure 3, the tracer was transported into the northern half of the Sacramento Valley during the night after the release.

The apparent contradiction between the results of the first and second tests from near Vallejo (Test 1 and Test 4), may have been due to different meteorological conditions. Since a small amount of tracer released late in the first test was also transported towards the Sacramento Valley, however, it appears likely that the different transport paths observed were largely due to the different release times. During the afternoon, the marine intrusion is more fully developed than during the morning, perhaps resulting in more effective transport into the Sacramento Valley.

The second, third, and fifth experiments were designed to determine the downwind impact of the Sacramento urban plume. During the second experiment, SF_6 was released from downtown (western) Sacramento between 0600 and 1100 PDT in order to tag the peak morning pollutant emissions in the city. Winds with a southerly component are typically observed at Sacramento throughout the day (Duckworth and Crowe, 1978 or Schultz, 1975). The winds shift more and more westerly during the day as slope heating on the Sierra Nevada foothills leads to flow oriented upslope. Throughout the period of the Test 2 release, however, no westerly component was observed at the release site. Automobile

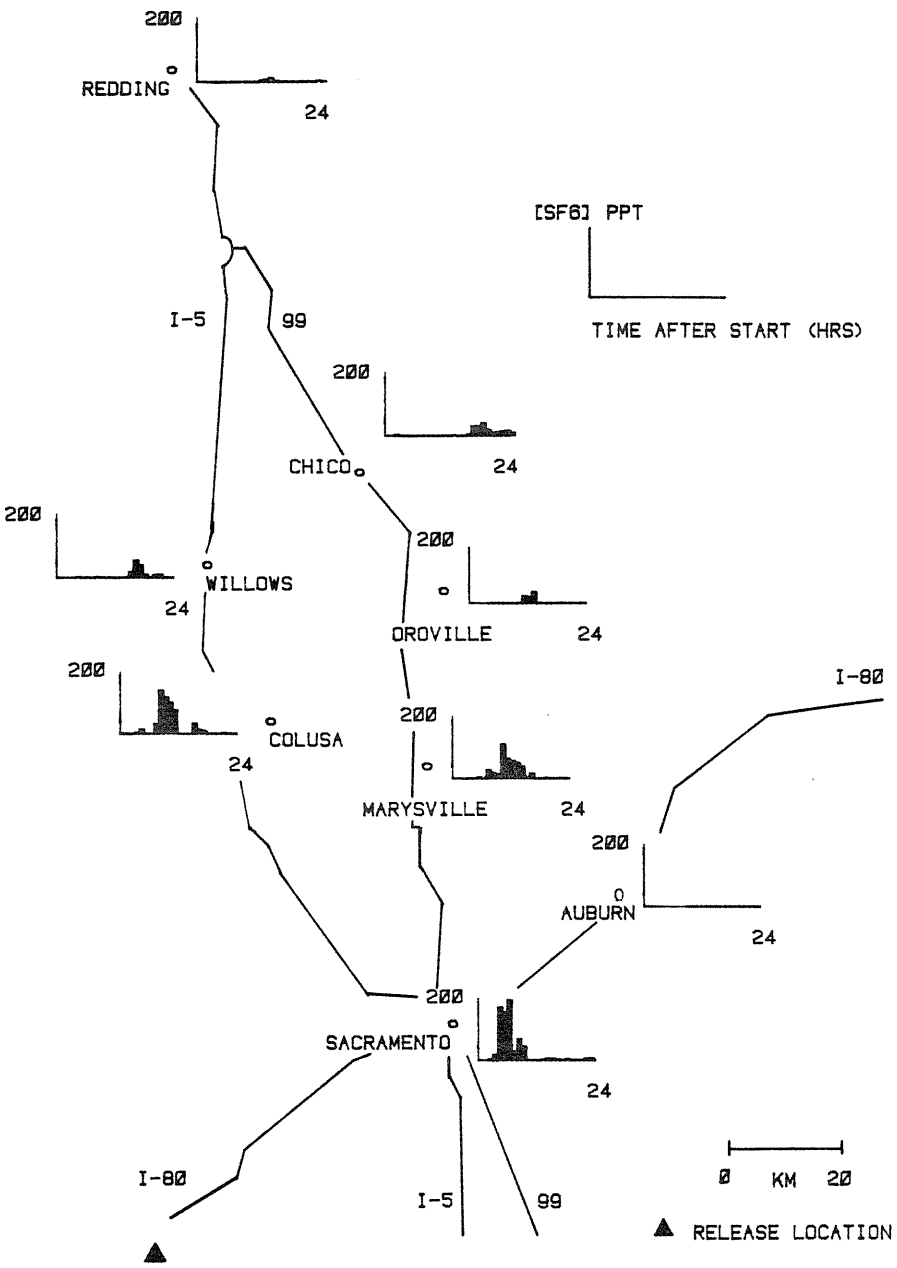

Figure 3 - Map of Sacramento Valley indicating the hourly-averaged tracer concentrations observed at sites within the valley after the second release from near Vallejo (Test 4, 8/23/80).

traverse data indicated that the tracer was initially transported northward in an essentially Gaussian plume. The horizontal dispersion of the tracer was consistent with that expected during atmospheric conditions corresponding to Pasquill-Gifford Stability Class B or C (Turner, 1970). Since the timing of the release was such that the westerly upslope winds had not fully developed, essentially all of the tracer released during this experiment was transported into the northern half of the Sacramento Valley. The hourly-averaged concentrations detected at sites in the Sacramento Valley are shown in Figure 4. Concentrations as high as 205 PPT (0.64 PPB/kg-mole released/hr) were observed at Marysville, and as high as 21 PPT (0.07 PPB/kg-mole released/hr) at Redding in the extreme northern end of the valley. The detection of SF_6 at Redding indicated that the tracer was transported northward at an average speed of about 4 mps. The transport path of the tracer was very similar to that observed during the second test from near Vallejo (Test 4, described previously).

Because the tracer in the previous test was never influenced significantly by the afternoon upslope winds, the third tracer release was conducted from eastern Sacramento during the afternoon. The fully developed afternoon winds transported the tracer directly towards the slopes. As indicated by Figure 5, concentrations as high as about 120 PPT SF_6 (0.44 PPB/kg-mole released/hr) were observed about 45 km east of the release site. On the day after the release, however, the tracer was observed in an elevated layer over the northern half of the Sacramento Valley. Airplane traverse data collected between 450 and 750 m in altitude

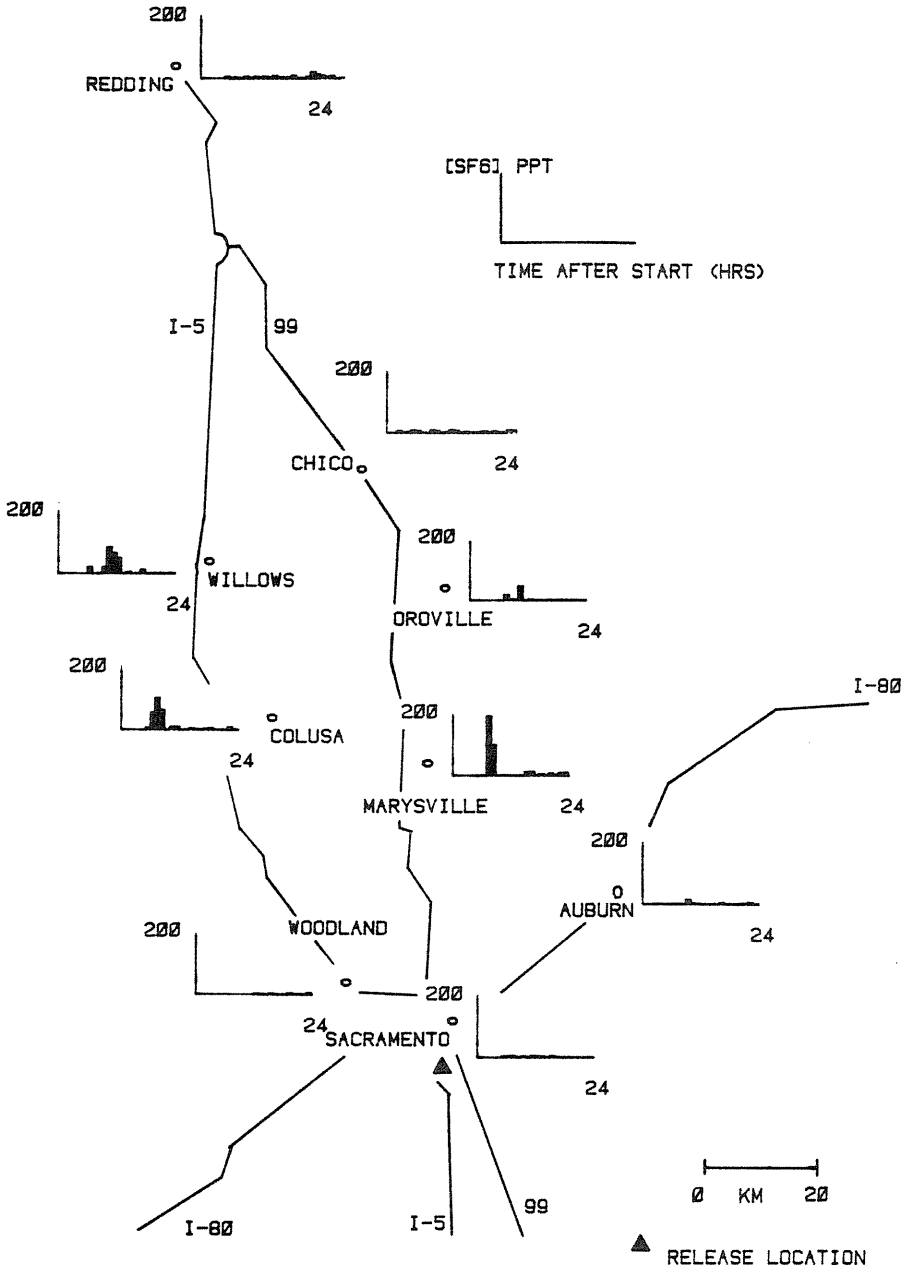

Figure 4 - Map of Sacramento Valley indicating the hourly-averaged tracer concentrations observed at sites within the valley after the first release from downtown Sacramento (Test 2, 8/13/80).

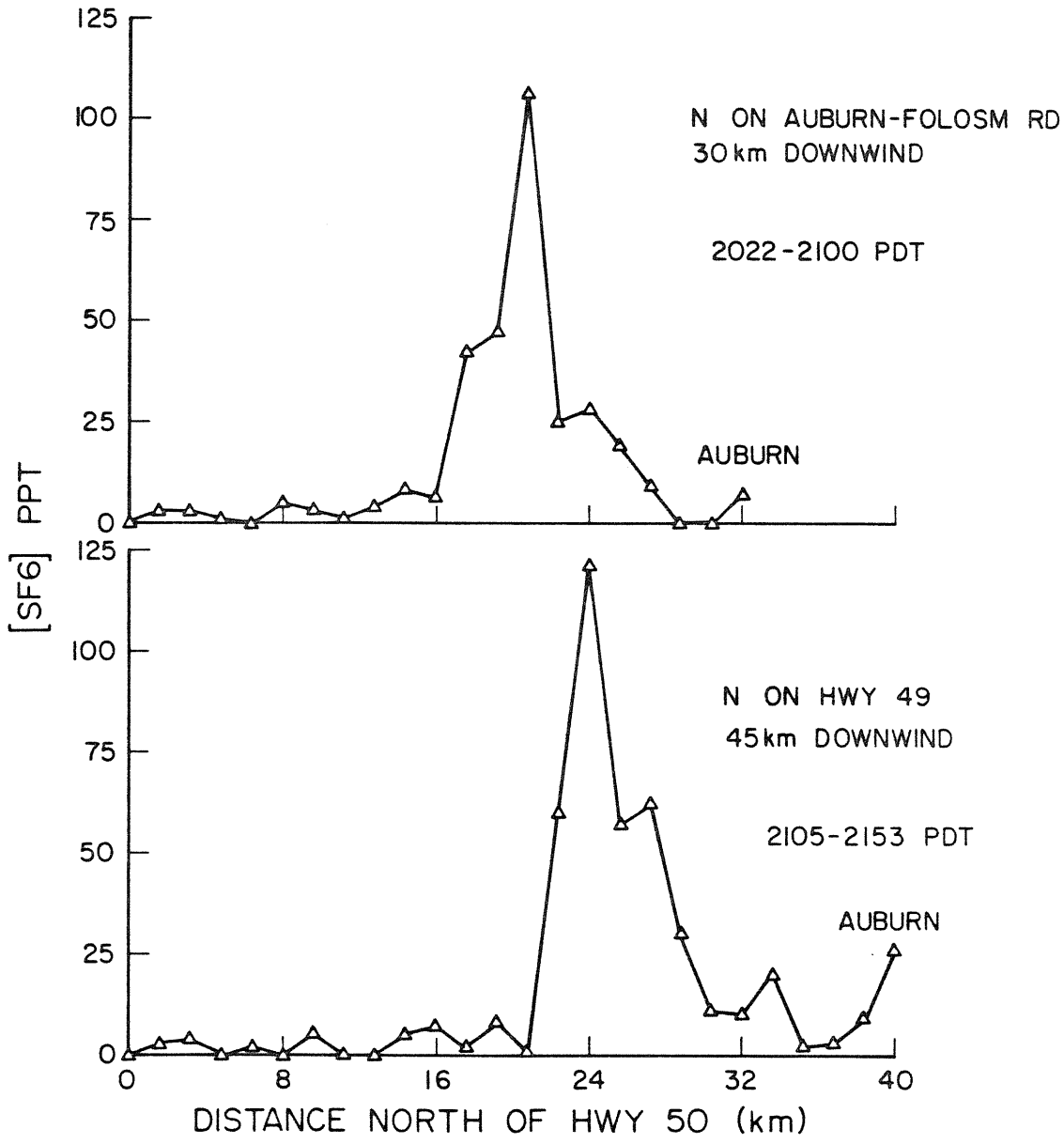

Figure 5 - Tracer concentrations observed in the foothills of the Sierra Nevada, east of Sacramento, during the evening after the release from near Mac Clellan AFB (Test 3, 8/20/80).

(msl) is shown in Figure 6. The inset figure shows that essentially none of the tracer was observed above or below these altitudes. The concentrations observed during these airplane traverses, and the area over which non-zero concentrations were measured suggest that the majority of the tracer released on the preceding day was observed. The transport of the tracer into the elevated layer above the valley may have been linked to the upslope flow, in that it may represent a return flow aloft that balances the air drawn from the valley by the upslope flow. The entrapment of pollutants aloft may be significant in that these pollutants can be transported back to ground level if the polluted air is incorporated into the mixing layer during the afternoon. This mechanism may lead to pollutant impacts, such as high ozone concentrations, that cannot be correlated to either local sources or to more conventional transport from distant sources. Unfortunately, airborne sampling was not conducted on the day after any other experiment. Thus it was not possible to determine the frequency of occurrence of this carryover mechanism.

During Test 5, the last experiment designed to evaluate the impact of the Sacramento urban plume, the release was made from downtown Sacramento between 0700 and 1100 PDT. The initial transport path of the tracer plume was virtually identical to that observed during Test 2 in which the tracer was also released during the morning from downtown Sacramento. The tracer plume observed at 4 and 8 km downwind of the release site was essentially Gaussian, the crosswind dispersion of which corresponded to that expected in Pasquill-Gifford Stability Class

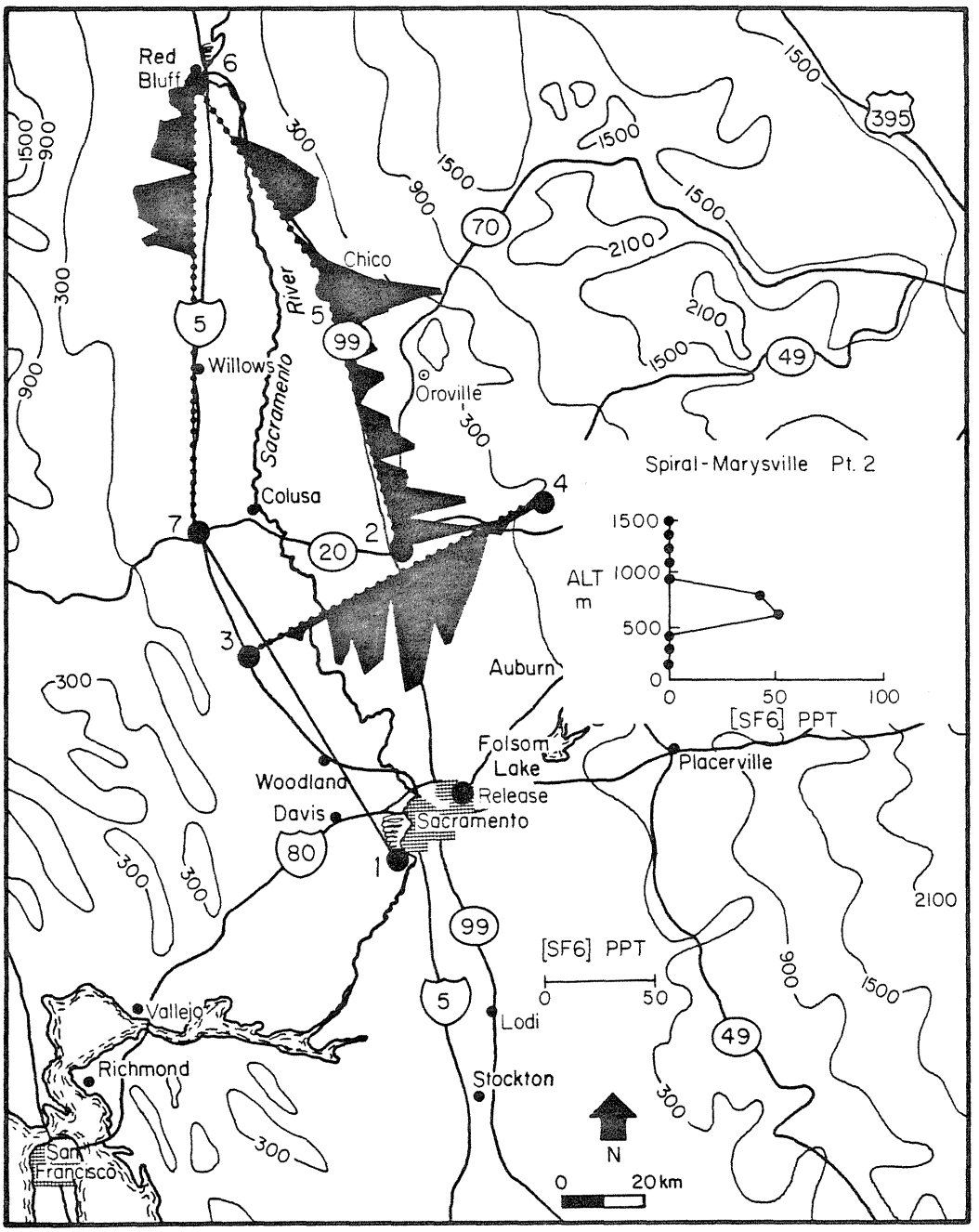

Figure 6 - Tracer concentrations observed during an airplane spiral over Marysville (inset) and airplane traverses between 450 m and 600 m throughout the northern valley on 8/21/80. The release was conducted from eastern Sacramento during afternoon westerly winds.

C. An hourly-averaged concentration of 182 PPT SF_6 (0.54 PPB/kg-mole released/hr) was observed at Marysville beginning about 5 hours after the start of the release. For comparison, a maximum hourly-averaged concentration of 205 PPT SF_6 (0.64 PPB/kg-mole released/hr) was observed at Marysville during Test 2. Partly due to the slightly later release time and to an earlier development of the upslope flow during this test, however, the latter half of the release was transported more eastward than during the earlier test. During automobile traverses in the mid-afternoon, the highest tracer concentrations were observed about 20 km east of Marysville, and by about 1800 PDT the highest tracer concentrations were observed in the foothills northeast of Sacramento, almost 50 km east of Marysville. The hourly-averaged data at all Sacramento Valley sampling sites are included in Figure 7. Note the detection of SF_6 at White Cloud Ranger Station in the foothills of the Sierra Nevada Mountains, beginning about 12 hours after the start of the release. This test clearly indicated the temporal variation of the flow divergence at Sacramento. During the morning, southerly or southeasterly winds were observed throughout Sacramento. As the upslope winds developed, however, the eastern side of the city exhibited more westerly winds. As the afternoon progressed, the upslope flow became stronger and slowly enveloped the entire city. Thus pollutants released at different times or locations within Sacramento could have an entirely different impact on receptor zones downwind. During the morning, the primary receptor zone downwind of Sacramento consistently appeared to be the northern half of the valley.

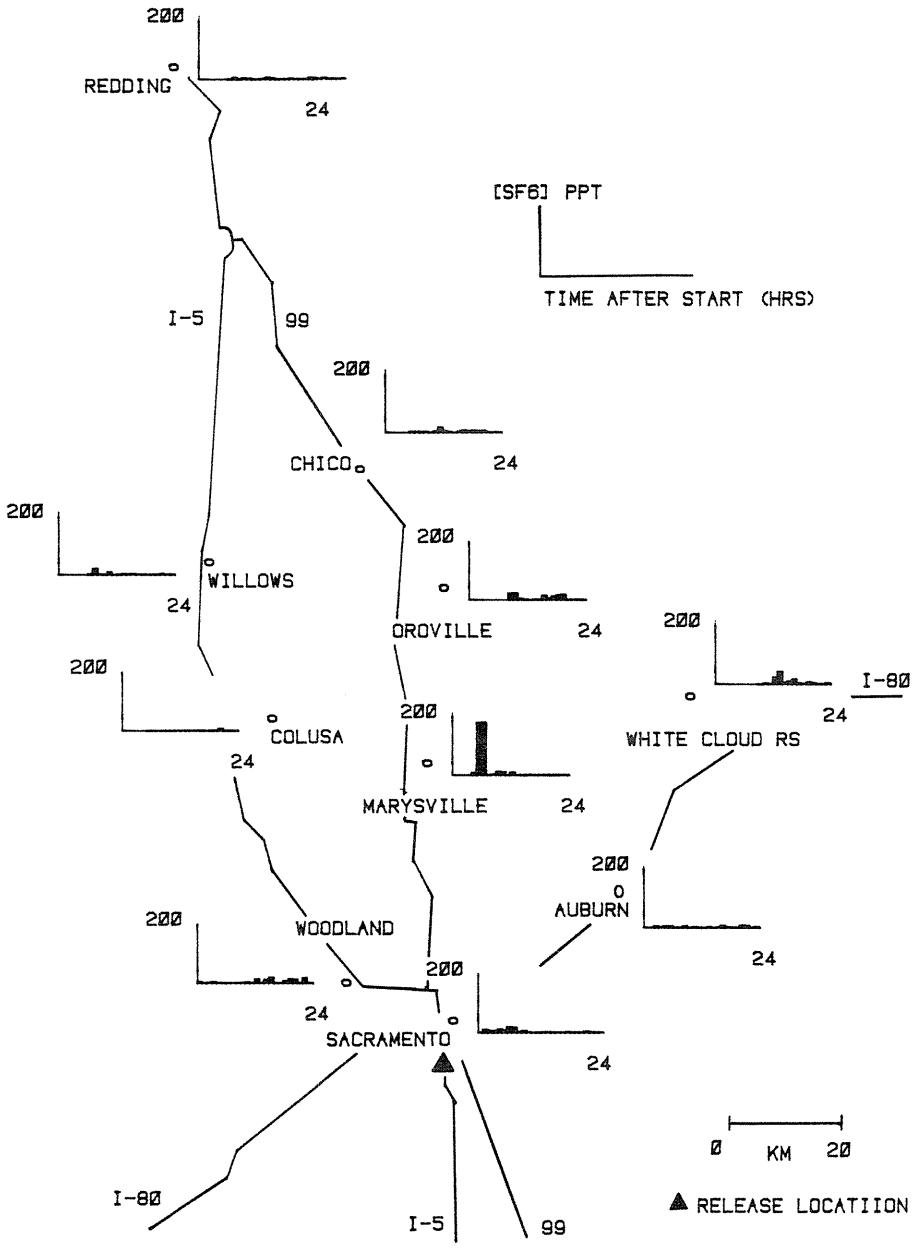

Figure 7 - Map of Sacramento Valley indicating the hourly-averaged tracer concentrations observed at sites within the valley after the second release from downtown Sacramento (Test 5, 8/25/80).

During the afternoon and evening, however, the bulk of the emissions were transported towards the northeast, no doubt contributing to the high afternoon ozone concentrations typically observed in the direction of the foothills (Duckworth and Crowe, 1979).

The final tracer experiment was designed to investigate the potential of the Schultz Eddy for recirculation of valley pollutants and for limiting the transport of pollutants from San Francisco into the Sacramento Valley. The Schultz Eddy is characterized by a northerly flow on the western side of the valley during the morning. During this experiment, SF_6 was released from the Woodland Airport. As indicated in Figure 8, the tracer was observed near Davis, southeast of the release site, and later, between Sacramento and the Sacramento Airport, directly east of the release site. This transport path clearly indicated the existence of an eddy and that it could potentially recirculate valley pollutants back into Sacramento. The Schultz Eddy probably influences the flow divergence over Sacramento. The southeasterly winds often observed in Sacramento during the morning may represent the corresponding return flow from the east to the west sides of the valley, indicating that, given sufficient time, pollutants might be transported from Sacramento to the western side of the valley and back. Because the eddy generally exists only during the morning, however, the complete cycle probably does not occur during any single day.

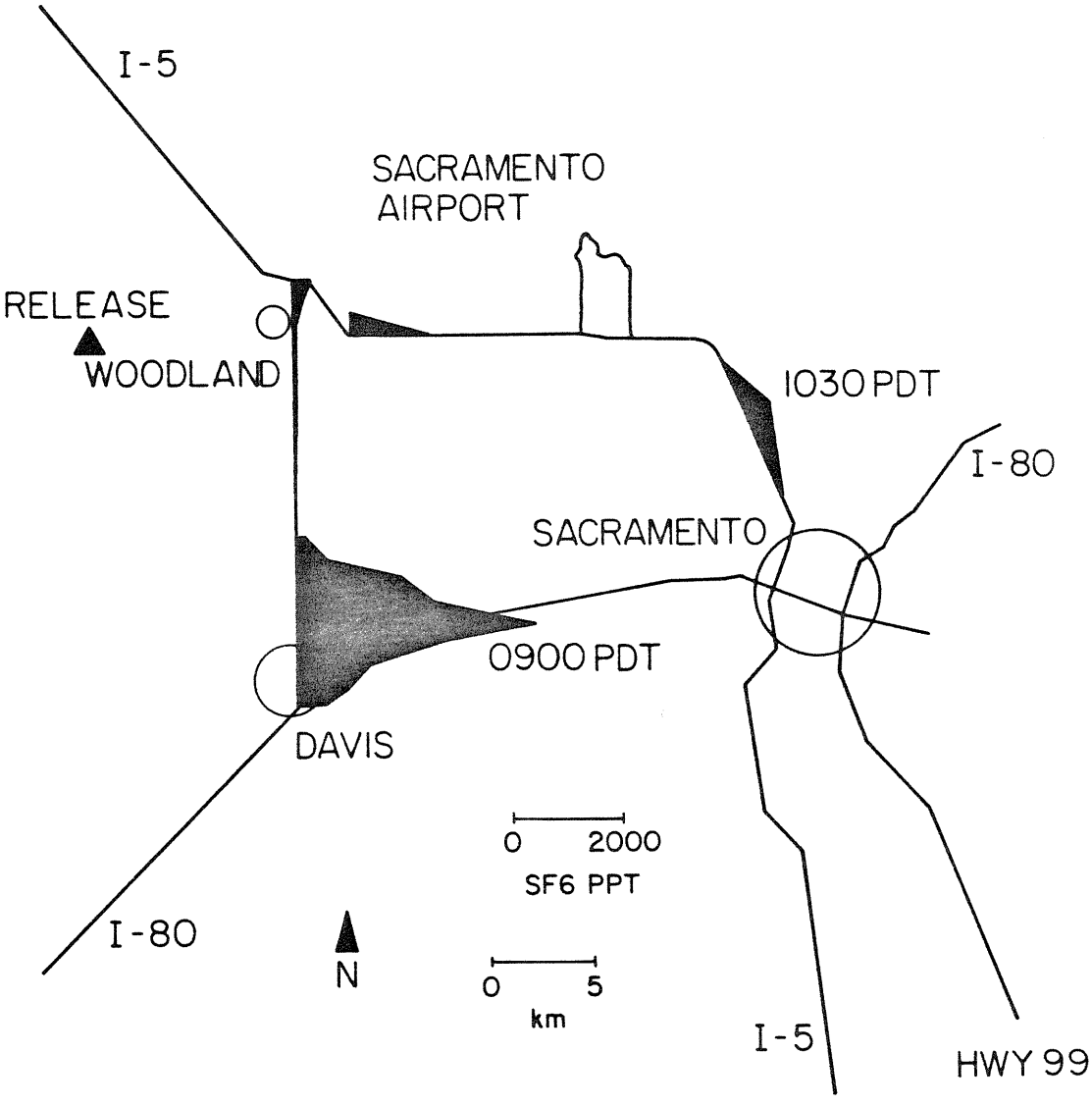

Figure 8 - Map of southern Sacramento Valley indicating the tracer concentrations observed during selected automobile traverses downwind of the release from Woodland Airport (Test 6, 8/28/80). Height of shaded region proportional to observed concentration.

Summary and Conclusions

A series of 6 atmospheric tracer experiments were conducted during August of 1980 to determine the transport routes of pollutants into, within, and out of the Sacramento Valley. The experiments were supported by existing and supplemental meteorological measurements and by airborne observations of air quality.

Based upon the results of the six tests, the following conclusions can be made:

1) Early morning emissions from the San Francisco Bay area and the California Delta apparently have a limited effect on air quality in the Sacramento Valley due to the lack of a well-developed sea breeze and the blockage effect of the Schultz Eddy. Afternoon emissions probably have a more significant effect on the Sacramento Valley but a number of previous studies (e.g. Lamb, et al., 1978) have indicated that the main downwind receptor of California Delta pollutants is still the San Joaquin Valley. The divergence of the winds through the Carquinez Straits makes it difficult to determine the source area for those pollutants that do impact the Sacramento Valley.

2) Due to a slow westward shift of the center of the flow divergence observed at Sacramento, the downwind impact of a tracer and/or pollutant source within the city varied from the northern valley to foothill locations northeast of the city. During the morning, air from Sacramento was

transported northward for later impact in the northern half of the valley. During the late afternoon, air from Sacramento was transported towards the Sierra Nevada foothills. During mid-day, however, pollutant emissions separated by small timing or location differences could impact vastly different areas later in the day.

3) The Schultz Eddy, in addition to limiting the morning transport of pollutants from sources south of the Sacramento Valley, is a potential mechanism for recirculation of aged valley pollutants, especially those emitted near Sacramento during the night and early morning hours.

4) A mechanism exists for the transport and entrapment of pollutants in elevated layers. The pollutants carried aloft can lead to ground level impacts on the following day as the surface mixing layer grows to include the polluted layer. The transport of pollutants aloft may be linked to the afternoon upslope flow on the foothills of the Sierra Nevada, perhaps indicating a balancing return flow aloft. The existence of this mechanism should be probed in other mountain-valley environments due to its potential significance.

5) The Sacramento Valley was effectively ventilated throughout the August, 1980 test period. During most tracer tests, essentially none of the tracer was detected at ground level on the day following a release. As described previously, however, a significant amount of tracer may have been trapped aloft on the day after a test.

References

Demarrais, G.A., Holworth, G.C., and Hosler, C.R. (1965). Meteorological summaries pertinent to atmospheric transport and dispersion over southern California. U.S. Weather Bureau, Technical Paper #54.

Duckworth, S. and Crowe, D. (1979). Ozone patterns on the western Sierra slope. California Air Resources Board, Technical Services Division, Sacramento, Ca.

Lamb, B.K. (1978). Development and application of dual atmospheric tracer techniques for the characterization of pollutant transport and dispersion. Ph.D. Thesis, California Institute of Technology, 16-26, Pasadena, Ca. 91125.

Lamb, B.K., Shair, F.H., and Smith, T.B. (1978). Atmospheric dispersion and transport within coastal regions- Part II, tracer study of industrial emissions in the California Delta region. Atmospheric Environment,12,2101-2118.

Reible and Shair (1982). The transport and dispersion of airborne contaminants in the Santa Barbara Channel area of southern California. Submitted for publication in Atmospheric Environment.

Reible, D.D., Shair, F.H., Smith, T.B., and D.E. Lehrman (1982a). The origin and fate of air pollutants in California's San Joaquin Valley, I. Winter. Submitted for publication in Atmospheric Environment.

Reible, D.D., Shair, F.H., Smith, T.B., and D.E. Lehrman (1982b). The origin and fate of air pollutants in California's San Joaquin Valley, II. Summer. Submitted for publication in Atmospheric Environment.

Schultz, H.B. (1975). Meso-climatic wind patterns and their application for abatement of air pollution in the central California valley. Final report to the California Air Resources Board, Project No. 111.

Turner, D.B. (1970). Workbook of atmospheric dispersion estimates, Environmental Protection Agency. AP-26, 84 pp.

Chapter 12

The Transport and Dispersion of Airborne Contaminants in the Santa Barbara Channel of Southern California

by

D.D. Reible and F.H. Shair

(Submitted to Atmospheric Environment)

Abstract

A series of eight atmospheric tracer experiments using sulfur hexafluoride (SF_6) were conducted during summer and early fall conditions in the Santa Barbara Channel area of southern California. The tests were designed to elucidate the behavior of airborne contaminants in an atmosphere exhibiting diurnal wind reversals and to determine the impact of offshore pollutant sources on the surrounding coastline.

In the Santa Barbara Channel, generally westerly daytime winds led to afternoon impacts of the tracer upon the surrounding coastline. The directly impacting plume was approximately Gaussian in shape, the width of which corresponded to that expected during stable atmospheric conditions. Vertical dispersion of the tracer was generally limited to the lower 150 m of the atmosphere. While the highest onshore tracer concentrations were observed during the afternoon, the diurnal wind reversals tended to well-mix the tracer over large zones and limit the net ventilation of the air basin. The uniform background concentrations of tracer observed during the night and on the day following the release suggested that pollutant carryover into days subsequent to their release can be a significant air quality problem in the Santa Barbara Channel and other similar coastal environments.

INTRODUCTION

In order to meet the nation's and the world's energy requirements in the coming years, many locations, which had heretofore faced little or no human influence, have become increasingly subjected to the environmental pressures inherent with commercial and industrial development. One of the more complex policy issues facing the world today is achieving a balance between the commericial development of energy resources and protection of the environment. Any policy attempting to balance these often conflicting pressures requires a sound technical basis as well as a thorough understanding of the social and economic implications of the policy.

In the United States, there currently exists an attempt to address these questions with respect to the development of off-shore oil resources. The current work is addressed to the technical issue of assessing the impact of gaseous off-shore pollutant sources on air quality in coastal and inland areas. This is a difficult task in that the wind field, which transports and disperses airborne pollutants, is typically not well characterized off-shore. Differential heating between the water and land surfaces gives rise to a sea breeze directed on-shore during the afternoon and a reversed land breeze directed off-shore during the night (see e.g. Defant, 1951). The diurnal wind reversals in the surface layer can potentially limit the net ventilation of an air basin by "recycling" pollutants. The dispersion of pollutants during the transition between the daytime and nighttime winds is particularly unclear. The wind reversals generally take place over a 1-3 hour time period. During this time, winds are generally light, often below threshold velocities of conventional anemometers. Thus the transport and dispersion of a pollutant during a wind reversal are difficult to predict.

In order to better understand the transport and dispersion of airborne pollutants in a diurnally varying atmosphere and to quantify the impact of off-shore pollutant sources on coastal receptor zones, a series of atmospheric tracer experiments was conducted in the Santa Barbara Channel of Southern California. The Santa Barbara Channel is an area of relatively pristine air quality widely known for its beautiful coastline. The ecologically fragile Channel Islands (some of which form the Channel Islands National Monument) are about 30 km offshore and form the southern boundary of the channel. The area faces the possibility of extensive development in the coming years to exploit off-shore oil reserves. Parts of the Santa Barbara Channel have been included in exploratory lease sales conducted by the United States Department of the Interior. While the results of this study do not strictly pertain to locations other than the Santa Barbara Channel area, it is clear that the basic structure of the flow field and the air pollution implications of that flow structure are repeated in other coastal environments.

EXPERIMENTAL PROCEDURE

To ensure the validity of the results of this study for typical meteorological conditions, a total of eight atmospheric tracer experiments were conducted from the Santa Barbara Channel. The first experiment was conducted during July, 1977 while the subsequent seven experiments were conducted during September and October of 1980. Ozone, the pollutant of primary interest in southern California, is found in higher concentrations during late summer and early fall than at any other time of year. During all eight experiments, sulfur hexafluoride (SF_6) was used as the tracer. Sulfur hexafluoride is a non-toxic, colorless, odorless, inert gas that can be detected at concentrations as low as 1-10 parts SF_6 per trillion parts air. The relative lack of natural or anthropogenic sources of SF_6 makes the gas an ideal atmospheric tracer. By releasing a known amount of the tracer and determining the 3-dimensional concentration profile downwind, source strength-receptor concentration relationships are established directly, and the flow field can be inferred. The grid over which tracer concentrations can be determined is typically much finer than the grid over which it is physically possible to determine wind speed and direction. For this reason, it is often easier to infer the transport wind field from tracer data than with wind measurements.

During each experiment, the tracer was released from cylinders each containing about 45 kg of liquid SF_6 under its own vapor pressure (about 2100 kN/m^2 at room temperature). The SF_6 was vaporized during its release to atmospheric pressure. The gas flow was monitored via a calibrated high-volume rotameter, and at the conclusion of an experiment, the SF_6 cylinders were weighed for an independent check of the release rate. The locations of all SF_6 releases conducted during this experiment are included in Figure 1. The release times as well as locations are listed in Table 1. Only the second tracer release was

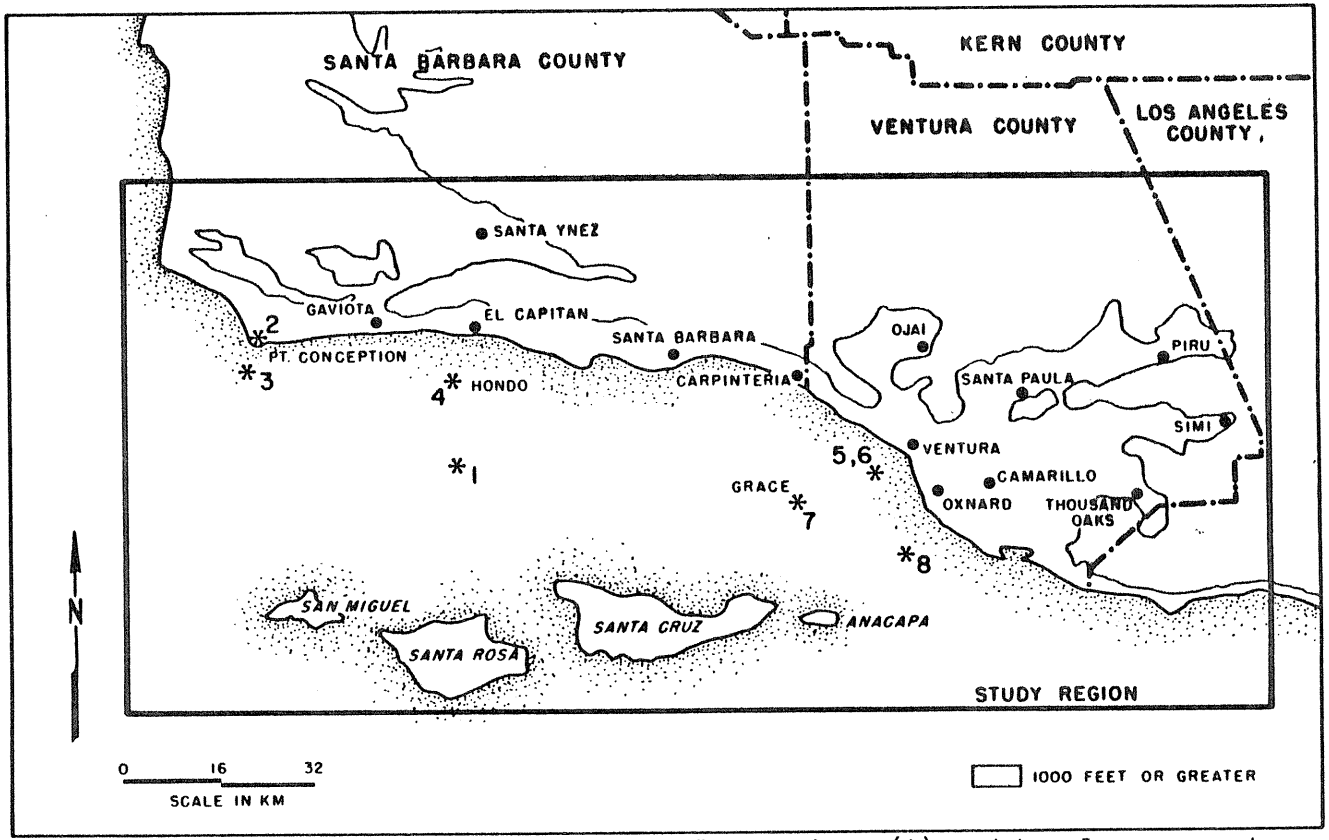

Figure 1 - Map of study area showing SF_6 release sites (*) and hourly-averaged sampling sites (●).

Table 1

Test 1 - 39 kg SF_6/hr from a location midway between Santa Rosa Island and El Capitan Beach between 0502 and 0714 PDT on 7/28/77.

Test 2 - 38 kg SF_6/hr from Pt. Conception between 1100 and 1600 PDT on September 17, 1980.

Test 3 - 32 kg SF_6/hr from 5 km south of Pt. Conception between 1100 and 1600 PDT on September 22, 1980.

Test 4 - 28 kg SF_6/hr from beside Platform Hondo in the Santa Barbara Channel. The release took place between 0200 and 0700 PDT on September 26, 1980.

Test 5 - 22 kg SF_6/hr from 9 km west of Ventura in the Santa Barbara Channel. The release took place between 1135 and 1900 PDT on September 24, 1980.

Test 6 - 22 kg SF_6/hr from 9 km west of Ventura in the Santa Barbara Channel. The release took place between 1240 and 1900 PDT on September 28, 1980.

Test 7 - 21 kg SF_6/hr from beside Platform Grace in the Santa Barbara Channel. The release took place between 0600 and 1100 PDT on October 1, 1980.

Test 8 - 30 kg SF_6/hr from 6 km southwest of Pt. Hueneme in the Santa Barbara Channel. The release took place between 0045 and 0545 PDT on October 3, 1980.

conducted from on-shore (Pt. Conception, at the extreme western end of the Santa Barbara Channel). All other releases were conducted from on-board various ships located at the positions depicted in Figure 1.

The 3-dimensional tracer concentration profile downwind of the source was measured via collection of both hourly-averaged and grab samples at fixed sites. In addition, grab samples were collected at regular time or distance intervals from a specified start point during airplane, automobile and boat traverses. All air samples were collected in 30 cm^3 plastic syringes. The hourly-averaged samples were collected by an automatic device that pulled 1 syringe over the course of an hour, sealed the syringe, and then pulled the next syringe over the course of the following hour. The location of the automatic samplers are shown in Figure 1. The automatic samplers were run for 24 hours during each test.

All samples were analyzed at the conclusion of an experiment by electron capture gas chromatography. This technique allows detection of SF_6 concentrations as low as 10 parts-per-trillion (PPT) with an error of less than $\pm$ 20%. Lower concentrations can be detected but with larger relative error. Details of the detection technique can be found in Drivas (1975) or Lamb (1978). In addition to the quantitative determination of SF_6 concentration at the conclusion of an experiment, a portable electron capture gas chromatograph was used during each experiment to spot check collected samples so that automobile and airplane traverses could be routed in the most effective manner.

In order to characterize the meteorological conditions which existed on the day of an experiment, wind speeds and directions, both at the surface and aloft, were measured at a number of sites. Airplanes were used to characterize the vertical temperature structure of the atmosphere. An acoustic sounder was located at Santa Paula to assist in the determination of the vertical

mixing height. Within the channel, additional meteorological data, including wind speeds and vertical temperature structure, were collected by personnel on the US Navy ship Acania as part of a separate study of the direct onshore impact of pollutant sources close to the coast (Schacher, et al., 1981).

PRESENTATION AND DISCUSSION OF RESULTS

The first tracer release was conducted from onboard a ship located near the center of the Santa Barbara Channel where 39 kg of SF_6/hr was released between 0502 and 0714 on 7/28/77. As shown in Figure 1, the location of the release was about 20 km offshore. The tracer was transported onshore by the afternoon sea breeze, impacting locations between Santa Barbara and Carpinteria by 1100 PDT. Grab sample concentrations as high as about 6 PPB/kg-mole/hr were detected near Santa Barbara. By 1200 PDT, concentrations about an order of magnitude lower were detected at Ventura due to the predominantly westerly winds observed in the channel. This test clearly showed that pollutants could be transported onshore from sources located at least as far as 20 km from shore. The subsequent seven experiments conducted during the late summer and early fall of 1980 were designed to further explore the onshore impact of channel pollutant sources.

The first tracer release during the 1980 experimental series was conducted from Pt. Conception at the extreme western edge of the study area (see Figure 1). 38 kg of SF_6 per hour was released from this location between 1100 and 1600 PDT, 9/17/80. Surface winds at Pt. Conception were northwesterly at 7 to 12 m/s throughout the release period. This is a typical late summer wind condition at Pt. Conception and can lead to transport into the Santa Barbara Channel. The winds within the channel are typically westerly during the afternoon and local on-shore winds can transport pollutants onto the surrounding coastline. Pt. Conception has been suggested as a possible site for a major liquified natural gas terminal and thus an understanding of the transport and dispersion of airborne pollutants from this area is necessary to accurately assess the impact of spills or accidental discharges of large amounts of liquified

natural gas on urban coastal areas around the Santa Barbara Channel. In addition, this test illustrates most of the basic flow structure in the Santa Barbara Channel and will thus be described in detail while subsequent tests will be outlined and compared to this test.

The trajectory or transport path of the tracer released at Pt. Conception is shown in Figure 2. Grab samples collected at Anacapa, Santa Cruz and San Miguel Islands indicated that none of the tracer was transported across the center of the channel during the afternoon. At oil drilling platform Hondo an average of 2600 $\pm$ 1400 PPT (10 parts per billion (PPB) per kg-mole SF_6 released per hour) was detected between 1330 and 1600 PDT. The arrival of SF_6 at the drilling platform by 1330 PDT indicated an average speed of about 4 m/s over the 32 km separating the drilling platform and the release point. Airplane traverses indicated that the tracer was mixed to an altitude of 150 m or less over the channel. Assuming that the Gaussian plume model (Turner, 1970) and stable atmospheric conditions (F stability) are applicable, the centerline concentration of the plume at this distance downwind should be about 9.7 PPB/kg-mole/hr. The excellent agreement between observed and estimated concentrations may be fortuitous, but it does suggest that the platform was very close to the centerline of the tracer plume. Later in the afternoon, the sea breeze led to transport of the tracer onshore. During automobile traverses along the coastline, an essentially Gaussian concentration profile was detected near Santa Barbara during mid-afternoon. The maximum grab sample concentrations observed during most of these traverses were about 1800 PPT (6.9 PPB/kg-mole/hr). The maximum hourly average concentration detected onshore was about 3 PPB/kg-mole SF_6 released/hr at both Santa Barbara and Carpinteria. These observations compare to predicted centerline concentrations (again via the Gaussian plume model, a 150 m mixing height and F stability) of 4.6 PPB/kg-mole/hr at Santa

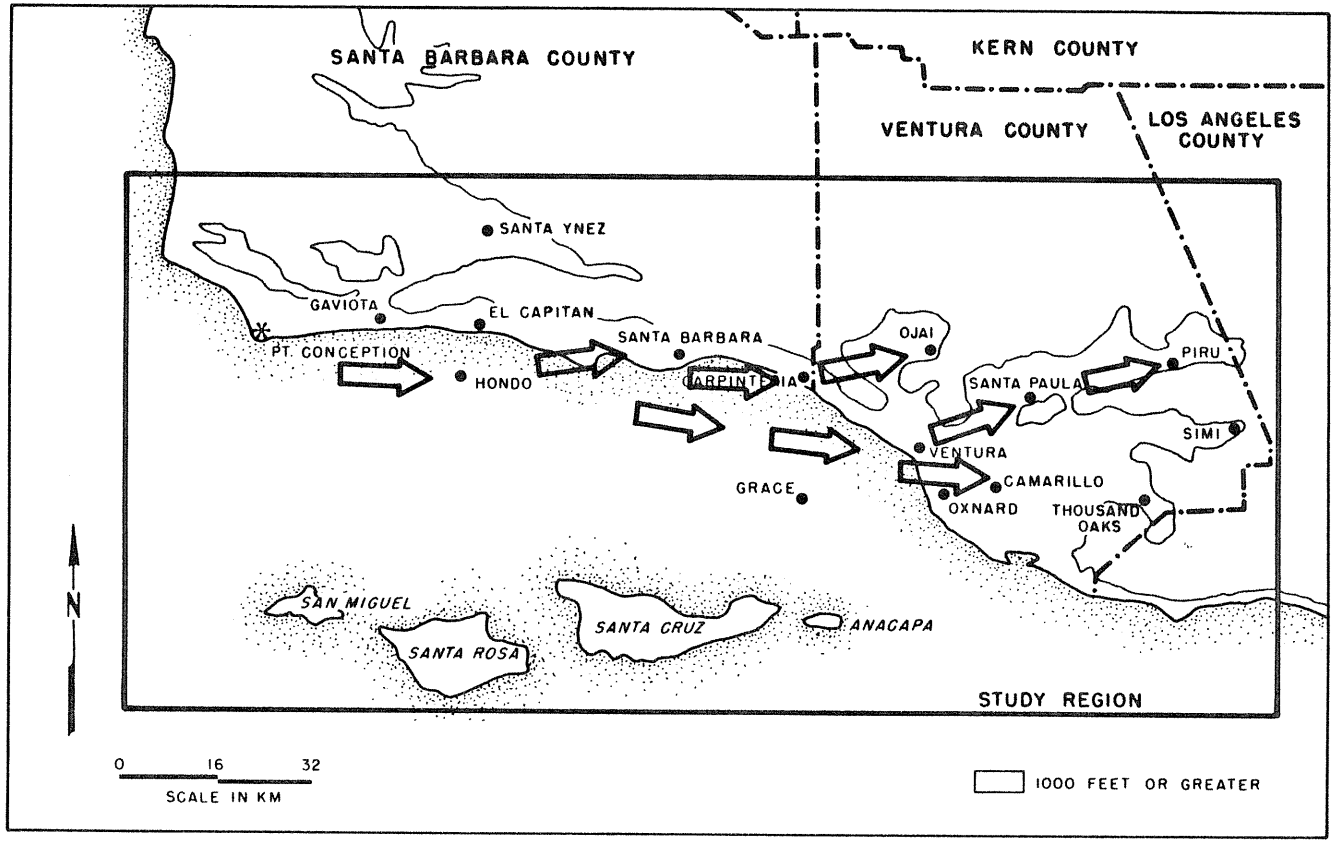

Figure 2 - Afternoon trajectory of SF_6 tracer released from Pt. Conception on 9/17/80.

Barbara and 2.2 PPB/kg-mole/hr at Carpinteria. While the maximum impact of the tracer was along the Santa Barbara County coastline, SF_6 concentrations about an order of magnitude lower were detected along the Ventura County coastline. As would be expected from the westerly afternoon winds, the tracer was transported toward the eastern end of the study area throughout the afternoon. The easternmost sampling site, Piru, detected concentrations as high as about .22 PPB/kg-mole by 2000 PDT. Airplane sampling indicated that the mixing height of the tracer was 2-4 times higher over the warmer inland areas than over the coastline, no doubt contributing to the dilution of the tracer.

At about the time that the tracer was first detected at Piru, nightfall brought increasing stabilization to the atmosphere and differential cooling of the land and sea surfaces led to the development of an easterly flow directed off-shore, reversing the transport path of the tracer. As shown in Figure 3, essentially uniform concentrations were detected at many of the inland and coastal hourly-averaged sampling sites during the night. Between 0400 and 0700 PDT an average of 32 PPT SF_6 (standard deviation 10 PPT) was detected over an area bounded by Piru to the east, Camarillo to the south, El Capitan State Beach to the west and Ojai to the north.

As mentioned previously, the tracer was mixed to an altitude of about 150 m along the coast, to as high as 3-600 m at inland locations. Assuming that the tracer was well-mixed at the above concentration (32 PPT) to an average height of 300 m, about 60 grams of SF_6 was distributed over each 1 km^2 of surface area. The total land area below 300 m bounded as described previously is approximately 1500 km^2. Thus the SF_6 detected onshore on the night after the release accounted for 90 kg of SF_6, about 47% of the 190 kg originally released. When allowance is made for that part of the SF_6 located

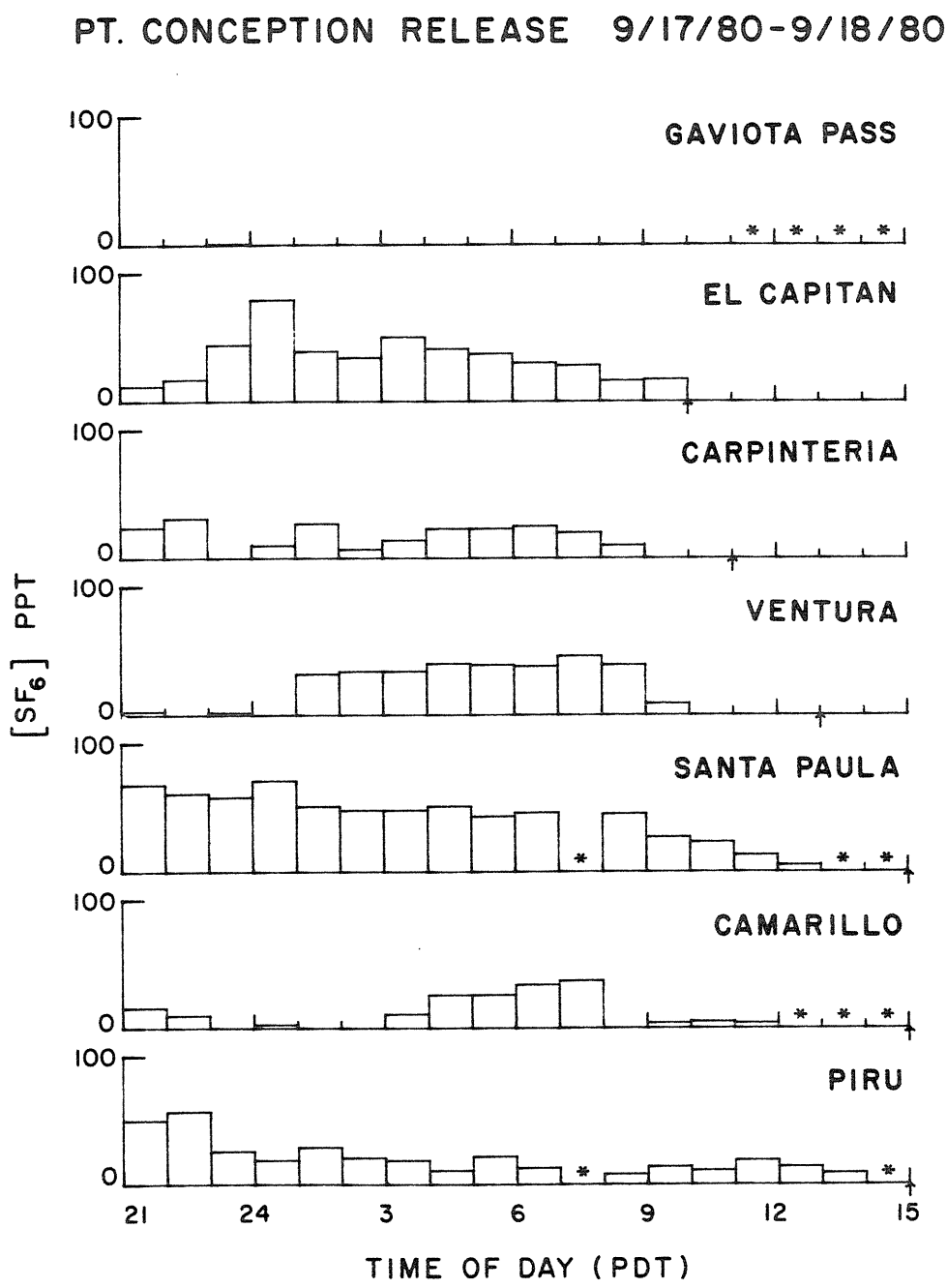

Figure 3 - Hourly-averaged tracer concentrations detected at various sites during the night after Pt. Conception release of 9/17/80.

off-shore during the night, the mass balance calculation indicates that most of the SF_6 originally released was not transported out of the study area before the onset of the reversed nighttime winds. Note also that the nighttime wind reversal led to efficient lateral mixing of the tracer such that essentially uniform concentrations were detected throughout the night at all impacted sites. The 5 hour release of tracer led to a measurable impact for at least 19 hours at sites along the Santa Barbara County coastline.

One other experiment was conducted from Pt. Conception, on 9/22/80, but in this experiment the tracer was released at a rate of 32 kg/hr from on a ship about 5 km south of the shoreline. As in the previous test, the tracer was released between 1100 and 1600 PDT, but the afternoon westerly winds failed to develop until about 1400 PDT, 3 hours after the beginning of the release. The initially light and variable winds thus spread the tracer laterally, giving the appearance of a complex area source to the receptor zones onshore. The primary impact of the tracer, however, was again detected near Santa Barbara as in the previous test. The maximum concentrations detected onshore (due to that part of the tracer transported directly to shore) were about a factor of three lower than observed during the previous test, consistent with the difference in estimated mixing depth between the two tests. The maximum mixing depth over the channel surface during this test was about 500 m, the highest observed during the experimental program. Due to the delayed onset of the afternoon onshore winds, the tracer was not transported as far inland as during the previous test. Thus the onshore impacts were limited to the Santa Barbara County coastal sites. As in the previous test, SF_6 was detected at these sites throughout the night. The observed nighttime concentrations were approximately double those found during the previous experiment because the tracer was not dispersed over as wide an

area as in the first experiment. During the day after the release, the tracer was again transported towards the east by the afternoon westerly sea breezes and by mid afternoon, tracer concentrations as high as 30 PPT were detected during automobile traverses between Ventura and Carpinteria. By late afternoon, SF_6 concentrations as high as 20 PPT were detected between Simi and Ventura. In summary, the delayed onset of the westerly afternoon winds and the deep mixing layer on the day of the release led to an initially reduced impact on shore, although the primary location of the impact was in Santa Barbara County as in the previous test. Since the tracer was not dispersed over as large an area as in the first test, however, the coastal impact during the night and early morning hours was higher during this experiment and higher concentrations were detected on the second day after the release than during the previous test.

A third tracer release was conducted from the western half of the Santa Barbara Channel. 28 kg/hr of SF_6 was released from near Platform Hondo (see Figure 1) on the night of 9/26/80 between the hours of 0200 and 0700 PDT. Due to the early release time, the prevailing surface flow was easterly until well after the end of the release. As might be expected from the previous experiment, the tracer plume was initially transported towards the west and significantly diluted before the onset of the afternoon onshore winds. The wind reversal that marked the beginning of the sea breeze led to efficient lateral dispersal of the tracer plume. The impact of the tracer was thus essentially uniform on both the Santa Barbara and Ventura County coastlines during mid-afternoon (see Figure 4). Tracer concentrations along the coastline from Gaviota Pass to Ventura during the traverses depicted in Figure 4 averaged about 20 PPT with a standard deviation of 9 PPT. The effective dispersal of the tracer over a wide area led to very low concentrations throughout the study area on 9/27/80, the day after the release.

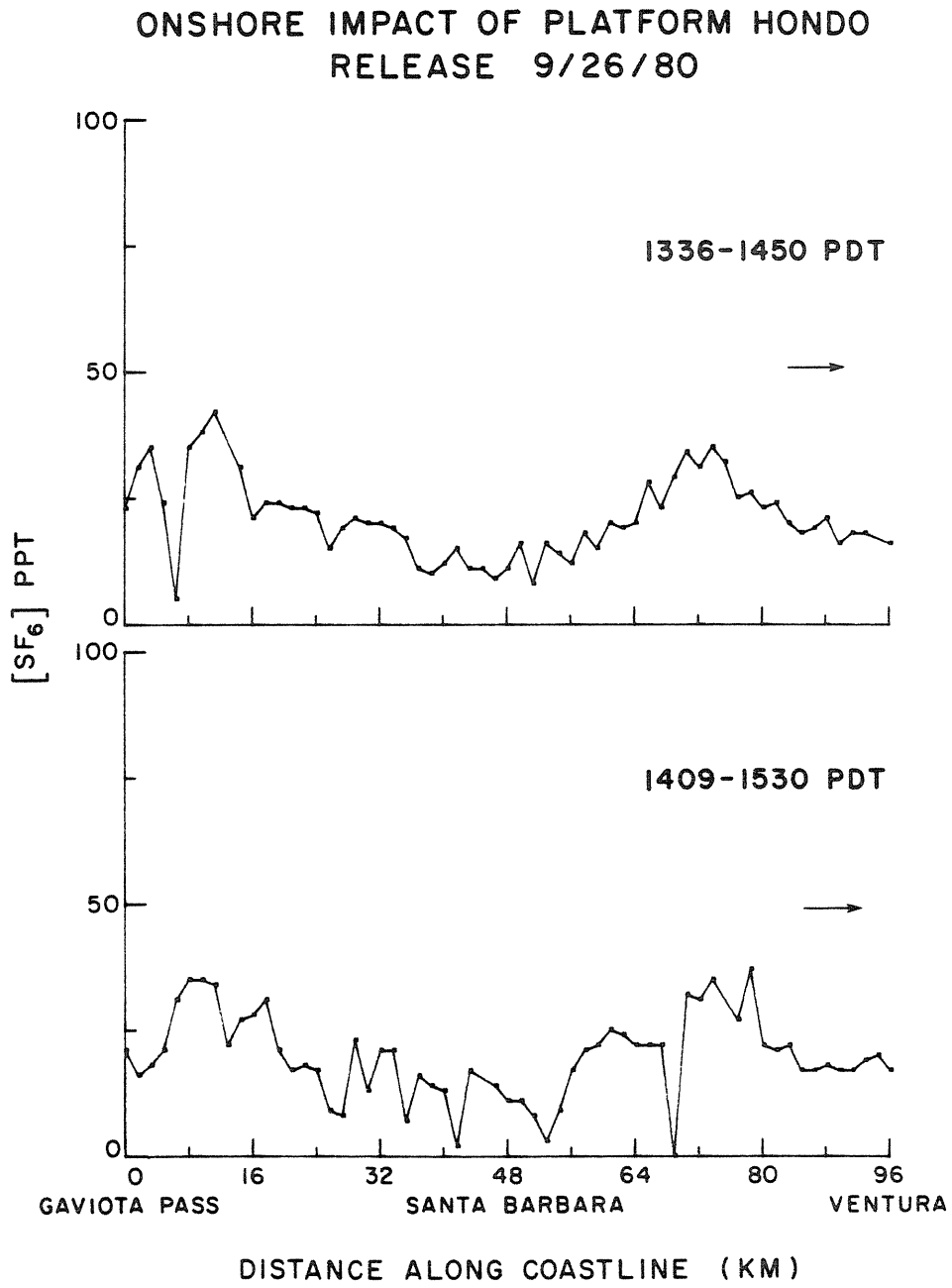

Figure 4 - SF_6 tracer concentrations detected during automobile traverses along the coastline between Gaviota Pass and Ventura during platform Hondo release of 9/26/80.

The concentrations detected were too low to estimate the total mass of the carryover.

The other four tracer experiments investigated the transport of pollutants in similar flow regimes for sources nearer the eastern end of the Santa Barbara Channel. Two releases were conducted from a ship located about 9 km west of Ventura during the afternoon westerly flow. The releases were conducted by Aerovironment, Inc. and the US Navy Postgraduate School as part of a separate study of the direct coastal impact of pollutant sources close to shore (Schacher, et al.). During the first of these releases (9/24/80) our sampling was limited to automobile traverses along a road that parallels the Ventura County coastline, while in the second (9/28/80) a complete sampling network was employed as in the previous tests. About 22 kg/hr of SF_6 was released during the afternoon sea breeze in both experiments. As shown in Figure 5, essentially Gaussian shaped plumes were detected by automobile traverses along the coast. During the experiment of 9/24/80, the best-fit crosswind standard deviation in concentration was about 330 m. Based upon mass balance considerations, the vertical standard deviation in concentration was calculated to be about 90 m. These calculated dispersion parameters correspond to those expected in E stability atmospheric conditions (Turner, 1970). During the experiment of 9/28/80, the best-fit crosswind standard deviation in concentration was about 200 m. The vertical standard deviation in concentration was calculated to be about 50 m. These dispersion parameters correspond to F atmospheric stability. During both experiments, the calculated atmospheric stability was one class more stable than that expected from the vertical temperature distribution. It should be remembered, however, that this conclusion is based on grab sample data. Time averaged samples would tend to indicate a lower maximum concentration and a larger lateral spread due to plume meander.

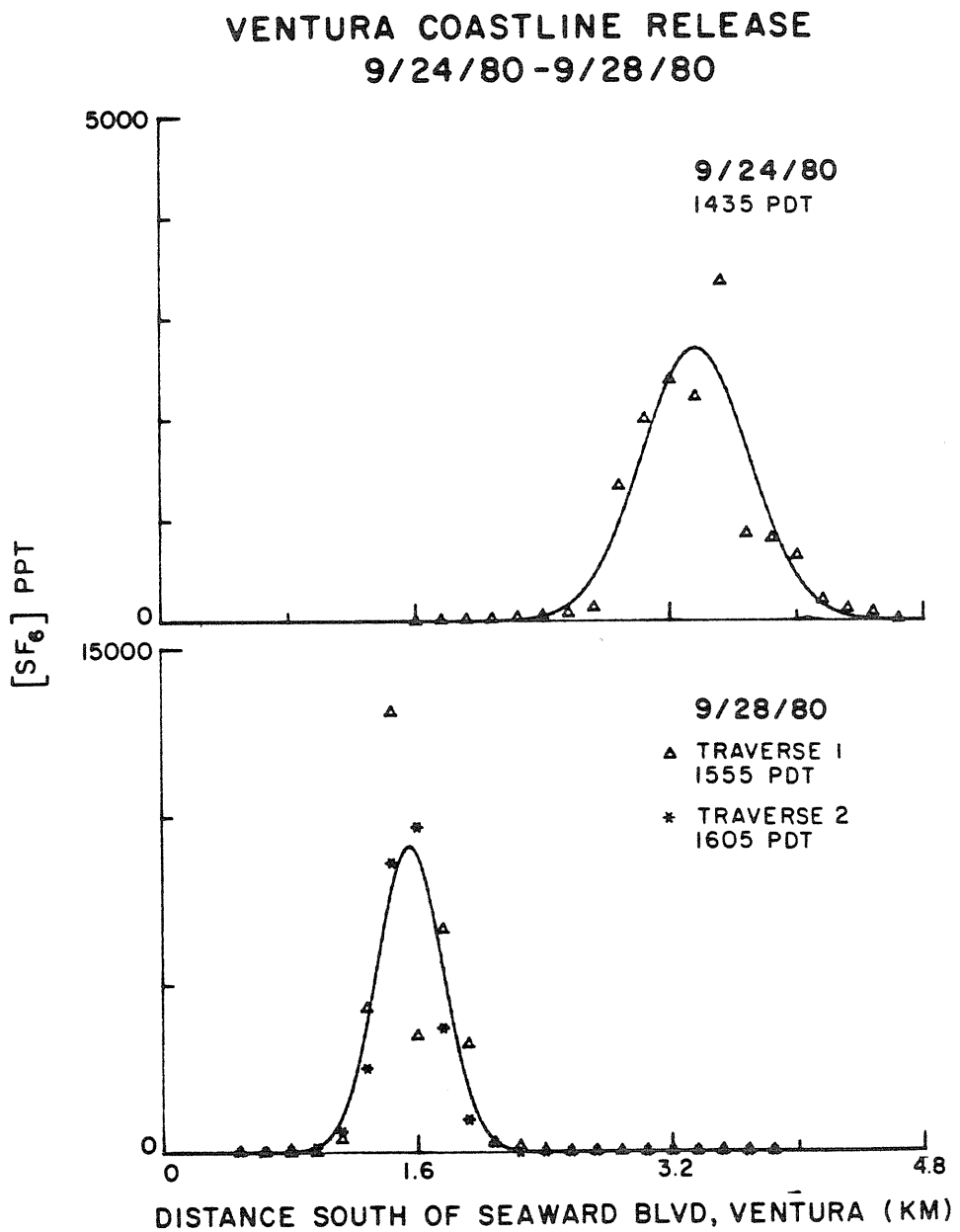

Figure 5 - Gaussian comparison for automobile traverses conducted between Ventura and Oxnard during offshore releases of 9/24/80 and 9/28/80.

During the experiment of 9/28/80, SF_6 sampling was continued inland. As expected from previous experiments, the tracer was primarily transported towards Santa Paula and Piru. A maximum concentration of 8 PPB/kg-mole SF_6 released/hr was detected at Santa Paula, approximately 30 km east of the release point. Between 1700 and 1800 PDT, the tracer was first detected at Piru where about 2 PPB/kg-mole SF_6 released/hr was detected between 2000 and 2100 PDT. As in the previous experiments, the stabilization of the atmosphere near nightfall and the development of the land breeze arrested the movement of the tracer and directed the transport back toward the coast. While some of the tracer was probably transported east of Piru and out of the Santa Barbara Channel air basin, most of the SF_6 apparently remained within the basin. Tracer concentrations in excess of 200 PPT were detected after midnight at Santa Paula and Oxnard and a maximum of about 80 PPT SF_6 was detected at Santa Barbara, about 50 km west of the release point. Between 0700 and 0800 PDT, an average of 41 PPT, with a standard deviation of 21 PPT, was detected over roughly the same area impacted by the nighttime land breeze during Test 1 (i.e. bounded on the west by the El Capitan State Beach area and on the east by Camarillo and Piru). Assuming an average afternoon mixing height of 300 m, this concentration level accounts for 80% of the tracer originally released. Again note that this calculation includes only that material over land. Essentially all of the released tracer was apparently within the channel area when allowance is made for that part of the tracer over the sea surface.

The seventh tracer experiment was conducted during the transition from the nighttime land breeze to the daytime sea breeze. 31 kg/hr of SF_6 was released from near off-shore drilling platform Grace on 10/1/80 between 0600 and 1100 PDT. The initial dispersion and weak westward transport of the tracer gave the appearance of an area source to onshore receptor locations. As

expected from the second tracer experiment, when the wind reversal also occurred during the release, the onshore impact of the tracer possessed characteristics of both a directly impacting plume and a more dilute reversed plume. The direct plume, resulting from that part of the release conducted after the onset of the onshore flow (after about 1000 PDT), impacted Santa Barbara and Carpinteria. A maximum hourly averaged tracer concentration of about 10 PPB per kg-mole of SF_6 released per hour was detected at Santa Barbara between 1500 and 1600 PDT. As in all previous tests, the tracer was transported eastward throughout the afternoon. Unlike the previous tests, however, the nighttime land breeze was not sufficiently strong to transport the tracer back towards the coast. The nighttime stabilization of the atmosphere did, however, retard the eastward movement of the tracer and as in previous tests, tracer concentrations throughout the study area remained essentially constant during the night. About 20 PPT (standard deviation 9 PPT) was detected over the entire zone from Santa Barbara to Thousand Oaks and Piru. Again assuming a 300 m mixing depth (corresponding to about 1700 km^2 surface area), the average on-land concentration of 20 PPT accounts for 60% of the tracer released. As in the previous tests, after allowing for that part of the tracer located offshore, most of the released tracer probably remained within the study area on the night following the release.

Because the diurnal land-sea breeeze cycle is generally reproducible from day to day, the results of the first seven experiments showed a remarkably consistent flow and transport structure in the atmosphere above the study area. The last experiment, however, clearly illustrated the difficulties in predicting the onshore impact of an offshore pollutant source without knowledge of the details of the mid-channel air flow. 30 kg/hr of the tracer was released from a location about 6 km southwest of Pt. Hueneme between 0045 and 0545 PDT,

10/3/80. 2-3 m/s southeasterly winds were observed at the release site. The tracer was expected to be transported into the center of the channel and then across the coastline (primarily the Ventura County coastline) during the afternoon sea breeze. The mid-channel southeasterly flow showed surprising strength and persistence, however, in that the tracer was first detected onshore at about 1200 PDT at Gaviota Pass. SF_6 concentrations as high as about 2 PPB per kg-mole SF_6 released per hour were observed. As shown in Figure 6, essentially none of the tracer was detected at other sampling sites along the coastline. The easternmost release point thus resulted in the westernmost onshore impact. Clearly, pollutants released from any location within the channel can impact any other location depending on the timing and strength of the diurnal wind flows. The tracer during this experiment was transported through Gaviota Pass and impacted inland areas in the Santa Ynez Valley. Tracer concentrations as high as 20-30 PPT were detected throughout the Santa Ynez Valley during the afternoon on the day following the release.

The tracer results can be used to develop a quantitative, empirical model of the onshore impacts of an offshore pollutant source. The tracer data resulting from an individual test directly indicate the onshore impact of a finite length source in a given meteorological condition. Since the basic flow field was quite reproducible, at least during the first 7 tests of the experimental program, the onshore impact of a continuous source of an essentially conserved pollutant can be predicted by a simple superposition of the appropriate tracer studies. Caution is warranted, however, in that this simple analysis cannot predict the behavior of the tracer during Test 8, in that there was inadequate characterization of the conditions that led to the enhanced westward transport of the tracer.

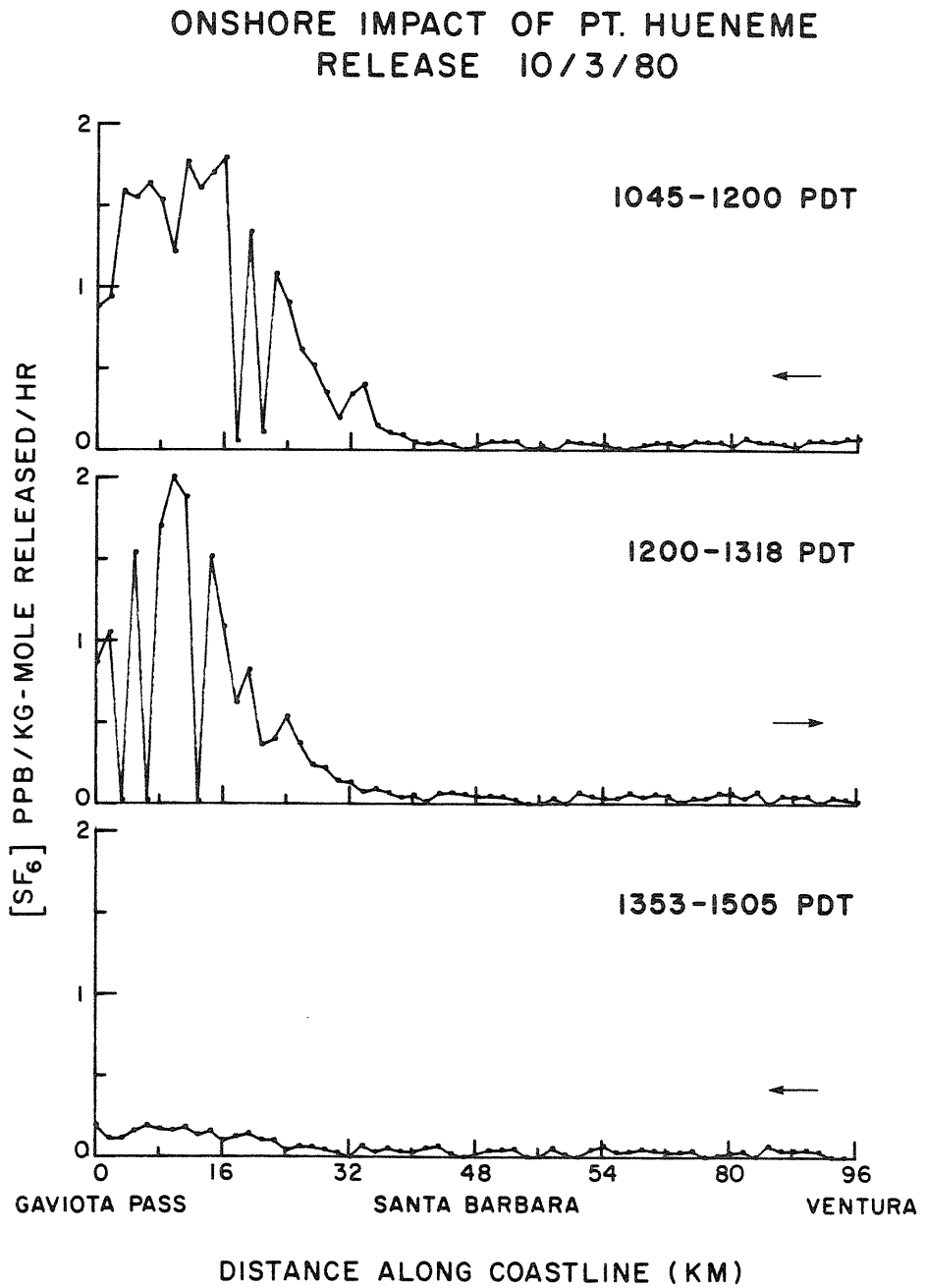

Figure 6 - SF_6 tracer concentrations detected during automobile traverses along the coastline between Gaviota Pass and Ventura during Pt. Hueneme release of 10/3/80.

An interesting and useful application of the tracer experiments is the prediction of the onshore impact of a pollutant source at Pt. Conception. Pt. Conception is a possible site for a major liquefied natural gas (LNG) terminal. Also, the area in the immediate vicinity of the point faces development in order to exploit off-shore oil reserves. An estimate of the air quality impact of a continuous pollutant source of known strength at Pt. Conception can be made by making the following assumptions,

a) Pollutants released during the first part of the afternoon westerly flow (about 1100 PDT to 1600 PDT) directly impact the coastal areas in a manner similar to the tracer released from Pt. Conception during Test 2.

b) Pollutants released prior to the onset of the afternoon flow impact the coastal areas after mixing laterally during the morning wind reversal. It was assumed that only pollutants released into a wind with a westerly component at Pt. Conception would later be detected in the Santa Barbara Channel. Between 9/13/80 and 10/11/80, surface winds with a westerly component were detected at Pt. Conception an average of 16 hours/day.

c) Since pollutants transported into the channel are efficiently mixed during the light nighttime winds and the morning wind reversal, the impact of pollutants released prior to the onset of the onshore winds was assumed to scale with the total mass of pollutants in the channel at the onset of the afternoon flow rather than the release rate at Pt. Conception. These pollutants were assumed to impact the shoreline uniformly as in the release from near platform Hondo (Test 4).

d) The impact onshore was calculated as the sum of the direct plume component, based on the Test 2 hourly-averaged tracer sampler data, and the uniformly mixed background component, based on the Test 4 hourly-averaged sampler data. The Test 4 hourly-averaged tracer data were shifted 3 hours to account for the observed transit time of the tracer from Pt. Conception to platform Hondo.

e) The carryover of pollutants at coastal sites was assumed negligible beyond one day subsequent to their release.

f) To replace missing data during the early morning hours of Test 4, the tracer concentrations were assumed constant throughout the night at the average of the 2100, 2200 and 2300 hour samples. This assumption was verified during other tracer experiments in which sampling continued through the night.

Employing these assumptions, the coastal impact of a continuous pollutant source at Pt. Conception is as shown in Figure 7. The continuous pollutant source would result in high pollutant concentrations during the afternoon, especially in Santa Barbara County (solid and dotted lines). The solid curve is based on the average tracer concentrations observed at El Capitan, Santa Barbara and Carpinteria and thus represents a regional average. The actual peak concentrations detected along the Santa Barbara County coastline could be much higher, as indicated by the dotted line, which is based on the peak tracer concentration detected among the three sites for each hour. As shown by the broken line, the impact of a continuous pollutant source at Pt. Conception is much smaller in Ventura County. This curve was based on the average tracer concentration detected during Tests 2 and 4 at Oxnard and Ventura during each

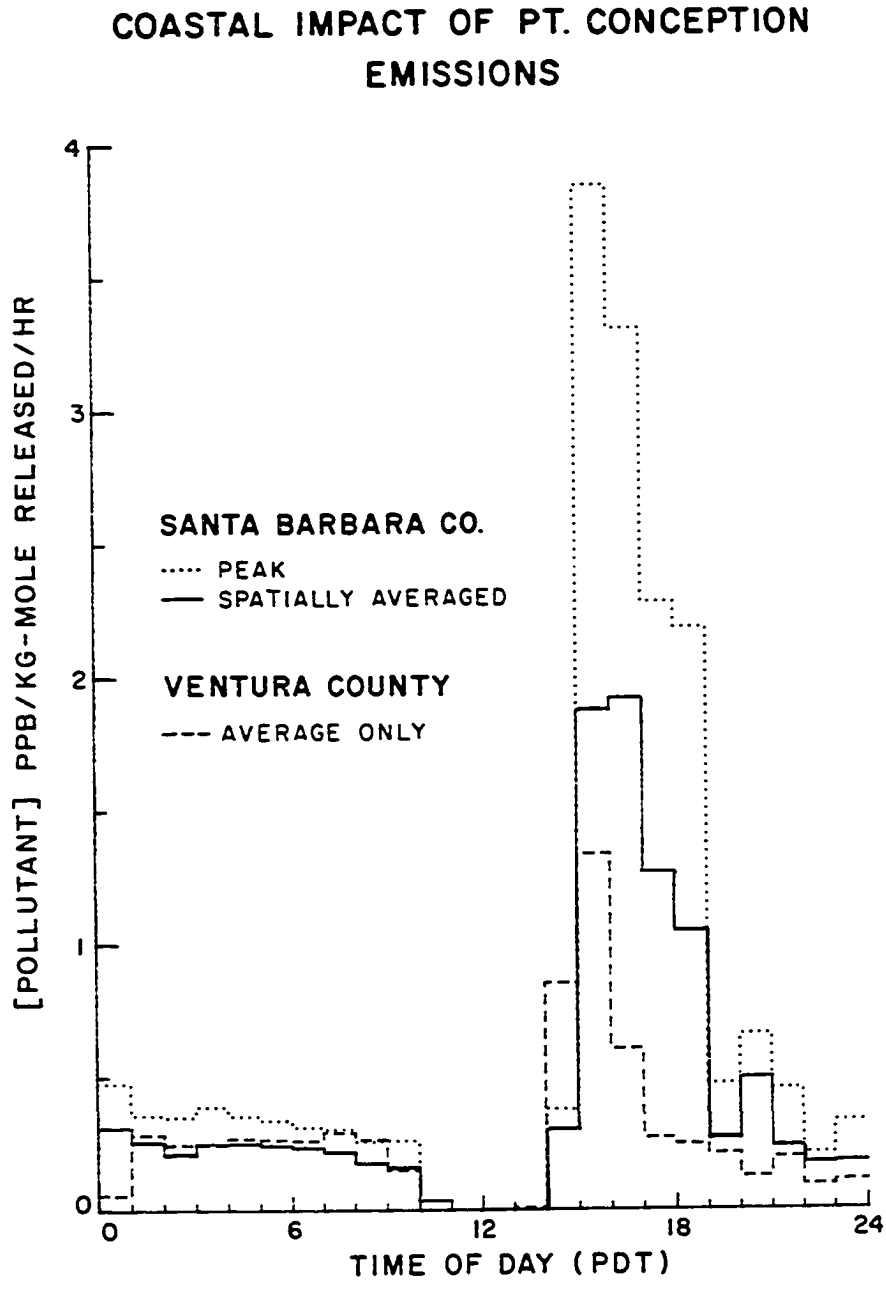

Figure 7 - Hourly-average coastal impact of a continuous pollutant source at Pt. Conception. Curves drawn from maximum tracer concentration observed among Santa Barbara, El Capitan Beach and Carpinteria (...), average tracer concentration observed at these sites (——), and the average of the Ventura and Oxnard tracer concentrations (----).

hour. The peak concentrations predicted during mid-afternoon are primarily due to the direct impact of pollutants released during the afternoon. The diluted pollutant released prior to the onset of the afternoon flow, however, contributes half or more of the essentially constant background levels detected throughout the night. Thus, after nightfall, the directly impacting plume does not appear significantly more concentrated than the initially reversed plume. The nighttime background concentrations are significant in that the integrated concentration, or dosage, between 1900 and 1200 the following day is 37% of the averaged total daily dosage in Santa Barbara County and almost 50% of the averaged total daily dosage in Ventura County. Clearly, the diurnal wind reversals and the resulting carryover of pollutants into at least the first day after their release must be considered in order to accurately assess the air quality implications of development of the Santa Barbara Channel.

SUMMARY AND CONCLUSIONS

The transport and dispersion of the tracer during each of the eight experiments was controlled by the diurnal variations in the surface winds. Over most of the coastal region, the average afternoon mixing height was about 150 m. Thus the tracer was generally limited to the surface layer, which is controlled by the diurnal variations, and to a large degree decoupled from the synoptic flow evident aloft. For this reason, the basic character of the tracer transport and dispersion was complex but generally reproducible from day to day. Two distinct types of tracer plumes were noted during the experiments. A release conducted during the afternoon on-shore flow caused a distinctly structured, essentially Gaussian type plume to impact the coastline. During these experiments, the dispersion of the tracer corresponded to that expected under stable atmospheric conditions. This was approximately consistent with the generally stable vertical atmospheric temperature gradients observed.

When the tracer release was conducted entirely within the nighttime off-shore flow, however, the wind reversal during the subsequent afternoon effectively mixed the tracer laterally and produced an essentially uniform on-shore impact. Widespread lateral mixing was also noted after the early evening transition from the sea breeze to the land breeze. Since the winds during a wind reversal are generally light, often below the measurable threshold velocity of about 0.5-1 m/s, it is difficult to predict the lateral dispersion of an airborne contaminant in such conditions. The concept of a trajectory has little or no meaning during a wind reversal in that the contaminant may no longer be embodied in a well-defined plume. Trajectory analysis should not be used to estimate the impact of a pollutant source after a wind reversal. Instead, a better estimate could be made by assuming that the pollutant was

spread laterally over some area at a uniform background concentration. Clearly, the background concentration is dependent upon the width of the lateral mixing during the wind reversal. In the Santa Barbara Channel, the pollutant can be spread uniformly over the entire Santa Barbara and Ventura County coastlines.

While the results of these tracer experiments are directly applicable only to the Santa Barbara Channel, it appears likely that the basic structure of the wind flow and resulting pollutant transport are repeated in other coastal environments. The synoptic scale flow is often masked by the local diurnal wind variations, thus the importance of the return of aged pollutants via wind reversals is probably significant in other coastal areas.

Acknowledgements

The authors wish to acknowledge the support and cooperation of Douglas Tubbs of the Ventura County Air Pollution Control District, John English and Donald Jones of the Santa Barbara County Air Pollution Control District, as well as Jack Suder and Charles Bennett of the California Air Resources Board. The authors would also like to acknowledge the cooperation of Dave Wilbur and the personnel of Aerovironment, Inc. during those tests conducted jointly. The work was performed under Ventura County Air Pollution Control District Contract #814.

References

Defant, F. (1951). Local Winds. Compendium of Meteorology, American Meteorological Society, Boston, Mass., 655-672.

Drivas, P. J. (1975). Investigation of atmospheric dispersion problems by means of a tracer technique. Ph.D. Thesis, California Institute of Technology, Pasadena, California 91125.

Lamb, B. K. (1978). Development and application of dual atmospheric tracer techniques for the characterization of pollutant transport and dispersion. Ph.D. Thesis, California Institute of Technology, Pasadena, California 91125.

Reible, D. D. and Shair, F. H. (1981). Tracer investigations of atmospheric transport into, within, and out of the Santa Barbara Channel and the coastal areas of Santa Barbara and Ventura Counties. Final report to Ventura Air Pollution Control District, Contract #814.

Schacher, G. E., Davidson, K. L., Leonard, C. A., Spiel, D. E. and Fairall, C. W. (1981). Offshore transport and diffusion in the Los Angeles Bight-I, NPS data summary. Report by Environmental Physics Group, Naval Postgraduate School to Bureau of Land Management, Los Angeles, California 90017

Turner, D. B. (1970): Workbook of Atmospheric Dispersion Estimates, Environmental Protection Agency. AP-26, 84 pp.

Chapter 13

A Two-Layer Model of the Atmosphere Indicating the Effects of Mixing between the Surface Layer and the Air Aloft

by

D.D. Reible, F.H. Shair and R. Aris

(Submitted to Atmospheric Environment)

Abstract

A two-layer air pollution model is developed for the case when inter-layer mixing is continuous, but slower than intra-layer vertical mixing. The model was designed to examine the implications of inter-layer transport for ground-level impacts. The model equations, consisting of two coupled partial differential equations, are solved numerically by the method of characteristics. In the case of first order chemical reactions, the zero and first order moments are computed in order to determine the locations of the centroids of pollutant mass.

The model indicated that a pulse of pollutants emitted at ground level can result in bifurcation of a pollutant plume due to the wind directional shear between the two atmospheric layers. The residual concentrations due to the transport between layers can move upwind, downwind or remain stationary with respect to the ground level winds, depending on the speed and orientation of the winds aloft. Several specific cases are described, and, in each case, the behavior of the residual plume would not be expected from the surface layer winds that are normally used to predict the transport and dispersion of pollutants. It appears that the characteristic exchange rate between the air aloft and the surface mixing layer is large enough that the winds aloft must be considered when describing long range transport or the multi-day impacts of a pollutant.

INTRODUCTION

In recent years it has become increasingly clear that the measurable impact of an air pollutant often extends into days subsequent to its emission or formation. This problem was first identified with respect to the long range transport of pollutants, such as the transport of sulfur compounds from western Europe into Scandinavia (Swedish Preparatory Committee for the U.N. Conference on the Human Environment, 1971), and the transport of ozone across the northeastern United States (Wolff, et al., 1977). The long term impact of a pollutant has also been linked, however, to episodic behavior in a single air basin (i.e. the buildup of abnormally high pollutant concentrations over a period of days). Johnson and Singh (1976) and Blumenthal, et al. (1978) described ozone-rich layers aloft that can be entrained into the surface mixing layer, thus providing a background of aged pollutants that supplement those emitted or produced on any given day. The development of ozone-rich elevated layers was linked to the diurnal variation in the surface layer mixing height. During the day, surface heating effectively mixes pollutants vertically throughout a relatively deep layer. At night, a much shallower mixing depth results in a polluted layer aloft that can be incorporated into the mixing layer on the subsequent afternoon. Indications of the multi-day impact of pollutants can also be found in statistical prediction models; for example, Aron and Aron (1978a and b) developed such models for carbon monoxide and ozone in the Los Angeles Basin. Aron and Aron found that the previous

day's pollutant concentration was a significant indicator of the levels observed on a given day. Along the same lines, Dabberdt and Singh (1977) found that short-term control strategies may not be a very effective means of alleviating episodic ozone levels in the Los Angeles Basin. A significant portion of the pollutant burden on a given episodic day may be due to the background levels remaining from previous days. As stated in their paper, "The potential effect of witholding new pollutants is therefore limited by the residence time of old ones". Pollutant carryover into days subsequent to their release or formation can generally be attributable to one of two mechanisms, 1) limited net transport in the surface layer, such as by diurnal wind reversals that continually "recycle" air over source and receptor areas, and 2)dynamic interactions of the surface layer with the air aloft. The latter mechanism is potentially important for both the long range transport of pollutants and the carryover of pollutants within a given area, and is the subject of this work.

Although carryover of pollutants into days subsequent to their release or initial formation has been recognized, the development of an accurate multi-day air quality model of an air basin has proven quite difficult. Benarie (1980) summarized the difficulities associated with such a simulation, perhaps the most serious of which are the impossibility of describing motion on a scale smaller than the grid size of the model and the difficulties in describing even the macroscopic motion of a large air parcel for many days. An air quality model might be composed, for example, of a number of grid cells of uniform height. Generally

no attempt is made to incorporate the interaction of these grid cells with the air above, beyond simple dilution as the cell height increases. In coastal or mountain-valley environments, the problems are compounded by highly variable local winds. These local winds often involve diurnal wind reversals in the surface layer, during which the mean speed and direction of the air motion is poorly characterized.

While accurate numerical simulation of the multi-day behavior of pollutants in the atmosphere is generally lacking, ultra-sensitive tracer techniques have allowed the basic characteristics of pollutant carryover to be observed. These experiments typically employ sulfur hexafluoride, which can be detected by electron capture gas chromatography at concentrations as low as 1-10 parts-per-trillion (PPT). The authors have conducted a number of atmospheric tracer studies, primarily in California, which have directly exhibited the potential for pollutant carryover into days subsequent to its release or formation within a single air basin. In the San Joaquin Valley of California, tracer was transported from the northern end of the valley to its southern end, a distance of about 400 km, within 24 hours, apparently due to the action of an accelerated layer of air above the stable nighttime surface layer (Reible, et al.,1982). In the Los Angeles Basin, tracer released during the night from a power plant plume was transported above the mixing layer and out over the sea surface (Shair, et al., 1982). Since the mixing height was higher over the sea, essentially all of the tracer was transported to the surface and back across the shoreline during

the subsequent afternoon sea breeze. Similarly, tracer released from a height of 30 m above ground level during a nighttime drainage flow in the northern California coastal mountains was transported up into the synoptic winds above the drainage flow and then back through the stable drainage layer to ground level (Reible, et al., 1981). Significant wind directional shear was noted at the interface between the two flows, indicating the degree of decoupling between the air aloft and the shallow surface layer. In an atmosphere composed of two or more layers of different stability, the interface between the two layers is commonly considered a barrier to significant transport (although the location of that interface may change). It was estimated, however, that the tracer was transported through the interface between the two flows (and the stable layer below) at a mean vertical velocity of about 2 cm/s. This estimate was based upon the transit time to the location of maximum ground-level impact and the 30 m vertical distance. While the 2 cm/s velocity indicates much slower vertical mixing than would be expected in a daytime free convection layer (vertical speeds in excess of 10 cm/s), it indicates that significant transport can occur through the interface between the two flow regimes. During this particular study, an estimated 80% of the released tracer was transported through this zone. The remaining 20% of the released tracer was transported in a separate (i.e. bifurcated) plume by the surface drainage layer.

Perhaps the clearest example of the potential for significant interaction between the surface layer and the air aloft was

observed in the Sacramento Valley of California (Reible and Shair, 1982a). An experiment was conducted during which a tracer was released into the westerly winds directed upslope from the valley towards the Sierra Nevada Mountains. As indicated in Figure 1, however, airplane traverses on the day following the release detected tracer concentrations as high as 50 PPT (180 PPT/gr-mole released/hr) betwen 450 and 700 m altitude. The inset figure indicates that essentially none of the tracer was observed either above or below this layer. The inset figure also indicates that elevated ozone concentrations were observed in this layer, presumably due to transport from pollutant sources in and near Sacramento (i.e. from the same source area as the tracer). The tracer concentration levels and the area of the impacted zone suggested that most of the released tracer was observed within the elevated layer. Because the maximum depth of mixing exceeded 1000 m, the contaminated air aloft was probably transported to ground-level during the afternoon. The ground-level impacts would have been difficult to correlate with a source area, based only upon surface wind and tracer data.

Interaction between a convectively mixed layer and a more stable layer aloft has also been the subject of laboratory scale experiments. These experiments have generally been designed to evaluate the rate at which a stable region is entrained via thermal overshoot from the convectively mixed region. Deardorff, et al. (1980), for example, found that a convectively mixed region entrained a neutrally stable layer at a rate approximately equal to 1/4 of the velocity scale within the mixed region. More stably

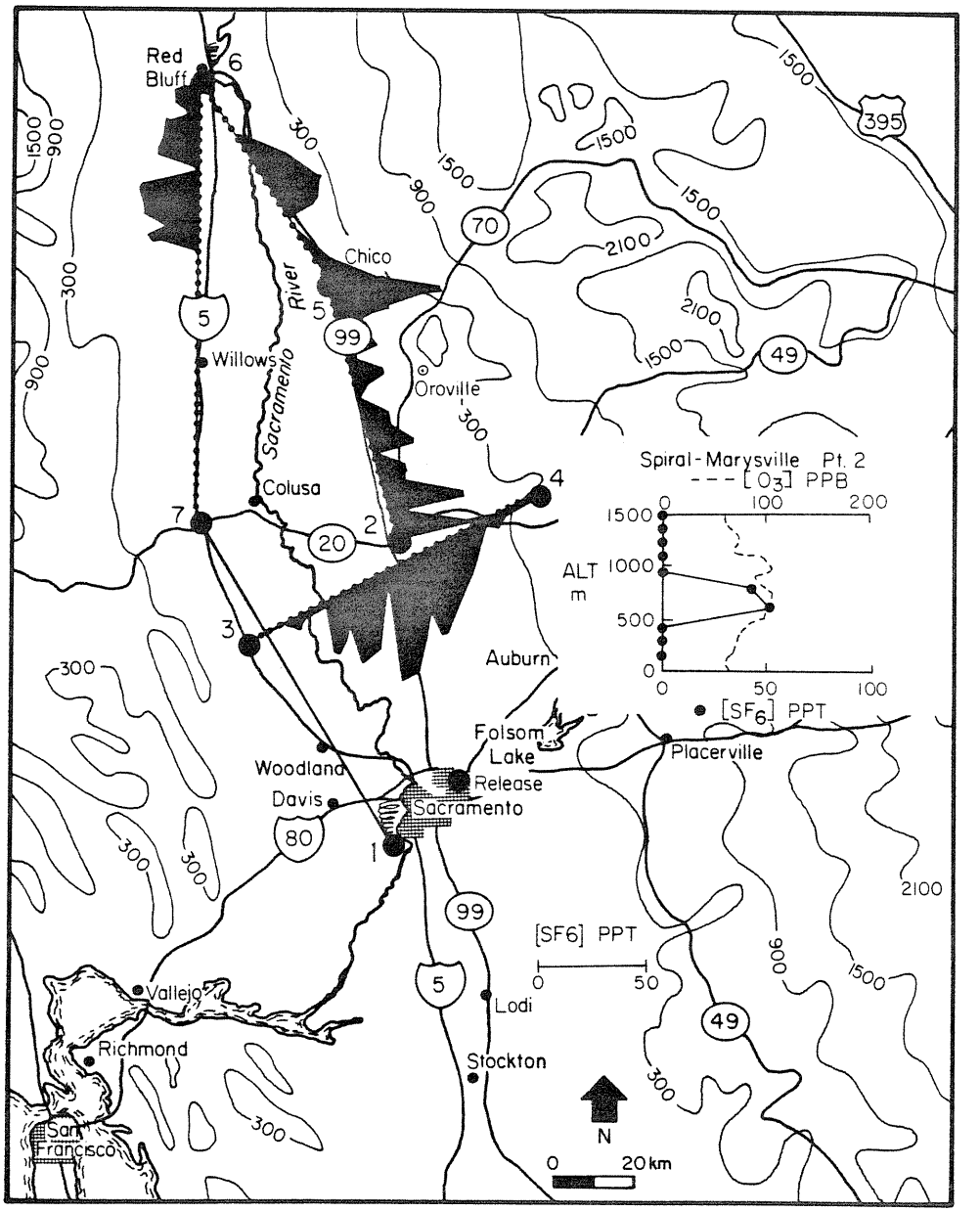

Figure 1 - Map of Sacramento Valley of northern California indicating tracer concentrations observed aloft on afternoon of day following the tracer release.

stratified layers "aloft" resulted in much slower entrainment velocities; these velocities were approximately proportional to the inverse of an overall Richardson's number. Deardorff and coworkers also found that the thickness of the entrainment layer, the layer influenced but not yet incorporated into the convectively mixed layer, was typically 20-40% of the mixed layer height. These data indicate that a relatively well-defined layer of substantial thickness may typically lie above the surface layer of the atmosphere.

In summary, pollutants can apparently be transported through the interface separating the air aloft and the surface layer by,

1) slow and continuous transport across the relatively stagnant interface between the layers (as described in Reible, et al, 1981).

2) generally more rapid transport due to the diurnal growth and shrinkage of the surface layer (as in Blumenthal, et al., 1978)

3) transport due to spatial variations in the mixing height, such as near the land-sea, or mountain-valley interface (as in Reible and Shair, 1982a and Shair, et al., 1982)

While the atmospheric tracer data as well as the results of small-scale laboratory experiments indicate that significant interaction between the surface layer and the air aloft can occur, the implications of such interaction on ground-level air quality is not clear. In order to indicate the importance of this transport, a two-dimensional mathematical model of a layered

atmosphere was developed. For simplicity and clarity, diffusional processes were neglected and the interaction between the layers was assumed proportional to the concentration gradient across them. Because of these and other simplifications, the model was not necessarily intended to quantitatively describe the behavior of pollutants in a layered atmosphere, but instead designed to indicate the basic structure and implications of such behavior. More specifically, the primary objective of the model was to compare the magnitude of the impact of a pollutant source on various locations in such an atmosphere. The model was intended to describe the transport of pollutants in an atmosphere such as that indicated in Figure 2. The figure qualitatively depicts the daytime structure of the atmosphere near a land-sea interface. Emissions from the pollutant source are transported inland due to the surface layer sea breeze. The arrows at the base of the temperature inversion indicate the possibility of vertical transport either through the stable layer or by vertical movement of the stable layer. Since the winds above the mixing layer are driven by synoptic scale pressure gradients, and are, in general, not coupled to the surface winds, these winds are shown as being directed offshore.

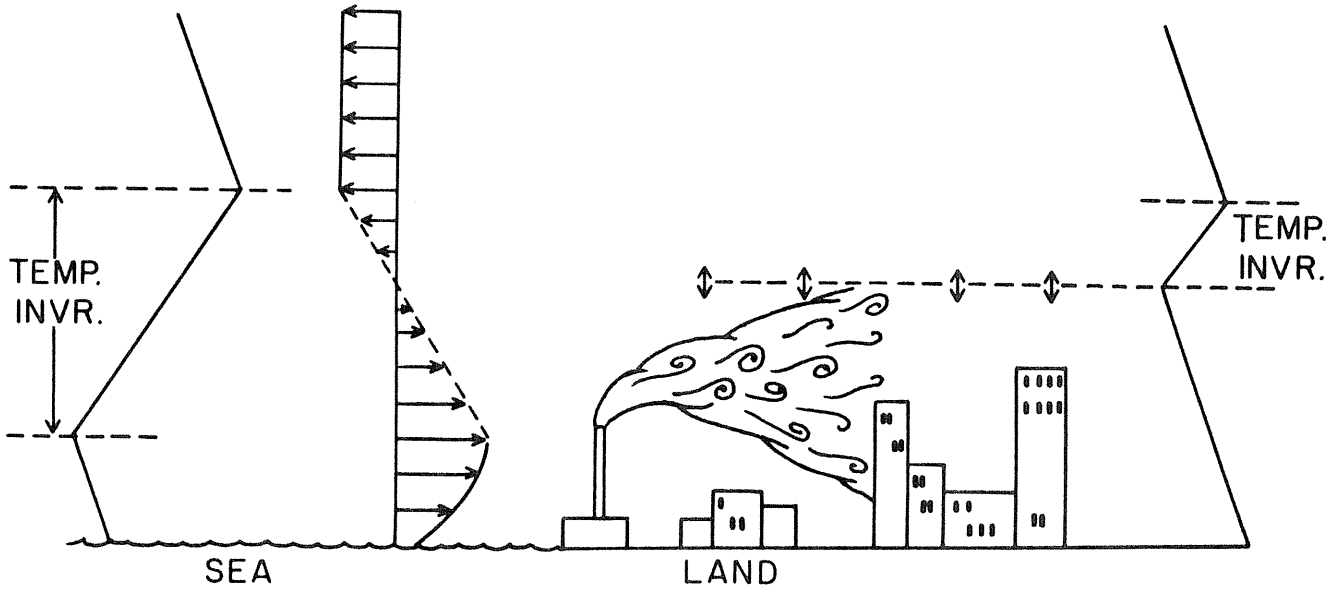

Figure 2: Hypothetical atmospheric temperature and velocity profiles near a land-sea interface, indicating physical application of model.

DESCRIPTION OF THE MODEL AND ITS SOLUTION

Consider two atmospheric layers as shown in Figure 3. The bottom layer extends from ground level to a vertical height, L_B, in the z-direction and has a uniform velocity, U, in the positive x-direction. The concentrations of constituents (e.g. pollutants) within this layer may change through (1) surface deposition (characterized by a surface deposition velocity, α_1), (2) reaction within the layer (characterized by a rate constant k_B), and (3) inter-layer exchange (characterized by an exchange velocity, α_2). The layer above, which extends in the vertical direction from L_B to (L_A+L_B), has a uniform velocity, V. The velocity in the upper layer is also positive if it is oriented in the positve x-direction. The concentration of constituents within the upper layer may change as a result of (1) inter-layer exchange, (2) reactions within the layer (characterized by a rate constant, k_A), and (3) loss to the upper atmosphere (characterized by an exchange velocity, α_3).

We shall consider situations in which the characteristic times required for vertical mixing within each layer are short compared to that associated with the rate of exchange. This assumption is clearly valid for a convectively mixed layer capped by stable air, but may be less valid for vertical transport in a stable layer. Thus, at any position, x, the concentrations within each layer are taken as uniform in the z-direction. We shall also neglect the effects of molecular and turbulent diffusion in either the x or y-directions. The exclusion of diffusional processes

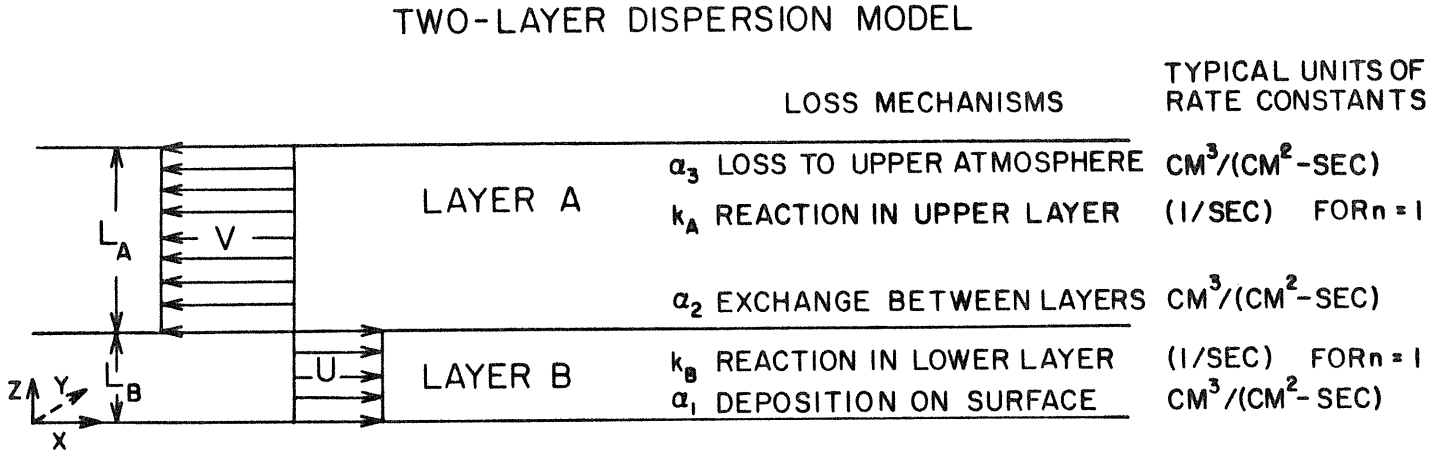

$$\text{LAYER A:}\quad \frac{\partial C_A}{\partial t} + V\frac{\partial C_A}{\partial X} = -\frac{\alpha_3}{L_A}C_A - k_A C_A^n - \frac{\alpha_2}{L_A}(C_A - C_B)$$

$$\text{LAYER B:}\quad \frac{\partial C_B}{\partial t} + U\frac{\partial C_B}{\partial X} = -\frac{\alpha_1}{L_B}C_B - k_B C_B^n - \frac{\alpha_2}{L_B}(C_B - C_A)$$

Figure 3: The conceptual and mathematical model of the transport of pollutants in a layered atmosphere.

does not alter the results of the model for the purposes of this work. The assumption of negligible lateral and axial diffusion is only strictly applicable, however, to a continuous, line source in a strong, uniform wind field. The assumption may also be accurate after wind reversals, however, in that pollutants tend to become well-mixed laterally in the light and variable wind conditions that are observed during wind reversals (Reible and Shair, 1982b). The concentration of constituents in each layer is described by the coupled, constant coefficient partial differential equations included in Figure 3. For convenience, we shall use the corrsponding non-dimensional equations for a first order reaction (i.e. n=1),

$$\frac{\partial \Theta_A}{\partial \tau} + \beta \frac{\partial \Theta_A}{\partial \eta} + A\Theta_A = B\Theta_B \tag{1}$$

and,

$$\frac{\partial \Theta_B}{\partial \tau} + \frac{\partial \Theta_B}{\partial \eta} + D\Theta_B = \Theta_A \tag{2}$$

where,

$$\tau = \frac{\alpha_2 t}{L_B} , \quad \eta = \frac{\alpha_2 X}{U L_B} , \quad \Theta_i = \frac{C_i}{C_{REF}} , \quad \beta = \frac{V}{U} \tag{3}$$

$$A = \frac{L_B}{L_A}\left(1 + \frac{\alpha_3}{\alpha_2}\right) + \frac{k_A L_B}{\alpha_2} , \quad B = \frac{L_B}{L_A} , \quad D = \left(1 + \frac{\alpha_1}{\alpha_2}\right) + \frac{k_B L_B}{\alpha_2} \tag{4}$$

The dimensionless time coordinate, τ, is the characteristic time required for an air exchange in a layer (i.e. the time required

for concentrations to decay to 1/e of their initial levels). The dimensionless distance coordinate, η, is the distance that an air parcel moves due to the winds in the lower level during this time. The appropriate reference concentration, C_{REF} is dependent upon the method of source introduction.

Given appropriate initial and boundary conditions, and if the reactions in each layer are first or zeroth order ($n<=1$), the system of equations can be solved by the method of the Laplace Transform. Inversion of the resulting transformed solution is difficult, however, and the inversion integrals are unlikely to be tabulated. The rigor of the calculation is inconsistent with the degree of approximation employed in the model. The authors currently plan to explore an analytical solution to a more complete model of transport and dispersion in a layered atmosphere (e.g. one that incorporates diffusional processes). For the current model, however, a much simpler means of solution is available through recognition of the hyperbolic nature of the equations. The solution to such an system is propagated along the characteristics of the equations. In Layer A, note that along the curve defined by,

$$\frac{d\eta}{d\tau} = \beta \left(= \frac{V}{U}\right) \tag{5}$$

the left hand side of Equation (1) reduces to a total derivative. Equation (2) is reduced to an ordinary differential equation in a similar manner. Thus the model can be reduced to the following set of equations, valid along the indicated characteristic curves,

$$\frac{d\Theta_A}{d\tau} = - A\Theta_A + B\Theta_B \quad \text{along } \frac{d\eta}{d\tau} = \beta \tag{6}$$

and,

$$\frac{d\Theta_B}{d\tau} = - D\Theta_B + \Theta_A \quad \text{along } \frac{d\eta}{d\tau} = 1 \tag{7}$$

A numerical solution to the system of equations can be constructed by first specifying an intial condition on a finite grid of points. Characteristic curves drawn from adjacent points intersect at a unique value of η and τ, as shown in Figure 4. The value of the dependent variables, the concentrations in each layer, can be determined at the intersection of the characteristics by evaluation of the appropriate ordinary differential equation. The following finite difference approximation to the ordinary differential equations was found to be convenient,

$$(\Theta_A)_{i+1} = \left[- A(\Theta_A)_i + B(\Theta_B)_i\right] \Delta\tau + (\Theta_A)_i \tag{8}$$

and,

$$(\Theta_B)_{i+1} = \left[- D(\Theta_B)_i + (\Theta_A)_i\right] \Delta\tau + (\Theta_B)_i \tag{9}$$

Thus the concentrations at $\eta+\Delta\eta$ and $\tau+\Delta\tau$ can be determined with knowldge of the concentrations at τ for all η. Note that the equations are valid only along the characteristic curves. Thus,

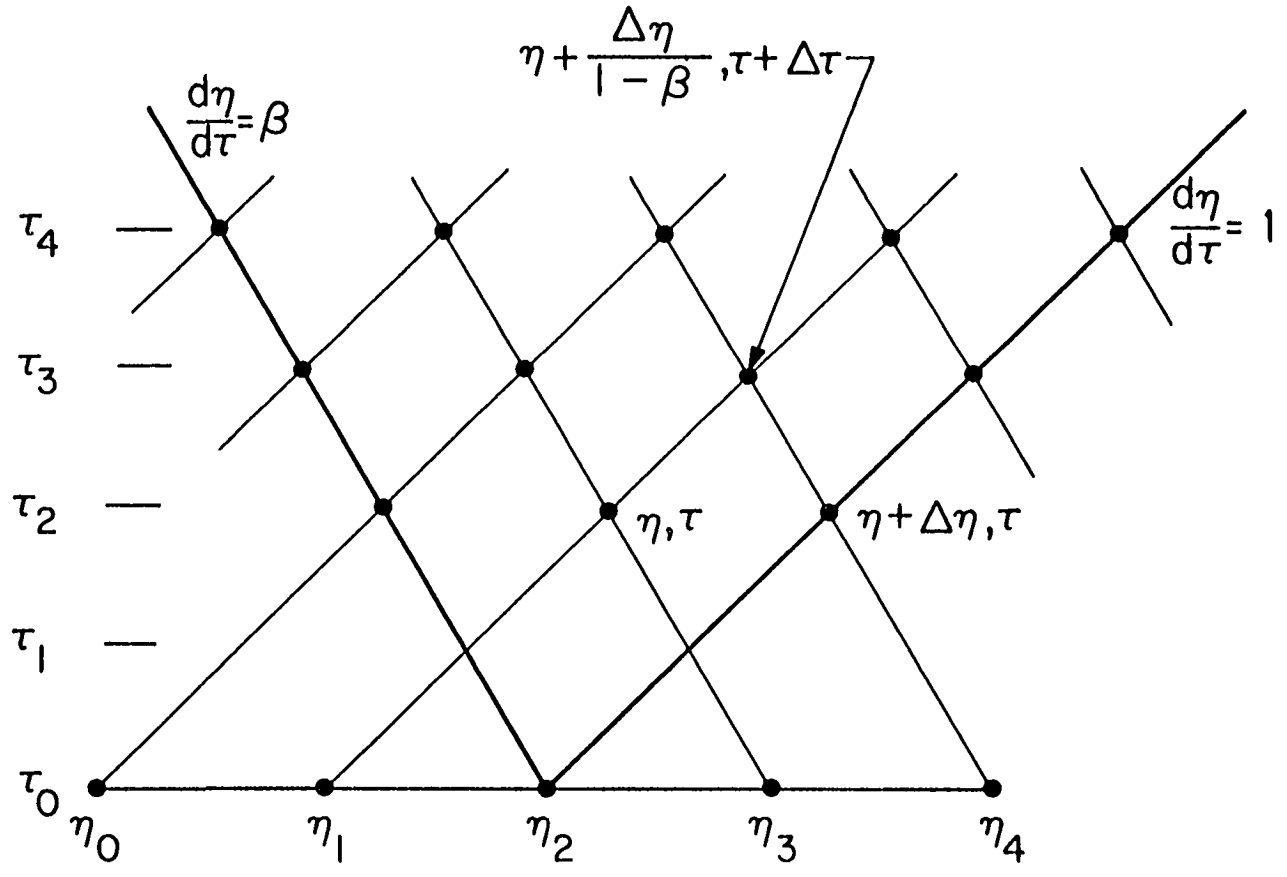

Figure 4 - Construction of solution via the method of characteristics.

for the example in Figure 4, the concentration in the lower layer at location $\eta+(\Delta\eta)/(1-\beta)$ and time $\tau+\Delta\tau$, is evaluated from the concentrations at η and τ, while the concentration in the upper layer is evaluated from the concentrations at $\eta+\Delta\eta$ and τ. The calculation proceeds in the same manner, with the concentrations at any location and time being dependent upon the concentrations at the two closest locations at the previous time step. This procedure is a relatively simple application of the method of characteristics (Stoker, 1957).

While much information can be gained from the numerical solution of the equations, an analytical approach allows easier generalization of the results. As described earlier, the development of a complete solution to the model equations is not warranted due to the degree of approximation employed in the model. The Method of Moments (Aris, 1956), however, can be used to probe the structure of the model for additional information. For this reason, integrals of the model equations were also evaluated for the special case of linear reaction terms and with an instantaneous pollutant source approximated by a delta function. Integration of the model equations with respect to the dimensionless distance coordinate gives,

$$\frac{d\gamma_A}{d\tau} + A\gamma_A = B\gamma_B \tag{10}$$

and,

$$\frac{d\gamma_B}{d\tau} + D\gamma_B = \gamma_A \tag{11}$$

where,

$$\gamma_i = \int_{-\infty}^{\infty} \theta_i \, d\eta \tag{12}$$

These equations can be solved, with appropriate intitial conditions, for the zeroth order moment of the concentration distribution. The zeroth order moment describes the distribution of mass between the two layers. Integrating the equations again with respect to the distance coordinate allows calculation of the first order moment of the concentration distribution:

$$\frac{d\delta_A}{d\tau} + A\delta_A - \beta\gamma_A = B\delta_B \tag{13}$$

and,

$$\frac{d\delta_B}{d\tau} + D\delta_B - \gamma_B = \delta_A \tag{14}$$

where,

$$\delta_i = \int_{-\infty}^{\infty} \eta\theta_i \, d\eta \tag{15}$$

The first order moment, when normalized with respect to the total mass in the layer (the zeroth moment), represents the center of mass of the pollutant in each layer. The first moment thus determines the location of the maximum impact of a pollutant source at any time, as long as the concentration distribution is unimodal.

PRESENTATION AND DISCUSSION OF RESULTS

Using the methods presented in the last section, the model was evaluated for an essentially instantaneous pollutant source in either the top or the bottom layer and for various combinations of the winds in each layer. These cases were chosen because they clearly indicate the behavior of a pollutant whose transport can be described by the model. Although the equations were presented with allowance for pollutant deposition, loss to the upper atmosphere, and reaction in each layer, we shall initially consider a persistent pollutant, for which these loss terms are identically zero. An instantaneous pollutant source was approximated numerically by introducing a source of strength, C0, over a zone of width 0.1 η, centered about η=0 and for a time equal 0.1τ.

Case 1 - Lower layer instantaneous source with β=-1 (V=-U)

If the winds in each layer are of equal magnitude and direction, a pollutant simply becomes mixed over a larger height than would be the case if the mixing between layers were neglected. A more interesting case occurs if the upper level winds are oriented in the opposite direction from the lower level winds. Because the surface layer is often essentially decoupled from the air aloft in mountain-valley or coastal environments, such wind conditions occur quite often. The 1200 PST summertime (Jun-Aug) winds at Los Angeles, for example, are predominantly from the southwest at 300 m above the surface while at 915 m above

the surface the most common wind direction is southeasterly (Lorenzen, 1979). Application of the method of characteristics to the case of $\beta=-1$ gives the concentration profiles indicated in Figure 5. The concentrations in the figure are shown as a fraction of the concentration at the source. The profiles are shown beginning at 3τ and ending at 9τ. The concentration profiles at each time are shifted on the concentration axis for clarity (i.e. the observed concentrations do not increase with time). Note the exponentially decaying primary peak. This peak moves downwind at the speed of the lower layer, losing concentration by exchange with the upper layer. It is this plume that is the subject of most models of dispersion in the atmosphere, e.g. the Gaussian plume model (Turner, 1970). Because the purpose of this model is to illustrate the long term impact of a pollutant that is allowed to interact with the upper atmosphere, however, the most interesting attribute of the concentration profile is the development of a secondary peak, or residual, due to the interaction between the two layers. Whereas intitially the secondary maximum is quite small compared to the primary plume, the exponential decay of the primary plume rapidly increases the relative importance of the former peak. After even 3τ, the bulk of the material released lies within the "residual" plume. After 5τ, the residual concentrations exceed those observed in the primary peak. Perhaps the most interesting characteristic of the residual, however, is that the location of the maximum concentration always occurs at a single location, in this case, a distance η, downwind of the source. Thus, after a sufficient

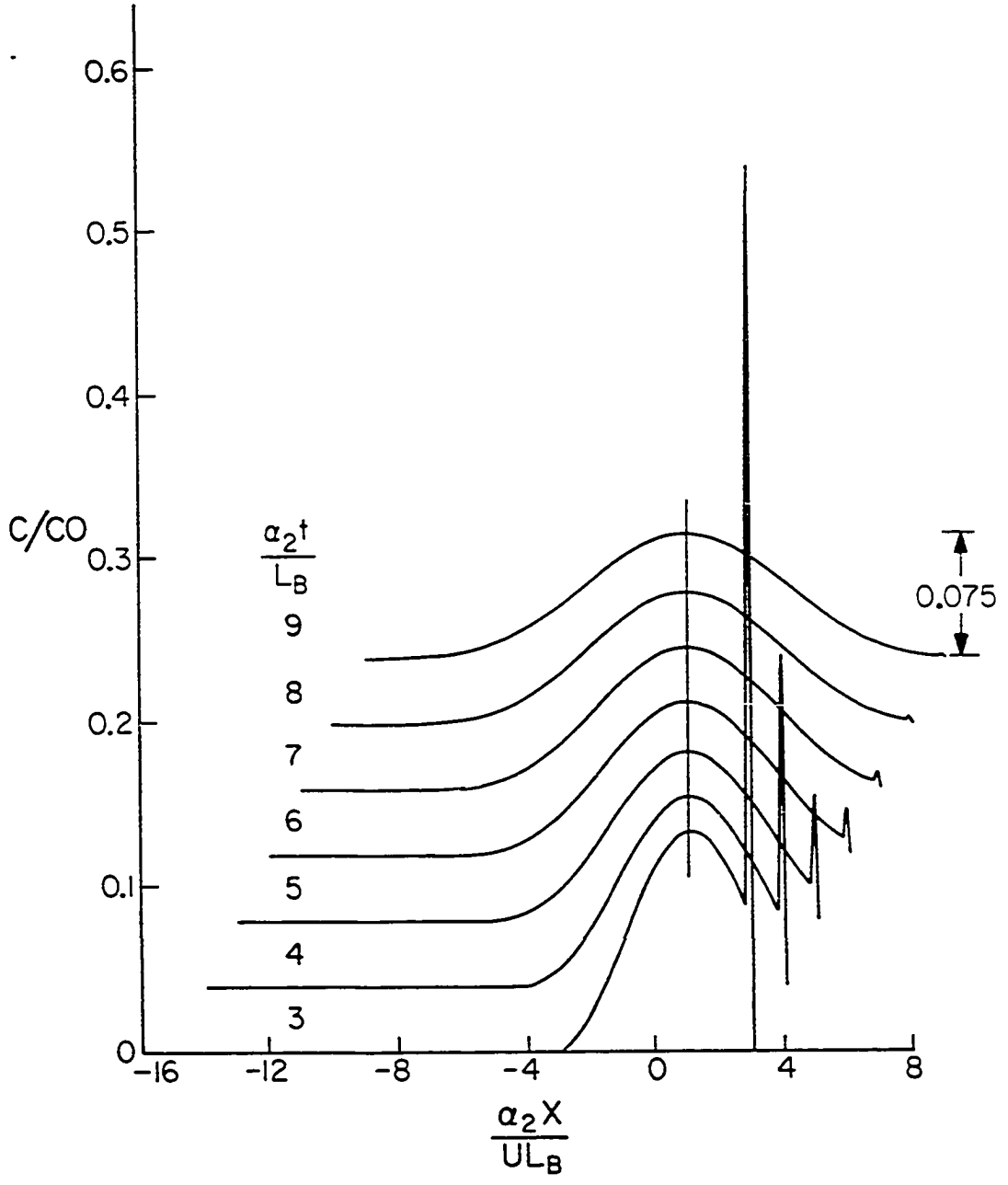

Figure 5 - Ground-level impact predicted by the model for a pulse source in the lower layer, β=-1 (V=-U) and identical layers with no reactions or losses at the boundaries of the atmosphere.

period of time, the maximum impact of an instantaneous pollutant source is at a single location and does not move with the winds observed at ground level.

Restating the results in terms of dimensional quantities rather than the non-dimensional coordinate system is difficult due to the simplifications of the model. In an experiment in the northern California coastal mountains, however, Reible, et al. (1981) found that an atmospheric tracer was transported from the air aloft through a stable layer to ground level. The average velocity of this transport was estimated to be about 2 cm/s. The entrainment velocity of the air aloft is likely to be much higher during the day when a convectively mixed layer erodes the typically more stable air aloft. In the Los Angeles Basin (at Los Angeles Airport), the average depth of the surface mixing layer at 1200 PST between 1965 and 1979 was 460 m (Lorenzen, 1979). Assuming that 2 cm/s is a reasonable value for the average vertical velocity through the interface between the atmospheric layers, the characteristic exchange rate between the layers is about 6.3 hours. Thus 1 day corresponds to about 4τ in dimensionless units for the Los Angeles Basin. While this is little more than an order of magnitude estimate, it again indicates that the interaction between the layers can be significant over the time scales important to pollutant transport and dispersion.

Case 2 - Lower layer instantaneous source with $\beta=-2$ ($V=-2U$)

The concentration profiles downwind of the essentially instantaneous source in such an atmosphere appear in Figure 6. As before, the source results in a primary maxima, which represents the direct downwind impact of the pollutant source, and a residual peak, which represents material transported into the upper layer and back. This and the previous results differ, however, in that the location of the maximum residual concentration is moving to the left, or upwind with respect to the lower layer. Thus, after a sufficient period of time, 3 to 5τ, the maximum impact of the pollutant is upwind of the source with respect to the ground level winds. By time, 9τ, the location of maximum impact is about 4η upwind of the source. For the case of the upper level winds oriented in the same direction as those in the lower layer, but at twice their velocity, a similar concentration profile results. In that case, however, the "residual" concentrations precede the primary, or directly impacting plume. The separation between the directly impacting plume and the residual can be quite large. If an average wind speed of 2 mps and a characteristic exchange time of about 6 hours is assumed (i.e the Los Angeles Basin example referred to earlier), each dimensionless distance unit, η, corresponds to about 40 km. Note, however, that wind reversals in the surface layer would reduce the horizontal extent of the pollutant plume.

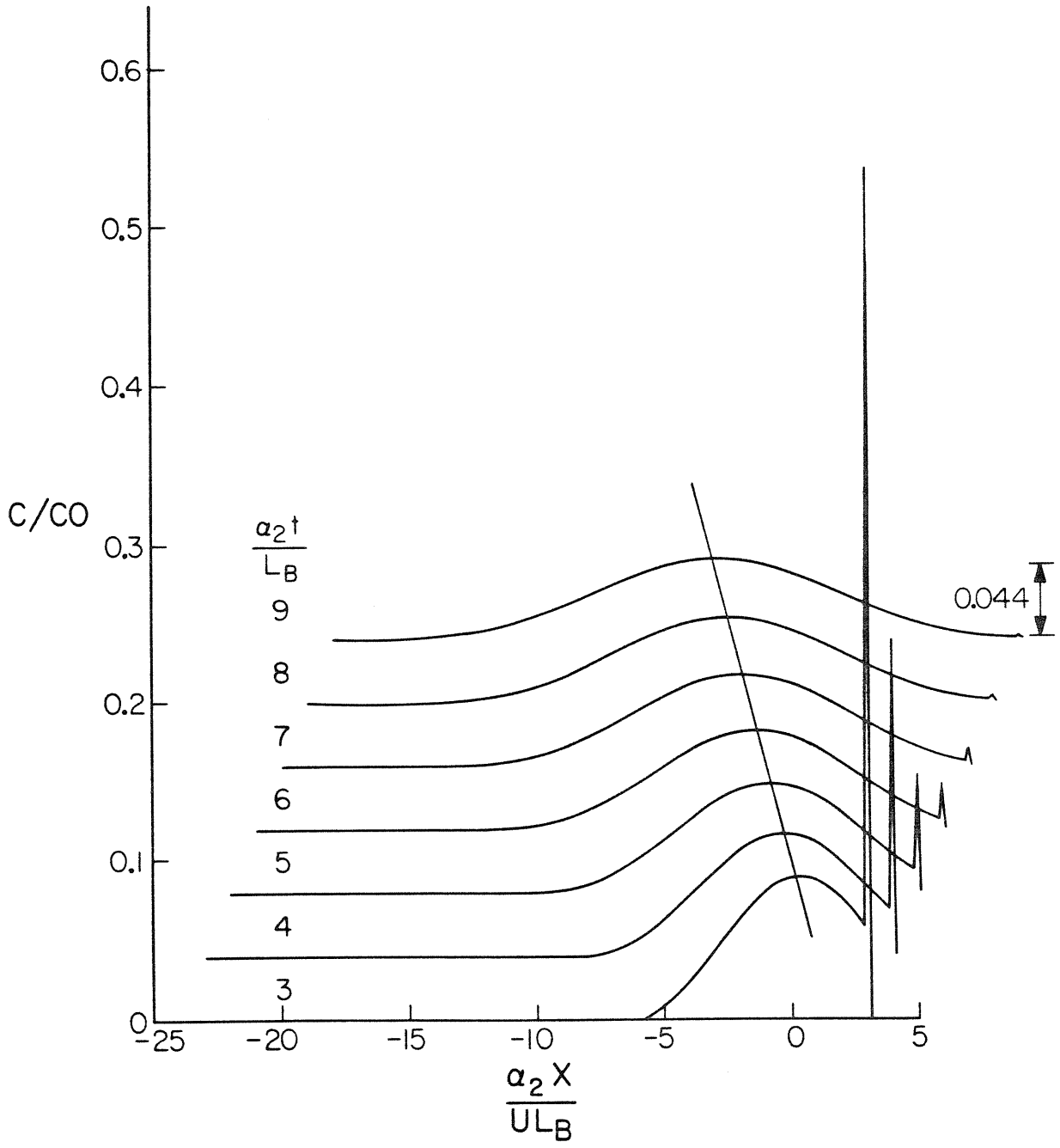

Figure 6 - Ground-level impact predicted by the model for a pulse source in the lower layer, β=-2 (V=-2U) and identical layers with no reactions or losses at the boundaries of the atmosphere.

Case 3 - Upper layer instantaneous source with $\beta=-1$ ($V=-U$)

Because of the symmetry of the model, this case is essentially the same as case 1. Here, however, the impact on the lower layer due to a source in the upper layer will be examined. This case corresponds to an elevated source, such as a buoyant power plant plume. The resulting concentration profile in the lower level is shown in Figure 7. The most interesting observation to be made about this case is that the maximum ground level impact is directly below the source at all times. Thus, if buoyant gases from a power plant stack are carried into an elevated layer in which the winds are of equal magnitude but directed opposite to those in the surface layer, the highest ground level concentrations are observed at the pollutant source, due to transport through the top of the mixing layer. Thus the development of a tall stack can effectively reduce the magnitude of the ground level impact but it may not be an effective means of shifting the location of that impact.

Application of the Method of Moments

To ensure that the results reported above were not numerical artifacts, and to gain a clearer understanding of the structure of the solution, the Method of Moments (Aris, 1956) was applied to the model equations. The equations from which the zeroth and first order moments of the concentration distribution can be evaluated have been given previously. If we consider a source

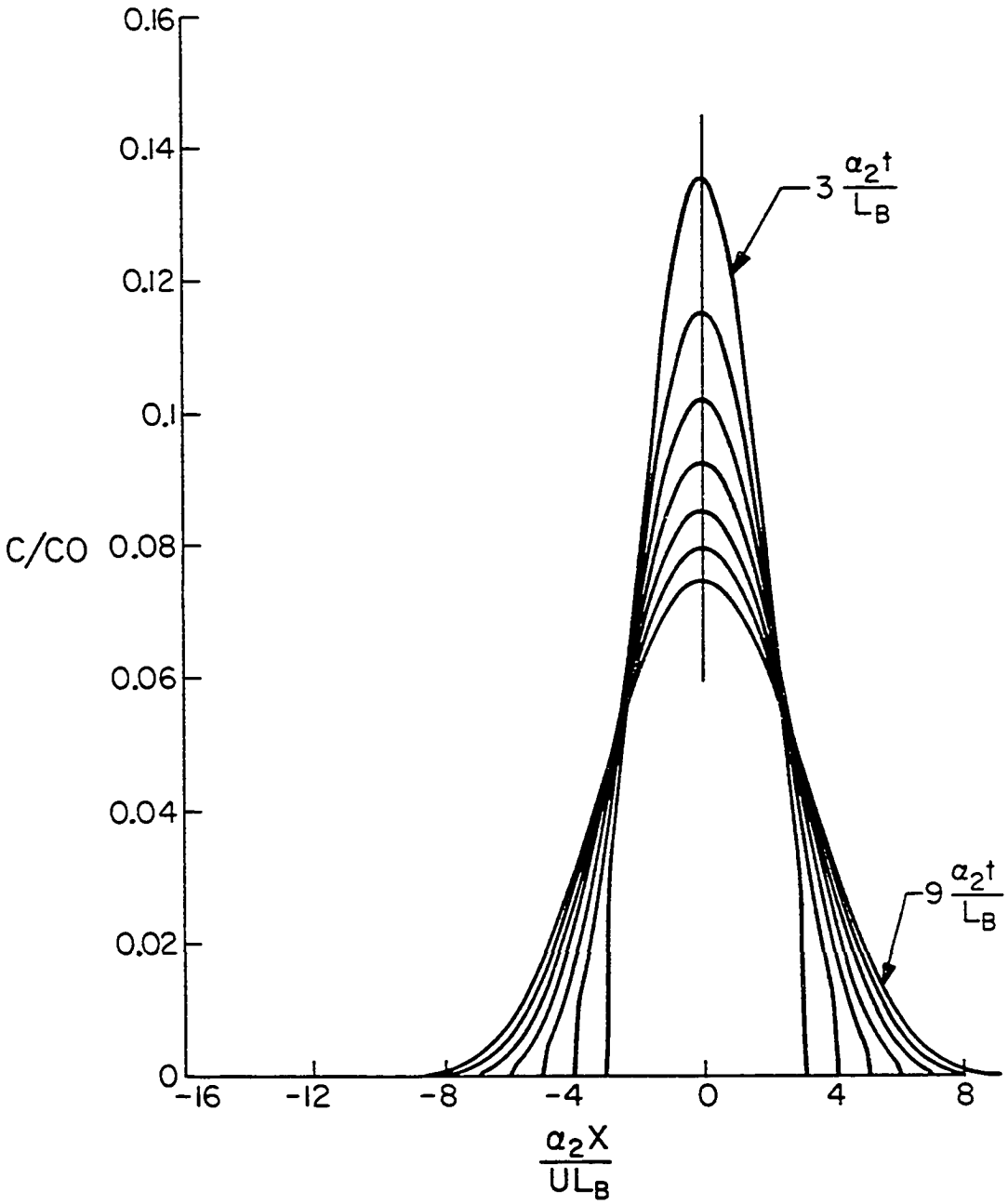

Figure 7 - Ground-level impact predicted by the model for a pulse source in the upper layer, β=-1 (V=-U) and identical layers with no reactions or losses at the boundaries of the atmosphere.

strength of unit mass in the lower layer at time zero, the applicable initial conditions are,

$$\left.\begin{aligned} \gamma_A &= 0 \\ \gamma_B &= 1 \end{aligned}\right\} \tau = 0 \qquad (16)$$

This initial condition allow solution of Equations (10) and (11), resulting in,

$$\gamma_A = \frac{B}{\lambda_2 - \lambda_1}\left(e^{\lambda_2 \tau} - e^{\lambda_1 \tau}\right) \qquad (17)$$

and,

$$\gamma_B = \frac{1}{\lambda_2 - \lambda_1}\left[(A + \lambda_2)e^{\lambda_2 \tau} - (A + \lambda_1)e^{\lambda_1 \tau}\right] \qquad (18)$$

where,

$$\lambda_1 = \frac{-(A + D) + \sqrt{(A + D)^2 - 4(AD - B)}}{2} \qquad (19)$$

and

$$\lambda_2 = \frac{-(A + D) - \sqrt{(A + D)^2 - 4(AD - B)}}{2} \qquad (20)$$

For short times, the zeroth moment of the concentration distribution in the upper layer (γ_A) indicates that the mass rate of transfer across the interface is directly proportional to time. As expected, the long time behavior of the solution indicates

that, for identical layers ($L_A=L_B$, $\alpha_1=\alpha_3$, $k_A=k_B$, or A=D, B=1, $\lambda_1=-(A-1)$, $\lambda_2=-(A+1)$), the mass becomes evenly distributed between the two layers.

The first moments of the concentration distributions, which are related to the center of mass of the pollutant, can be evaluated from Equations (13) and (14). Assuming that the initial distribution of mass is symmetric about the origin, the appropriate initial condition is,

$$\left.\begin{aligned}\delta_A &= 0\\ \delta_B &= 0\end{aligned}\right\} \quad \tau = 0 \tag{21}$$

As indicated previously, the center of mass, which is also the location of the maximum concentrations for a unimodal distribution, is given by,

$$\mu_i = \frac{\delta_i}{\gamma_i} \tag{22}$$

Solving for δ_A and dividing by γ_A gives,

$$\mu_A = -\frac{\left[(\lambda_1+\lambda_2+2A) + \beta(\lambda_1+\lambda_2+2D)\right]}{(\lambda_2-\lambda_1)^2} - \frac{\tau e^{\lambda_1\tau}}{\lambda_2-\lambda_1}\left[\frac{\lambda_1(1+\beta)+(A+\beta D)}{e^{\lambda_1\tau} - e^{\lambda_2\tau}}\right]$$

$$- \frac{\tau e^{\lambda_2\tau}}{\lambda_2-\lambda_1}\left[\frac{\lambda_2(1+\beta)+(A+\beta D)}{e^{\lambda_1\tau} - e^{\lambda_2\tau}}\right] \tag{23}$$

Similarly, solving for δ_B and dividing by γ_B gives,

$$\mu_B = -\frac{2}{(\lambda_2-\lambda_1)^2}\left[(\lambda_1+A)(\lambda_2+A)+\beta B\right]\left[\frac{e^{\lambda_1\tau}-e^{\lambda_2\tau}}{(A+\lambda_1)e^{\lambda_1\tau}-(A+\lambda_2)e^{\lambda_2\tau}}\right]$$

$$-\frac{\tau e^{\lambda_1\tau}}{\lambda_2-\lambda_1}\left[\frac{(\lambda_1+A)^2+\beta B}{(A+\lambda_1)e^{\lambda_1\tau}-(A+\lambda_2)e^{\lambda_2\tau}}\right]-\frac{\tau e^{\lambda_2\tau}}{\lambda_2-\lambda_1}\left[\frac{(\lambda_2+A)^2+\beta B}{(A+\lambda_1)e^{\lambda_1\tau}-(A+\lambda_2)e^{\lambda_2\tau}}\right] \quad (24)$$

For identical layers in which no reaction occurs, these relations reduce to,

$$\mu_A = \left(\frac{1+\beta}{2}\right)\tau \quad (25)$$

$$\mu_B = \left(\frac{1+\beta}{2}\right)\tau + \left(\frac{1-\beta}{2}\right)\left(\frac{1-e^{-2\tau}}{1+e^{-2\tau}}\right) \quad (26)$$

At short times, the center of mass in the upper layer is zero while in the lower layer, its location is equal to τ. This is simply a reflection of the fact that the primary, directly impacting plume initially contains all of the pollutant mass. After long time, however, the residual contains essentially all of the pollutant mass, as alluded to by the numerical results. The long time asymptotic behavior of the center of mass in the lower layer is,

$$\mu_B \sim \left(\frac{1-\beta}{2}\right) + \left(\frac{1+\beta}{2}\right)\tau \quad (27)$$

This equation indicates that the maximum residual concentration shifts with time according to the ratio of the velocities in each

layer. For Case 1, in which V=-U, the residual concentration in the lower layer is always peaked a distance η downwind of the source, as indicated previously by the numerical analysis (Figure 5). For Case 2, in which V=-2U, the residual concentration in the lower layer shifts upwind at the average speed of the two layers, as indicated in Figure 6. Comparison of Equations (25) and (27) indicates that the center of mass in the upper layer is shifted with respect to the center of mass in the lower layer. For winds that are of equal magnitude but in opposite directions, V=-U, the center of mass in the upper layer is at the origin. By symmetry, the maximum impact in the lower layer due to a pollutant source in the upper layer is also at the origin, as indicated by the numerical evaluation of Case 3 (Figure 7). Thus the moments of the concentration distribution verify the numerical results.

The model can also be analyzed for non-zero reaction terms but no new information about the solution is observed. Reactive decay, in either or both layers reduces the relative impact of the residual when compared to the primary plume, but its structure remains the same. The method of characteristics can also be used to evaluate the effect of wind reversals on the concentration distribution, since wind reversals simply change the characteristic curves on which the equations propagate. Its inclusion, however, tends to complicate rather than elucidate the structure of the solution.

SUMMARY AND CONCLUSIONS

The results of pollutant transport between the surface layer of the atmosphere and the air aloft were examined via development and solution of a simple mathematical model of the process. Previous experimental work had indicated that such interaction could be significant, especially for the long-range transport or multi-day impact of a pollutant source. Solutions to the model equations were developed numerically via the method of characteristics and analytically by the method of moments. Although the model excluded diffusional processes and the diurnal variation of the atmospheric layers, the structure of its solution retained many of the characteristics that had been observed in experiments conducted in an atmosphere with significant vertical structure, such as the possibility of plume bifurcation due to transport through directionally sheared wind flows.

The model indicated that a pulse of pollutants emitted at ground level when the upper and lower level winds are of equal magnitude, but oriented in the opposite direction, can result in a residual impact that remains centered over a single location for all time. Similarly, a pulse of pollutants emitted when the upper level winds are stronger and oriented in the direction opposite to those at the surface, can result in a residual impact that moves upwind with respect to the surface winds. The residual concentrations move at the average speed of the two layers. The model also indicates that the maximum ground-level impact of an elevated source is directly below the source, when the winds in

each layer are of equal magnitude but in opposite directions.

In each case, the behavior of the residual plume would not be expected from the surface layer winds that are normally used to predict the transport and dispersion of pollutants. It appears, however, that the characteristic exchange rate between the air aloft and the surface mixing layer is large enough that the winds aloft must be considered when describing long range transport or the multi-day impacts of a pollutant.

References

Aris, R. (1956). On the dispersion of a solute in a fluid flowing through a tube. Procedures of the Royal Society (London), A235, 67-77.

Aron, R.H., and Aron, I. (1978). Statistical forecasting models: I. Carbon monoxide concentrations in the Los Angeles Basin. Journal of the Air pollution Control Association, 28, No. 7, 681-684.

Aron, R.H., and Aron, I. (1978). Statistical forecasting models: II. Oxidant concentrations in the Los Angeles Basin. Journal of the Air pollution Control Association, 28, 7, 684-688.

Benarie, M.M. (1980). Urban Air Pollution Modeling. MIT Press, Cambridge, Massachusetts, 405 pp.

Blumenthal, D.L., White, W.H., and Smith, T.B. (1978). Anatomy of a Los Angeles smog episode: pollutant transport in the daytime sea breeze regime. Atmospheric Environment, 12, 893-907.

Dabberdt, W.F., and Singh, H.B. (1977). Objective evaluation of emergency plans for oxidant control. Journal of the Air Pollution Control Association, 27, 9, 876-881.

Deardorff, J.W., Willis, G.E. and Stockton, B.H. (1980). Laboratory studies of the entrainment zone of a convectively mixed layer. Journal of Fluid Mechanics,100, 1, 41-64.

Johnson, W.B., and Singh, H.B. (1977). Oxidant layers aloft: their origin and significance. presented at the International Ozone Conference, NC, 1976.

Lorenzen, A. (1979). Summary of California upper air meteorological data. California Air Resources Board, Technical Services Division, PO Box 2815, Sacramento, Ca. 95812.

Reible, D.D., Shair, F.H., and Kauper, E. (1981). Plume dispersion and bifurcation in directional shear flows associated with complex terrain. Atmospheric Environment, 15, 7, 1165-1172.

Reible, D.D., and Shair, F.H. (1982a). The transport of airborne pollutants into, within, and out of the Sacramento Valley of California. Submitted for publication in Atmospheric Environment.

Reible, D.D., and Shair, F.H. (1982b). The transport and

dispersion of airborne contaminants in the Santa Barbara Channel area of Southern California. Submitted for publication in Atmospheric Environment.

Reible, D.D., Shair, F.H., Smith, T.B., and Lehrman, D.E. (1982). The origin and fate of air pollutants in California's San Joaquin Valley, II. Summer. Submitted for publication to Atmospheric Environment.

Shair, F., Sasaki, E., Carlan, D. Cass, G., Goodin, W., Edinger, J., and Schacher, G. (1982). Transport and dispersion of airborne pollutants associated with the land-sea breeze system. In press, Atmospheric Environment.

Stoker, J.J. (1957). Water Waves, Wiley-Interscience, Ney York.

Swedish Preparatory Committee for the UN conference on the Human Environment (1971). Air Pollution Across National Boundaries: The Impact on the Environment of Sulphur in Air and Precipitation, Royal Ministries of Foreign Affairs and Food, Stockholm.

Turner, D.B. (1970). Workbook of atmospheric dispersion estimates, Environmental Protection Agency, AP-26, 84 pp.

Wolff, G.T., Lioy, P.J., Wight, G.D., Meyers, R.E., Cederwall, R.T. (1977). An investigation of long-range transport of ozone across the midwestern and eastern United States. Atmospheric Environment, 11, 797-802.